frontiers | Research Topics

Advances in the endocrine role of the skeleton, volume II

Edited by
Andrea Del Fattore, Michela Rossi and Helen Knowles

Published in
Frontiers in Endocrinology

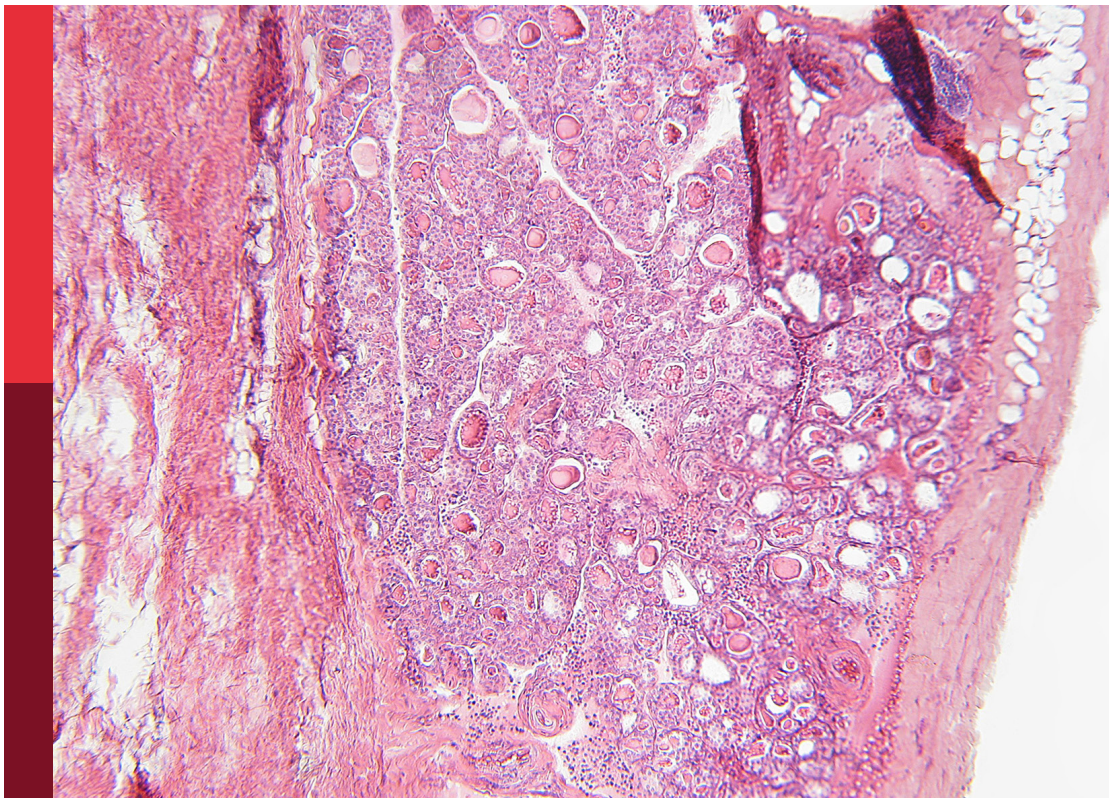

ISSN 1664-8714
ISBN 978-2-8325-4248-4
DOI 10.3389/978-2-8325-4248-4

About Frontiers

Frontiers is more than just an open access publisher of scholarly articles: it is a pioneering approach to the world of academia, radically improving the way scholarly research is managed. The grand vision of Frontiers is a world where all people have an equal opportunity to seek, share and generate knowledge. Frontiers provides immediate and permanent online open access to all its publications, but this alone is not enough to realize our grand goals.

Frontiers journal series

The Frontiers journal series is a multi-tier and interdisciplinary set of open-access, online journals, promising a paradigm shift from the current review, selection and dissemination processes in academic publishing. All Frontiers journals are driven by researchers for researchers; therefore, they constitute a service to the scholarly community. At the same time, the *Frontiers journal series* operates on a revolutionary invention, the tiered publishing system, initially addressing specific communities of scholars, and gradually climbing up to broader public understanding, thus serving the interests of the lay society, too.

Dedication to quality

Each Frontiers article is a landmark of the highest quality, thanks to genuinely collaborative interactions between authors and review editors, who include some of the world's best academicians. Research must be certified by peers before entering a stream of knowledge that may eventually reach the public - and shape society; therefore, Frontiers only applies the most rigorous and unbiased reviews. Frontiers revolutionizes research publishing by freely delivering the most outstanding research, evaluated with no bias from both the academic and social point of view. By applying the most advanced information technologies, Frontiers is catapulting scholarly publishing into a new generation.

What are Frontiers Research Topics?

Frontiers Research Topics are very popular trademarks of the *Frontiers journals series*: they are collections of at least ten articles, all centered on a particular subject. With their unique mix of varied contributions from Original Research to Review Articles, Frontiers Research Topics unify the most influential researchers, the latest key findings and historical advances in a hot research area.

Find out more on how to host your own Frontiers Research Topic or contribute to one as an author by contacting the Frontiers editorial office: frontiersin.org/about/contact

Advances in the endocrine role of the skeleton, volume II

Topic editors

Andrea Del Fattore — Bambino Gesù Children's Hospital (IRCCS), Italy

Michela Rossi — Bambino Gesù Children's Hospital (IRCCS), Italy

Helen Knowles — University of Oxford, United Kingdom

Citation

Del Fattore, A., Rossi, M., Knowles, H., eds. (2024). *Advances in the endocrine role of the skeleton, volume II*. Lausanne: Frontiers Media SA.

doi: 10.3389/978-2-8325-4248-4

Table of contents

frontiers | Frontiers in Endocrinology

TYPE Editorial
PUBLISHED 20 December 2023
DOI 10.3389/fendo.2023.1345813

OPEN ACCESS

EDITED AND REVIEWED BY
Jonathan H Tobias,
University of Bristol, United Kingdom

*CORRESPONDENCE
Andrea Del Fattore
andrea.delfattore@opbg.net

RECEIVED 28 November 2023
ACCEPTED 12 December 2023
PUBLISHED 20 December 2023

CITATION
Rossi M, Knowles HJ and Del Fattore A (2023) Editorial: Advances in the endocrine role of the skeleton volume II.
Front. Endocrinol. 14:1345813.
doi: 10.3389/fendo.2023.1345813

Editorial: Advances in the endocrine role of the skeleton volume II

Michela Rossi[1], Helen J. Knowles[2] and Andrea Del Fattore[1]*

[1]Bone Physiopathology Research Unit, Translational Pediatrics and Clinical Genetics Research Division, Bambino Gesù Children's Hospital, IRCCS, Rome, Italy, [2]Botnar Institute for Musculoskeletal Sciences, Nuffield Department of Orthopaedics Rheumatology & Musculoskeletal Sciences, University of Oxford, Oxford, United Kingdom

KEYWORDS

bone, bone disease, endocrinology, osteoclast, osteoblast

Editorial on the Research Topic
Advances in the endocrine role of the skeleton volume II

In the last years, the identification of crosstalk between bone tissue and other organs and the analysis of its involvement in different diseases, have been of great interest to the research community. Indeed, from the archaic description of the skeleton exclusively as a support and protective scaffold for the body, this research has discovered novel functions associated with bone and has dissected the mechanisms of its interplay with other organs (1, 2).

In the paper published in this Research Topic, Cui et al. investigated the causal association between non-alcoholic fatty liver disease (NAFLD) and osteoporosis. NAFLD comprises of steatosis, non-alcoholic steatohepatitis, and fibrosis in obese children and adolescents. Interestingly, the possible correlation between NAFLD and osteoporosis has already been explored by previously published papers with inconsistent results (3). In this paper, the authors employed a Mendelian randomization analysis to evaluate the potential causal effect of NAFLD on the development of osteoporosis, fractures, and falling risk, and discovered that the genetic prediction of NAFLD was linked with an increased risk of osteoporosis without observing a correlation between NAFLD variants and fractures and falling risk.

Moreover, Xiong et al. investigated the link between thyroid dysfunction and bone tissue, analysing a potential correlation between thyroid dysfunction and hallux valgus (HV, bunion). Although thyroid diseases have widespread systemic manifestations, including the alteration of bone metabolism (4), the causal effect of thyroid alterations on hallux valgus is still unknown. The etiology of HV is currently under investigation since many factors can contribute to the development of this forefoot deformity including genetic factors, improper habits, inflammatory and neuromuscular joint disease. The authors performed a Mendelian randomization analysis considering hypothyroidism, hyperthyroidism, thyroxine (FT4; free T4) and thyroid stimulating hormone (TSH) as exposure and HV as outcome. They found that high risk of Hallux valgus recurrence is observed in hypothyroidism, without revealing correlation with hyperthyroidism, FT4 and TSH.

Also in this Research Topic, Wang et al. investigated the interaction between obesity and diabetes with bone alterations. Using data from the National Health and Nutrition Examination Survey (NHANES), the authors revealed a potential correlation between weight-adjusted waist index (WWI) and total BMD (Bone Mineral Density) in nearly 7,000 US adolescents. They performed a multivariate linear regression analysis that revealed a negative correlation between WWI and total BMD; they also detected an L-shaped association between WWI and total BMD, with a flex point at 9.98 cm/√kg.

Additionally, Li et al. analysed how type 1 diabetes could influence periodontal ligament and alveolar bone remodeling during axial tooth movement in mice. Using streptozotocin (STZ)-injected mice, the authors investigated how axial tooth movement was inhibited in type 1 diabetic mice, potentially due to alterations of the periodontal ligament collagen fibers or to osteoclasts.

The endocrine role of osteocalcin was also investigated within this Research Topic. Verdelli et al. analysed how osteocalcin regulates the function of parathyroid tumor cells. They performed *in vitro* experiments with primary cells isolated from parathyroid adenomas and HEK cells, and reported how both osteocalcin with gamma-carboxyglutamic acid residues (GlaOC) and the uncarboxylated form (GluOC) control pERK/ERK and active β-catenin, mainly through the activation of the calcium-sensing receptor (CASR).

Bone remodelling can be influenced by external factors including lifestyle choices such as inadequate sun exposure, minimal physical activity, malnutrition, smoking, or excessive alcohol intake, as well as environmental factors that can adversely affect bone health and contribute to bone loss (5). In the elegant review published by Romano et al., osteoporosis and dermatoporosis are described as consequences of the aging process respectively in the bone and skin and share vitamin D deficiency. The term "Dermatoporosis" was introduced about 15 years ago to describe a condition characterized by thinner skin that becomes fragile and tends to rip, leading to deep dissecting hematomas (6). Vitamin D has well-established effects on bone tissue but further investigation is required to understand how it regulates aging in other tissues, including the skin, to decipher the role of Vitamin D deficiency in the development of dermatoporosis.

Moreover, in the paper published by Zhang et al., a cross-sectional study on a Chinese cohort of 3433 individuals was performed to evaluate the effects of cooking oil fumes (COFs) and fume extractors on BMD. They found significant correlations between the non-use of fume extractors and total Lombar Spine BMD, as well as bone formation markers including PINP (Procollagen type I N-terminal propeptide) and ALP(Alkaline phosphatase).

In this Research Topic, advances in the understanding of bone physiology were also reported, directing attention to the potential translational impact of bone endocrinology. Janssen et al. investigated gene expression in calvarial and cortical bone of juvenile female mice. They did not report alterations in classic bone gene expression (e.g. Runx2, Osx, ALP, Col1a1, Col1a2 and Dentin matrix protein 1) between calvaria and cortical bones. However, they did find alterations in genes involved in skeletal diseases, craniosynostosis and weight loading.

Currently, research on ferroptosis may hold promise for the prevention and treatment of primary osteoporosis. Ferroptosis is an iron-dependent cell death and it differs from apoptosis, necrosis, autophagy, and other forms of cell death as it is caused by unrestricted lipid peroxidation and accumulation of reactive oxygen species (ROS). Using bioinformatic methods, Xia et al. identified 5 key ferroptosis-DEGs (differentially expressed genes) associated with primary osteoporosis and ferroptosis, including SIRT1, HSPA5, MTOR, HIF1A and BECN1.

This Research Topic is of interest both to basic and clinical researchers since it takes into consideration a wide range of topics regarding bone research. Original studies and reviews have been published to describe the latest discoveries in skeleton physiology and function.

Author contributions

MR: Writing – original draft. HJK: Writing – original draft. ADF: Writing – original draft, Writing – review & editing.

Funding

The author(s) declare financial support was received for the research, authorship, and/or publication of this article. MR is supported by the Fondazione Umberto Veronesi. This work was also supported by the Italian Ministry of Health with the "Current Research funds".

Conflict of interest

The authors declare that the research was conducted in the absence of any commercial or financial relationships that could be construed as a potential conflict of interest.

The author(s) declared that they were an editorial board member of Frontiers, at the time of submission. This had no impact on the peer review process and the final decision.

Publisher's note

References

1. Karsenty G. Update on the biology of osteocalcin. *Endocr Pract* (2017) 23 (10):1270–4. doi: 10.4158/EP171966.RA

2. Rossi M, Battafarano G, Pepe J, Minisola S, Del Fattore A. The endocrine function of osteocalcin regulated by bone resorption: A lesson from reduced and increased bone mass diseases. *Int J Mol Sci* (2019) 20(18):4502. doi: 10.3390/ijms20184502

3. Yang YJ, Kim DJ. An overview of the molecular mechanisms contributing to musculoskeletal disorders in chronic liver disease: osteoporosis, sarcopenia, and osteoporotic sarcopenia. *Int J Mol Sci* (2021) 22(5):2604. doi: 10.3390/ijms22052604

4. Bassett JHD, Williams GR. Role of thyroid hormones in skeletal development and bone maintenance. *Endocr Rev* (2016) 37(2):135–87. doi: 10.1210/er.2015-1106

5. Rubio-Gutierrez JC, Mendez-Hernández P, Guéguen Y, Galichon P, Tamayo-Ortiz M, Haupt K, et al. Overview of traditional and environmental factors related to bone health. *Environ Sci pollut Res Int* (2022) 29(21):31042–58. doi: 10.1007/s11356-022-19024-1

6. Kaya G, Saurat JH. Dermatoporosis: a chronic cutaneous insufficiency/fragility syndrome. Clinicopathological features, mechanisms, prevention and potential treatments. *Dermatology* (2007) 215(4):284–94. doi: 10.1159/000107621

frontiers | Frontiers in Endocrinology

TYPE Original Research
PUBLISHED 25 August 2022
DOI 10.3389/fendo.2022.980867

OPEN ACCESS

EDITED BY
Michela Rossi,
Bambino Gesù Children's Hospital, (IRCCS), Italy

REVIEWED BY
Yufei Zhou,
Fudan University, China
Elizabeth Rendina-Ruedy,
Vanderbilt University Medical Center, United States
Guotian Luo,
Université de Paris, France

*CORRESPONDENCE
Huilin Yang
suzhouspine@163.com
Dechun Geng
szgengdc@suda.edu.cn

†These authors have contributed equally to this work and share first authorship

SPECIALTY SECTION
This article was submitted to Bone Research, a section of the journal Frontiers in Endocrinology

RECEIVED 29 June 2022
ACCEPTED 12 August 2022
PUBLISHED 25 August 2022

CITATION
Xia Y, Zhang H, Wang H, Wang Q, Zhu P, Gu Y, Yang H and Geng D (2022) Identification and validation of ferroptosis key genes in bone mesenchymal stromal cells of primary osteoporosis based on bioinformatics analysis. *Front. Endocrinol.* 13:980867. doi: 10.3389/fendo.2022.980867

Identification and validation of ferroptosis key genes in bone mesenchymal stromal cells of primary osteoporosis based on bioinformatics analysis

Yu Xia[1†], Haifeng Zhang[1†], Heng Wang[1†], Qiufei Wang[2], Pengfei Zhu[1], Ye Gu[2], Huilin Yang[1*] and Dechun Geng[1*]

[1]Department of Orthopedics, The First Affiliated Hospital of Soochow University, Suzhou, China, [2]Department of Orthopedics, Changshu Hospital Affiliated to Soochow University, First People's Hospital of Changshu City, Changshu, China

Primary osteoporosis has long been underdiagnosed and undertreated. Currently, ferroptosis may be a promising research direction in the prevention and treatment of primary osteoporosis. However, the specific mechanism of ferroptosis in primary osteoporosis remains a mystery. Differentially expressed genes (DEGs) were identified in bone mesenchymal stromal cells (BMSCs) of primary osteoporosis and heathy patients from the GEO databases with the help of bioinformatics analysis. Then, we intersected these DEGs with the ferroptosis dataset and obtained 80 Ferr-DEGs. Several bioinformatics algorithms (PCA, RLE, Limma, BC, MCC, etc.) were adopted to integrate the results. Additionally, we explored the potential functional roles of the Ferr-DEGs *via* GO and KEGG. Protein–protein interactions (PPI) were used to predict potential interactive networks. Finally, 80 Ferr-DEGs and 5 key Ferr-DEGs were calculated. The 5 key Ferr-DEGs were further verified in the OVX mouse model. In conclusion, through a variety of bioinformatics methods, our research successfully identified 5 key Ferr-DEGs associated with primary osteoporosis and ferroptosis, namely, sirtuin 1(*SIRT1*), heat shock protein family A (*Hsp70*) member 5 (*HSPA5*), mechanistic target of rapamycin kinase (*MTOR*), hypoxia inducible factor 1 subunit alpha (*HIF1A*) and beclin 1 (*BECN1*), which were verified in an animal model.

KEYWORDS

primary osteoporosis, ferroptosis, bioinformatics, bone mesenchymal stromal cells (BMSCs), autophagy

Introduction

As a complex bone metabolism disorder mainly characterized by bone loss and bone microstructure changes, primary osteoporosis has long been underdiagnosed and undertreated (1–4). Approximately 40% of postmenopausal white women are affected by osteoporosis. The aging population will exacerbate the medical and socioeconomic effects of osteoporosis. A patient with osteoporosis has a 40% lifetime fracture risk, and most of them occur in the spine, hip or wrist (5). Osteoporotic fractures affect 8.9 million people around the world per year. It is expected that osteoporotic hip fractures among elderly men will increase by 310% and 240% in women by 2050 (6, 7). Osteoporosis and its complications have become a worldwide health crisis.

As a recently identified regulated cell death (RCD), ferroptosis differs from apoptosis (8), necrosis (9), autophagy (10), pyroptosis (11), etc. The main characteristics of ferroptosis are iron-dependent lipid peroxidation and reactive oxygen species (ROS) accumulation (12, 13). It involves multiple signaling pathways and their regulators (14) and has been extensively studied in the treatment of cancers, such as renal carcinoma and leukemia (15, 16) and hepatocellular carcinoma (17). Ferroptosis has been observed to be associated with various noncancer diseases, such as neurological diseases (18, 19), viral infection, ischemia and reperfusion injury, and atherosclerosis (20). Interestingly, a number of studies have suggested that ferroptosis may be a promising research direction in the prevention and treatment of osteoporosis (21–23).

Bone mesenchymal stromal cells (BMSCs) are pluripotent mesenchymal cells that can differentiate into different lineages, such as osteoblasts and adipocytes (24). BMSCs play an important role in maintaining bone homeostasis. As a result, osteoporosis is always accompanied by the low osteogenic potential of circulating BMSCs (25), the two form a vicious cycle, exacerbating the progression of osteoporosis. The delicate balance between osteogenic and lipogenic differentiation of BMSCs will be disrupted during the onset of osteoporosis (26). Under certain conditions, ferroptosis can also occur during the process of directional differentiation of BMSCs (27). At present, some researchers have also studied the mechanisms related to ferroptosis and several signaling pathways had been confirmed to play a role in the process of ferroptosis related osteoporosis (28). It is the existing basic research that provides inspiration and guidance for this study. Despite this, the specific mechanisms and related signaling pathways of ferroptosis remain mysterious in osteoporosis.

Bioinformatics analysis of ferroptosis genes in primary osteoporosis has not been reported to date. Thus, we identified DEGs in BMSCs of primary osteoporosis and healthy patients from the GEO databases with the help of bioinformatics analysis. By intersecting these DEGs with the ferroptosis dataset, ferroptosis DEGs (Ferr-DEGs) were obtained. After that, protein–protein interactions (PPI) were used to predict potential interactive networks. Then, the key Ferr-DEGs we obtained were further verified by an experimental OVX model. We have discovered the potential functional role of ferroptosis in BMSCs for the first time and have laid a possible foundation for understanding the pathological mechanism of primary osteoporosis.

Abbreviations: BC, Betweenness Centrality; BP, Biological Process; BMSCs, Bone Mesenchymal Stromal Cells; BMD, Bone Mineral Density; BV, Bone Volume; BV/TV, Bone Volume Per Tissue Volume; CC, Cellular Component; CMA, Chaperone-Mediated Autophagy; DEGs, Differentially Expressed Genes; ER, Endoplasmic Reticulum; Ferr-DEGs, Ferroptosis DEGs; GEO, Gene Expression Omnibus; GO, Gene Ontology; HPA, Human Protein Atlas Database; IF, Immunofluorescence; KEGG, Kyoto Encyclopedia of Genes and Genomes; MCC, Maximal Clique Centrality; MCODE, Molecular Complex Detection; MF, Molecular Function; OVX, Ovariectomy; PCA, Principal Component Analysis; PPI, Protein–Protein Interactions; ROS, Reactive Oxygen Species; ROI, Region of Interest; RCD, Regulated Cell Death; RLE, Relative Log Expression; Tb. N, Trabecular Number; Tb.Sp, Trabecular Separation.

Materials and methods

Microarray data collection

Information on primary osteoporosis patients was downloaded from the Gene Expression Omnibus (GEO; http://www.ncbi.nlm.nih.gov/geo), a public database that collects gene sequencing results (29). We downloaded the raw data of GSE35958 uploaded by Benisch from GEO (30). Five samples of primary osteoporosis (GSM878104, GSM878105, GSM878106, GSM878107, GSM878108; op group) and four controls (GSM878100, GSM878101, GSM878102, GSM878103; ctrl group) in GSE35958 were collected. A detailed table of patients' parameters can be seen in Supplementary Table S1.

Datasets analysis

Bioconductor was used to download the annotated R 4.0.3 package, and R was used to convert the microarray probes to symbols. When multiple probes corresponded to one gene ID, the average value was taken for analysis. Principal component analysis (PCA) was used to determine the significant difference dimensions with a P value < 0.05 (31). Relative log expression (RLE) was used for quality control (32). We used Limma to identify the DEGs. P-Value <0.05 and |log2-fold change (FC)| >1 were considered statistically significant (33). In addition, the Ferroptosis Database (FerrDb; http://www.zhounan.org/ferrdb) provided us with a dataset containing 259 genes (34). Then, we intersected it with the DEGs of GSE35958 to obtain ferroptosis DEGs (Ferr-DEGs).

Functional enrichment analysis and visualization

Metascape (http://metascape.org) was used to determine gene functions (35). Biological process (BP), cellular component (CC) and molecular function (MF) are the three major components of gene ontology (GO), which are used to describe gene functions and interactions (36).. The Kyoto Encyclopedia of Genes and Genomes (KEGG) Pathway Database is an extensive database for mapping pathway annotation results (37, 38). GO and KEGG analyses were performed to explore the functional roles of the Ferr-DEGs *via* Metascape, and Cytoscape (V3.7.2) was used for visualization (39, 40). We then chose molecular complex detection (MCODE) to identify the interconnected central genes. Different colors are used to represent each MCODE network and the close interactions between molecules. During the interaction enrichment analysis, the minimum and maximum sizes of the selection network were 3 and 500, respectively.

Protein–protein interaction network analysis

Then, Ferr-DEGs were uploaded to STRING (https://string-db.org/) to predict and construct PPI networks with a confidence level of >0.4 (41, 42). The node degree of proteins analyzed by STRING was used for ranking. Cytoscape was used to visualize the network. Nodes represent genes, and edges represent connections between genes. Genes were ranked by size according to the betweenness centrality (BC) score analyzed by the CytoNCA plugin. The cytoHubba plugin was used to rank genes by depth of the color corresponding to the weighted score based upon maximal clique centrality (MCC) algorithms (43, 44).

Identification of key Ferr-DEGs

Protein and gene expression profiles at the tissue level (high, medium, low, NA) were obtained from the Human Protein Atlas database (HPA, https://www.proteinatlas.org). After calculation, we regarded the top ranked genes of each algorithm as hub genes and then took the trend of tissue expression and intersected most of those algorithms as the 5 most likely key Ferr-DEGs.

OVX model construction and cell culture

We selected twelve eight-week-old female C57BL/6 mice (provided by the Experimental Animal Center of Soochow University) for osteoporosis induction experiments (45). Mice were randomly divided into two groups: the ovariectomy (OVX) and sham groups. Eight weeks after surgery, all the specimens of the left femurs were removed for microCT and histological experiments. The right femurs were removed for BMSCs collection. Blood was collected by eyeballs removing, and the serum was separated by centrifugation at 2,000 r/m for 20 min and frozen at -80°C for future analysis. All procedures and experiments were approved by the Animal Ethics Committee of the First Affiliated Hospital of Soochow University.

BMSCs were obtained from the right femurs according to the protocol (46). Cells were seeded in a 10-cm^2 dish and incubated in a 37°C incubator with 5% CO_2. BMSCs after three passages were used for subsequent experiments.

Micro-CT analysis

Left femur samples were scanned with a SkyScan 1176 micro-CT (Aartselaar, Belgium) (n = 6/group) after fixation in 10% buffered formalin for 48 h. Three-dimensional (3D) histomorphometric images were constructed by using NRecon software (SkyScan micro-CT, Aartselaar, Belgium). Bone mineral density (BMD), bone volume (BV), trabecular number (Tb. N), bone volume per tissue volume (BV/TV) and trabecular separation (Tb.sp) were used to evaluate bone mass. The region of interest (ROI) began with 100 pieces below the femur growth plate, and 200 pieces (6 μm each) were read per sample.

RT–PCR

Total cellular RNA was obtained from BMSCs using TRIzol reagent (Beyotime, China), reverse transcription and amplification were performed using qRT supermix and SYBR qPCR master mix (Vazyme, China) according to the protocol. RT–PCR was performed in a CFX96™ thermal cycler (Bio-Rad Laboratories, USA). GAPDH was used as an internal reference to calculate the relative mRNA expression level. The primers are listed below: forward 5′-3′: GGTTGTCTCCTGCGACTTCA, reverse 5′-3′: TGGTCCAGGGTTTCTTACTCC for *Gapdh*. Forward 5′-3′: CGCTGTGGCAGATTGTTATTAA, reverse 5′-3′: TTGATCTGAAGTCAGGAATCCC for *Sirt1*. Forward 5′-3′: ATGATGAAGTTCACTGTGGTGG, reverse 5′-3′: CTGATCGTTGGCTATGATCTCC for *Hspa5*. Forward 5′-3′: CTGATCCTCAACGAGCTAGTTC, reverse 5′-3′: GGTC TTTGCAGTACTTGTCATG, for *Mtor*. Forward 5′-3′: GAAT GAAGTGCACCCTAACAAG, reverse 5′-3′: GAG GAATGGGTTCACAAATCAG for *Hif1a*. Forward 5′-3′: TAATAGCTTCACTCTGATCGGG, reverse 5′-3′: CAA ACAGCGTTTGTAGTTCTGA for *Becn1*.

Lipid peroxidation assay

A Lipid Peroxidation Malondialdehyde (MDA) Assay Kit (Beyotime, China) was used to measure lipid peroxidation levels. Serum can be used directly for MDA detection. Cells were homogenized on ice in cell lysis buffer (Beyotime, China). After homogenization followed by centrifugation at 12,000×g for 10 minutes, the supernatant was collected for MDA assays. A 100 μl sample was added to each vial containing 200 μl of MDA detection working solution. The samples were mixed and incubated at 100°C for 15 mins. The samples were cooled to room temperature in a water bath and centrifuged at 1000×g for 10 minutes at room temperature. Then, 200 μl supernatant from each sample was pipetted into a 96-well plate, and the absorbance was measured at 532 nm with a microplate reader. MDA content was determined according to the standard curve.

Iron assay

Serum and cellular iron levels were measured by an iron Content Assay Kit (Solarbio, China). Serum can be used directly for iron assay. 100μl serum was mixed with 250 μl of working solution and incubated at 100°C for 5 mins. The samples were cooled to room temperature in a water bath, mixed with 62 μl chloroform, and centrifuged at 10000×g for 10 minutes at room temperature. Then, 210 μl supernatant from each sample was pipetted into a 96-well plate, and the absorbance was measured at 520 nm. BMSCs were homogenized on ice in cell lysis buffer (Beyotime, China). After homogenization followed by centrifugation at 12,000×g for 10 minutes, 20 μl supernatant was collected and mixed with 180 μl working buffer at 25°C for 10 min, and then the absorbance was measured at 510 nm. A standard curve was simultaneously generated according to the manufacturer's instructions.

Immunofluorescence staining

We used immunofluorescence (IF) staining to detect the expression of Ferr-DEGs between the two groups. Antigen repair of the sections was performed, and the sections were blocked with horse serum. Finally, the primary antibody was incubated at 4°C overnight, and fluorescent-labeled secondary antibodies (ab150079, abcam, UK) were incubated at room temperature for 1 hour. The localization and protein expression level of *Becn1* (A7353, ABclonal, China) were observed by IF staining under an AxioCam HRC microscope (Carl Zeiss, Germany).

Statistical analysis

The quantitative data are presented as the mean ± SD. Student's t test was used to compare the differences between two groups. Each assay condition was performed in triplicate for all quantitative assays. A P value <0.05 was defined as statistically significant.

Results

Data quality control and identification of Ferr-DEGs

A schematic diagram of this study and the main findings is shown in Figure 1. Samples from GEO were divided into two groups [primary osteoporosis (OP) group versus control (Ctrl) group]. PCA and RLE analysis were performed to determine available dimensions and screen correlated samples according to quality control standards and the normalization of raw data. PCA demonstrated significant differences between the op group and the ctrl group (Supplementary Figure S1A). The RLE plots showed that the normalization was acceptable (Supplementary Figure S1B).

We first analyzed the DEGs of GSE35958 by using the "Limma" package and presented it in a volcano plot

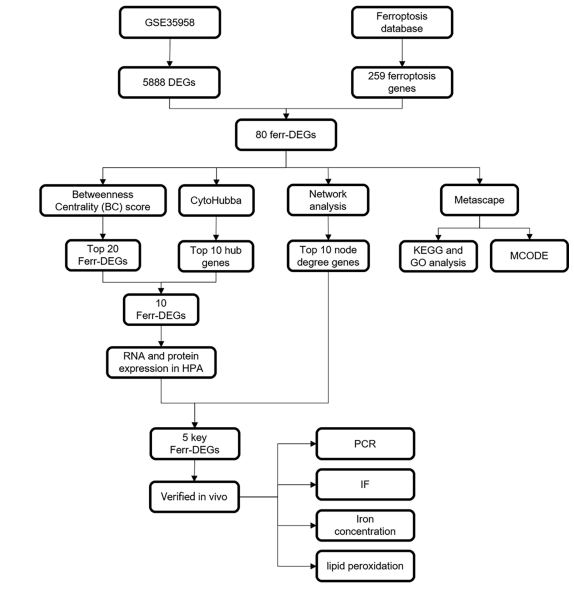

FIGURE 1
Schematic diagram showing the study design.

(Figure 2B) and heatmap (Supplementary Figure S2). Then, we obtained a gene set including 259 genes from FerrDb and intersected them with the DEGs of GSE35958 to identify Ferr-DEGs. Eighty Ferr-DEGs were found and are shown in a heatmap and Venn diagram (Figures 2A, C). The Ferr-DEGs were further divided into driver, suppressor and marker according to FerrDb (Table 1).

Enrichment analysis of Ferr-DEGs

Gene Ontology (GO) enrichment and Kyoto Encyclopedia of Genes and Genomes (KEGG) Pathway Database were used to analyze the biological classification of Ferr-DEGs by using Meyascape. The respective results of BP, CC, MF and KEGG are shown in detail (Supplementary Figure S3). The results showed that the significantly enriched genes were involved in the cellular response to stress, response to starvation, ferroptosis, autophagy, response to iron ion, etc. To further understand the relationships between different terms, we visualized it as a network plot (Figures 3A, B). Details of the top 20 terms are listed in the table (Figure 3C).

The MCODE algorithm was applied to explore those highly connected modules, and three of them were found (Figures 4A–D), The genes in Module 1 were associated with nongenomic actions of 1,25 dihydroxyvitamin D3,

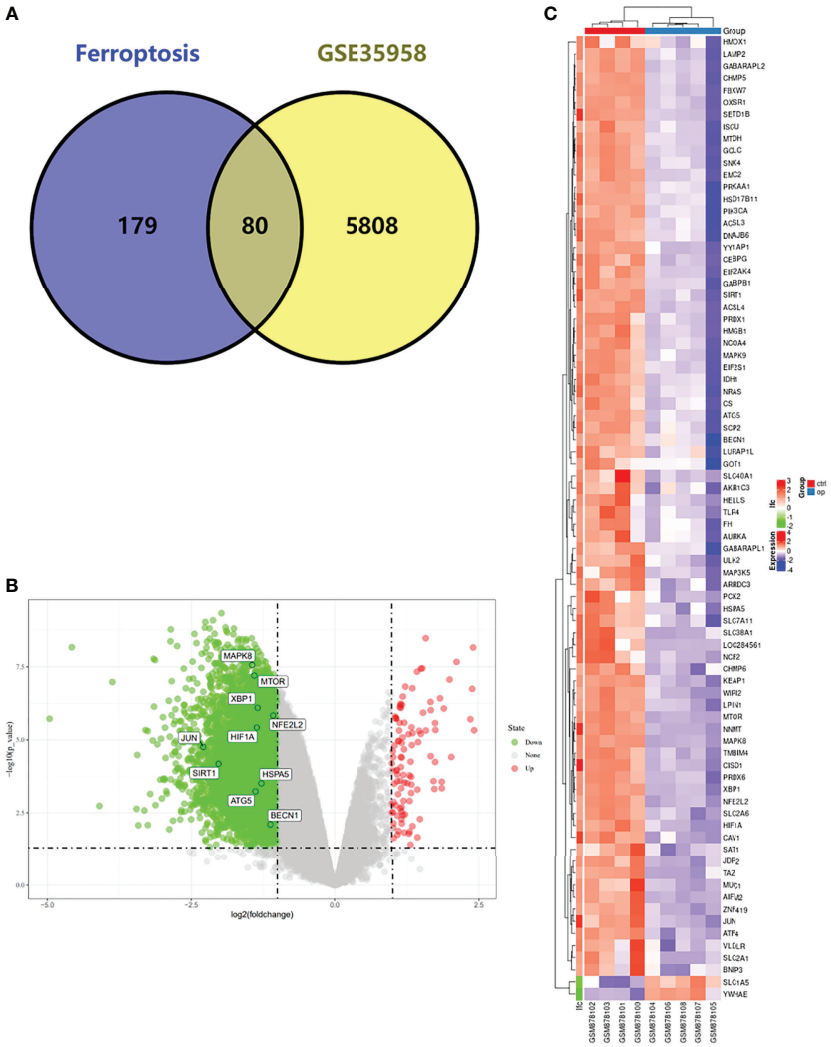

FIGURE 2
Detection of differentially expressed genes (DEGs) in the GSE35958 and Identification of shared DEGs with ferroptosis. **(A)** Venn diagram of DEGs in ferroptosis and GSE35958. **(B)** Volcano map of GSE35958, red represent up-regulated genes and green represent down-regulated genes, The top 10 genes identified by CytoHubba were marked in the diagram. **(C)** An expression heat map of the 80 Ferr-DEGs in GSE35958 dataset.

TABLE 1 Summary of the Ferr-DEGs.

Driver	Suppressor	Marker
EMC2, PIK3CA, SCP2, ACSL4, TAZ, NRAS, SLC38A1, SLC1A5, GOT1, KEAP1, HMOX1, ATG5, NCOA4, IDH1, BECN1, GABARAPL2, SIRT1, DNAJB6, GABARAPL1, WIPI2, CS, SNX4, ULK2, SAT1, MAPK8, LPIN1, MAPK9, PRKAA1, HIF1A, HMGB1, TLR4, YY1AP1, MTDH, FBXW7	*SLC7A11, AKR1C3, GCLC, NFE2L2, HMOX1, MUC1, SLC40A1, CISD1, HSPA5, ATF4, HELLS, MTOR, FH, ISCU, ACSL3, PRDX6, HIF1A, JUN, TMBIM4, AIFM2, LAMP2, CHMP5, CHMP6, CAV1*	*NCF2, BNIP3, OXSR1, SLC7A11, LOC284561, VLDLR, LURAP1L, XBP1, ZNF419, ARRDC3, JDP2, AURKA, CEBPG, EIF2S1, PRDX1, PCK2, GABPB1, HSD17B11, SETD1B, HMOX1, SLC40A1, ATF4, NFE2L2, MAP3K5, NNMT, SLC2A1, SLC2A6, IF2AK4, HMGB1, YWHAE,*

transcriptional activation by NFE2 like bZIP transcription factor 2(*NFE2L2*) in response to phytochemicals and regulation of protein transport. The genes in Module 2 were associated with autophagy and the response to starvation. The genes in Module 3 were related to protein processing and cellular responses to stress (Figure 4E).

PPI network analysis and construction of Ferr-DEGs

Because one of the 80 genes was not related to other molecules and did not form a molecular network, we obtained a PPI network containing 79 nodes and 348 edges. Node degree

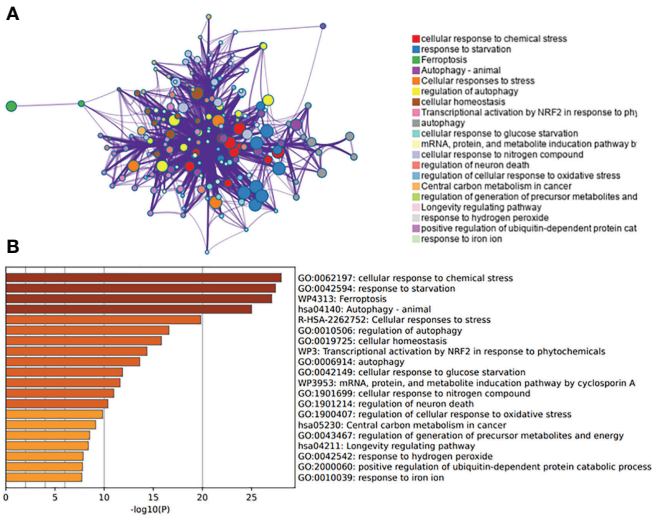

C

Term	Description	Count	%	Log10(P)	Log10(q)
GO:0062197	cellular response to chemical stress	23	28.75	-28.01	-23.66
GO:0042594	response to starvation	21	26.25	-27.42	-23.37
WP4313	Ferroptosis	16	20	-27.04	-23.17
hsa04140	Autophagy - animal	18	22.5	-25	-21.49
R-HSA-2262752	Cellular responses to stress	25	31.25	-19.83	-16.58
GO:0010506	regulation of autophagy	17	21.25	-16.59	-13.45
GO:0019725	cellular homeostasis	20	25	-15.82	-12.77
WP3	Transcriptional activation by NRF2 in response to phytochemicals	7	8.75	-14.35	-11.42
GO:0006914	autophagy	14	17.5	-13.62	-10.75
GO:0042149	cellular response to glucose starvation	8	10	-11.87	-9.1
WP3953	mRNA, protein, and metabolite induction pathway by cyclosporin A	5	6.25	-11.62	-8.91
GO:1901699	cellular response to nitrogen compound	16	20	-10.98	-8.34
GO:1901214	regulation of neuron death	12	15	-10.38	-7.81
GO:1900407	regulation of cellular response to oxidative stress	8	10	-9.84	-7.32
hsa05230	Central carbon metabolism in cancer	7	8.75	-9.13	-6.69
GO:0043467	regulation of generation of precursor metabolites and energy	8	10	-8.52	-6.17
hsa04211	Longevity regulating pathway	7	8.75	-8.39	-6.06
GO:0042542	response to hydrogen peroxide	7	8.75	-7.86	-5.58
GO:2000060	positive regulation of ubiquitin-dependent protein catabolic process	7	8.75	-7.8	-5.54
GO:0010039	response to iron ion	5	6.25	-7.73	-5.47

FIGURE 3
Functional enrichment analysis of DEGs. **(A)** Network of enriched terms. **(B)** A bar chart of top 20 biological pathways based on the P-value and the percentage of genes. **(C)** Details of top 20 biological pathways were listed in table.

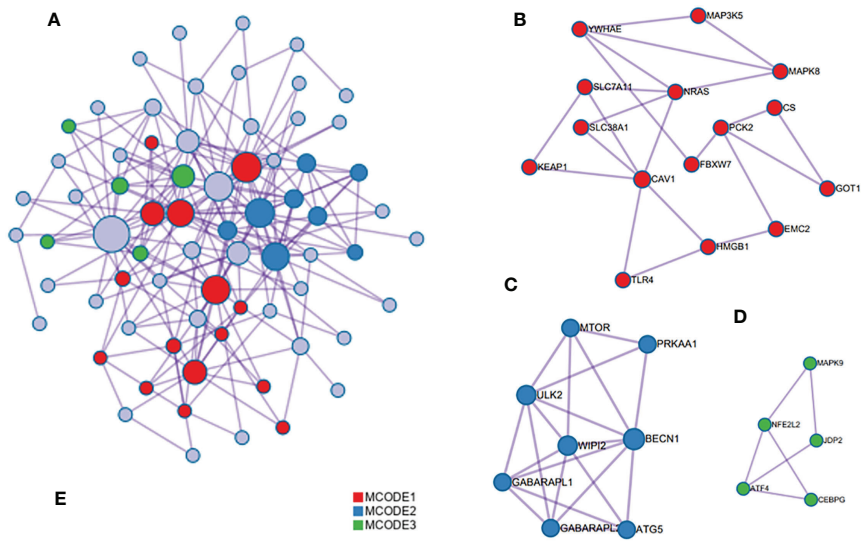

Color	MCODE	GO	Description	Log10(P)
	MCODE_1	WP4341	Non-genomic actions of 1,25 dihydroxyvitamin D3	-7.4
	MCODE_1	WP3	Transcriptional activation by NRF2 in response to phytochemicals	-7.3
	MCODE_1	GO:0051223	regulation of protein transport	-7.1
	MCODE_2	hsa04136	Autophagy - other	-20.2
	MCODE_2	hsa04140	Autophagy - animal	-18.7
	MCODE_2	GO:0042594	response to starvation	-17.5
	MCODE_3	GO:0140467	integrated stress response signaling	-8.1
	MCODE_3	hsa04141	Protein processing in endoplasmic reticulum	-5.8
	MCODE_3	R-HSA-2262752	Cellular responses to stress	-5.7

FIGURE 4
Construction of interactive network. **(A)** GO enrichment analysis was applied to each MCODE network. The same color nodes represent an interactive network and perform similar biological functions. **(B–D)** Three MCODE components were constructed with the screened hub genes. **(E)** Details of the 3 clusters were shown in table.

of proteins analyzed by STRING was used to rank, and the top 10 genes were mechanistic target of rapamycin kinase (*MTOR*), hypoxia inducible factor 1 subunit alpha (*HIF1A*), beclin 1 (*BECN1*), sirtuin 1(*SIRT1*), heat shock protein family A (Hsp70) member 5 (*HSPA5*), Jun proto-oncogene (*JUN*), *NFE2L2*, kelch like ECH associated protein 1(*KEAP1*), autophagy related 5 (*ATG5*) and heme oxygenase 1 (*HMOX1*) (details in Supplementary Table S2). Then, Cytoscape was used to visualize the network. The Ferr-DEG PPI network was constructed by CytoNCA. The top 20 genes are shown inside the circle, and the genes were ranked by size according to the betweenness centrality (BC) score (Figure 5A). Furthermore, we obtained the top 10 hub genes with the highest degree values by using CytoHubba (Figure 5B). Their descriptions and functions are shown in the table (Figure 5C).

Selection and analysis of key Ferr-DEGs

We took the top gene in each algorithm as hub genes of different algorithms. After calculation, 10 Ferr-DEGs were obtained for further research. According to the literature, BMSCs tend to differentiate into adipogenic cells rather than osteogenic cells in osteoporosis patients. Therefore, protein and gene expression profiles at the tissue level (high, medium, low, NA) were obtained from HPA. We used the differences in their expression levels in adipose and bone marrow tissues as a preliminary reference for key Ferr-DEGs (Supplementary Figure S4). At the protein level, the expression of SIRT1, MAPK8*(Mitogen-activated protein kinase 8)*, NFE2L2, HIF1A and BECN1 in bone marrow was higher than that in adipose tissues. In contrast, the expression of ATG5 was higher in

10.3389/fendo.2022.980867

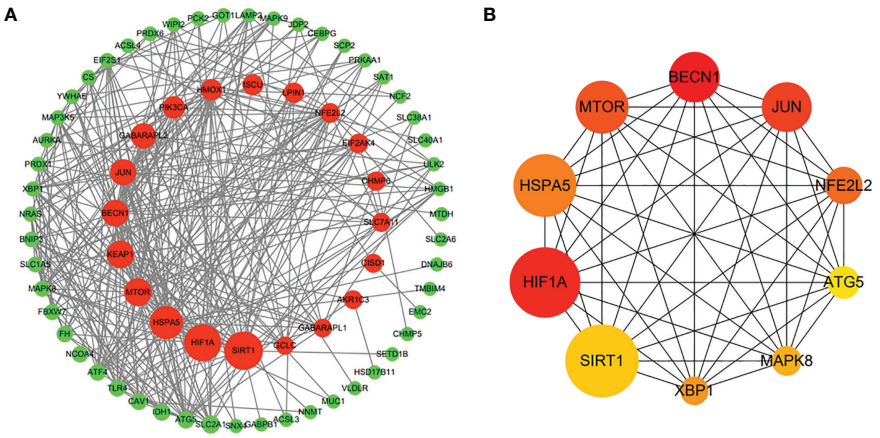

C

Gene symbol	Description	Function
BECN1	Beclin 1	Regulates autophagy ,tumorigenesis, neurodegeneration and apoptosis
HIF1A	Hypoxia Inducible Factor 1 Subunit Alpha	Functions as a master regulator of cellular and systemic homeostatic response to hypoxia
JUN	Jun Proto-Oncogene, AP-1 Transcription Factor Subunit	Involved in NF-kappaB pathway and apoptosis
MTOR	Mechanistic Target Of Rapamycin Kinase	Mediate cellular responses to stresses such as DNA damage and nutrient deprivation,as a part of the PI3K/Akt pathway,
NFE2L2	NFE2 Like BZIP Transcription Factor 2	DNA-binding transcription factor activity and protein domain specific binding
HSPA5	Heat Shock Protein Family A (Hsp70) Member 5	Acts as a repressor of the unfolded protein response (UPR) and also plays a role in cellular apoptosis and senescence.
XBP1	X-Box Binding Protein 1	Regulates DNA-binding transcription factor activity and sequence-specific DNA binding.
MAPK8	Mitogen-Activated Protein Kinase 8	Involved in NF-kappaB pathway and apoptosis and survival anti-apoptotic action of nuclear ESR1 and ESR2.
SIRT1	Sirtuin 1	Associates with aging,identical protein binding and transcription factor binding.
ATG5	Autophagy Related 5	Involved in autophagic vesicle formation, mitochondrial quality control after oxidative damage

FIGURE 5
Hub gene identification **(A)** DEG PPI network constructed using Cytoscape, top 20 genes were shown inside the circle, genes were ranked by size according to Betweenness Centrality (BC) score. **(B)** Top 10 genes with the highest degree values were identified using CytoHubba and the depth of the color correspond to the weighted score. **(C)** The description and function of 10 hub genes were shown in table.

adipose tissues, and the expression level of HSPA5 was the same, while XBP1(X-box binding protein 1) and JUN were not detected in either tissue. At the gene level, the expression of *SIRT1*, *MAPK8*, *XBP1*, *HSPA5*, *HIF1A* and *BECN1* in bone marrow was higher than that in adipose tissues, and in contrast, the expression of *ATG5*, *NFE2L2*, *MTOR* and *JUN* was higher in adipose tissues. Finally, we considered the trends of protein level and gene expression in tissues and intersected most of those algorithms as the 5 most likely key Ferr-DEGs, including *SIRT1*, *HSPA5*, *MTOR*, *HIF1A* and *BECN1* (Figures 6A, B).

Validation of the key Ferr-DEGs *in vivo*

To verify the key Ferr-DEGs *in vivo*, an OVX mouse model was used for validation. The OVX model was successfully established in C57BL/6 mice 8 weeks after surgery. The microCT results showed that the BMD, BV, BV/TV and Tb. N of the OVX group were decreased, while Tb.sp was increased (Figure 7). Meanwhile, the mRNAs of BMSCs isolated from the femurs were used to detect the expression of those 5 key Ferr-DEGs. The results showed that the relative mRNA expression levels of *Sirt1*, *Hspa5*, *Mtor*, *Hif1a* and *Becn1* in the OVX group were significantly lower than those in the sham group (Figures 8A–E). To further validate the expression of these five differentially expressed genes *in vivo*, we chose *Becn1* as the representative target, and IF staining was used for evaluation. The results showed that BECN1 was significantly more highly expressed in the sham group than in the OVX group (Figures 8F, G).

To further demonstrate the involvement of ferroptosis in the development of osteoporosis, lipid peroxidation levels and iron concentrations in serum and BMSCs from OVX mice were measured. The results showed that MDA levels and iron concentrations were significantly increased both in serum and BMSCs from OVX group (Figures 9A–D). Lipid peroxidation

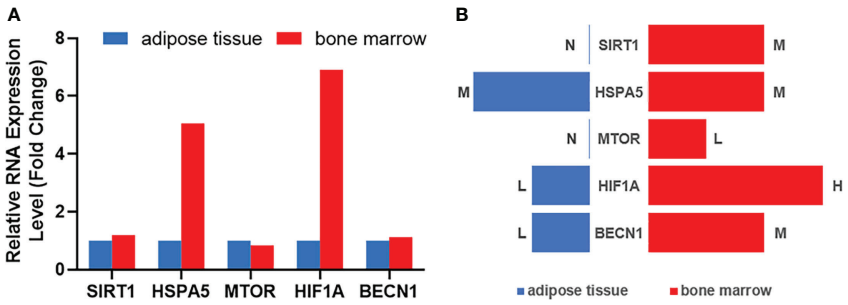

FIGURE 6
The expression analysis of hub genes in human tissues according to Human Protein Atlas data base. **(A)** Summary of RNA expression (fold change). **(B)** Summary of protein expression. H: high; M: medium; L: low; N: not detected.

and iron overload are the characteristic manifestations of ferroptosis.

In summary, these *in vivo* results are consistent with the bioinformatics analysis, demonstrating that there is a high correlation between ferroptosis genes and the progression of osteoporosis in a mouse model. However, the exact mechanism needs to be further elucidated.

Discussion

Different types of osteoporosis, such as diabetic osteoporosis, glucocorticoid-induced osteoporosis, and postmenopausal osteoporosis, were confirmed to be associated with ferroptosis (22, 47–50). However, the specific mechanisms and signaling pathways of ferroptosis involved in osteoporosis remain a mystery. We first intersected microarrays on primary osteoporosis patients in GEO with FerrDb, especially the detection and analysis of BMSCs, which has not been reported in previous studies. We aimed to identify the key genes of ferroptosis and explore its mechanisms in primary osteoporosis. Therefore, we compared the gene expression of primary osteoporosis patients with controls. To be more statistically persuasive, several bioinformatics algorithms (PCA, RLE, Limma, BC, MCC, etc.) were adopted to integrate the results. Additionally, PPI network construction, GO and KEGG were performed to explore the potential functional roles of the Ferr-DEGs. Finally, 80 Ferr-DEGs and 5 key Ferr-DEGs were calculated for further study.

As a newly discovered form of RCD, ferroptosis is accompanied by iron overload, lipid peroxidation and oxidative stress and is regulated by manifold genes. There appears to be a synergistic or antagonistic effect between ferroptosis and other RCDs because they have cross regulators in some pathways (51–53). Interestingly, according to our findings in this research, autophagy was regarded as the most crucial biological process after ferroptosis. Autophagy is an intracellular degradation system that maintains the stability of the intracellular environment (54, 55). Including three subtypes: microautophagy, macroautophagy and chaperone-mediated autophagy (CMA) (56–58). Several stress-related proteins were reported to be important regulators of autophagy-dependent ferroptosis in cancer therapy (59). New evidence suggests that abnormal levels of autophagy and mitochondrial autophagy disrupt the balance of bone metabolism. Osteoporotic BMSCs exhibit impaired osteogenic and increased adipogenic differentiation due to decreased autophagy (60, 61). Our results indicate that ferroptosis is involved in the process of osteoporosis and that autophagy is also involved. This conclusion was further supported by the MCODE results, which suggested that the Ferr-DEGs in different modules were connected with nongenomic actions of 1,25-dihydroxyvitamin D3, autophagy, and response to starvation and stress. We verified the potential connection between ferroptosis and autophagy in osteoporosis *via* various bioinformatics methods. The interaction between ferroptosis and autophagy deserves further study.

As a group of cells with the potential for multidirectional differentiation, BMSCs can differentiate into osteoblasts, chondrocytes and adipocytes. There is an opposite relationship between the differentiation of BMSCs into osteoblasts and adipocytes (62, 63). When osteoporosis occurs, BMSCs tend to differentiate into adipocytes rather than osteoblasts (64, 65). To test and verify our hypothesis, based on the HPA database, we compared the protein and gene expression levels of 10 hub genes between human bone marrow and adipose tissue. We considered the trends of protein and gene expression in tissues and intersected most of those algorithms as the 5 most likely key Ferr-DEGs, including *SIRT1*, *HSPA5*, *MTOR*, *HIF1A* and *BECN1*. Ultimately, these 5 key Ferr-DEGs were considered to be a preliminary reference for determining whether they are differentially expressed when osteoporosis occurs.

SIRT1 is an important regulator of bone homeostasis. The results of HPA showed that the expression level of SIRT1 in adipose tissue is NA, which is not entirely consistent with what is known thus far as SIRT1 is a potential regulator in adipose tissue inflammation and metabolism. The conflicting results may be due

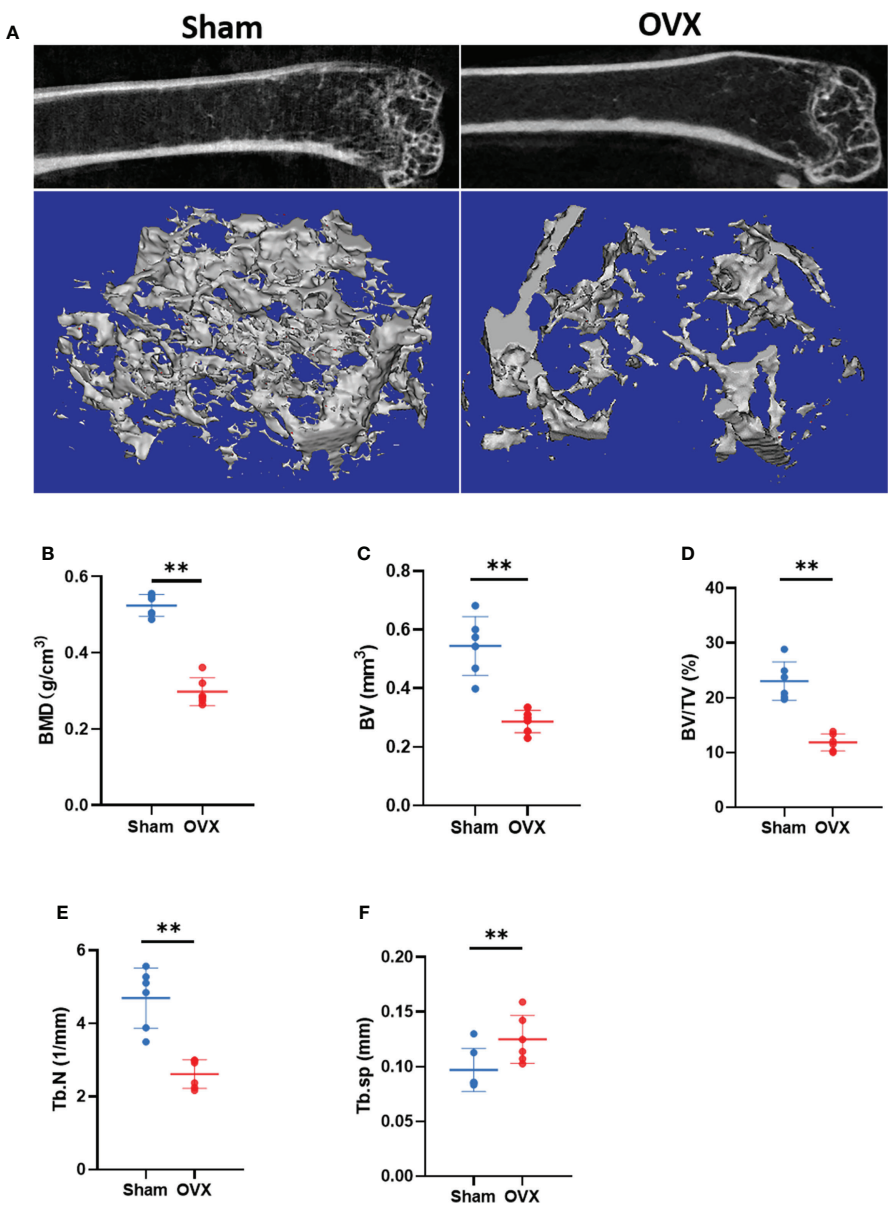

FIGURE 7
Micro CT results and analysis. **(A)** Representative 3D micro-CT reconstruction images of Sham and OVX group. **(B–F)** Quantitative analysis of bone parameters. (The data are expressed as the mean ± sd **P < 0.01).

to delays in updating the site. However, the relative expression levels of SIRT1 in adipose tissue and bone marrow tissue were consistent, which did not affect the conclusion of this study. *Sirt1* KO mice presented with osteoporosis characterized by decreased osteogenesis and increased adipogenesis in BMSCs (66). In contrast, BMSCs overexpressing *Sirt1* repressed the increased expression of superoxide dismutase 2 (*Sod2*) and forkhead box O3A (*Foxo3a*), which promoted the differentiation of BMSCs into osteoblasts and delayed senescence (67). A study in head and neck cancer cells showed that silencing *SIRT1* expression can inhibit epithelial-mesenchymal transition and decrease ferroptosis, while *SIRT1* agonists can promote ferroptosis (68). *SIRT1* was also reported to be associated with mitophagy (69). *HSPA5* is a chaperone protein mainly expressed in the Endoplasmic reticulum (ER) that maintains the stability of glutathione peroxidase 4 (*GPX4*) by forming the *HSPA5-GPX4* complex, thereby causing resistance to ferroptosis (70, 71). There seems to be no current research on the potential role of *HSPA5* in osteoporosis, which would be an interesting direction. *HIF1A* degradation, circadian rhythm and lipid peroxidation play a role in the regulation of ferroptosis, and *HIF1A* is a key factor (72).

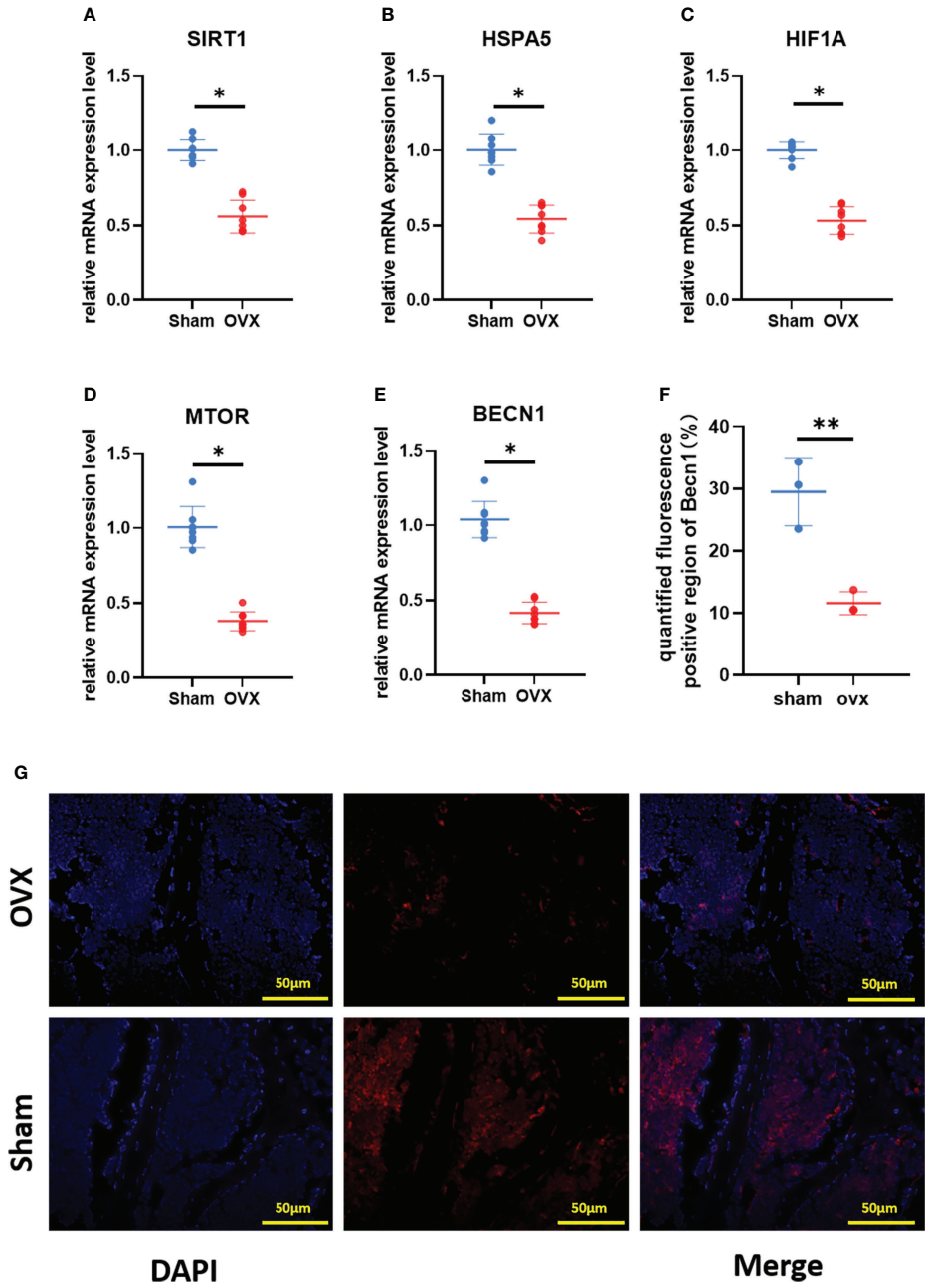

FIGURE 8
Validation of key Ferr-DEGs *in vivo*. **(A–E)** The mRNA expression level of Ferr-DEGs (*Sirt1*, *Hspa5*, *Mtor*, *Hif1a* and *Becn1*) in Sham and OVX group. **(F)** Quantitative analysis of fluorescence intensity. **(G)** Immunofluorescence staining of BECN1. (The data are expressed as the mean ± sd *P < 0.05, **P < 0.01).

Feng et al. reported that ferroptosis might enhance diabetic nephropathy and damage renal tubules in diabetic mouse models (73). In orthopedic-related fields, it has been reported that *Hif1a*-dependent *Bcl2* interacting protein 3 (*Bnip3*) expression is increased and participates in hypoxia-induced autophagy activation, ultimately leading to osteoclastogenesis (74). The *Hif1a*-specific inhibitor 2ME2 can prevent osteoporosis in OVX mice, and the induction of ferroptosis by targeting *Hif1a* in osteoclasts may be a novel approach for the treatment of osteoporosis (50). Most studies on *BECN1* in ferroptosis are based on autophagy. *AMPK*-mediated *BECN1* phosphorylation can promote ferroptosis (75). The process of ferroptosis after erastin treatment was blocked by knockdown of *BECN1*, suggesting that ferroptosis may be a type of autophagy-dependent RCD (76). The osteogenic capability of an osteoblastic

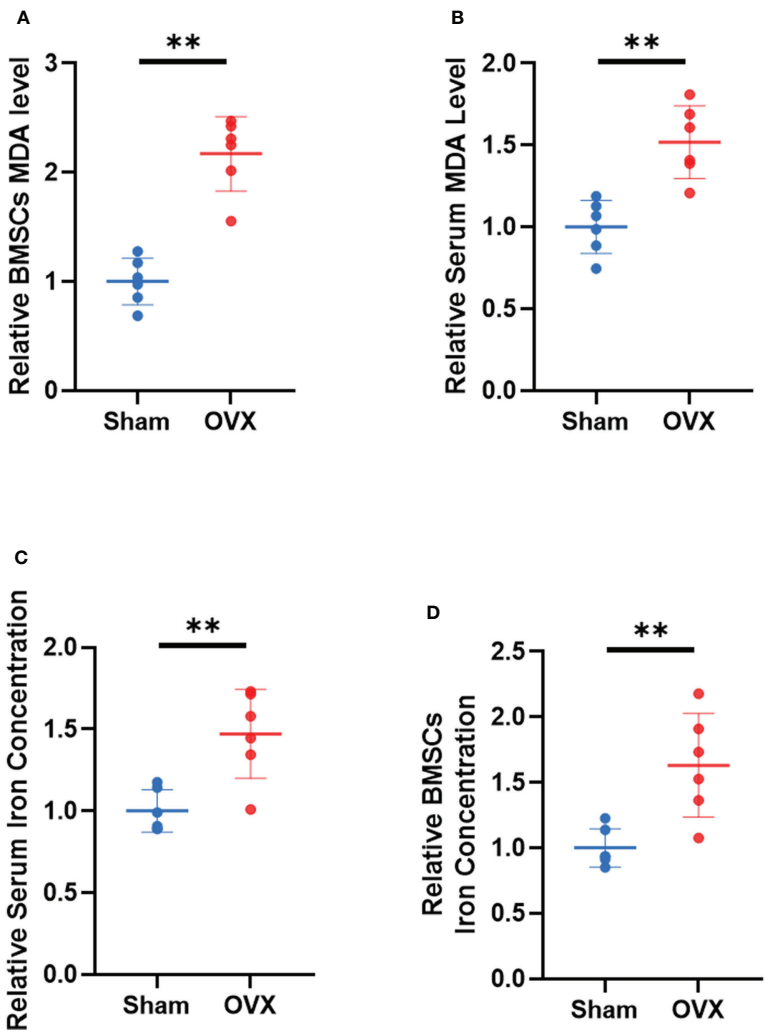

FIGURE 9
Validation of lipid peroxidation and iron level *in vivo*. **(A, B)** Relative expression of MDA in serum and BMSCs. **(C, D)** relative iron concentrations in serum and BMSCs. (The data are expressed as the mean ± sd **P < 0.01).

cell line was significantly reduced after knockdown of autophagy related 7 (*Atg7*) and *Becn1* (77). Our previous study also found that tet methylcytosine dioxygenase 2(*Tet2*) promoted bone loss in OVX mice. It positively regulates BECN1-dependent autophagy by inhibiting BCL2 expression and promoting osteoclast differentiation (78). However, whether *BECN1* is involved in ferroptosis during BMSCs differentiation is still unclear and will be further researched. Acts as a central regulator of the cellular response to growth stimulation, *MTOR* can inhibit autophagy-dependent ferroptosis. In cancer cells, interactions between *MTOR* and *GPX4* can regulate autophagy-dependent ferroptosis by inhibiting CMA (79), and *MTOR* inhibitors may promote *GPX4* degradation by activating the CMA pathway. *MTOR* also has a protective effect on ferroptosis in BMSCs, and autophagy mediated by the *MTOR* pathway can regulate the regeneration function of BMSCs, thereby influencing the occurrence and development of osteoporosis in postmenopausal women (61). Collectively, there are few studies about the specific functions and related mechanisms of these 5 key Ferr-DEGs in ferroptosis during osteoporosis progression. Our results provide a very meaningful direction for future research.

To further verify our conclusions, an osteoporotic model was successfully established in OVX mice. We found that the expression of *Sirt1*, *Hspa5*, *Mtor*, *Hif1a* and *Becn1* in BMSCs from the OVX group was lower than that in BMSCs from the control group, which is consistent with our bioinformatic analysis results. The results of immunofluorescence staining were also consistent with our expectations. Detection of lipid peroxidation and iron levels at serum and cellular levels also confirmed that ferroptosis may be involved in the development

of primary osteoporosis. These outcomes suggest that ferroptosis of BMSCs may be involved in the pathological process of primary osteoporosis. Finally, we believe that our results will offer new insight into the role of ferroptosis in primary osteoporosis and identify the 5 key Ferr-DEGs as potential biomarkers for primary osteoporosis diagnosis and treatment.

Conclusion

In summary, through a variety of bioinformatics methods, our research successfully identified 5 key Ferr-DEGs associated with primary osteoporosis and ferroptosis, namely, *SIRT1*, *HSPA5*, *MTOR*, *HIF1A* and *BECN1*. In addition, autophagy may also be involved in ferroptosis-related primary osteoporosis. In the future, we intend to collect enough bone tissues from patients with primary osteoporosis for further research. We aimed to clarify the regulatory roles of these genes to explore the differentiation mechanisms of BMSCs.

Data availability statement

The datasets presented in this study can be found in online repositories. The names of the repository/repositories and accession number(s) can be found in the article/Supplementary Material.

Ethics statement

The animal study was reviewed and approved by Animal Ethics Committee of the First Affiliated Hospital of Soochow University.

Author contributions

YX and HZ: conception and design. HW and PZ: Acquisition and analysis of data. Investigation and software operation: QW. Validation: YX and YG. Writing and revising: YX and DG. Funding: DG and HY. All authors contributed to the article and approved the submitted version.

Funding

This study was supported by grants from the National Natural Science Foundation of China (Nos. 82072425, 82072498, 81873991, 81873990, 81672238 and 81472077), the Young Medical Talents of Jiangsu Province (No. QNRC2016751), the Natural Science Foundation of Jiangsu Province (Nos. BK20180001 and BE2021650), and the Priority Academic Program Development of Jiangsu Higher Education Institutions (PAPD) and Special Project of Diagnosis and Treatment Technology for Key Clinical Diseases in Suzhou (LCZX202003).

Conflict of interest

The authors declare that the research was conducted in the absence of any commercial or financial relationships that could be construed as a potential conflict of interest.

Publisher's note

Supplementary material

The Supplementary Material for this article can be found online at: https://www.frontiersin.org/articles/10.3389/fendo.2022.980867/full#supplementary-material

SUPPLEMENTARY FIGURE 1
Principal component analysis (PCA) and Relative log expression (RLE) plots of gene chips **(A)** PCA plot of GSE35958. Red and blue spots represent samples from op group and ctrl group respectively. **(B)** RLE plots of GSE35958.

SUPPLEMENTARY FIGURE 2
expression heat map of DEGs in GSE35958 dataset.

SUPPLEMENTARY FIGURE 3
GO and KEGG enrichment analysis. **(A–C)** A histogram of GO enrichment analysis of DEGs, included biological process, cellular component and molecular function. **(D)** Enrichment KEGG pathways.

SUPPLEMENTARY FIGURE 4
RNA and protein expression of top 10 hub genes in different human tissues. **(A)** Relative Rna expression level. **(B)** Summary of protein expression (H: high; M: medium; L: low; N: not detected)

References

1. Compston JE, McClung MR, Leslie WD. Osteoporosis. *Lancet* (2019) 393 (10169):364–76. doi: 10.1016/s0140-6736(18)32112-3

2. Lomholt LB, Dahl AJ. Treatment of osteoporosis: Unmet needs and emerging solutions. *J Bone Metab* (2018) 25(3):133. doi: 10.11005/jbm.2018.25.3.133

3. NIH Consensus Development Panel on Osteoporosis Prevention, Diagnosis and Therapy. Osteoporosis prevention, diagnosis and therapy. *JAMA* (2001) 285 (6):785–95. doi: 10.1001/jama.285.6.785

4. Khosla S, Shane E. A crisis in the treatment of osteoporosis. *J Bone Mineral Res* (2016) 31(8):1485–7. doi: 10.1002/jbmr.2888

5. Rachner TD, Khosla S, Hofbauer LC. New horizons in osteoporosis. *Lancet* (2011) 377(9773):1276. doi: 10.1016/S0140-6736(10)62349-5

6. Hernlund E, Svedbom A, Ivergård M, Compston J, Cooper C, Stenmark J, et al. Osteoporosis in the European union: Medical management, epidemiology and economic burden. a report prepared in collaboration with the international osteoporosis foundation (Iof) and the European federation of pharmaceutical industry associations (Efpia). *Arch Osteoporosis* (2013) 8(1):136. doi: 10.1007/s11657-013-0136-1

7. Bass MA, Sharma A, Nahar VK, Chelf S, Zeller B, Pham L, et al. Bone mineral density among men and women aged 35 to 50 years. *J Am Osteopathic Assoc* (2019) 119(6):357–63. doi: 10.7556/jaoa.2019.064

8. Mirzayans R, Murray D. Do tunel and other apoptosis assays detect cell death in preclinical studies? *Int J Mol Sci* (2020) 21(23):9090. doi: 10.3390/ijms21239090

9. Wu J, Ye J, Kong W, Zhang S, Zheng Y. Programmed cell death pathways in hearing loss: A review of apoptosis, autophagy and programmed necrosis. *Cell Prolif* (2020) 53(11):e12915. doi: 10.1111/cpr.12915

10. Galluzzi L, Baehrecke EH, Ballabio A, Boya P, Bravo-San Pedro JM, Cecconi F, et al. Molecular definitions of autophagy and related processes. *EMBO J* (2017) 36(13):1811–36. doi: 10.15252/embj.201796697

11. Liu P, Zhang Z, Li Y. Relevance of the pyroptosis-related inflammasome pathway in the pathogenesis of diabetic kidney disease. *Front Immunol* (2021) 12:603416. doi: 10.3389/fimmu.2021.603416

12. Xie Y, Hou W, Song X, Yu Y, Huang J, Sun X, et al. Ferroptosis: Process and function. *Cell Death Differ* (2016) 23(3):369–79. doi: 10.1038/cdd.2015.158

13. Dixon SJ, Lemberg KM, Lamprecht MR, Skouta R, Zaitsev EM, Gleason CE, et al. Ferroptosis: An iron-dependent form of nonapoptotic cell death. *Cell* (2012) 149(5):1060–72. doi: 10.1016/j.cell.2012.03.042

14. Liu P, Wang W, Li Z, Li Y, Yu X, Tu J, et al. Ferroptosis: A new regulatory mechanism in osteoporosis. *Oxid Med Cell Longevity* (2022) 2022:2634431. doi: 10.1155/2022/2634431

15. Yang WS, SriRamaratnam R, Welsch ME, Shimada K, Skouta R, Viswanathan VS, et al. Regulation of ferroptotic cancer cell death by Gpx4. *Cell* (2014) 156(1-2):317–31. doi: 10.1016/j.cell.2013.12.010

16. Yu Y, Xie Y, Cao L, Yang L, Yang M, Lotze MT, et al. The ferroptosis inducer erastin enhances sensitivity of acute myeloid leukemia cells to chemotherapeutic agents. *Mol Cell Oncol* (2015) 2(4):e1054549. doi: 10.1080/23723556.2015.1054549

17. Sun X, Ou Z, Chen R, Niu X, Chen D, Kang R, et al. Activation of the P62-Keap1-Nrf2 pathway protects against ferroptosis in hepatocellular carcinoma cells. *Hepatol (Baltimore Md)* (2016) 63(1):173–84. doi: 10.1002/hep.28251

18. Bao WD, Zhou XT, Zhou LT, Wang F, Yin X, Lu Y, et al. Targeting mir-124/Ferroportin signaling ameliorated neuronal cell death through inhibiting apoptosis and ferroptosis in aged intracerebral hemorrhage murine model. *Aging Cell* (2020) 19(11):e13235. doi: 10.1111/acel.13235

19. Wen S, Aki T, Unuma K, Uemura K. Chemically induced models of parkinson's disease: History and perspectives for the involvement of ferroptosis. *Front Cell Neurosci* (2020) 14:581191. doi: 10.3389/fncel.2020.581191

20. Le Y, Zhang Z, Wang C, Lu D. Ferroptotic cell death: New regulatory mechanisms for metabolic diseases. *Endocr Metab Immune Disord Drug Targets* (2021) 21(5):785–800. doi: 10.2174/1871530320666200731175328

21. Zhang J. The osteoprotective effects of artemisinin compounds and the possible mechanisms associated with intracellular iron: A review of in vivo and in vitro studies. *Environ Toxicol Pharmacol* (2020) 76:103358. doi: 10.1016/j.etap.2020.103358

22. Yang RZ, Xu WN, Zheng HL, Zheng XF, Li B, Jiang LS, et al. Exosomes derived from vascular endothelial cells antagonize glucocorticoid-induced osteoporosis by inhibiting ferritinophagy with resultant limited ferroptosis of osteoblasts. *J Cell Physiol* (2021) 236(9):6691–705. doi: 10.1002/jcp.30331

23. Ma H, Wang X, Zhang W, Li H, Zhao W, Sun J, et al. Melatonin suppresses ferroptosis induced by high glucose *Via* activation of the Nrf2/Ho-1 signaling pathway in type 2 diabetic osteoporosis. *Oxid Med Cell Longevity* (2020) 2020:9067610. doi: 10.1155/2020/9067610

24. Chamberlain G, Fox J, Ashton B, Middleton J. Concise review: Mesenchymal stem cells: Their phenotype, differentiation capacity, immunological features, and potential for homing. *Stem Cells (Dayton Ohio)* (2007) 25(11):2739–49. doi: 10.1634/stemcells.2007-0197

25. Dalle Carbonare L, Valenti MT, Zanatta M, Donatelli L, Lo Cascio V. Circulating mesenchymal stem cells with abnormal osteogenic differentiation in patients with osteoporosis. *Arthritis Rheum* (2009) 60(11):3356–65. doi: 10.1002/art.24884

26. Wang QL, Li HF, Wang DP, Liu ZY, Xiao WW, Xu LL, et al. Effect of ggcx on the differentiation function of osteoporosis bone marrow mesenchymal stem cells through regulating Tgfβ/Smad signaling pathway. *Eur Rev Med Pharmacol Sci* (2019) 23(17):7224–31. doi: 10.26355/eurrev_201909_18825

27. Song X, Xie Y, Kang R, Hou W, Sun X, Epperly MW, et al. Fancd2 protects against bone marrow injury from ferroptosis. *Biochem Biophys Res Commun* (2016) 480(3):443–9. doi: 10.1016/j.bbrc.2016.10.068

28. Luo C, Xu W, Tang X, Liu X, Cheng Y, Wu Y, et al. Canonical wnt signaling works downstream of iron overload to prevent ferroptosis from damaging osteoblast differentiation. *Free Radical Biol Med* (2022) 188:337–50. doi: 10.1016/j.freeradbiomed.2022.06.236

29. Patra BG, Maroufy V, Soltanalizadeh B, Deng N, Zheng WJ, Roberts K, et al. A content-based literature recommendation system for datasets to improve data reusability - a case study on gene expression omnibus (Geo) datasets. *J Biomed Inf* (2020) 104:103399. doi: 10.1016/j.jbi.2020.103399

30. Benisch P, Schilling T, Klein-Hitpass L, Frey SP, Seefried L, Raaijmakers N, et al. The transcriptional profile of mesenchymal stem cell populations in primary osteoporosis is distinct and shows overexpression of osteogenic inhibitors. *PloS One* (2012) 7(9):e45142. doi: 10.1371/journal.pone.0045142

31. Ma S, Dai Y. Principal component analysis based methods in bioinformatics studies. *Briefings Bioinf* (2011) 12(6):714–22. doi: 10.1093/bib/bbq090

32. Brettschneider J, Collin F, Bolstad BM, Speed TP. Quality assessment for short oligonucleotide microarray data. *Technometrics* (2008) 50(3):241–64. doi: 10.1198/004017008000000334

33. Ritchie ME, Phipson B, Wu D, Hu Y, Law CW, Shi W, et al. Limma powers differential expression analyses for rna-sequencing and microarray studies. *Nucleic Acids Res* (2015) 43(7):e47. doi: 10.1093/nar/gkv007

34. Zhou N, Bao J. Ferrdb: A manually curated resource for regulators and markers of ferroptosis and ferroptosis-disease associations. *Database* (2020) 2020: baaa021. doi: 10.1093/database/baaa021

35. Zhou Y, Zhou B, Pache L, Chang M, Khodabakhshi AH, Tanaseichuk O, et al. Metascape provides a biologist-oriented resource for the analysis of systems-level datasets. *Nat Commun* (2019) 10(1):1523. doi: 10.1038/s41467-019-09234-6

36. Pomaznoy M, Ha B, Peters B. Gonet: A tool for interactive gene ontology analysis. *BMC Bioinf* (2018) 19(1):470. doi: 10.1186/s12859-018-2533-3

37. Kanehisa M, Sato Y, Kawashima M, Furumichi M, Tanabe M. Kegg as a reference resource for gene and protein annotation. *Nucleic Acids Res* (2016) 44 (D1):D457–62. doi: 10.1093/nar/gkv1070

38. Kanehisa M, Furumichi M, Tanabe M, Sato Y, Morishima K. Kegg: New perspectives on genomes, pathways, diseases and drugs. *Nucleic Acids Res* (2017) 45 (D1):D353–d61. doi: 10.1093/nar/gkw1092

39. Shannon P, Markiel A, Ozier O, Baliga NS, Wang JT, Ramage D, et al. Cytoscape: A software environment for integrated models of biomolecular interaction networks. *Genome Res* (2003) 13(11):2498–504. doi: 10.1101/gr.1239303

40. Saito R, Smoot ME, Ono K, Ruscheinski J, Wang PL, Lotia S, et al. A travel guide to cytoscape plugins. *Nat Methods* (2012) 9(11):1069–76. doi: 10.1038/nmeth.2212

41. Szklarczyk D, Gable AL, Lyon D, Junge A, Wyder S, Huerta-Cepas J, et al. String V11: Protein-protein association networks with increased coverage, supporting functional discovery in genome-wide experimental datasets. *Nucleic Acids Res* (2019) 47(D1):D607–13. doi: 10.1093/nar/gky1131

42. Szklarczyk D, Morris JH, Cook H, Kuhn M, Wyder S, Simonovic M, et al. The string database in 2017: Quality-controlled protein-protein association networks, made broadly accessible. *Nucleic Acids Res* (2017) 45(D1):D362–8. doi: 10.1093/nar/gkw937

43. Chin CH, Chen SH, Wu HH, Ho CW, Ko MT, Lin CY. Cytohubba: Identifying hub objects and Sub-networks from complex interactome. *BMC Syst Biol* (2014) 8 Suppl 4(Suppl 4):S11. doi: 10.1186/1752-0509-8-s4-s11

44. Tang Y, Li M, Wang J, Pan Y, Wu FX. Cytonca: A cytoscape plugin for centrality analysis and evaluation of protein interaction networks. *Bio Syst* (2015) 127:67–72. doi: 10.1016/j.biosystems.2014.11.005

45. Jee WS, Yao W. Overview: Animal models of osteopenia and osteoporosis. *J Musculoskeletal Neuronal Interact* (2001) 1(3):193–207.

46. Zhu H, Guo ZK, Jiang XX, Li H, Wang XY, Yao HY, et al. A protocol for isolation and culture of mesenchymal stem cells from mouse compact bone. *Nat Protoc* (2010) 5(3):550–60. doi: 10.1038/nprot.2009.238

47. Anagnostis P, Paschou SA, Gkekas NN, Artzouchaltzi AM, Christou K, Stogiannou D, et al. Efficacy of anti-osteoporotic medications in patients with type 1 and 2 diabetes mellitus: A systematic review. *Endocrine* (2018) 60(3):373–83. doi: 10.1007/s12020-018-1548-x

48. Lu J, Yang J, Zheng Y, Chen X, Fang S. Extracellular vesicles from endothelial progenitor cells prevent steroid-induced osteoporosis by suppressing the ferroptotic pathway in mouse osteoblasts based on bioinformatics evidence. *Sci Rep* (2019) 9(1):16130. doi: 10.1038/s41598-019-52513-x

49. D'Amelio P, Cristofaro MA, Tamone C, Morra E, Di Bella S, Isaia G, et al. Role of iron metabolism and oxidative damage in postmenopausal bone loss. *Bone* (2008) 43(6):1010–5. doi: 10.1016/j.bone.2008.08.107

50. Ni S, Yuan Y, Qian Z, Zhong Z, Lv T, Kuang Y, et al. Hypoxia inhibits rankl-induced ferritinophagy and protects osteoclasts from ferroptosis. *Free Radical Biol Med* (2021) 169:271–82. doi: 10.1016/j.freeradbiomed.2021.04.027

51. Duan JY, Lin X, Xu F, Shan SK, Guo B, Li FX, et al. Ferroptosis and its potential role in metabolic diseases: A curse or revitalization? *Front Cell Dev Biol* (2021) 9:701788. doi: 10.3389/fcell.2021.701788

52. Chen X, Li J, Kang R, Klionsky DJ, Tang D. Ferroptosis: Machinery and regulation. *Autophagy* (2021) 17(9):2054–81. doi: 10.1080/15548627.2020.1810918

53. Zheng J, Conrad M. The metabolic underpinnings of ferroptosis. *Cell Metab* (2020) 32(6):920–37. doi: 10.1016/j.cmet.2020.10.011

54. Mizushima N, Levine B, Cuervo AM, Klionsky DJ. Autophagy fights disease through cellular self-digestion. *Nature* (2008) 451(7182):1069–75. doi: 10.1038/nature06639

55. Klionsky DJ, Emr SD. Autophagy as a regulated pathway of cellular degradation. *Sci (New York NY)* (2000) 290(5497):1717–21. doi: 10.1126/science.290.5497.1717

56. Glick D, Barth S, Macleod KF. Autophagy: Cellular and molecular mechanisms. *J Pathol* (2010) 221(1):3–12. doi: 10.1002/path.2697

57. Mizushima N, Komatsu M. Autophagy: Renovation of cells and tissues. *Cell* (2011) 147(4):728–41. doi: 10.1016/j.cell.2011.10.026

58. Parzych KR, Klionsky DJ. An overview of autophagy: Morphology, mechanism, and regulation. *Antioxid Redox Signaling* (2014) 20(3):460–73. doi: 10.1089/ars.2013.5371

59. Li C, Zhang Y, Liu J, Kang R, Klionsky DJ, Tang D. Mitochondrial DNA stress triggers autophagy-dependent ferroptotic death. *Autophagy* (2021) 17(4):948–60. doi: 10.1080/15548627.2020.1739447

60. Wang Z, Liu N, Liu K, Zhou G, Gan J, Wang Z, et al. Autophagy mediated cocrmo particle-induced peri-implant osteolysis by promoting osteoblast apoptosis. *Autophagy* (2015) 11(12):2358–69. doi: 10.1080/15548627.2015.1106779

61. Qi M, Zhang L, Ma Y, Shuai Y, Li L, Luo K, et al. Autophagy maintains the function of bone marrow mesenchymal stem cells to prevent estrogen deficiency-induced osteoporosis. *Theranostics* (2017) 7(18):4498–516. doi: 10.7150/thno.17949

62. Beresford JN, Bennett JH, Devlin C, Leboy PS, Owen ME. Evidence for an inverse relationship between the differentiation of adipocytic and osteogenic cells in rat marrow stromal cell cultures. *J Cell Sci* (1992) 102(Pt 2):341–51. doi: 10.1242/jcs.102.2.341

63. Abdallah BM, Jafari A, Zaher W, Qiu W, Kassem M. Skeletal (Stromal) stem cells: An update on intracellular signaling pathways controlling osteoblast differentiation. *Bone* (2015) 70:28–36. doi: 10.1016/j.bone.2014.07.028

64. Taipaleenmäki H, Abdallah BM, AlDahmash A, Säämänen AM, Kassem M. Wnt signalling mediates the cross-talk between bone marrow derived pre-adipocytic and pre-osteoblastic cell populations. *Exp Cell Res* (2011) 317(6):745–56. doi: 10.1016/j.yexcr.2010.12.015

65. Justesen J, Stenderup K, Ebbesen EN, Mosekilde L, Steiniche T, Kassem M. Adipocyte tissue volume in bone marrow is increased with aging and in patients with osteoporosis. *Biogerontology* (2001) 2(3):165–71. doi: 10.1023/a:1011513223894

66. Cohen-Kfir E, Artsi H, Levin A, Abramowitz E, Bajayo A, Gurt I, et al. Sirt1 is a regulator of bone mass and a repressor of sost encoding for sclerostin, a bone formation inhibitor. *Endocrinology* (2011) 152(12):4514–24. doi: 10.1210/en.2011-1128

67. Sun W, Qiao W, Zhou B, Hu Z, Yan Q, Wu J, et al. Overexpression of Sirt1 in mesenchymal stem cells protects against bone loss in mice by Foxo3a deacetylation and oxidative stress inhibition. *Metab: Clin Exp* (2018) 88:61–71. doi: 10.1016/j.metabol.2018.06.006

68. Lee J, You JH, Kim MS, Roh JL. Epigenetic reprogramming of epithelial-mesenchymal transition promotes ferroptosis of head and neck cancer. *Redox Biol* (2020) 37:101697. doi: 10.1016/j.redox.2020.101697

69. Yoshii SR, Mizushima N. Autophagy machinery in the context of mammalian mitophagy. *Biochim Biophys Acta* (2015) 1853(10 Pt B):2797–801. doi: 10.1016/j.bbamcr.2015.01.013

70. Zhu S, Zhang Q, Sun X, Zeh HJ3rd, Lotze MT, Kang R, et al. Hspa5 regulates ferroptotic cell death in cancer cells. *Cancer Res* (2017) 77(8):2064–77. doi: 10.1158/0008-5472.Can-16-1979

71. Chen C, Wang D, Yu Y, Zhao T, Min N, Wu Y, et al. Legumain promotes tubular ferroptosis by facilitating chaperone-mediated autophagy of Gpx4 in aki. *Cell Death Dis* (2021) 12(1):65. doi: 10.1038/s41419-020-03362-4

72. Yang M, Chen P, Liu J, Zhu S, Kroemer G, Klionsky DJ, et al. Clockophagy is a novel selective autophagy process favoring ferroptosis. *Sci Adv* (2019) 5(7):eaaw2238. doi: 10.1126/sciadv.aaw2238

73. Feng X, Wang S, Sun Z, Dong H, Yu H, Huang M, et al. Ferroptosis enhanced diabetic renal tubular injury *Via* hif-1α/Ho-1 pathway in Db/Db mice. *Front Endocrinol* (2021) 12:626390. doi: 10.3389/fendo.2021.626390

74. Zhao Y, Chen G, Zhang W, Xu N, Zhu JY, Jia J, et al. Autophagy regulates hypoxia-induced osteoclastogenesis through the hif-1α/Bnip3 signaling pathway. *J Cell Physiol* (2012) 227(2):639–48. doi: 10.1002/jcp.22768

75. Song X, Zhu S, Chen P, Hou W, Wen Q, Liu J, et al. Ampk-mediated Becn1 phosphorylation promotes ferroptosis by directly blocking system X(C)(-) activity. *Curr Biol CB* (2018) 28(15):2388–99.e5. doi: 10.1016/j.cub.2018.05.094

76. Park E, Chung SW. Ros-mediated autophagy increases intracellular iron levels and ferroptosis by ferritin and transferrin receptor regulation. *Cell Death Dis* (2019) 10(11):822. doi: 10.1038/s41419-019-2064-5

77. Nollet M, Santucci-Darmanin S, Breuil V, Al-Sahlanee R, Cros C, Topi M, et al. Autophagy in osteoblasts is involved in mineralization and bone homeostasis. *Autophagy* (2014) 10(11):1965–77. doi: 10.4161/auto.36182

78. Yang C, Tao H, Zhang H, Xia Y, Bai J, Ge G, et al. Tet2 regulates osteoclastogenesis by modulating autophagy in ovx-induced bone loss. *Autophagy* (2022), 1–13. doi: 10.1080/15548627.2022.2048432

79. Liu Y, Wang Y, Liu J, Kang R, Tang D. Interplay between mtor and Gpx4 signaling modulates autophagy-dependent ferroptotic cancer cell death. *Cancer Gene Ther* (2021) 28(1-2):55–63. doi: 10.1038/s41417-020-0182-y

frontiers | Frontiers in Endocrinology

TYPE Original Research
PUBLISHED 23 January 2023
DOI 10.3389/fendo.2023.1098702

OPEN ACCESS

EDITED BY
Michela Rossi,
Bambino Gesù Children's Hospital (IRCCS), Italy

REVIEWED BY
Xianqi Li,
Matsumoto Dental University, Japan
Bing Wu,
GE Healthcare, China
Xiaochun Wei,
Second Hospital of Shanxi Medical University, China
Wei Chen,
Southwest Hospital, China
Rongjie Bai,
Beijing Jishuitan Hospital, China
Zhengwei Huang,
Shanghai Jiao Tong University, China

*CORRESPONDENCE
Jinliang Niu
sxlscjy@163.com

SPECIALTY SECTION
This article was submitted to Bone Research, a section of the journal Frontiers in Endocrinology

RECEIVED 15 November 2022
ACCEPTED 09 January 2023
PUBLISHED 23 January 2023

CITATION
Li W, Zheng J, Xu Y, Niu W, Guo D, Cui J, Bian W, Wang X and Niu J (2023) Remodeling of the periodontal ligament and alveolar bone during axial tooth movement in mice with type 1 diabetes. *Front. Endocrinol.* 14:1098702. doi: 10.3389/fendo.2023.1098702

Remodeling of the periodontal ligament and alveolar bone during axial tooth movement in mice with type 1 diabetes

Wenjin Li[1], Jing Zheng[2], Yao Xu[3], Weiran Niu[4], Dong Guo[3], Jianing Cui[5], Wenjin Bian[5], Xiaohui Wang[2] and Jinliang Niu[6*]

[1]Department of Stomatology, 2nd Hospital, Shanxi Medical University, Taiyuan, Shanxi, China, [2]School of Basic Medicine, Shanxi Medical University, Taiyuan, Shanxi, China, [3]Stomatological Hospital of Shanxi Medical University, Taiyuan, Shanxi, China, [4]Department of Mental Health, Shanxi Medical University, Taiyuan, Shanxi, China, [5]Medical Imaging Department of Shanxi Medical University, Taiyuan, Shanxi, China, [6]Department of Radiology, 2nd Hospital, Shanxi Medical University, Taiyuan, Shanxi, China

Objectives: To observe the elongation of the axial tooth movement in the unopposed rodent molar model with type 1 diabetes mellitus and explore the pathological changes of periodontal ligament and alveolar bone, and their correlation with tooth axial movement.

Methods: The 80 C57BL/6J mice were randomly divided into the streptozotocin (STZ)-injected group (n = 50) and the control group (n = 30). Mice in the streptozotocin(STZ)-injected group were injected intraperitoneal with streptozotocin (STZ), and mice in the control group were given intraperitoneal injection of equal doses of sodium citrate buffer. Thirty mice were randomly selected from the successful models as the T1DM group. The right maxillary molar teeth of mice were extracted under anesthesia, and allowed mandibular molars to super-erupt. Mice were sacrificed at 0, 3, 6,9, and 12 days. Tooth elongation and bone mineral density (BMD) were evaluated by micro-CT analysis(0,and 12 days mice). Conventional HE staining, Masson staining and TRAP staining were used to observe the changes in periodontal tissue(0, 3, 6, 9, and 12 days mice). The expression differences of SPARC, FGF9, BMP4, NOGGIN, and type I collagen were analyzed by RT-qPCR.

Results: After 12 days of tooth extraction, our data showed significant super-eruption of mandibular mouse molars of the two groups. The amount of molar super-eruption in the T1DM group was 0.055mm($\pm$ 0.014mm), and in the control group was 0.157($\pm$ 0.017mm). The elongation of the T1DM mice was less than that of the control mice($P<0.001$). It was observed that the osteoclasts and BMD increased gradually in both groups over time. Compared with the control group, the collagen arrangement was more disordered, the number of osteoclasts was higher ($P<0.05$), and the increase of bone mineral density was lower(2.180 $\pm$ 0.007g/cm^3 vs. 2.204 $\pm$ 0.006g/cm^3, $P<0.001$) in the T1DM group. The relative expression of SPARC, FGF9, BMP4, and type I collagen in the two groups increased with the extension of tooth extraction time while NOGGIN decreased. The relative expression of all of SPARC, FGF9, BMP4, and type I collagen in the T1DM group

were significantly lower, and the expression of NOGGIN was higher than that in the control group ($P<0.05$).

Conclusion: The axial tooth movement was inhibited in type 1 diabetic mice. The result may be associated with the changes of periodontal ligament osteoclastogenic effects and alveolar bone remodeling regulated by the extracellular matrix and osteogenesis-related factors.

KEYWORDS

tooth movement, periodontal ligament, type 1 diabetes, alveolar bone remodeling, osteogenesis

1 Introduction

Tooth movement is a multi-factor process involving the motion of existing tissues and the formation of new tissues coordinated by a set of genetic events (1), commonly occurring in tooth eruption, tooth loss, adaptation to mastication, orthodontic tooth movement, etc. (2). The alveolar bone surrounding the teeth is constantly remodeled throughout life (3) and presents a high turnover rate during tooth movement, including bone resorption and bone formation. The periodontal ligament(PDL) anchors the tooth in the alveolar socket. Extrinsic and intrinsic stimuli trigger the response of periodontal ligament fibroblasts to induce periodontal tissue reorganization, which is the biological basis of tooth movement (4). The tooth movement process involves high levels of elaborate interactions between growth factors, transcription factors, and structural proteins (5). Establishing the dynamic relationship among tooth movement, alveolar bone remodeling, and periodontal ligament biological responses is of great significance for orthodontics.

At present, studies of tooth movement have focused on tissue remodeling of horizontal tooth movement caused by orthodontic force (6). The horizontal movement during orthodontic treatment is affected by the traction force of the orthodontic device, and the mechanical stress or traction generated during orthodontic tooth movement also can cause tissue damage and triggers an inflammatory response (7), which cannot reflect the intrinsic physiological mechanism of tooth movement. The study of tooth axial movement is mainly related to tooth eruption, which is defined as the axial movement of the tooth from its site of development in the alveolar bone to its functional position in the oral cavity (8). Therefore, the research on axial tooth movement is of great significance to the study of the physiological mechanism of tooth movement and tooth eruption. However, there were few empirical researches on it. The research had demonstrated that after removing the upper molars unilaterally, the lower molars would erupt continuously without an antagonist, which was used to study the axial tooth movement (9).

In addition, tooth movement is also affected by medication or systemic pathological factors. Diabetes mellitus(DM) is a group of clinical syndromes, which will result in diminished bone-mineral density and osteoporosis (10–12). The study showed that DM not only induces higher alveolar bone resorption but also enhances fibroblast inflammation and osteoclastogenic effects of periodontal ligament (13). Some results suggested that tooth movement in T2DM animals was higher than in healthy animals with adapted orthodontic appliances (14), while another study observed that the amount of orthodontic tooth movement in T2DM was not compromised (15). However, relatively few data are available for type 1 diabetes mellitus (T1DM) (16). Studies have found that children with T1DM with age younger than 11.5 years had teeth eruption acceleration, while children older than 11.5 years had delayed teeth eruption process (17). Type 1 T1DM is becoming more prevalent among young individuals worldwide who is also the main population needing orthodontic treatment. Compared with T2DM, T1DM affects bone more severely and *via* a pathophysiological mechanism dependent on a decrease in bone mineral density (BMD) (18).The cellular and molecular related to T1DM that may affect the elongation movement of teeth in the axial direction are still unclear, and it is necessary to investigate these mechanisms.

The present study was performed to visualize the process of axial tooth movement by using T1DM the model of unopposed rodent molar with type 1 diabetes mellitus, and investigate the related changes of the periodontal ligament biological responses and alveolar bone remodeling.

2 Material and methods

2.1 Animals

C57BL/6J mice(six weeks old, male, 19~25g) were purchased from the Animal Laboratory Center of Shanxi Medical University (Animal Permit NO: DW2022038) and kept in a standard lab housing with a 12 h light/dark cycle at a temperature of 22 ± 2°C and 30% - 50% humidity with diet and water ad libitum. Study protocols were approved by the Animal Ethics Committee of the Second Hospital of Shanxi Medical University.

2.2 Induction of T1DM model

Eighty mice were divided into control(n=30) and streptozotocin (STZ)-injected groups(n=50) randomly. The mice were fasted for 8h before STZ injection. Injected mice were intraperitoneally injected a

single dose of 150mg/kg STZ (Sigma S-0130) dissolved in 0.1 M citrate buffer at pH 4.2. The control group received the same volume of 0.1 M citrate buffer. 72h after the STZ injection, mice with consistent blood glucose levels ≥11.1 mmol/L for three consecutive days were regarded as successful diabetic models (19). T1DM mice were fed a diet high in fat and sugar. Plasma glucose concentration was recorded during the experimental period. The model was considered to be unsuccessful if blood glucose returned to normal or the mice died during feeding.

2.3 Induction of un-opposed molar model

The T1DM group(n=30) and the control group(n=30) were anesthetized with Ketamine (100mg/kg) and Xylazine (5mg/kg). All three right maxillary molars were extracted under anesthesia. The mice were intraperitoneally injected with buprenorphine (0.05 mg/kg) to manage pain after the operation.

2.4 Mandible morphometric analyses by microcomputerized

Mice were sacrificed using an excess of isoflurane anesthesia at 0 and 12 days after surgery. The mandibular alveolar bone was harvested, and bone specimens were scanned with a micro-CT scanner equipped with a custom software package (Micro-CTCH-8306, Scanco Medical, Basserdorf, Switzerland). Specimens were scanned at 70 kVp and 114 μA at high resolution (37 μm). The images were processed by three-dimensional reconstruction software (μCT Evaluation Program v6.0, Scanco Medical). Taking the line of the outermost tangent point above the bilateral mandibular foramen of mice as the reference line, the distance between the two parallel lines at 12 day after tooth extraction was measured from the highest point of the right mandibular first molar as the parallel line with the reference line, and the distance between the two parallel lines at 0 days after tooth extraction was subtracted as the eruption rate. Each sample was analyzed by two different investigators independently. The analysis software Mimics Medical 17.0 was used to measure bone mineral density (BMD).

2.5 Tissue processing

Mice were sacrificed using an excess of isoflurane anesthesia at 0, 3, 6, 9 and 12 days after surgery. Collected mandibles were fixed in 10% neutral formalin for 24h followed by decalcification for 30~40 days with 10% EDTA. After decalcification and paraffin embedding, the samples were cut in 4 μm sagittal sections along the long axis of the molar teeth, and the sections were stained with hematoxylin and eosin (H&E) Masson and Tartrate-resistant acid phosphatase (TRAP) staining. The results were observed under a microscope(Olympus, Tokyo, Japan). Scanscope scanning system was used to scan the stained sections, and Spectrum software was used to analyze the sections. Five high-magnification fields (×200) were randomly selected from the sections of each group of the diabetes group and the control group to count the osteoclasts. The results was analyzed by two different investigators independently.

2.6 RNA extraction and real-time quantitative PCR

Total RNA was extracted from the mandibles of three mice (per group). The expression of SPARC, FGF9, BMP4, type I collagen, and NOGGIN gene expression in the periodontal tissues were assessed by real-time quantitative PCR. RNAs underwent RT-PCR using Sprint RT Complete kit (Clontech). Real-time quantitative PCR was performed using Taqman Fast Universal PCR Master Mix (Applied Biosystems) with DLUX fluorogenic primers. Reaction conditions were as follows: 30s at 95°C (one cycle), 5s at 95°C, and 30s at 60°C (40 cycles). PCR products were continuously monitored with an ABI PRISM 7900 detection system (Applied Biosystems). Primer sequences used for real-time PCR analysis are shown in Table 1. The CT value of each group was computed and processed according to $2^{-\Delta\Delta Ct}$, and the results were plotted by the software GraphPad Prism.

2.7 Statistical analyses

SPSS27.0 statistical software was used for statistical analysis. The normality test was performed on measurement data. Quantitative data were presented as mean ± Standard Error of Mean (SEM), and the data were analyzed by Independent-Samples T-Test. Differences were considered significant at $P < 0.05$.

3 Results

3.1 T1DM animal model

A total of 46 mice were modeled, and all 30 mice in the control group survived. The body weight of mice in STZ-injected was significantly

TABLE 1 Primer sequences used for real-time PCR.

Genes	Forward Primer (5′ -3′)	Reverse Primer (5′ -3′)
BMP4	TTGATACCTGAGACCGGGAAG	ACATCTGTAGAAGTGTCGCCTC
NOGGIN	GCCAGCACTATCTACACATCC	GCGTCTCGTTCAGATCCTTCTC
Col1	CGTCGGAGCAGACGGGAGTTT	CAGAGTTTGGAACTTACTGTC
SPARC	CTGCGTGTG AAGAAGATCCA	CATGTGGGTTCTGACTGGTG
FGF9	CCAGGACTAAACGGCACCAGAA	AATAAGAACCCACCGCATGAAAG

lower than that of the control mice(19.44 ± 1.92g vs. 22.76 ± 2.08g, P = 0.016). Mice in the STZ-injected group, the blood glucose levels were significantly higher than that of control mice(16.49 ± 2.75mmol/L vs. 6.94 ± 0.83 mmol/L, $P < 0.001$). The induction of the T1 T1DM model is characterized by a significant increase in fasting blood glucose and weight loss. These characteristics indicated that the T1DM model was successfully established (Figure 1).

3.2 Eruption rate

There was a significant amount of super-eruption on the unopposed side of both groups (Figure 2). The results demonstrated that the amount of tooth movement in the control group was significantly more than that in the T1DM group at 12 day after surgery(0.055 ± 0.014mm vs. 0.157 ± 0.017mm, $P < 0.001$).

3.3 Bone mineral density of the right mandible

After 12 days of tooth extraction, the density of the right mandible increased in both groups (Figure 3A). Compared with control mice, the T1DM group showed less increase in bone mineral density (2.180 ± 0.006 g/cm^3 vs. 2.204 ± 0.0061 g/cm^3, *P<0.001*).

3.4 Histological analysis

Histological analysis in all groups showed changes in the periodontal tissue structure of mice by HE staining (Figure 4) and Masson staining (Figure 5). TRAP staining (Figure 6) showed changes in the number of osteoclasts (Figure 3B). The histological trend of the T1DM group was consistent with that of the control group. In both groups of mice, the periodontal ligament was mainly composed of fibroblasts interspersed with collagen fibers and vascular and neural elements. Three days after the extraction of the right maxillary molars, cells were arranged irregularly, the periodontal collagen fiber bundles were arranged disorderly, and the cells on the surfaces of cementum and alveolar bone gradually increased. Collagen fibers also became more compact at 9~12days. In the control group, cells in the periodontal ligament were arranged in order, and the periodontal ligament fibers were orderly arranged. Compared with the control group, collagen arrangement was disordered and the number of osteoclasts (Figure 3B) was higher in the T1DM group (At days 3,6,9, and 12, $p<0.05$). There were fewer cellular components and sparse collagen fibers per unit area of alveolar bone in the T1DM mice.

3.5 RT–qPCR analysis

The relative expression of SPARC, FGF9, BMP4, and type I collagen increased with the extension of tooth extraction time, while the relative expression of noggin decreased in the two groups. The relative expression of SPARC, FGF9, BMP4, and type I collagen in the T1DM mice were significantly lower than that in the control mice, and the relative expression of NOGGIN was higher (Figure 7) (At days 3,6,9, and 12, $p<0.05$).

4 Discussion

The axial tooth movement is the physiological mechanism of tooth eruption. The loss of antagonists results in varying degrees of axial tooth movement in the post-emergent phase of tooth eruption (20). Moreover, diabetes mellitus(DM) was a common disease which affected tooth movement. T1DM usually starts during adolescence, at a time of accelerated skeletal growth, and because the bone becomes compromised at a younger age, the adverse consequences are more severe relative to T2DM (21). In our study, the maxillary molars of mice were extracted to establish the model of the unopposed mouse molar, and we found that T1DM mice had a lower tendency of tooth super-eruption than normal mice($P<0.001$). The periodontal ligament biological responses were inhibited, and the alveolar bone remodeling was weakened in type 1 diabetic T1DM mice.

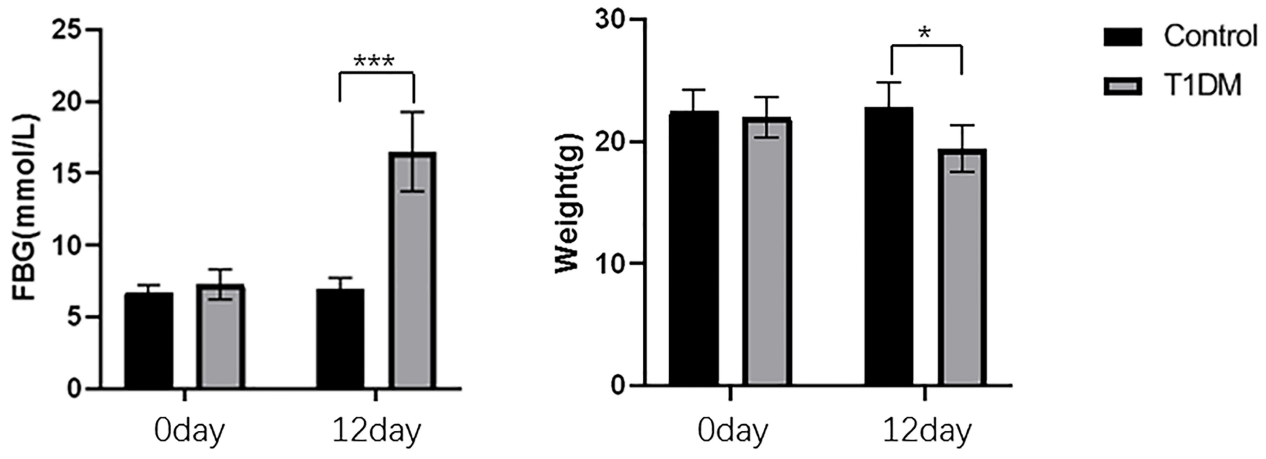

FIGURE 1
The changes of FBG and body weight in control and T1DM groups. Compared with the control group, the blood glucose was significantly increased, and the body weight was decreased in the T1DM group. *P < 0.05; ***P < 0.001

10.3389/fendo.2023.1098702

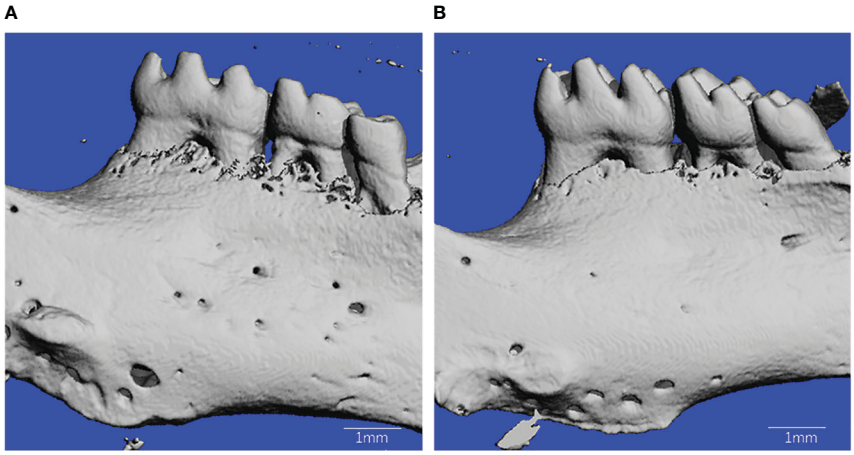

FIGURE 2
Microcomputed tomography reconstruction of mandibles in T1DM and control mice. **(A)** is from T1DM mice, and **(B)** is from control mice.

Measurements of tooth movement were made through 3D reconstructed images and showed that the mandibular molars of T1DM mice in each group elongated after tooth extraction, and the elongation of type 1 diabetic T1DM mice was smaller. To find out whether external forces such as bite force or intrinsic genetic mechanisms worked for physiological tooth movement mechanisms, researchers developed the model of the unopposed mouse molar (22–24). Previous studies had established significant axial movement of first and second mandibular mouse molars following the complete extraction of antagonists (1). A study showed that diabetes significantly reduced orthodontic tooth movement (25). However, how type 1 diabetes T1DM affects axial tooth movement and its physiological mechanisms have not been studied.

In this study, bone mineral density BMD was measured during tooth elongation in both groups. The generation and functional regulation of osteoblasts and osteoclasts lead to changes in the bone mineral density BMD (26). The results showed that BMD increased in mandible of both groups, but the increment in diabetic group was smaller than that in control group. Previous studies had suggested that the decreased BMD in patients with type 1 diabetes T1DM was due to the retardation of osteoblast activity and the inhibition of bone remodeling (27). Uncontrolled blood glucose levels and insulin deficiency are thought to be the main causes of osteopenia in T1DM. Insulin can directly affect bone cells and may lead to low bone mineral density BMD in T1DM.

Our results showed that periodontal ligament collagen fibers and osteoclasts responded actively with increasing time, whereas T1DM mice had smaller responses and more osteoclast. Changes in the periodontal tissue were similar to those observed during physiological tooth development. It has been demonstrated in previous studies that axial tooth movement induced by unloading in mice was due to osteoclastic bone resorption on the distal aspect of the alveolar socket combined with alveolar bone and cementum formation on the mesial and apical parts of the alveolar socket (28). The changes of periodontal collagen and cells reflected the response of periodontal ligament during tooth movement with orthodontic treatment (29). Nevertheless, the detailed molecular mechanisms underlying the role of individual molecules in unloading-induced bone remodeling remain unclear.

The results of qPCR showed that the relative expression of extracellular matrix gene products SPARC and type I collagen in all mice increased with the extension of tooth extraction time, however, the relative expression of them in the T1DM group were significantly lower. Type I collagen is the main structural component of the PDL,

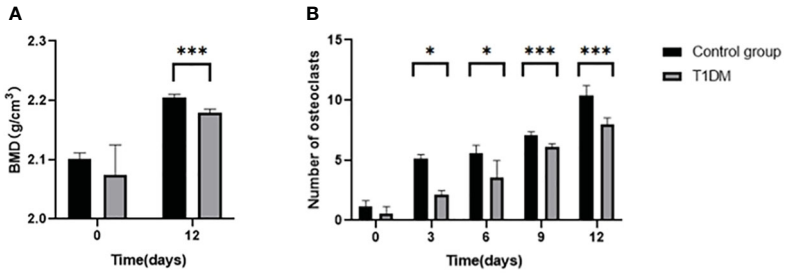

FIGURE 3
(A) is the bone mineral density(BMD) of the right mandible in control and T1DM groups on days 0 and 12 of the experiment.. After 12 days of tooth extraction, the bone mineral density in both groups increased during the axial tooth movement, and the increase of bone mineral density in the T1DM mice was significantly less than that in the control group. **(B)** is the number of right mandibular osteoclasts in both groups on days 0, 3, 6, 9, and 12 of the experiment. The number of osteoclasts in the two groups increased gradually. Compared with the control group, the number of osteoclasts in the T1DM mice was higher, which was particularly obvious at day 9 and day 12. *P < 0.05; ***P < 0.001.

10.3389/fendo.2023.1098702

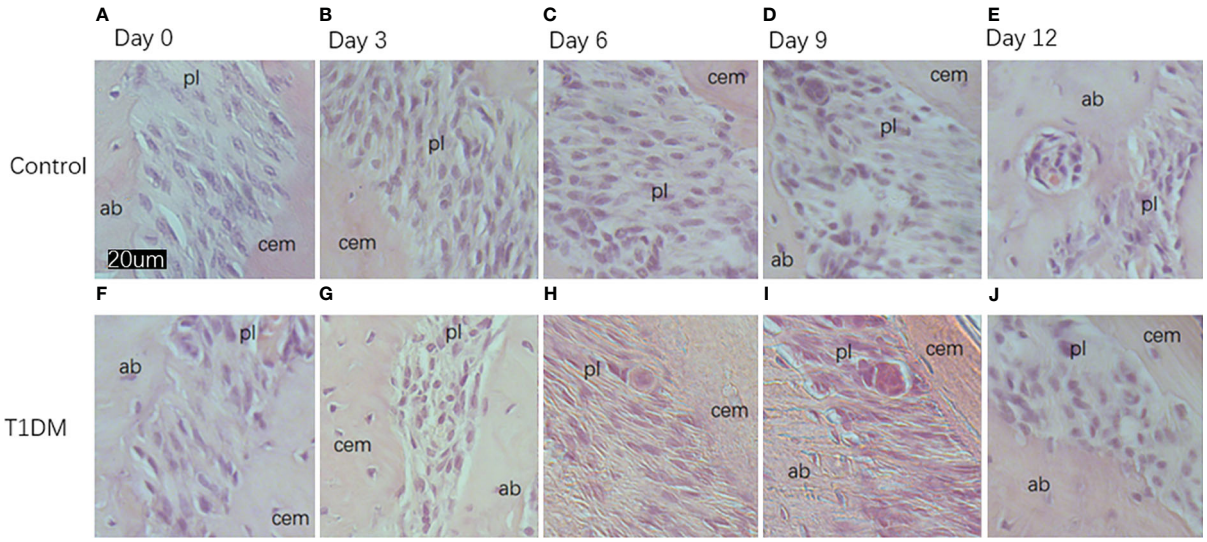

FIGURE 4
Histological appearance (HE staining)of the periodontium of mandibular molars in both groups on days 0, 3, 6, 9, and 12 of the experiment. **(A–E)** are from control mice, and **(F–J)** are from T1DM mice.3 to 12 days after the extraction of the surgery, the periodontal ligament of the corresponding mandibular molar showed irregular arrangement of cells. The cells in the periodontal ligament space, cementum, and alveolar bone surface gradually increased, and osteoclasts and osteoblasts could be observed in both groups of mice. In contrast, diabetic mice had fewer cellular components and a greater proportion of osteoclasts. cem, cementum; ab, alveolar bone; pl, periodontal ligament (×200).

which maintains periodontal health (30). In previous orthodontic experiments, the expression of type I collagen increased during tooth movement (31). SPARC (secreted protein, autogenous and rich in cysteine) could modulate osteoblasts and osteoclasts and was critical for normal bone remodeling. SPARC also could mediate the *in vitro* mineralization of type I collagen by binding firmly to type I collagen (32, 33). The regeneration capacity of PDL and bone formation were reduced in Sparc-null mice (34, 35). In previous studies, the relative expression of SPARC in the type 2 diabetes T2DM mice was higher than that in the control mice (36, 37), and this might be the result of SPARC promoting insulin resistance.

The relative expression of osteogenesis-related factors BMP4 and FGF9 were continuously increased while NOGGIN (Extracellular BMP antagonist, acts by binding BMP4 with high affinity, and as a consequence, blocks its biological effects) decreased. Compared with the control mice, the expression level of BMP4 and FGF9 was lower, while the NOGGIN expression level was higher in the T1DM mice. Bone morphogenetic proteins

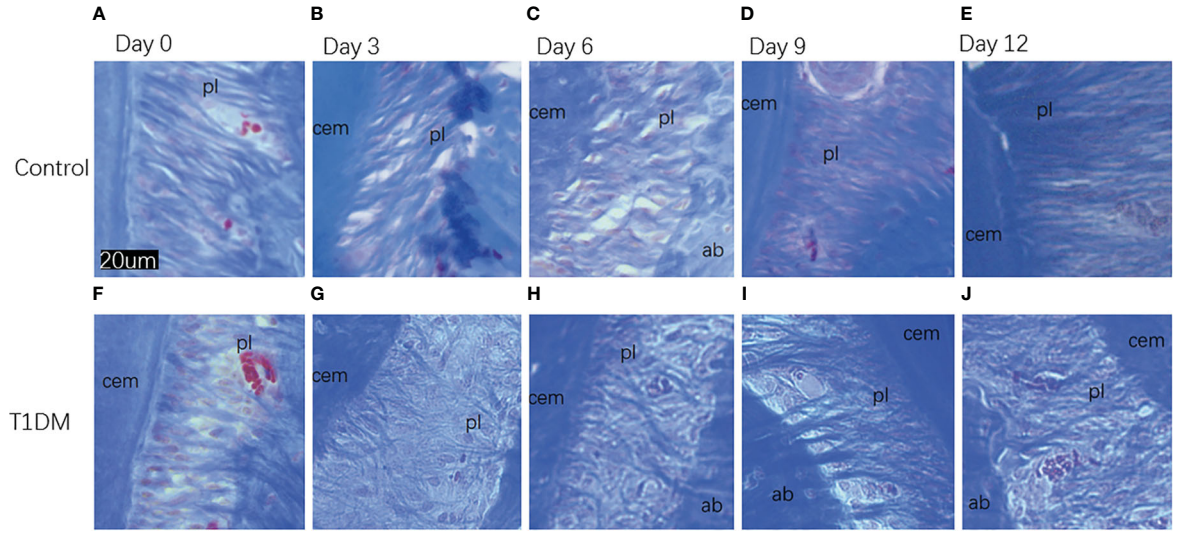

FIGURE 5
Histological appearance (Masson staining)of collagen fibers in the periodontal ligament in both groups on days 0, 3, 6, 9, and 12 of the experiment. **(A–E)** are from control mice, **(F–J)** are from T1DM mice.In both groups, at 3 and 6 days after the extraction of the right maxillary molar, the collagen fibers in the periodontal tissue of the mandibular molar began to arrange disorderly. At 9 and 12 days after the extraction, the collagen fibers became compact. Compared with the control group, the collagen fibers in the T1DM group were more sparse and disordered. cem, cementum; ab, alveolar bone; pl, periodontal ligament (×200).

10.3389/fendo.2023.1098702

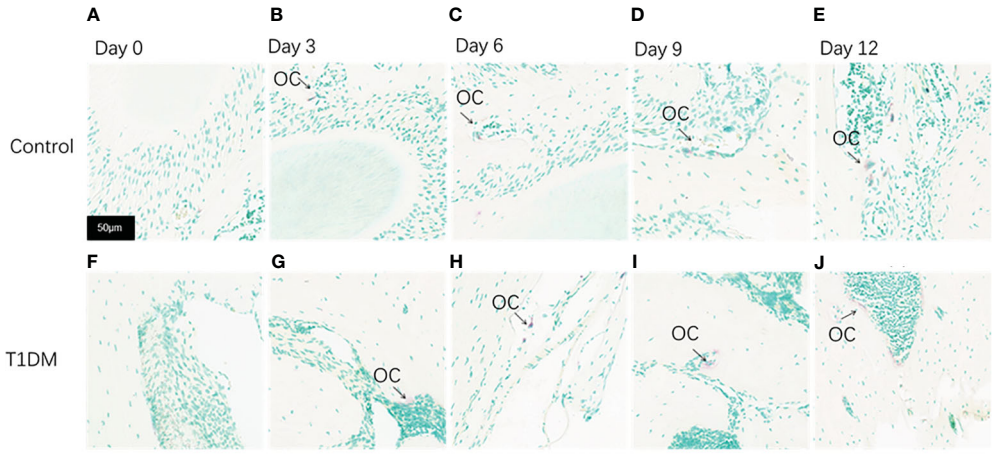

FIGURE 6
Tartrate-resistant acid phosphatase staining(TRAP staining) of the periodontium of mandibular molars in both groups on days 0, 3, 6, 9, and 12 of the experiment. **(A–E)** are from control mice, and **(F–J)** are from T1DM mice. 0 to 12 days after the extraction of the surgery, the number of osteoclasts increased gradually in both groups, however, the number of osteoclasts in the T1DM group was higher than that in the control group. The arrows indicate the site of positive osteoclast staining. OC, osteoclast (×200).

(BMPs) play a crucial role in regulating alveolar bone formation (38). BMP4 is identified as a bone-inducing factor, and injection of BMP4-transduced MSCs induced bone formation in mice (39). FGF9 has complex and essential roles in skeletal development and repair, inducing osteoblast proliferation and new bone formation (40). Some studies had demonstrated that Type 2 diabetes T2DM affected bone remodeling, leading to decreased bone regeneration. These effects could be reversed by the local application of FGF9 (41). Hyperglycemia is the main feature of T1DM. Hyperglycemia affects alveolar bone and periodontal ligament repair and reconstruction. Therefore, the unusual expression of these extracellular matrix gene products and osteogenesis-related factors in T1DM may be due to the impaired cells function and abnormal changes of bone protein matrix induced, leading to a chronic inflammatory state of bone (42).

However, this study had several limitations. First, our study only observed the expression changes of factors associated with tissue remodeling during tooth movement. The related genes should be knocked out in subsequent studies to determine whether the tissue remodeling ability is weakened or enhanced. Second, in this study, only the axial movement of mandibular teeth was observed, where the direction of gravity was opposite to the tooth elongation. The movement of maxillary teeth in the same direction of gravity should also be observed to research whether there was any influence in the next experiment. Finally, these experiments were currently limited to animal models, and further studies are needed to explore the data of axial tooth movement in type 1 diabetic T1DM patients.

In conclusion, the axial tooth movement was inhibited in type 1 diabetic T1DM mice. The mechanisms responsible for these

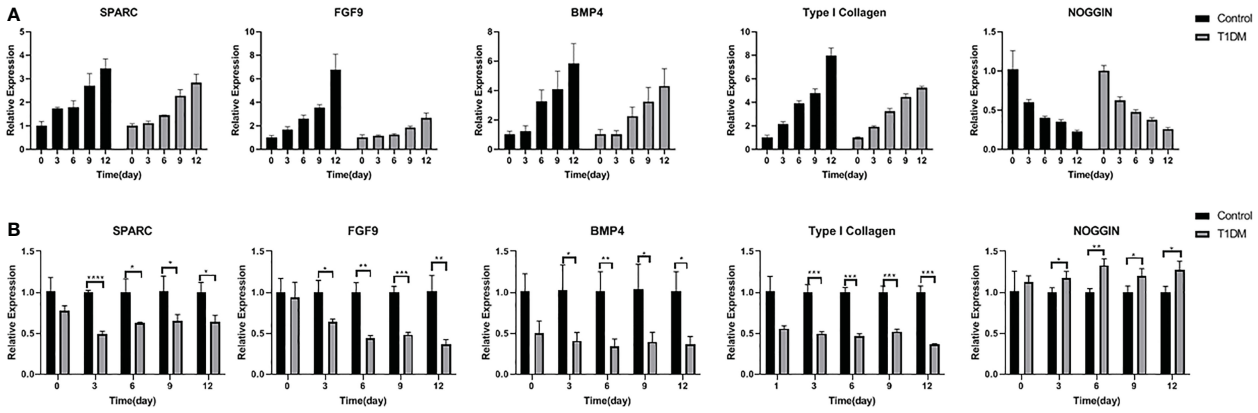

FIGURE 7
The relative expression of SPARC, FGF9, BMP4, Type I collagen and NOGGIN in control and T1DM group on days 0, 3, 6, 9, and 12 of the experiment. **(A)** The trend of relative expression levels in both groups at days o,3,6,9,12. Extraction of the opposing teeth resulted in a gradual increase in SPARC, FGF9, BMP4, and Type I collagen relative expression while the expression level of NOGGIN decreased, indicating that these osteogenesis-related factors were actively involved in bone remodeling during the axial tooth movement. **(B)** Comparison of the relative expression levels in two groups at different time points. The relative expression levels of SPARC, FGF9, BMP4, and Type I collagen were lower, and the NOGGIN expression was higher in T1DM mice compared with control mice, suggesting that osteogenesis was impaired in T1DM mice. *P < 0.05; **P < 0.01; ***P < 0.001; ****P < 0.0001.

pathological changes may be associated with enhanced periodontal ligament osteoclastogenic effects and reduced alveolar bone remodeling, based on the regulation of extracellular matrix and osteogenesis-related factors.

Data availability statement

The raw data supporting the conclusions of this article will be made available by the authors, without undue reservation.

Ethics statement

The animal study was reviewed and approved by Animal Ethics Committee of the Second Hospital of Shanxi Medical University.

Author contributions

Guarantor of integrity of entire study, JN; study concepts/study design or data acquisition or data analysis/interpretation, all authors; manuscript drafting or manuscript revision for important intellectual content, all authors; agrees to ensure any questions related to the work are appropriately resolved, all authors; literature research, JZ, YX, and WN; clinical studies, WL; experimental studies, WL and DG; statistical analysis, JZ; and manuscript editing, all authors. All authors contributed to the article and approved the submitted version.

Funding

This study was supported by the National Natural Science Fund of China (No. 82071898) and the Health Commission Fund of Shanxi Province(No. 2019042).

Conflict of interest

The authors declare that the research was conducted in the absence of any commercial or financial relationships that could be construed as a potential conflict of interest.

The reviewer XW declared a shared affiliation with the authors to the handling editor at the time of review.

Publisher's note

All claims expressed in this article are solely those of the authors and do not necessarily represent those of their affiliated organizations, or those of the publisher, the editors and the reviewers. Any product that may be evaluated in this article, or claim that may be made by its manufacturer, is not guaranteed or endorsed by the publisher.

References

1. Luan X, Ito Y, Holliday S, Walker C, Daniel J, Galang TM, et al. Extracellular matrix-mediated tissue remodeling following axial movement of teeth. *J Histochem Cytochem* (2007) 55(2):127–40. doi: 10.1369/jhc.6A7018.2006

2. Yan ZQ, Wang XK, Zhou Y, Wang ZG, Wang ZX, Jin L, et al. H-type blood vessels participate in alveolar bone remodeling during murine tooth extraction healing. *Oral Dis* (2020) 26(5):998–1009. doi: 10.1111/odi.13321

3. Shoji-Matsunaga A, Ono T, Hayashi M, Takayanagi H, Moriyama K, Nakashima T. Osteocyte regulation of orthodontic force-mediated tooth movement *via* RANKL expression. *Sci Rep* (2017) 7(1):8753. doi: 10.1038/s41598-017-09326-7

4. Brockhaus J, Craveiro RB, Azraq I, Niederau C, Schröder SK, Weiskirchen R, et al. *In vitro* compression model for orthodontic tooth movement modulates human periodontal ligament fibroblast proliferation, apoptosis and cell cycle. *Biomolecules* (2021) 11(7):932. doi: 10.3390/biom11070932

5. Shimono M, Ishikawa T, Ishikawa H, Matsuzaki H, Hashimoto S, Muramatsu T, et al. Regulatory mechanisms of periodontal regeneration. *Microsc Res Tech* (2003) 60 (5):491–502. doi: 10.1002/jemt.10290

6. Li Y, Zhan Q, Bao M, Yi J, Li Y. Biomechanical and biological responses of periodontium in orthodontic tooth movement: Up-date in a new decade. *Int J Oral Sci* (2021) 13(1):20. doi: 10.1038/s41368-021-00125-5

7. Koletsi D, Iliadi A, Papageorgiou SN, Konrad D, Eliades T. Evidence on the effect of uncontrolled diabetes mellitus on orthodontic tooth movement. A systematic review with meta-analyses in pre-clinical in- vivo research. *Arch Oral Biol* (2020) 115:104739. doi: 10.1016/j.archoralbio.2020.104739

8. Aldowsari M, Alsaif FS, Alhussain MS, AlMeshary BN, Alosaimi NS, Aldhubayb SM, et al. Prevalence of delayed eruption of permanent upper central incisors at a tertiary hospital in Riyadh, Saudi Arabia. *Children (Basel)* (2022) 9(11):1781. doi: 10.3390/children9111781

9. Walker CG, Dangaria S, Ito Y, Luan X, Diekwisch TG. Osteopontin is required for unloading-induced osteoclast recruitment and modulation of RANKL expression during tooth drift-associated bone remodeling, but not for super-eruption. *Bone* (2010) 47 (6):1020–9. doi: 10.1016/j.bone.2010.08.025

10. Li Y, Ling J, Jiang Q. Inflammasomes in alveolar bone loss. *Front Immunol* (2021) 12:691013. doi: 10.3389/fimmu.2021.691013

11. DiMeglio LA, Evans-Molina C, Oram RA. Type 1 diabetes. *Lancet* (2018) 391 (10138):2449–62. doi: 10.1016/S0140-6736(18)31320-5

12. Ferreira CL, da Rocha VC, da Silva Ursi WJ, De Marco AC, Santamaria MJr, Santamaria MP, et al. Periodontal response to orthodontic tooth movement in diabetes-induced rats with or without periodontal disease. *J Periodontol* (2018) 89(3):341–50. doi: 10.1002/JPER.17-0190

13. Zheng J, Chen S, Albiero ML, Vieira GHA, Wang J, Feng JQ, et al. Diabetes activates periodontal ligament fibroblasts *via* NF-κB in vivo. *J Dent Res* (2018) 97(5):580–8. doi: 10.1177/0022034518755697

14. Gomes MF, Goulart MDGV, Giannasi LC, Hiraoka CM, Melo GFS, Zangaro RA, et al. Effects of the photobiomodulation using different energy densities on the periodontal tissues under orthodontic force in rats with type 2 diabetes mellitus. *Braz Oral Res* (2018) 32:e61. doi: 10.1590/1807-3107bor-2018.vol32.0061

15. Plut A, Sprogar Š, Drevenšek G, Hudoklin S, Zupan J, Marc J, et al. Bone remodeling during orthodontic tooth movement in rats with type 2 diabetes. *Am J Orthod Dentofacial Orthop* (2015) 148(6):1017–25. doi: 10.1016/j.ajodo.2015.05.031

16. Chakraborty P, Mukhopadhyay P, Bhattacharjee K, Chakraborty A, Chowdhury S, Ghosh S. Periodontal disease in type 1 diabetes mellitus: Influence of pubertal stage and glycemic control. *Endocr Pract* (2021) 27(8):765–8. doi: 10.1016/j.eprac.2021.01.010

17. Mandura RA, Meligy OAE, Attar MH, Alamoudi RA. Diabetes mellitus and dental health in children: A review of literature. *Int J Clin Pediatr Dent* (2021) 14(5):719–25. doi: 10.5005/jp-journals-10005-2006

18. Napoli N, Chandran M, Pierroz DD, Abrahamsen B, Schwartz AV, Ferrari SL, et al. Mechanisms of diabetes mellitus-induced bone fragility. *Nat Rev Endocrinol* (2017) 13 (4):208–19. doi: 10.1038/nrendo.2016.153

19. Li Y, Li B, Wang B, Liu M, Zhang X, Li A, et al. Integrated pancreatic microcirculatory profiles of streptozotocin-induced and insulin-administrated type 1 diabetes mellitus. *Microcirculation* (2021) 28(5):e12691. doi: 10.1111/micc.12691

20. Dorotheou D, Bochaton-Piallat ML, Giannopoulou C, Kiliaridis S. Expression of α-smooth muscle actin in the periodontal ligament during post-emergent tooth eruption. *J Int Med Res* (2018) 46(6):2423–35. doi: 10.1177/0300060518769545

21. Cortet B, Lucas S, Legroux-Gerot I, Penel G, Chauveau C, Paccou J. Bone disorders associated with diabetes mellitus and its treatments. *Joint Bone Spine* (2019) 86(3):315–20. doi: 10.1016/j.jbspin.2018.08.002

22. Schneider BJ, Meyer J. Experimental studies on the interrelations of condylar growth and alveolar bone formation. *Angle Orthod* (1965) 35:187–99. doi: 10.1043/0003-3219(1965)035

23. Cohn SA. Disuse atrophy of the periodontium in mice following partial loss of function. *Arch Oral Biol* (1966) 11(1):95–105. doi: 10.1016/0003-9969(66)90120-8

24. Levy GG, Mailland ML. Histologic study of the effects of occlusal hypofunction following antagonist tooth extraction in the rat. *J Periodontol* (1980) 51(7):393–9. doi: 10.1902/jop.1980.51.7.393

25. Arita K, Hotokezaka H, Hashimoto M, Nakano-Tajima T, Kurohama T, Kondo T, et al. Effects of diabetes on tooth movement and root resorption after orthodontic force application in rats. *Orthod Craniofac Res* (2016) 19(2):83–92. doi: 10.1111/ocr.12117

26. Wang C, Cao L, Yang C, Fan Y. A novel method to quantify longitudinal orthodontic bone changes with *In vivo* micro-CT data. *J Healthc Eng* (2018) 2018:1651097. doi: 10.1155/2018/1651097

27. Dixit M, Liu Z, Poudel SB, Yildirim G, Zhang YZ, Mehta S, et al. Skeletal response to insulin in the naturally occurring type 1 diabetes mellitus mouse model. *JBMR Plus* (2021) 5(5):e10483. doi: 10.1002/jbm4.10483

28. Lira Dos Santos EJ, Salmon CR, Chavez MB, de Almeida AB, Tan MH, Chu EY, et al. Cementocyte alterations associated with experimentally induced cellular cementum apposition in hyp mice. *J Periodontol* (2021) 92(11):116–27. doi: 10.1002/JPER.21-0119

29. Ullrich N, Schröder A, Jantsch J, Spanier G, Proff P, Kirschneck C. The role of mechanotransduction versus hypoxia during simulated orthodontic compressive strain-an *in vitro* study of human periodontal ligament fibroblasts. *Int J Oral Sci* (2019) 11(4):33. doi: 10.1038/s41368-019-0066-x

30. Morimoto C, Takedachi M, Kawasaki K, Shimomura J, Murata M, Hirai A, et al. Hypoxia stimulates collagen hydroxylation in gingival fibroblasts and periodontal ligament cells. *J Periodontol* (2021) 92(11):1635–45. doi: 10.1002/JPER.20-0670

31. K S, Vijayaraghavan N, Krishnan V. Time-dependent variation in expression patterns of lysyl oxidase, type I collagen and tropoelastin mRNA in response to orthodontic force application. *Arch Oral Biol* (2019) 102:218–24. doi: 10.1016/j.archoralbio.2019.04.016

32. Rosset EM, Bradshaw AD. SPARC/osteonectin in mineralized tissue. *Matrix Biol* (2016) 52-54:78–87. doi: 10.1016/j.matbio.2016.02.001

33. Ribeiro N, Sousa SR, Brekken RA, Monteiro FJ. Role of SPARC in bone remodeling and cancer-related bone metastasis. *J Cell Biochem* (2014) 115(1):17–26. doi: 10.1002/jcb.24649

34. Trombetta-eSilva J, Rosset EA, Hepfer RG, Wright GJ, Baicu C, Yao H, et al. Decreased mechanical strength and collagen content in SPARC-null periodontal ligament is reversed by inhibition of transglutaminase activity. *J Bone Miner Res* (2015) 30 (10):1914–24. doi: 10.1002/jbmr.2522

35. Delany AM, Hankenson KD. Thrombospondin-2 and SPARC/osteonectin are critical regulators of bone remodeling. *J Cell Commun Signal* (2009) 3(3-4):227–38. doi: 10.1007/s12079-009-0076-0

36. Atorrasagasti C, Onorato A, Gimeno ML, Andreone L, Garcia M, Malvicini M, et al. SPARC Is required for the maintenance of glucose homeostasis and insulin secretion in mice. *Clin Sci (Lond)* (2019) 133(2):351–65. doi: 10.1042/CS20180714

37. Wu D, Li L, Yang M, Liu H, Yang G. Elevated plasma levels of SPARC in patients with newly diagnosed type 2 diabetes mellitus. *Eur J Endocrinol* (2011) 165(4):597–601. doi: 10.1530/EJE-11-0131

38. Ou M, Zhao Y, Zhang F, Huang X. Bmp2 and Bmp4 accelerate alveolar bone development. *Connect Tissue Res* (2015) 56(3):204–11. doi: 10.3109/03008207.2014.996701

39. Chen Y, Ma B, Wang X, Zha X, Sheng C, Yang P, et al. Potential functions of the BMP family in bone, obesity, and glucose metabolism. *J Diabetes Res* (2021) 2021:6707464. doi: 10.1155/2021/6707464

40. Wang L, Roth T, Abbott M, Ho L, Wattanachanya L, Nissenson RA. Osteoblast-derived FGF9 regulates skeletal homeostasis. *Bone* (2017) 98:18–25. doi: 10.1016/j.bone.2016.12.005

41. Wallner C, Schira J, Wagner JM, Schulte M, Fischer S, Hirsch T, et al. Application of VEGFA and FGF-9 enhances angiogenesis, osteogenesis and bone remodeling in type 2 diabetic long bone regeneration. *PLoS One* (2015) 10(3):e0118823. doi: 10.1371/journal.pone.0118823

42. Kheniser KG, Polanco Santos CM, Kashyap SR. The effects of diabetes therapy on bone: A clinical perspective. *J Diabetes Complications* (2018) 32(7):713–9. doi: 10.1016/j.jdiacomp.2018.04.005

frontiers | Frontiers in Endocrinology

TYPE Original Research
PUBLISHED 08 March 2023
DOI 10.3389/fendo.2023.1115834

OPEN ACCESS

EDITED BY
Michela Rossi,
Bambino Gesù Children's Hospital (IRCCS), Italy

REVIEWED BY
Shihua Gao,
Guangzhou University of Chinese Medicine, China
JunFang Xiao,
Guangzhou University of Chinese Medicine, China
Linjing Lin,
Shenzhen Hospital of Integrated Traditional Chinese and Western Medicine, China

*CORRESPONDENCE
Weidong Sun
sunweidong8239@aliyun.com

†These authors have contributed equally to this work

SPECIALTY SECTION
This article was submitted to Bone Research, a section of the journal Frontiers in Endocrinology

RECEIVED 04 December 2022
ACCEPTED 21 February 2023
PUBLISHED 08 March 2023

CITATION
Xiong B, Bai Z, Cao X, Nie D, Zhang C, Sun X, Guo Z, Wen J and Sun W (2023) Causal relationship between thyroid dysfunction and hallux valgus: A two-sample Mendelian randomization study. *Front. Endocrinol.* 14:1115834. doi: 10.3389/fendo.2023.1115834

Causal relationship between thyroid dysfunction and hallux valgus: A two-sample Mendelian randomization study

Binglang Xiong[1†], Zixing Bai[1†], Xuhan Cao[1], Duorui Nie[2], Cheng Zhang[3], Xudong Sun[1], Ziyan Guo[1], Jianmin Wen[1] and Weidong Sun[1*]

[1]Second Department of Orthopedics, Wangjing Hospital of China Academy of Chinese Medical Sciences, Beijing, China, [2]Graduate School, Hunan University of Traditional Chinese Medicine, Changsha, China, [3]Fourth Department of Orthopedics,Wangjing Hospital of China Academy of Chinese Medical Sciences, Beijing, China

Introduction: Previous observational studies have reported that thyroid dysfunction is associated with hallux valgus (HV). However, the causal effect of thyroid dysfunction on hallux valgus is still unknown. To assess whether there is a causal relationship between thyroid dysfunction and hallux valgus, we performed a two-sample Mendelian randomization (MR) study.

Methods: The data of the two-sample Mendelian randomization study were obtained from public databases. In this study, hypothyroidism, hyperthyroidism, free thyroxine (FT4), and thyrotropin (TSH) were chosen as exposures. The single nucleotide polymorphisms (SNP) of hypothyroidism and hyperthyroidism were from the genome-wide association studies (GWAS) of the IEU database, including 337,159 subjects. Data for FT4 and TSH (72,167 subjects) were extracted from the ThyroidOmics Consortium. HV was used as the outcome. The SNPs associated with HV were selected from a GWAS of 202,617 individuals in the fignngen database. The inverse variance weighted (IVW) method was used as the primary analysis. Four complementary methods were applied, including MR-presso, MR-Egger, and weighted median. In addition, Cochran's *Q* test, MR-presso, MR-Egger regression, and the leave-one-out test were used as sensitivity analysis, and the MR-pleiotropy test was performed to examine pleiotropy.

Results: According to the results of IVW, we found that there was a causal relationship between hypothyroidism and HV, and hypothyroidism increased the incidence of HV (OR = 2.838 (95% CI: 1.116–7.213); p = 0.028). There were no significant causal effects of hyperthyroidism, FT4, and TSH on HV (p > 0.05). Sensitivity analyses showed that the results were robust and reliable, and no horizontal pleiotropy was detected.

Conclusions: Our findings provided genetic support that hypothyroidism might increase the risk of HV. It will predict the occurrence of HV in patients with hypothyroidism and provide suggestions for early prevention and intervention.

KEYWORDS

thyroid, hypothyroidism, hallux valgus, causality, Mendelian randomization analysis

Introduction

Hallux valgus (HV) is one of the most common forefoot deformities (1), which is mainly characterized by the progressive aggravation of lateral hallux deviation and medial deviation of the first metatarsal, often leading to severe foot pain and walking dysfunction (2) and thus reducing the quality of life of patients (3). According to studies, women are more likely than men to develop HV, which affects 23% of individuals between the ages of 18 and 65 and 35.7% of adults over the age of 65 (2). However, the etiology of HV is currently unclear (4). Genetic factors, improper shoe habits, inflammatory joint disease, and neuromuscular disease can all contribute to the occurrence of this disease (5, 6). There are many treatments for HV, although etiology-specific therapies are still lacking. At present, there are hundreds of surgical procedures reported in the literature to correct HV deformity, but their postoperative complication rates range from 10% to 50% (7, 8). More than 25% to 33% of patients are dissatisfied with the outcomes of surgery (9), and the high expense of surgery also adds to the burden on the medical system (10). Therefore, it is of high clinical value and economic significance to actively explore the etiology of HV and find a treatment for the etiology.

Previous large-scale observational studies have found a significant correlation between hypothyroidism and HV (11), but no research has yet confirmed whether there is a causal relationship between the two disorders. Numerous earlier investigations have demonstrated a connection between thyroid dysfunction and various orthopedic diseases. For instance, Tagoe et al. (12) revealed that patients with higher antithyroid peroxidase antibody (TPOAb) were more likely to develop chondrocalcification. Cell research confirms that abnormal thyroid hormone signaling raises the risk of osteoporosis, osteoarthritis, and other degenerative orthopedic illnesses (13, 14). Other studies have demonstrated that thyroid hormones can affect the function of osteoblasts and osteoclasts (15). However, hallux valgus is a common orthopedic disease, and whether thyroid disease affects it has not been explored.

Based on previous studies, we hypothesize that there may be a causal relationship between thyroid dysfunction and the risk of HV, and in this study, two-sample Mendelian randomization (MR) analysis was used to verify this. MR is an epidemiological statistical method that uses genetic variation as an instrumental variable (IV) to infer causal relationships between exposures and outcomes (16). Because genetic variation follows Mendel's second law and is randomly assigned when fertilized eggs are formed, MR can reduce the interference of confounding factors on the results compared with previous studies and achieve the same effect as randomized controlled trials (17). MR also overcomes reverse causation because genetic variation is not affected by disease status (18). In this study, we considered hypothyroidism, hyperthyroidism, free thyroxine (FT4), and thyrotropin (TSH) as exposure and HV as outcome. This is the first study on the causal relationship between thyroid dysfunction and HV, with the purpose of further studying the etiology of HV and providing new ideas for the clinical treatment of HV.

Materials and methods

Study design and data sources

We aimed to investigate the causal relationship between thyroid dysfunction and the risk of HV. Because all of the data in this study were obtained from public databases, no consent was required from the participants. We reported our study according to the STROBE-MR statement (19). The key assumptions of the MR study can be seen in Figure 1.

In this study, hypothyroidism (increased TSH), hyperthyroidism (decreased TSH), FT4, and TSH were chosen as exposures. The single nucleotide polymorphisms (SNP) of hypothyroidism and hyperthyroidism were from the genome-wide association studies (GWAS) of the IEU database (https://gwas.mrcieu.ac.uk/), including 337,159 subjects and 10,894,596 SNPs. The study included 16,376 hypothyroidism samples and 320,783 control samples. There were also 2,547 hyperthyroidism cases and 334,612 ncases. The GWAS data of FT4 and TSH are all from The ThyroidOmics Consortium database (https://transfer.sysepi.medizin.uni-greifswald.de/thyroidomics/datasets/), containing 72,167 samples (Table 1).

HV was selected as the outcome, and its GWAS data were obtained from the FinnGen database (https://www.finngen.fi/en), which included 20,2617 samples (12,055 cases, 190,562 ncases) and 16,383,115 SNPs. All participants were of European ancestry.

Genetic IV selection

We selected effective instrumental variables (IV) based on three assumptions (Figure 1). First, we set that each IV was significantly

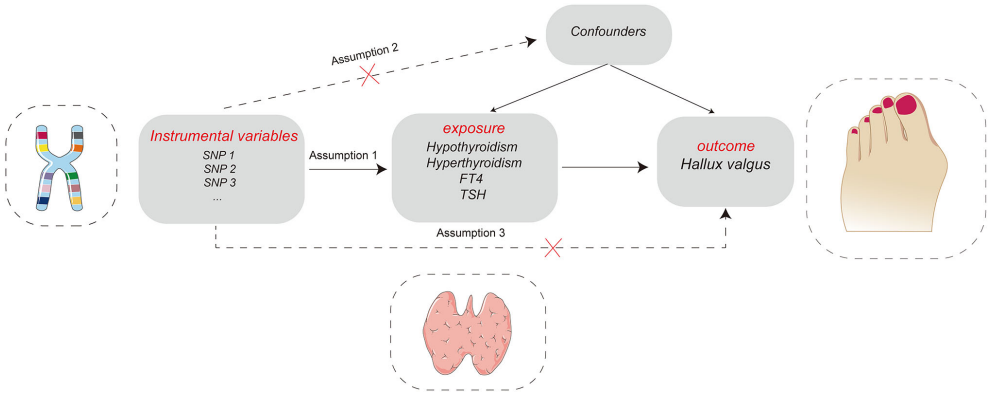

FIGURE 1
Key assumptions of the Mendelian randomization study: Assumption 1: instrumental variables should be robustly associated with exposure. Assumption 2: instrumental variables should not be associated with any confounders. Assumption 3: instrumental variables must not be associated with hallux valgus except through exposure.

correlated with exposure ($p< 5 \times 10^{-8}$ means that the instrumental variable is strongly correlated with exposure). To remove the linkage disequilibrium between each SNP, we set the distance to 10,000 KB and the LD r^2 to< 0.001 (20). To remove the possible horizontal pleiotropy of IV, use the Phenoscanner (http://www.phenoscanner.medschl.cam.ac.uk/) to search for phenotypes that may be affected by each SNP and remove the SNPs related to HV-associated phenotypes (21). SNPs for exposure and outcome should be harmonised, and palindromic and incompatible alleles should be removed (22). Finally, calculate the F value of each SNP ($F = \beta^2_{exposure}/SE^2_{exposure}$), and the SNPs with an F value<10 should be removed (23) (Figure 2).

Statistical analyses

All two-sample MR data analyses in this study were based on the TwoSampleMR package in the R software (version 4.5.0).

We used inverse variance weighting (IVW) as the primary method to evaluate the causal relationship between thyroid dysfunction and the risk of HV (24). IVW assumes that all selected IV are valid, so it has the highest statistical power and can provide the most accurate results (18). In addition, MR-Egger (25) and weighted median (26) were selected as supplementary methods. If all included SNPs match the effective IV assumption, then IVW can be considered the most reliable result (27). All results are expressed as OR values and 95% confidence intervals, with $p<$ 0.05 representing statistical significance.

Sensitivity analysis

Cochrane's Q was used as a heterogeneity test; $p< 0.05$ represents the existence of heterogeneity (28). MR-Egger regression was used to detect horizontal pleiotropy. The intercept value of MR-Egger regression represents the strength of horizontal pleiotropy, and a p-value of > 0.05 means that there is no horizontal pleiotropy (29). MR-PRESSO was used to detect SNPs that may lead to pleiotropic effects, remove outlier SNPs, and then perform MR analysis to compare whether the results have changed before and after correction (30). The leave-one-out test was used to detect the robustness of the results. This method gradually eliminated a single SNP and performed MR analysis on the remaining SNPs to detect whether the single SNP had a significant impact on the results.

Results

After a series of quality evaluations, the number of SNPs selected as effective IV in hypothyroidism, hyperthyroidism, FT4, and TSH was 70, 4, 14, and 36, respectively. In the Supplementary Material, information on SNPs as IV was provided (Supplementary

TABLE 1 Sources of GWAS data for instrumental variables.

Exposure	Outcome	Consortium	Population	Sample size
Hypothyroidism	HV	IEU	European	337,159
Hyperthyroidism	HV	IEU	European	337,159
FT4	HV	The ThyroidOmics Consortium	European	72,167
TSH	HV	The ThyroidOmics Consortium	European	72,167

FT4, free thyroxine; TSH, thyrotropin; HV, hallux valgus.

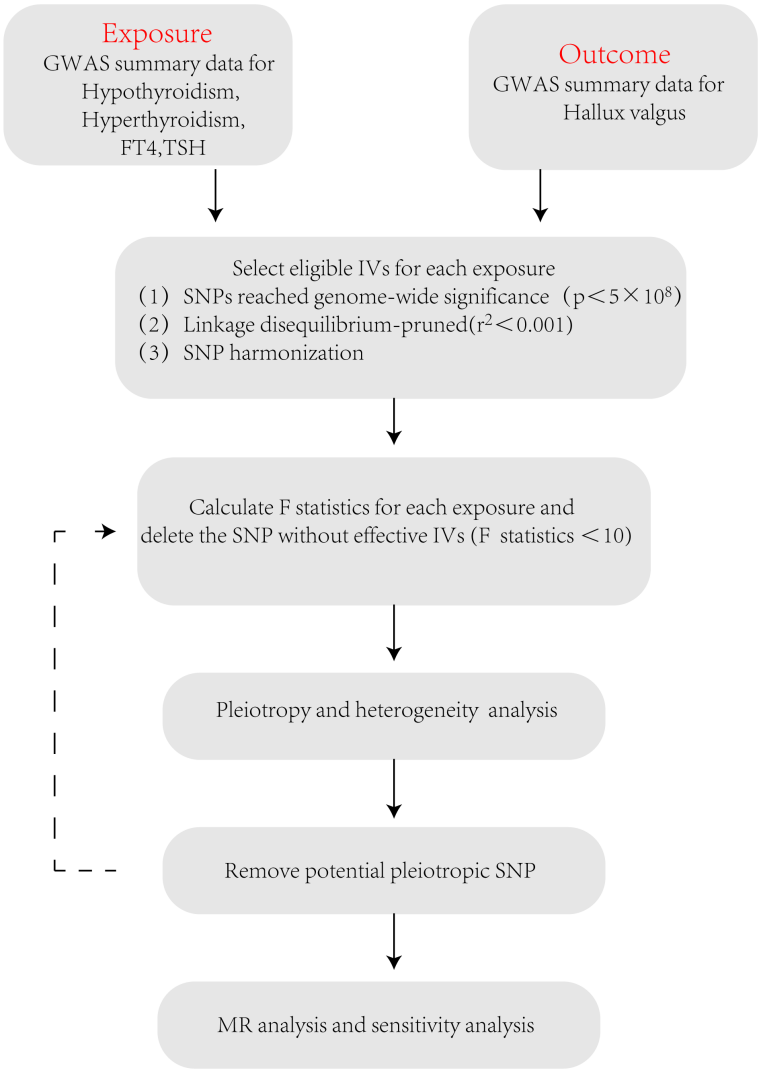

FIGURE 2
Flowchart of MR analysis in this study.

Tables S1–S4). The *F* values of all SNPs used as IV are greater than 10 (Supplementary Tables S1–S4), indicating that the included IV perform effectively.

Two-sample MR analysis for evaluating causal effects of FT4, TSH, hyperthyroidism, and hypothyroidism on HV

IVW, MR-Egger, and weighted median methods were used to assess whether there is a causal relationship between hypothyroidism, hyperthyroidism, FT4, TSH, and the risk of HV. According to IVW results, we found that there is a positive causal relationship between hypothyroidism and HV; hypothyroidism can increase the risk of HV (OR = 2.838, 95% CI: 1.116–7.213); p = 0.028) (Table 2; Figure 3), and there is no statistical difference in MR-Egger and weighted median (Table 2; Figure 3). At the same time, these three methods showed no statistical significance in the assessment of the causal relationship between hyperthyroidism, FT4, TSH, and the risk of HV (Table 2; Figure 3).

Heterogeneity, pleiotropy, and sensitivity analysis

All the results of this part are presented in Table 3. We found no heterogeneity when hyperthyroidism (p = 0.131) and FT4 (p = 0.132) were used as exposure. However, when hypothyroidism (p = 0.001) and TSH (p = 0.0004) were considered exposures, we discovered heterogeneity. The sources of these heterogeneities may be due to differences in the source of SNP data, experimental conditions, detection methods, and included populations. When heterogeneity was present, the random-effects model in IVW was

TABLE 2 MR estimates from different methods of assessing the causal effect of thyroid dysfunction on HV.

Exposure	MR methods	nSNP	Beta	OR (95% cl)	*p*-value
Hypothyroidism	IVW	70	1.043	2.838 (1.116, 7.213)	0.028
	MR-Egger	70	0.549	1.732 (0.230, 13.004)	0.594
	Weighted median	70	0.215	1.241 (0.369, 4.169)	0.727
Hyperthyroidism	IVW	4	−0.701	0.496 (1.733e−05, 1.419e+4)	0.893
	MR-Egger	4	−23.574	5.774e−11 (1.014e−44, 3.286e+23)	0.612
	Weighted median	4	−4.459	0.012 (7.848e−07, 1.704e+2)	0.361
FT4	IVW	12	−0.003	0.996 (0.863, 1.149)	0.961
	MR-Egger	12	−0.018	0.981 (0.700, 1.376)	0.917
	Weighted median	12	0.003	1.003 (0.847, 1.188)	0.969
TSH	IVW	36	−0.035	0.965 (0.862,1.079)	0.535
	MR-Egger	36	0.219	1.246 (0.949,1.634)	0.121
	Weighted median	36	−0.002	0.998 (0.876,1.138)	0.982

FT4, free thyroxine; TSH, thyrotropin; HV, Hallux valgus; SNP, single nucleotide polymorphism; MR, Mendelian randomization; IVW, inverse variance weighting.

chosen (30). MR-Egger regression showed that there was no horizontal pleiotropy for the SNPs of all exposures (Table 3). Neither MR-presso found outliers, and the results were consistent with IVW results (Table 3). the leave-one-out test further confirms that the results are stable, as shown in Figure 4. Funnel plots can be seen in Supplementary Figure S1, and the forest plots in MR analysis are shown in Supplementary Figure S2. Therefore, we considered the results of IVW to be reliable.

Discussion

In our two-sample MR study, we found a positive causal relationship between hypothyroidism and HV, with hypothyroidism associated with an increased risk of HV. However, there is no obvious causal relationship between hyperthyroidism, FT4, TSH, and HV. Our findings support the results of a previous observational study. Sterling et al. (11) investigated the prevalence of thyroid disease in 350 patients

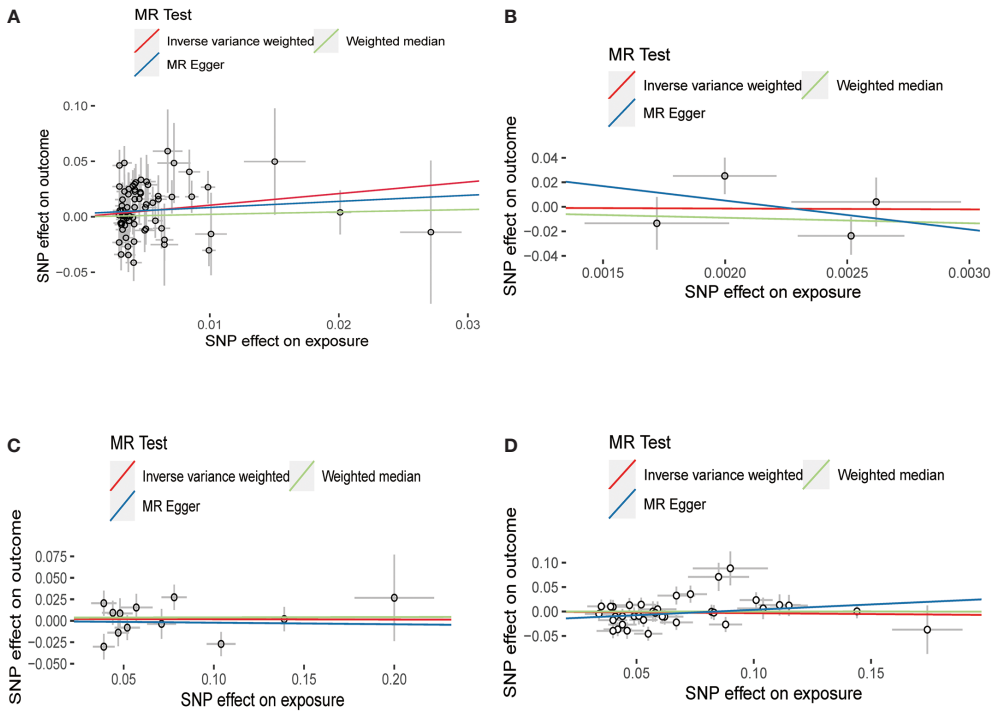

FIGURE 3
Scatter plots for Mendelian randomization (MR) analyses of the causal relationship between thyroid dysfunction and hallux valgus. **(A)** Hypothyroidism-HV. **(B)** Hyperthyroidism-HV. **(C)** FT4-HV. **(D)** TSH-HV.

10.3389/fendo.2023.1115834

TABLE 3 Sensitivity analysis of thyroid dysfunction causally linked to HV.

Exposure	Outcome	Pleiotropy		Heterogeneity		Outlier examination by MR-PRESSO	
		Horizontal pleiotropy (Egger intercept)	Horizontal pleiotropy (*p*-value)	Heterogeneity (*Q*)	Heterogeneity (*p*-value)	Before correction (*p*-value)	After correction (*p*-value)
Hypothyroidism	HV	0.002	0.589	109.245	0.001	0.032	NA
Hyperthyroidism	HV	0.052	0.618	5.648	0.130	0.902	NA
FT4	HV	0.001	0.925	16.229	0.132	0.962	NA
TSH	HV	−0.018	0.052	69.531	0.0004	0.539	NA

FT4, free thyroxine; TSH, thyrotropin; HV, hallux valgus; MR, Mendelian randomization.

with forefoot deformity who visited the doctor for the first time and found that the prevalence of hypothyroidism was the highest among patients (19.1%) and that patients with hallux valgus were more likely to have thyroid disease (61.5%). Subsequently, the researchers analyzed a national public database of 905,924 patients with forefoot deformities and found that 321,656 (35.5%) patients were diagnosed with thyroid disease. Finally, it was concluded that forefoot deformities, especially HV, were significantly associated with thyroid dysfunction (11). A limitation of this study is that it did not examine the causal relationship between thyroid dysfunction and hallux valgus, which our findings provide support for. Our findings provide a new perspective on the etiology of hallux valgus, which is that hypothyroidism may contribute to the development of HV.

A large number of experimental studies have confirmed that bones are sensitive to thyroid hormones, and the biological role of thyroid hormones in bone tissue and cartilage has also attracted more and more attention (13). However, the specific biological mechanism behind the positive causal relationship between hypothyroidism and HV remains unclear. Previous literature holds that the thyroid hormone is an important regulator of bone metabolism and is crucial for bone remodeling; any deficiency or excess may lead to bone metabolism disorder (31). Hyperthyroidism and TSH levels lower than normal can accelerate bone metabolism and lead to accelerated bone loss (32, 33). In contrast, histomorphological data from hypothyroid patients showed decreased bone turnover and increased bone calcification

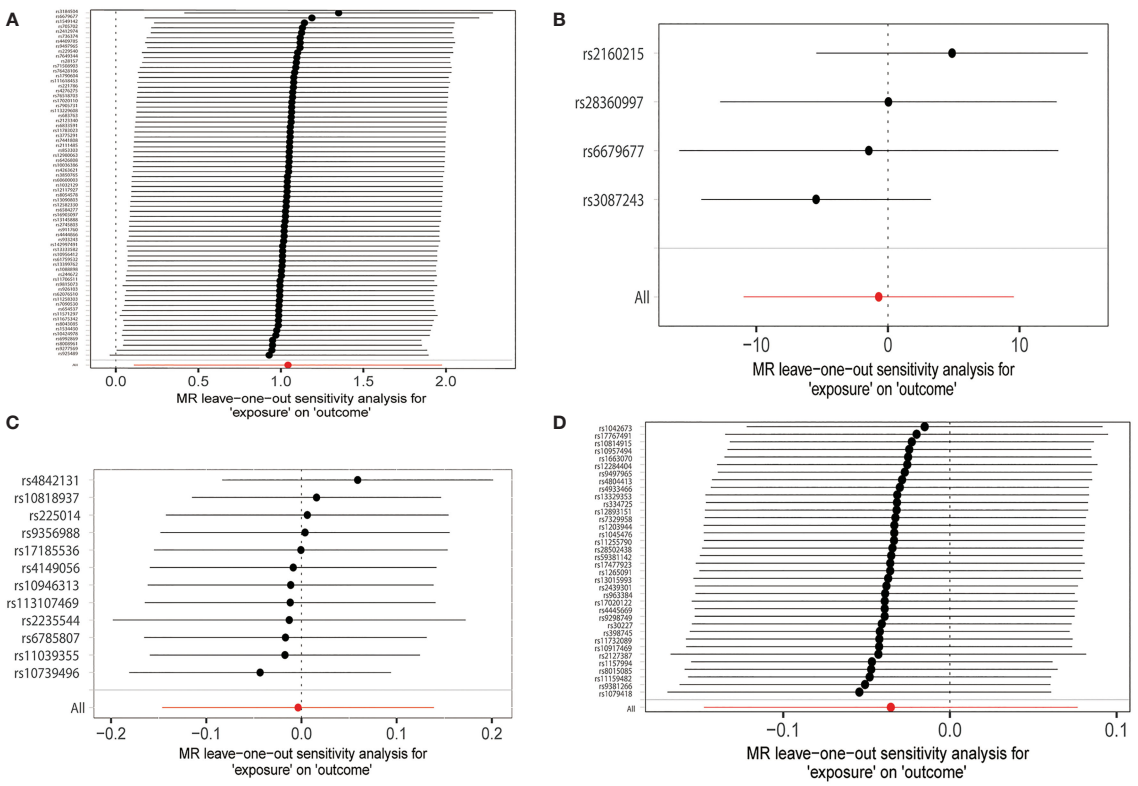

FIGURE 4
MR leave-one-out sensitivity analyses of the causal relationship between thyroid dysfunction and hallux valgus. **(A)** Hypothyroidism-HV. **(B)** Hyperthyroidism-HV. **(C)** FT4-HV. **(D)** TSH-HV.

(34). The study by Robinson et al. (35) found that there may be a specific cell population in the soft tissue surrounding HV, and cell experiments proved that when stimulated by fibroblast growth factor (FGF), it would lead to increased osteogenesis and the formation of HV. From this, we can speculate that patients with hypothyroidism may suffer from HV due to regionally impaired bone metabolism. Sclerostin, an osteocyte-derived protein encoded by the SOST gene, acts as an inhibitor of bone formation by stimulating the apoptosis of osteoblasts (36). Studies have shown that the content of sclerostin in the blood circulation of patients with hyperthyroidism is significantly higher than that of patients with hypothyroidism, and the level of sclerostin is positively correlated with FT4 and negatively correlated with TSH (37). This provides further evidence that hypothyroid patients are more likely to exhibit osteogenic dominance.

Some studies have studied the distribution of thyroid hormone receptors in human bone tissue. They found that at sites of endochondral ossification in osteophytes, TRalpha1, TRalpha2 variants, TRbeta1, and TRbeta2 mRNA were widely distributed in undifferentiated, proliferating, mature, and hypertrophic chondrocytes. Most osteoblasts (> 90%) express TRalpha-1 mRNA at regions of bone remodeling (38). A part of the concurrent clinical symptoms of HV is the formation of osteophytes, and studies have shown that there is a significant correlation between the cartilage degeneration of the first metatarsophalangeal joint and the severity of hallux valgus (39). Therefore, we can speculate that hypothyroidism may mediate cartilage degeneration leading to hallux valgus.

Other studies have found that the synovium of patients with rheumatoid arthritis (RA) and osteoarthritis (OA) contains a network of thyroid hormones. Thyroid hormones are strongly biodegraded in the synovium, and synoviocytes play an important role in the activation and degradation of thyroid hormones (40). HV is frequently present alongside synovitis, which is strongly connected with pain in this condition (41, 42). This leads us to hypothesize that a series of pathological changes caused by the action of thyroid hormone on the synovium may also contribute to the development of hallux valgus. However, the above speculations on the mechanism are all based on existing research results. No studies have investigated the mechanism of thyroid hormones on HV, which may be the subject of our upcoming study.

Most of the previous knowledge about the etiology of HV is that abnormalities in anatomy or biomechanics lead to the occurrence of the disease (43). No studies have investigated endocrine disorders as an etiology of HV. The surgical approaches for treating HV are varied since there are numerous pathologic variables, and the choice of surgical method is often based on the preference of the surgeon (5). However, the treatment satisfaction of the operation is poor (9). No consensus has been reached about the gold standard of HV treatment, despite the fact that there are several studies comparing the effectiveness of various surgical techniques (44, 45). However, there are still a large number of patients waiting for treatment every year. A 1994 study estimated that there are approximately 209,000 HV operations in the USA each year (46). Therefore, it is particularly important to actively explore other possible causes and establish a standardized treatment system. Our research suggests that hypothyroidism may be one of the causes of HV, and people with hypothyroidism are 2.838 times more likely to develop HV than normal people. Based on the results of this study, it may provide new ideas for the treatment of HV and provide a theoretical basis for the development of drug therapy for HV in the future. Early treatment of hypothyroid patients may reduce the incidence of hallux valgus and improve the quality of life of patients. Thyroid function screening and timely intervention in the HV patient population may slow the progression of HV and avoid the eventual development of surgery. In the USA, per HV surgery costs about $18,332 (10). Numerous surgical expenditures can be avoided if the amount of operations is decreased. Therefore, our findings have important implications for public health.

There are some advantages to our study. First of all, compared with observational studies, we use MR studies for causal inference and select genetic variation as IV, which can avoid the interference of other confounding factors and reverse causality. Second, all samples were drawn from European populations, and our results are less susceptible to differences in demographics. Most importantly, we demonstrate for the first time a causal relationship between hypothyroidism and HV, which may provide new strategies for the treatment of HV.

There are also some deficiencies in this study. First, thyroid hormones include multiple subtypes, such as T3 and T4, but due to research limitations, we cannot obtain the SNP data of the remaining subtypes. We were not able to explore other thyroid hormone subtypes as exposures for causal effects on HV. Second, FT4 and TSH are often used as indicators for the diagnosis of hypothyroidism, but they have not shown a causal relationship with hallux valgus. This may be caused by a relatively insufficient sample size of FT4 and TSH. Third, the participants we included were all from European populations, so it is not clear whether our findings are applicable to other populations. In addition, some of the methods we used in this study did not produce the same results as IVW, but all of the SNPs included in our study met the assumption of effective IV, and the MR-presso results were consistent with IVW, so our results are still reliable.

Conclusion

We used the two-sample MR to study the causal relationship between thyroid function and HV and proved that there is a positive causal relationship between hypothyroidism and HV. Hypothyroidism could increase the risk of HV. It will predict the occurrence of HV in patients with hypothyroidism and provide suggestions for early prevention and intervention. However, the results of this study need to be further confirmed by basic experiments.

Data availability statement

The original contributions presented in the study are included in the article/Supplementary Material. Further inquiries can be directed to the corresponding author.

Ethics statement

Ethical review and approval was not required for the study on human participants in accordance with the local legislation and institutional requirements. Written informed consent for participation was not required for this study in accordance with the national legislation and the institutional requirements.

Author contributions

BX: research design and paper writing. ZB, XC, and DN: collection and organization of data. CZ, XS, and ZG: analysis and visualization of results. JW and WS: research quality assessment. All authors contributed to the article and approved the submitted version.

Funding

This research was supported by the Beijing Municipal Science and Technology Project (Z191100006619024) and the Beijing Municipal Natural Science Foundation of China (7172244).

Conflict of interest

The authors declare that the research was conducted in the absence of any commercial or financial relationships that could be construed as a potential conflict of interest.

Publisher's note

All claims expressed in this article are solely those of the authors and do not necessarily represent those of their affiliated organizations, or those of the publisher, the editors and the reviewers. Any product that may be evaluated in this article, or claim that may be made by its manufacturer, is not guaranteed or endorsed by the publisher.

Supplementary material

The Supplementary Material for this article can be found online at: https://www.frontiersin.org/articles/10.3389/fendo.2023.1115834/full#supplementary-material

References

1. Ota T, Nagura T, Kokubo T, Kitashiro M, Ogihara N, Takeshima K, et al. Etiological factors in hallux valgus, a three-dimensional analysis of the first metatarsal. *J Foot Ankle Res* (2017) 10:43. doi: 10.1186/s13047-017-0226-1

2. Nix S, Smith M, Vicenzino B. Prevalence of hallux valgus in the general population: a systematic review and meta-analysis. *J foot ankle Res* (2010) 3:21. doi: 10.1186/1757-1146-3-21

3. Menz HB, Fotoohabadi MR, Wee E, Spink MJ. Validity of self-assessment of hallux valgus using the Manchester scale. *BMC musculoskelet Disord* (2010) 11:215. doi: 10.1186/1471-2474-11-215

4. Easley ME, Trnka HJ. Current concepts review: hallux valgus part 1: pathomechanics, clinical assessment, and nonoperative management. *Foot ankle Int* (2007) 28(5):654–9. doi: 10.3113/FAI.2007.0654

5. Smyth NA, Aiyer AA. Introduction: Why are there so many different surgeries for hallux valgus? *Foot ankle Clinics* (2018) 23(2):171–82. doi: 10.1016/j.fcl.2018.01.001

6. Piqué-Vidal C, Maled-García I, Arabi-Moreno J, Vila J. Radiographic angles in hallux valgus: differences between measurements made manually and with a computerized program. *Foot ankle Int* (2006) 27(3):175–80. doi: 10.1177/107110070602700304

7. Monteagudo M, Martínez-de-Albornoz P. Management of complications after hallux valgus reconstruction. *Foot ankle clinics* (2020) 25(1):151–67. doi: 10.1016/j.fcl.2019.10.011

8. Raikin SM, Miller AG, Daniel J. Recurrence of hallux valgus: a review. *Foot ankle clinics* (2014) 19(2):259–74. doi: 10.1016/j.fcl.2014.02.008

9. Ferrari J, Higgins JP, Williams RL. Interventions for treating hallux valgus (abductovalgus) and bunions. *Cochrane Database syst Rev* (2000) 2):CD000964. doi: 10.1002/14651858.CD000964.pub2

10. Willey JC, Reuter LS, Belatti DA, Phisitkul P, Amendola N. Availability of consumer prices for bunion surgery. *Foot ankle Int* (2014) 35(12):1309–15. doi: 10.1177/1071100714549045

11. Tran SK, Carr JB, Hall MJ, Park JS, Cooper MT. Incidence of thyroid disease in patients with forefoot deformity. *Foot ankle Surg* (2020) 26(4):445–8. doi: 10.1016/j.fas.2019.05.014

12. Tagoe CE, Wang W, Wang S, Barbour KE. Association of anti-thyroid antibodies with radiographic knee osteoarthritis and chondrocalcinosis: a NHANES III study. *Ther Adv musculoskelet dis* (2021) 13:1759720x211035199. doi: 10.1177/1759720X211035199

13. Bassett JH, Williams GR. Role of thyroid hormones in skeletal development and bone maintenance. *Endocr Rev* (2016) 37(2):135–87. doi: 10.1210/er.2015-1106

14. Nehls V. [Osteoarthropathies and myopathies associated with disorders of the thyroid endocrine system]. *Deutsche medizinische Wochenschrift* (2018) 143(16):1174–80. doi: 10.1055/s-0043-121381

15. Williams GR. Thyroid hormone actions in cartilage and bone. *Eur Thyroid J* (2013) 2(1):3–13. doi: 10.1159/000345548

16. Davey Smith G, Hemani G. Mendelian randomization: genetic anchors for causal inference in epidemiological studies. *Hum Mol Genet* (2014) 23(R1):R89–98. doi: 10.1093/hmg/ddu328

17. Davies NM, Holmes MV, Davey Smith G. Reading mendelian randomisation studies: a guide, glossary, and checklist for clinicians. *BMJ* (2018) 362:k601. doi: 10.1136/bmj.k601

18. Burgess S, Davey Smith G, Davies NM, Dudbridge F, Gill D, Glymour MM, et al. Guidelines for performing mendelian randomization investigations. *Wellcome Open Res* (2019) 4:186. doi: 10.12688/wellcomeopenres.15555.2

19. Skrivankova VW, Richmond RC, Woolf BAR, Yarmolinsky J, Davies NM, Swanson SA, et al. Strengthening the reporting of observational studies in epidemiology using mendelian randomization: The STROBE-MR statement. *Jama* (2021) 326 (16):1614–21. doi: 10.1001/jama.2021.18236

20. Shen Y, Li F, Cao L, Wang Y, Xiao J, Zhou X, et al. Hip osteoarthritis and the risk of lacunar stroke: A two-sample mendelian randomization study. *Genes* (2022) 13 (9):1584 doi: 10.3390/genes13091584

21. Staley JR, Blackshaw J, Kamat MA, Ellis S, Surendran P, Sun BB, et al. PhenoScanner: a database of human genotype-phenotype associations. *Bioinformatics* (2016) 32(20):3207–9. doi: 10.1093/bioinformatics/btw373

22. Emdin CA, Khera AV, Kathiresan S. Mendelian randomization. *Jama* (2017) 318(19):1925–6. doi: 10.1001/jama.2017.17219

23. Burgess S, Thompson SG. Avoiding bias from weak instruments in mendelian randomization studies. *Int J Epidemiol* (2011) 40(3):755–64. doi: 10.1093/ije/dyr036

24. Lawlor DA, Harbord RM, Sterne JA, Timpson N, Davey Smith G. Mendelian randomization: using genes as instruments for making causal inferences in epidemiology. *Stat Med* (2008) 27(8):1133–63. doi: 10.1002/sim.3034

25. Bowden J, Del Greco MF, Minelli C, Davey Smith G, Sheehan NA, Thompson JR. Assessing the suitability of summary data for two-sample mendelian randomization analyses using MR-egger regression: the role of the I2 statistic. *Int J Epidemiol* (2016) 45 (6):1961–74. doi: 10.1093/ije/dyw220

26. Bowden J, Davey Smith G, Haycock PC, Burgess S. Consistent estimation in mendelian randomization with some invalid instruments using a weighted median estimator. *Genet Epidemiol* (2016) 40(4):304–14. doi: 10.1002/gepi.21965

27. Hartwig FP, Davies NM, Hemani G, Davey Smith G. Two-sample mendelian randomization: avoiding the downsides of a powerful, widely applicable but potentially fallible technique. *Int J Epidemiol* (2016) 45(6):1717–26. doi: 10.1093/ije/dyx028

28. Greco MF, Minelli C, Sheehan NA, Thompson JR. Detecting pleiotropy in mendelian randomisation studies with summary data and a continuous outcome. *Stat Med* (2015) 34(21):2926–40. doi: 10.1002/sim.6522

29. Bowden J, Davey Smith G, Burgess S. Mendelian randomization with invalid instruments: effect estimation and bias detection through egger regression. *Int J Epidemiol* (2015) 44(2):512–25. doi: 10.1093/ije/dyv080

30. Verbanck M, Chen CY, Neale B, Do R. Detection of widespread horizontal pleiotropy in causal relationships inferred from mendelian randomization between complex traits and diseases. *Nat Genet* (2018) 50(5):693–8. doi: 10.1038/s41588-018-0099-7

31. Tuchendler D, Bolanowski M. The influence of thyroid dysfunction on bone metabolism. *Thyroid Res* (2014) 7(1):12. doi: 10.1186/s13044-014-0012-0

32. Eriksen EF, Mosekilde L, Melsen F. Trabecular bone remodeling and bone balance in hyperthyroidism. *Bone* (1985) 6(6):421–8. doi: 10.1016/8756-3282(85)90218-2

33. Bjerkreim BA, Hammerstad SS, Eriksen EF. Bone turnover in relation to thyroid-stimulating hormone in hypothyroid patients on thyroid hormone substitution therapy. *J Thyroid Res* (2022) 2022:8950546. doi: 10.1155/2022/8950546

34. Tsourdi E, Colditz J, Lademann F, Rijntjes E, Köhrle J, Niehrs C, et al. The role of dickkopf-1 in thyroid hormone-induced changes of bone remodeling in Male mice. *Endocrinology* (2019) 160(3):664–74. doi: 10.1210/en.2018-00998

35. Robinson D, Hasharoni A, Halperin N, Yayon A, Nevo Z. Mesenchymal cells and growth factors in bunions. *Foot ankle Int* (1999) 20(11):727–32. doi: 10.1177/107110079902001109

36. Sharifi M, Ereifej L, Lewiecki EM. Sclerostin and skeletal health. *Rev endocr Metab Disord* (2015) 16(2):149–56. doi: 10.1007/s11154-015-9311-6

37. Mihaljević O, Živančević-Simonović S, Lučić-Tomić A, Živković I, Minić R, Mijatović-Teodorović L, et al. The association of circulating sclerostin level with markers of bone metabolism in patients with thyroid dysfunction. *J Med Biochem* (2020) 39(4):436–43. doi: 10.5937/jomb0-24943

38. Abu EO, Horner A, Teti A, Chatterjee VK, Compston JE. The localization of thyroid hormone receptor mRNAs in human bone. *Thyroid* (2000) 10(4):287–93. doi: 10.1089/thy.2000.10.287

39. Bock P, Kristen KH, Kröner A, Engel A. Hallux valgus and cartilage degeneration in the first metatarsophalangeal joint. *J Bone Joint Surg Br* (2004) 86 (5):669–73. doi: 10.1302/0301-620x.86b5.14766

40. Pörings AS, Lowin T, Dufner B, Grifka J, Straub RH. A thyroid hormone network exists in synovial fibroblasts of rheumatoid arthritis and osteoarthritis patients. *Sci Rep* (2019) 9(1):13235. doi: 10.1038/s41598-019-49743-4

41. Siclari A, Piras M. Hallux metatarsophalangeal arthroscopy: indications and techniques. *Foot ankle clinics* (2015) 20(1):109–22. doi: 10.1016/j.fcl.2014.10.012

42. Lui TH. First metatarsophalangeal joint arthroscopy in patients with hallux valgus. *Arthroscopy* (2008) 24(10):1122–9. doi: 10.1016/j.arthro.2008.05.006

43. Zirngibl B, Grifka J, Baier C, Götz J. [Hallux valgus : Etiology, diagnosis, and therapeutic principles]. *Der Orthop* (2017) 46(3):283–96. doi: 10.1007/s00132-017-3397-3

44. Alimy AR, Polzer H, Ocokoljic A, Ray R, Lewis TL, Rolvien T, et al. Does minimally invasive surgery provide better clinical or radiographic outcomes than open surgery in the treatment of hallux valgus deformity? a systematic review and meta-analysis. *Clin orthop related Res* (2022) 4. doi: 10.1097/CORR.0000000000002471

45. Fukushi JI, Tanaka H, Nishiyama T, Hirao M, Kubota M, Kakihana M, et al. Comparison of outcomes of different osteotomy sites for hallux valgus: A systematic review and meta-analysis. *J orthop Surg* (2022) 30(2):10225536221110473. doi: 10.1177/10225536221110473

46. Menz HB, Roddy E, Marshall M, Thomas MJ, Rathod T, Peat GM, et al. Epidemiology of shoe wearing patterns over time in older women: Associations with foot pain and hallux valgus. the journals of gerontology series a. *Biol Sci Med Sci* (2016) 71(12):1682–7. doi: 10.1093/gerona/glw004

frontiers | Frontiers in Endocrinology

TYPE Original Research
PUBLISHED 30 March 2023
DOI 10.3389/fendo.2023.1129930

OPEN ACCESS

EDITED BY
Michela Rossi,
Bambino Gesù Children's Hospital (IRCCS), Italy

REVIEWED BY
Bin Wang,
Thomas Jefferson University, United States
Guido Zavatta,
University of Bologna, Italy

*CORRESPONDENCE
Sabrina Corbetta
sabrina.corbetta@unimi.it

†These authors have contributed equally to this work

SPECIALTY SECTION
This article was submitted to Bone Research, a section of the journal Frontiers in Endocrinology

RECEIVED 22 December 2022
ACCEPTED 14 March 2023
PUBLISHED 30 March 2023

CITATION
Verdelli C, Tavanti GS, Forno I, Vaira V, Maggiore R, Vicentini L, Dalino Ciaramella P, Perticone F, Lombardi G and Corbetta S (2023) Osteocalcin modulates parathyroid cell function in human parathyroid tumors. *Front. Endocrinol.* 14:1129930. doi: 10.3389/fendo.2023.1129930

Osteocalcin modulates parathyroid cell function in human parathyroid tumors

Chiara Verdelli[1†], Giulia Stefania Tavanti[1,2†], Irene Forno[3], Valentina Vaira[3,4], Riccardo Maggiore[5], Leonardo Vicentini[6], Paolo Dalino Ciaramella[7], Francesca Perticone[8], Giovanni Lombardi[9,10] and Sabrina Corbetta[2,11*]

[1]Laboratory of Experimental Endocrinology, IRCCS Istituto Ortopedico Galeazzi, Milan, Italy, [2]Department of Biomedical, Surgical and Dental Sciences, University of Milan, Milan, Italy, [3]Division of Pathology, Fondazione IRCCS Ca` Granda Ospedale Maggiore Policlinico, Milan, Italy, [4]Department of Pathophysiology and Transplantation, University of Milan, Milan, Italy, [5]Endocrine Surgery, IRCCS Ospedale San Raffaele, Milan, Italy, [6]Endocrine Surgery, IRCCS Istituto Auxologico, Milan, Italy, [7]Endocrinology Unit, ASST Grande Ospedale Metropolitano Niguarda, Milan, Italy, [8]Endocrinology Unit, IRCCS Ospedale San Raffaele, Milan, Italy, [9]Laboratory of Experimental Biochemistry and Molecular Biology, IRCCS Istituto Ortopedico Galeazzi, Milan, Italy, [10]Department of Athletics, Strenght and Conditioning, Poznań University of Physical Education, Poznań, Poland, [11]Endocrinology and Diabetology Service, IRCCS Istituto Ortopedico Galeazzi, Milan, Italy

Introduction: The bone matrix protein osteocalcin (OC), secreted by osteoblasts, displays endocrine effects. We tested the hypothesis that OC modulates parathyroid tumor cell function.

Methods: Primary cell cultures derived from parathyroid adenomas (PAds) and HEK293 cells transiently transfected with the putative OC receptor GPRC6A or the calcium sensing receptor (CASR) were used as experimental models to investigate γ-carboxylated OC (GlaOC) or uncarboxylated OC (GluOC) modulation of intracellular signaling.

Results: In primary cell cultures derived from PAds, incubation with GlaOC or GluOC modulated intracellular signaling, inhibiting pERK/ERK and increasing active β-catenin levels. GlaOC increased the expression of *PTH, CCND1* and *CASR*, and reduced *CDKN1B/p27* and *TP73*. GluOC stimulated transcription of *PTH*, and inhibited *MEN1* expression. Moreover, GlaOC and GluOC reduced staurosporin-induced caspase 3/7 activity. The putative OC receptor GPRC6A was detected in normal and tumor parathyroids at membrane or cytoplasmic level in cells scattered throughout the parenchyma. In PAds, the membrane expression levels of GPRC6A and its closest homolog CASR positively correlated; GPRC6A protein levels positively correlated with circulating ionized and total calcium, and PTH levels of the patients harboring the analyzed PAds. Using HEK293A transiently transfected with either GPRC6A or CASR, and PAds-derived cells silenced for *CASR*, we showed that GlaOC and GluOC modulated pERK/ERK and active β-catenin mainly through CASR activation.

10.3389/fendo.2023.1129930

Conclusion: Parathyroid gland emerges as a novel target of the bone secreted hormone osteocalcin, which may modulate tumor parathyroid CASR sensitivity and parathyroid cell apoptosis.

KEYWORDS

parathyroid tumor, osteocalcin, CASR, GPRC6A, ERK, beta-catenin

Introduction

Primary hyperparathyroidism (PHPT) is one of the most common endocrine disorder, and it is characterized by inappropriate secretion of PTH from parathyroid tumors and hypercalcemia (1). PHPT is one of the main causes of secondary osteoporosis, with a prevalence of 1 at 1000 in postmenopausal women (1). It is often associated with high bone turnover (2); high bone turnover induces the release of a number of bioactive molecules from bone, among which osteocalcin (OC) is thought to play extraskeletal endocrine functions. OC is a small non-collagenous protein mainly produced by osteoblasts and is highly represented in bones of most vertebrates. Human OC contains up to three highly conserved gamma-carboxyglutamic acid residues (GlaOC), at positions 17, 21 and 24 (3), which are thought to increase calcium-binding strength, improving mechanical properties of the bone matrix. Recent studies *in vitro* and in animal models revealed that OC may exert also important endocrine functions, affecting energy metabolism and male fertility (4). The endocrine effects seem to be mediated by the uncarboxylated form of OC (GluOC) (5), while data regarding the carboxylation state-related function of the active form of OC are controversial (6, 7).

Tumors of the parathyroid glands are common, mostly benign, though sometimes associated with severe and life-threatening PHPT. Parathyroid tumors are heterogeneous in the severity of PTH secretion, cell proliferation, and genetic background (8). It is known that persistent secondary hyperparathyroidism, such as that induced by idiopathic hypercalciuria or malabsorption-related vitamin D deficiency, may stimulate parathyroid cell proliferation and autonomous PTH hypersecretion (9).

Therefore, it may be conceived that increased bone turnover and consequent increased OC release from bone might promote parathyroid cell proliferation and/or modulate PTH secretion. In line with this hypothesis, both circulating GlaOC and GluOC levels have been found to be increased in PHPT patients (10–12), and elevated levels of circulating OC have been suggested to be predictors of multiglandular disease in PHPT patients (13). Indeed, a direct effect of OC on parathyroid cell function has never been investigated until now.

GPRC6A, a widely expressed G-protein coupled receptor, is proposed to be the putative receptor of OC and a master regulator of complex endocrine networks and metabolic processes (14, 15). GPRC6A is the closest mammalian homolog of the calcium-sensing receptor (CASR), which is the molecular mechanism inhibiting PTH secretion and parathyroid cell proliferation. CASR is the target of the currently available drugs cinacalcet and etelcalcetide for the control of hyperparathyroid diseases (16). Both CASR and GPCR6A are often modulated by the same orthosteric and allosteric ligands and have overlapping expression patterns (17). It is thus conceivable that the receptors could either directly form heterodimers or remain expressed as homodimers in the same cell, having different effects on intracellular signaling.

The present study aims to investigate: 1) the effects of GlaOC and GluOC on the modulation of intracellular signaling pathways and of the parathyroid specific genes expression in human parathyroid tumor cells, 2) the expression of GPRC6A in parathyroid adenomas-derived cells, 3) the distinct effects of the stimulation with GlaOC or GluOC in HEK293A cells transfected with GPRC6A or CASR, and 4) the effects of GlaOC and GluOC on parathyroid cell apoptosis.

Materials and methods

Parathyroid tissue samples

Fresh samples from 45 parathyroid adenomas (PAds) were collected immediately after surgical removal from patients with a diagnosis of PHPT, caused by a single parathyroid adenoma, partly snap frozen and partly dissociated for primary cell cultures. In all PHPT patients, fasting plasma ionized calcium, serum total calcium, and PTH were routinely measured to diagnose PHPT. This study was approved by the Institutional Ethical Committee (Ospedale San Raffaele Ethical Committee, protocol no. GPRC6A PARA, 07/03/2019; CE40/2019), and informed consent was obtained from all patients.

Cell cultures

Samples from PAds were cut into 1 mm^3 fragments, washed with PBS and partially digested with 2 mg/mL collagenase type I (Worthington, Lakewood, NJ, USA) for 90 minutes. Digested tissues were filtered with a cell strainer (100 µm Nylon, BD Falcon, Rignano Flaminio, Italy) to obtain a single cell suspension and cultured in DMEM supplemented with 10% fetal bovine serum, 2 mmol/L glutamine and 100 U/mL penicillin-streptomycin.

The human embryonic kidney HEK293A cell line (Catalog n.R705-07, Invitrogen, ThermoFisher Scientific, Carlsbad, CA, USA) was maintained until 30 passages and cultured in the same medium of PAds-derived cells, as described above.

Since a human parathyroid cell line is not commercially available and due to the difficulty in performing a long-term parathyroid primary cell culture, we used PAds-derived cells, two days after isolation, and transiently transfected HEK293A cell line as models for our experiments.

Treatment of PAds-derived cells with GlaOC and GluOC

Before treatment with GlaOC or GluOC, cells were serum-starved overnight and pretreated for 30 minutes with physiological saline solution PSS (NaCl 125 mM, KCl 4 mM, HEPES 20 mM, D-Glucose 0.1%, NaH_2PO_4 0.8 mM, $MgCl_2$ 1 mM, pH 7.45), containing 0.1% BSA. Then, PAds-derived cells were treated with increasing concentrations of GlaOC and GluOC (#4034491 and #4063516, respectively; BACHEM, Bubendorf, Switzerland) in presence of 1.5 mM extracellular calcium ($[Ca^{2+}]_o$) for 10 minutes for intracellular pathways' investigation and for 6 hours for gene expression analysis. Tested GlaOC and GluOC concentrations, previously used by Pi et al. (18), were identified from preliminary dose-effect experiments in GPRC6A-HEK293A and CASR-HEK293A cells. Due to the limited number of cells obtained from each PAd sample, dose-effect curves could not be performed and the GlaOC and GluOC concentrations were restricted to 60 and 80 ng/mL. Untreated cells (NT) were considered as controls.

RNA extraction and purification

Total RNA from PAds-derived cells cultures was isolated using TRIzol reagent (Invitrogen, ThermoFisher Scientific, Carlsbad, CA, USA) and genomic DNA contamination was removed by DNase I (Life Technologies, ThermoFisher Scientific, Carlsbad, CA, USA). Then, DNA-free RNA was quantified spectrophotometrically at Λ=260 nm.

Real-time quantitative RT-PCR

Total cellular DNA-free RNA (300 ng) was reverse transcribed using the iScript cDNA Synthesis Kit (Bio-Rad, Hercules, CA, USA). Then, cDNA was amplified using TaqMan gene expression assay and a StepOnePlus™ Real-Time PCR System. The following probes were used: *PTH* Hs00757710_g1, *CASR* Hs01047795_m1, *CCND1* Hs00765553_m1, *GCM2* Hs00899403_m1, *VDR* Hs01045843_m1, *MEN1* Hs00365720_m1, *CDKNB1* Hs01597588_m1, and *TP73* Hs01056231_m1. The reference genes *HMBS* and *B2M* (Hs00609297_m1 and Hs99999907_m1, respectively) were used to normalize expression data and to obtain relative quantities using $2^{(-\Delta\Delta Ct)}$ formula. Where not otherwise specified, reagents and instruments were from Thermo Fisher Scientific (Carlsbad, CA, USA).

Protein extraction and western blot analysis

Cells were homogenized using NP40 lysis buffer (FNN0021, ThermoFisher Scientific, Carlsbad, CA, USA) containing protease and phosphatase inhibitors to obtain total protein extracts. Membrane proteins were obtained from snap-frozen tissue sections (n=15) using a Dounce homogenizer and the Subcellular Protein Fractionation Kit for Tissues (ThermoFisher Scientific, Carlsbad, CA, USA). Protein concentration was measured using the Pierce BCA Protein Assay Kit (ThermoFisher Scientific, Carlsbad, CA, USA).

Twenty micrograms of total proteins per sample were loaded on a 10% or 7.5% SDS-PAGE, electrophoretically separated and then transferred to nitrocellulose membrane (Amersham Protran GE Healthcare Life Science, Chicago, Illinois, USA). For immunoblotting the following primary antibodies were used: GPRC6A (ab236964, Abcam, Cambridge, UK), CASR (ab19347, Abcam, Cambridge, UK), phosphorylated ERK and total ERK (#4370S and #9107S, respectively, Cell Signaling, Danvers, MA, USA), phosphorylated AKT and total AKT (#4060S and #4691S, respectively, Cell Signaling, Danvers, MA, USA), active unphosphorylated β-catenin (#8814, Cell Signaling, Danvers, MA, USA). Vinculin (ab129002, Abcam, Cambridge, UK) and GAPDH (ab9485, Abcam, Cambridge, UK) was used as loading controls for whole cell proteins, while Na^+/K^+-ATPase (ab76020, Abcam, Cambridge, UK) were used as loading control for membrane protein fractions. Binding of appropriate HRP-conjugated secondary antibodies was detected using the chemiluminescence ChemiDoc XRS System (Bio-Rad, Hercules, CA, USA). Analyses of bands densitometry were performed using Image Lab software (Bio-Rad, Hercules, CA, USA), and protein expression levels were normalized using vinculin, GAPDH, or Na^+/K^+-ATPase as reference.

ERK expression levels were considered as ratio of phosphorylated ERK/total ERK.

Immunohistochemistry

Formalin-fixed paraffin-embedded (FFPE) samples were collected from 7 normal parathyroid glands (PaNs) incidentally removed from normocalcemic patients treated with thyroid surgery, and 12 PAds removed from PHPT patients. Parathyroid tissue sections were incubated with a rabbit monoclonal primary antibody specific for GPRC6A (TA208322, Origine, Rockville, MD, USA). Immunohistochemical staining was performed using the automatic staining BioGenex i6000 Automated Staining System (BioGenex, Fremont, CA, USA). Reactions were detected by Novolink Polymer Detection System (Novocastra Laboratories, Leica Microsystems, Newcastle, UK), according to the manufacturer's instructions. Negative controls were incubated in the absence of primary antibody and human testis was used as positive control.

Immunofluorescence

PAds-derived cells were fixed in 4% paraformaldehyde, permeabilized in 0.2% Triton X-100, and blocked in serum-free block protein solution (DAKO) for 1 h. Cells were incubated with primary antibodies, GPRC6A (TA308322, Origene, Rockville, MD, USA), PTH (sc-80924, Santa Cruz Biotechnology, Dallas, TX, USA), and GCM2 (sc-79491, Santa Cruz Biotechnology, Dallas, TX, USA), washed thrice in PBS, and then incubated with secondary antibodies conjugated with Alexa488 or Cy3 (1:100; Jackson Immuno Research, West Grove, PA, USA). Hoechst 33342 was used as nuclear stain (blue). As negative control, PBS was used instead of primary antibodies to exclude unspecific binding of secondary antibody. Images were obtained using fluorescence microscopy (Zeiss Axioskop 2 Plus, Zeiss OberKochen, Germany).

CASR silencing in PAds-derived cells

PAds-derived cells were plated two days before transfection in antibiotic-free complete DMEM medium in 6-well plates. Cells were transiently transfected with 25 nM CaSR direct siRNA (L-005444-00-0005; ON-TARGET Plus siRNA SmartPool, Dharmacon, Lafayette, CO, USA) or 25 nM control siRNA (D-001810-10-05, ON-TARGETplus Non-targeting Pool, Dharmacon, Lafayette, CO, USA) in Opti-MEM medium (Gibco, ThermoFisher Scientific, Carlsbad, CA, USA), using DharmaFECT 1 (T-2001-02; Dharmacon, Lafayette, CO, USA) as transfection reagent. After 24 hours, transfected cells were treated for 10 minutes with either 80 ng/mL GlaOC or GluOC and analyzed by Western Blotting. All transfection conditions and reagent concentrations were previously optimized.

GPCR6A and CASR transfections

HEK293A cells were seeded at a density of $1.2x10^5$ cells/well in 6-well plates and cultured in DMEM without penicillin-streptomycin. The following day, cells were transiently transfected with plasmid encoding for *GPRC6A* (sc-306340, Santa Cruz Biotechnology, Dallas, TX, USA), or with plasmid encoding for *CASR*, obtained by site-directed mutagenesis, as previously described (19). Two micrograms of GPRC6A plasmid were transfected using Lipofectamine3000 (L3000008, ThermoFisher Scientific, Carlsbad, CA, USA) in OptiMEM serum-free medium (GPRC6A-HEK293A cells). For CASR plasmid transfection, 4 micrograms of DNA were transfected using TurboFect Transfection Reagent (R0533, ThermoFisher, Carlsbad, CA, USA) in DMEM serum-free medium (CASR-HEK293A cells), following the manufacturer's instructions. Preliminary experiments were performed to determine the optimal concentrations of both plasmids and to set up and optimize transfection conditions (Supplementary Figures 1A, D). GPRC6A and CASR transfections were functionally verified by documenting changes in pERK/ERK levels in response to stimulation with increasing concentrations of arginine and calcium as well as R568, respectively (Supplementary Figures 1B, C, E–H).

Treatment of HEK293A cells with GlaOC and GluOC

Forty-eight hours after transfection, both GPRC6A-HEK293A and CASR-HEK293A cells were treated with increasing concentrations (20, 40, 60, 80 ng/mL) of GlaOC or GluOC, in the same experimental conditions used for PAds-derived cells. Cells were treated with the two isoforms of OC in presence of 1.5 mM $[Ca^{2+}]_o$ for 10 minutes for intracellular pathways investigation. Untreated cells (NT) were used as controls. The same experiments were also conducted on HEK293A cells transfected with the empty vector to verify the receptor specificity of the observed GlaOC or GluOC effects (data not shown).

Apoptosis assays

For apoptosis experiments, PAds-derived cells and $8x10^4$ HEK293A cells transfected with GPRC6A or CASR plasmid (as described above) were seeded in 96-well plates. Cleaved Caspase 3/7 activity levels were measured using the Apo-One® Homogeneous Caspase 3/7 assay (Promega Corp., WI, USA) that provides a profluorescent substrate and a cell lysis/activity buffer for Caspase 3/7 (DEVDase) activity assay. After induction of apoptosis with 2 µM staurosporine (Merk Millipore, Burlington, MA, USA) and treatment with GlaOC and GluOC for 5 hours, 100 µl of Apo-One was added to each well, incubated for 2-18 hours and then fluorescence levels were measured (485Ex/527Em) according to the manufacturer's instructions.

Statistics

Densitometric data were log2 transformed, analyzed by One-way ANOVA adjusted for multiple comparisons and presented as mean±SEM. All data related to protein expression were normalized on the levels detected in untreated conditions.

Gene expression data were log2 transformed and presented as mean±SEM. Differences among the levels at each time point experiment were tested by One-way ANOVA analysis adjusted for multiple comparisons. Correlations between gene expression and biochemical parameters were analyzed by Pearson coefficient of correlation.

A probability value (P) less than 0.05 was considered statistically significant. Statistical analyses were performed using Prism v6.0 (GraphPad Inc., San Diego, CA, USA).

Results

Effects of GlaOC and GluOC stimulations on intracellular signaling pathways in human parathyroid adenomatous cells

We first tested the hypothesis that GlaOC or GluOC or both can affect parathyroid tumor cell biology. The OC putative receptor GPRC6A (20) is coupled to the modulation of the extracellular signal-regulated kinases (21–23), of the protein kinase B (24, 25),

10.3389/fendo.2023.1129930

and of the WNT/β-catenin signaling (26). Therefore, we investigated the effect of both GlaOC and GluOC on these intracellular signaling pathways in parathyroid adenomas (PAd)-derived cells. Specifically, changes in the levels of phosphorylated and total extracellular signal-regulated kinases (pERK/ERK), of phosphorylated and total protein kinase B (pAKT/AKT), and of the active unphosphorylated β-catenin in whole cell protein extracts were quantified by western blot analysis. PAds-derived primary cell preparations were incubated with increasing concentrations of GlaOC (60-80 ng/mL) and GluOC (60-80 ng/mL) for 10 minutes.

GlaOC, at both concentrations, inhibited the basal pERK/ERK levels of about two folds, while GluOC-induced changes were not significantly different from basal conditions (n=4) (Figure 1A). The two isoforms of OC did not exert any significant effect on pAKT/AKT levels (Figure 1B), while both GlaOC and GluOC stimulated the basal active β-catenin levels of about 8 folds (n=4) (Figure 1C).

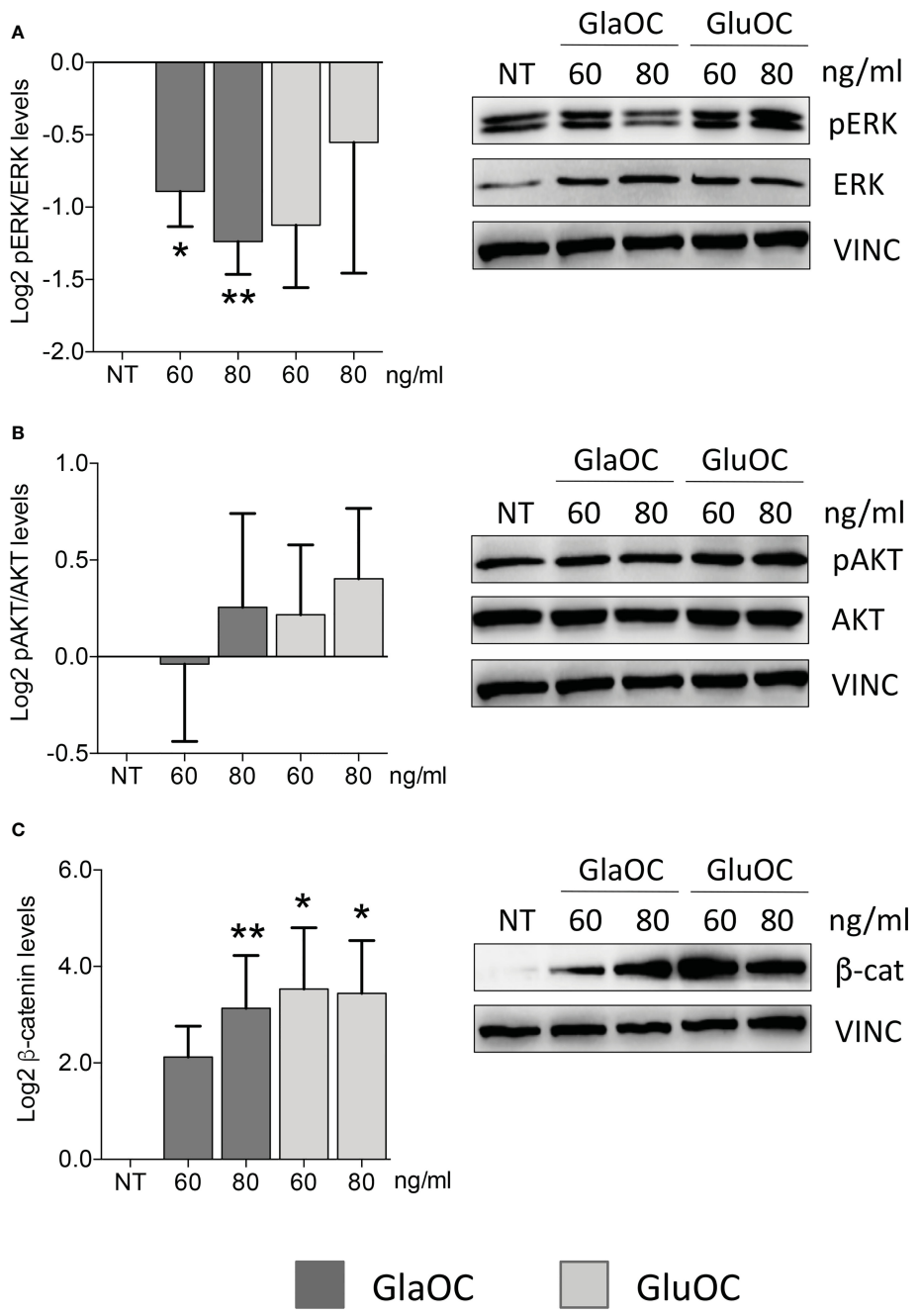

FIGURE 1
Effects of the GlaOC and GluOC stimulation on intracellular signaling pathways in human parathyroid cells. PAds-derived cells were incubated for 10 minutes with increasing concentrations of GlaOC (dark grey columns; 60-80 ng/mL) and GluOC (light grey columns; 60-80 ng/mL) (n=4). A representative western blot is shown for each experimental condition and data are expressed as mean ± SEM. **(A)** GlaOC and GluOC effects on basal pERK/ERK levels (*, P=0.019; **, P=0.004). **(B)** GlaOC and GluOC effects on basal pAKT/AKT levels. **(C)** GlaOC and GluOC effects on basal active β-catenin levels (*, P=0.048; **, P=0.042). VINC, vinculin was used as loading control.

10.3389/fendo.2023.1129930

Effects of GlaOC and GluOC stimulations on the expression of specific genes in human PAds-derived cells

Incubation for 6 hours of PAds-derived cell preparations (n=8) with increasing concentrations (60 and 80 ng/mL) of GlaOC elicited significant increases of the expression levels of the parathyroid specific gene *PTH* (Figure 2A). Modest but significant increases of *CCND1* transcripts were elicited by 80 ng/mL GlaOC (Figure 2B), in association with decreases in *CDKN1B* and *TP73* mRNA levels (Figures 2C, D, respectively). Besides, GlaOC did not affect the expression levels of the transcription factors *GCM2* (Figure 2E) and *MEN1* (Figure 2F). GlaOC stimulated the expression of *CASR* (Figure 2G), but not that of *VDR* mRNA levels (Figure 2H). As far as GluOC was concerned, increasing concentrations (60 and 80 ng/mL) induced *PTH* expression levels (Figure 2A), while GluOC did not affect the expression of *CCND1* (Figure 2B), *CDKN1B* (Figure 2C), *TP73* (Figure 2D), *GCM2* (Figure 2E), *CASR* (Figure 2G) and *VDR* (Figure 2H). At variance, GluOC reduced *MEN1* mRNA levels (Figure 2F).

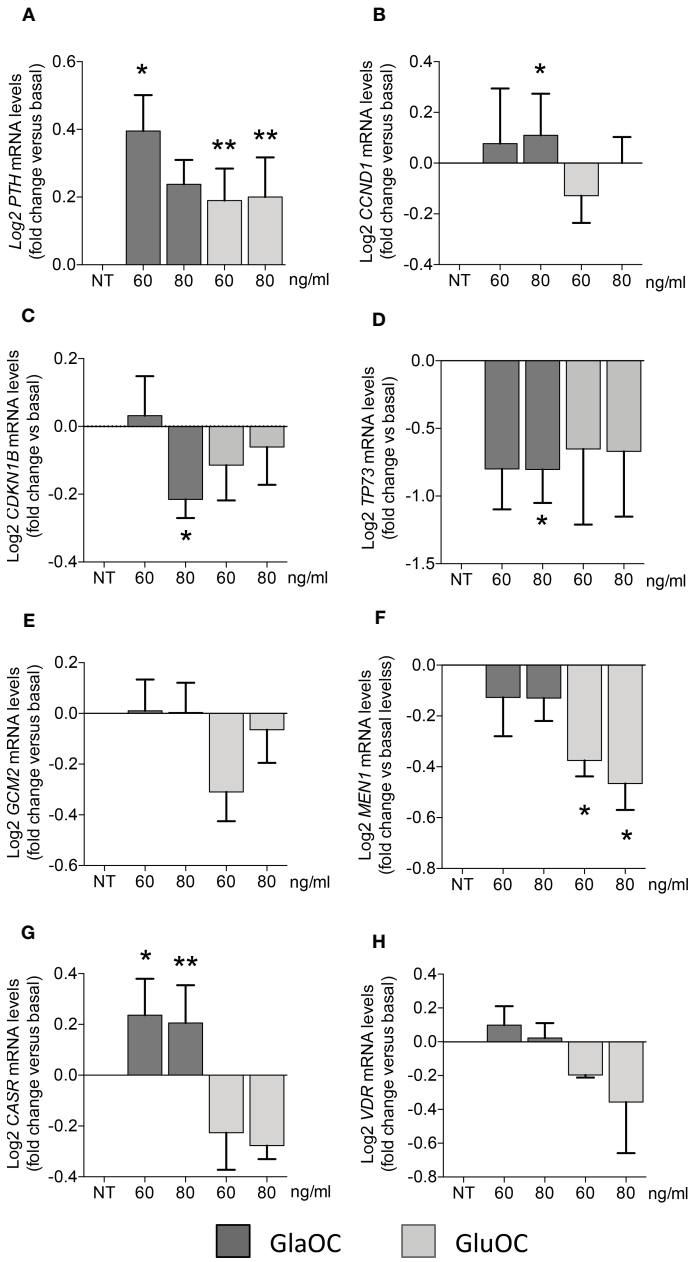

FIGURE 2
Effects of GlaOC and GluOC stimulation on the expression of specific genes in PAds-derived cells. PAds-derived cells were incubated for 6 hours with increasing concentrations (60-80 ng/mL) of GlaOC (dark grey columns) and GluOC (light grey columns). Data were expressed as fold change versus levels in non treated conditions (NT) and presented as mean ± SEM. GlaOC and GluOC modulated the expression of **(A)** *PTH* mRNA levels (*, P=0.015; **, P=0.008), **(B)** *CCND1* transcripts (*, P=0.002), **(C)** *CDKN1B* mRNA levels (*, P=0.041), and **(D)** *TP73* mRNA levels (*, P=0.042). Effects of GlaOC and GluOC on parathyroid specific transcription factors **(E)** *GCM2* mRNA levels, **(F)** *MEN1* mRNA levels (*, P=0.0001), and on **(G)** the receptors *CASR* (*, P=0.002; **, P=0.014) and **(H)** VDR mRNA levels are shown.

10.3389/fendo.2023.1129930

GPCR6A expression in human parathyroid gland

Our data suggests that GlaOC and GluOC induce biologic responses in PAds-derived cells, though at different extents, in term of modulation of intracellular signaling pathways and of parathyroid specific genes expression. These patterns of responses may be mediated by the membrane receptor GPRC6A. Therefore, we investigated GPRC6A expression in human parathyroid glands. Human *GPRC6A* transcripts were detected in total RNA extracted from a series of PAds derived from patients affected with sporadic PHPT (Figure 3A). Immunofluorescence with specific antibodies demonstrated that the GPRC6A protein was expressed in the PTH-expressing and GCM2-expressing PAds-derived cells (Figure 3B). GPRC6A expression was also investigated in normal parathyroid glands derived from normocalcemic subjects due to accidentally excision during thyroid surgery. IHC detected GPRC6A both at membrane and cytoplasmic levels, showing heterogeneity within sections from normal parathyroid glands (Figure 3C, a, b), where GPRC6A-expressing cells were scattered throughout the parenchyma or clusterized in defined areas. A similar pattern of expression was detected in sections from PAds (Figure 3C, c-f). Of

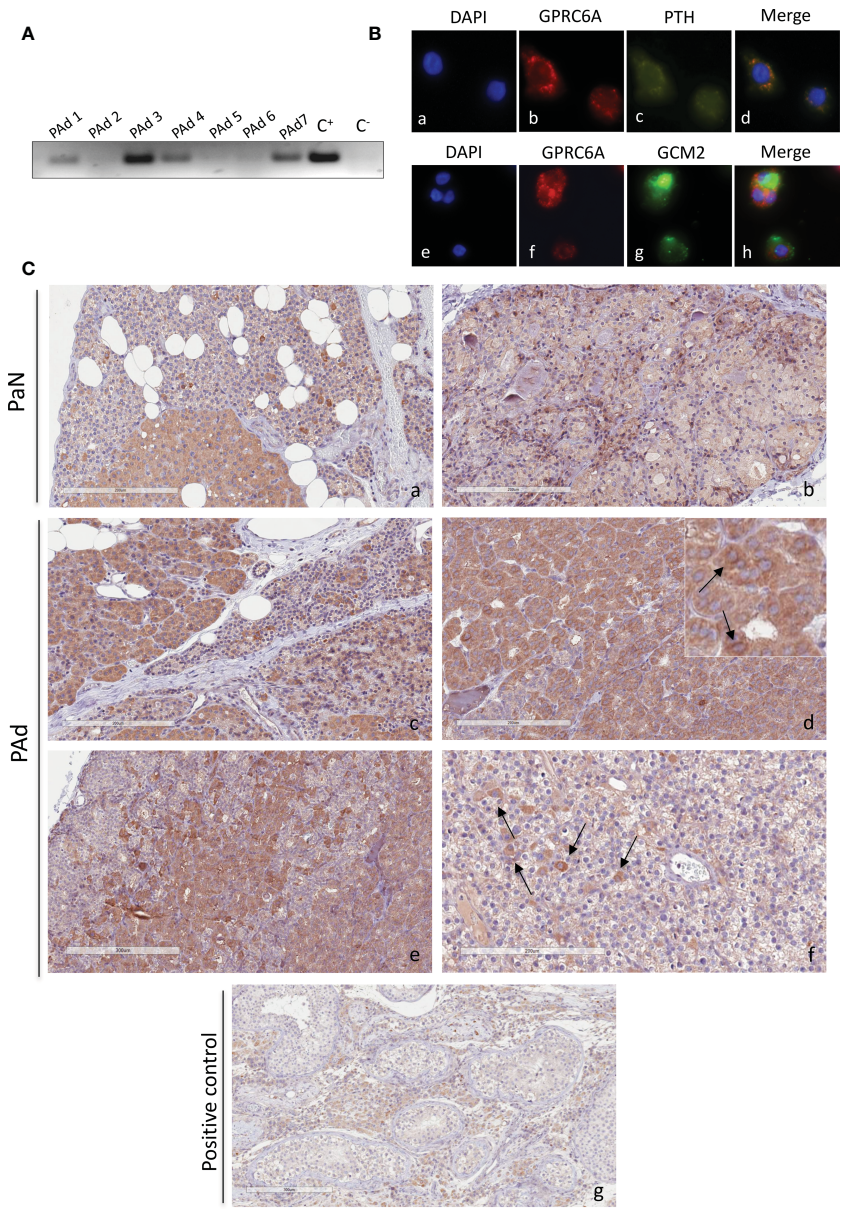

FIGURE 3
GPCR6A expression in human parathyroid cells. **(A)** *GPRC6A* transcripts were variably detected by RT-PCR in total RNA from PAds (n=7) of PHPT patients; C^+, plasmid encoding GPRC6A; C^-, water. **(B)** Immunofluorescence of short-term cultured PAds-derived cells showed cytoplasmic and membrane expression of GPRC6A (red, **b, f**); PTH (green, **c**) co-expressed with GPRC6A (merge, **d**) GCM2 (green, **g**) co-expressed with GPRC6A (merge, **h**). **(C)** Immunohistochemistry by a specific anti-GPRC6A antibody in normal parathyroid glands from normocalcemic patients with thyroid diseases **(a, b)** and in parathyroid adenomas (panels **c–f**). **(g)** Human testis with GPRC6A-expressing Leydig cells were used as positive control. Insert in **(d)** shows cells with GPRC6A expression at membrane level. Magnification 20X; bars, 200 µm.

note, GPRC6A protein was more abundant in parathyroid samples than in the human testicular Leydig cells (Figure 3C, g), used as positive control.

Relationships among GPRC6A, CASR expression levels and clinical features of parathyroid tumors

GPRC6A and CASR belong to class C G-protein coupled receptors and share a high degree of homology (27). The expression levels of GPRC6A and CASR proteins were analyzed by western blot in membrane protein fractions from 15 PAds (Figure 4A and Supplementary Figure 2A). Patients' clinical and biochemical features are reported in Supplementary Table 1. Both receptors were variably expressed among PAds, though their expression levels were positively correlated (r=0.618, P=0.014) (Figure 4B). Of note, considering the ratio between GPRC6A and CASR expression levels, PAds expressing higher levels of GPRC6A were associated with higher levels of circulating ionized calcium (r=0.552, P=0.033)(Figure 4C), total calcium (r=0.602, P=0.018) (Figure 4D), and PTH (r=0.539, P=0.038)(Figure 4E).

Effects of GPRC6A activation by GlaOC and GluOC in HEK293A cells transfected with GPRC6A

To define the contribution of GPRC6A in the signaling response to GlaOC and GluOC stimulation in PAds, we studied pERK/ERK

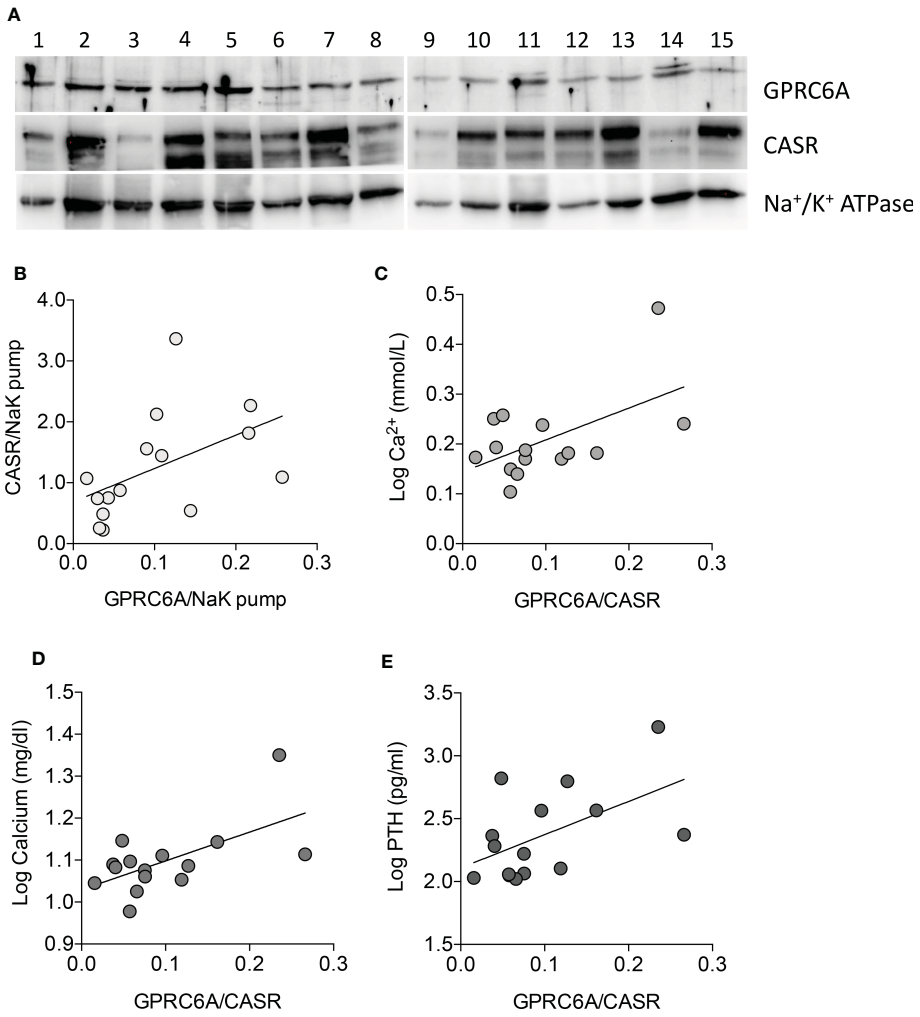

FIGURE 4
GPRC6A and CASR expression in membrane protein fractions from PAds and correlation with clinical features. **(A)** Western blot analysis of GPRC6A and CASR expression in membrane protein fractions from a series of PAds (n=15); GPRC6A specific band was detected at 105 kDa; specific CASR bands were detected at 130 and 150 kDa; Na^+/K^+ ATPAse was used as loading control. **(B)** Correlation between GPRC6A and CASR membrane proteins in the PAds series (r=0.618, P=0.014 by Spearman coefficient of correlation). **(C)** Correlation between GPRC6A/CASR ratio and plasma ionized calcium levels, expressed as log2 (r=0.552, P=0.033 by Pearson coefficient of correlation). **(D)** Correlation between GPRC6A/CASR ratio and serum total calcium levels, expressed as log2 (r=0.602, P=0.018 by Pearson coefficient of correlation). **(E)** Correlation between GPRC6A/CASR ratio and plasma PTH levels, expressed as log2 (r=0.539, P=0.038 by Pearson coefficient of correlation).

10.3389/fendo.2023.1129930

and β-catenin OC-stimulated responses using HEK293A cells transfected with the *GPRC6A* gene (GPRC6A-HEK293A cells) as experimental model (Supplementary Figures 1A–C). PhosphoAKT/AKT signaling was not evaluated as in PAds-derived cells it did not show significant changes in response to stimulation with isoforms of OC. Experiments were repeated four times in presence of 1.5 mM extracellular calcium ($[Ca^{2+}]_o$).

Increasing concentrations of both GlaOC and GluOC significantly stimulated of about 4 folds basal pERK/ERK levels (Figures 5A–C). Of note, this pattern of response was opposite to that observed in PAds-derived cells. Increasing concentrations of GlaOC induced small but significant increases of the basal active β-catenin levels (Figure 5D, F), while GluOC did not affect them (Figure 5E, F).

Effects of CASR activation by GlaOC and GluOC in HEK293A cells transfected with CASR

HEK293A cells transfected with CASR (CASR-HEK293A cells) (Supplementary Figures 1D-H) were used to test the hypothesis that

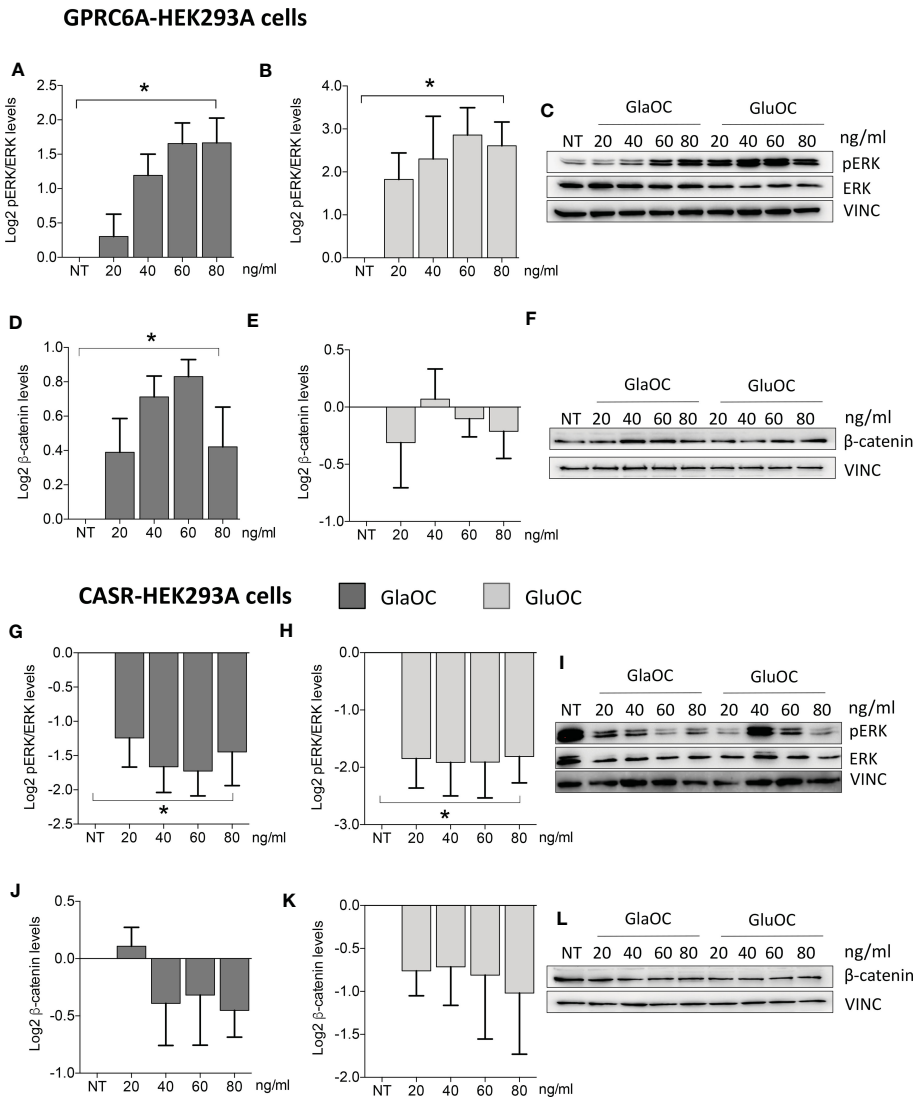

FIGURE 5
Effects of the treatment with GlaOC or GluOC in HEK293A cells transfected with GPCR6A and with CASR. HEK293A cells transiently transfected with GPRC6A (GPRC6A-HEK293A) or CASR (CASR-HEK293A) were incubated for 10 minutes with increasing concentrations (20, 40, 60, 80 ng/mL) of GlaOC (dark grey columns) and GluOC (light grey columns). Data were log2 transformed and presented as mean±SEM. **(A, B)** Effects of increasing concentrations of GlaOC and GluOC on pERK/ERK levels (*, P=0.006 and P=0.05, respectively) in GPRC6A-HEK293A cells. **(C)** Representative western blot. **(D, E)** Effects of increasing concentrations of GlaOC and GluOC on active β-catenin levels (*, P=0.025) in GPRC6A-HEK293A cells and representative western blot **(F)**. **(G, H)** Effects of increasing concentrations of GlaOC and GluOC on pERK/ERK levels (*, P=0.023 and P=0.048, respectively) in CASR-HEK293A cells and representative western blot **(I)**. **(J, K)** Effects of increasing concentrations of GlaOC and GluOC on β-catenin levels in CASR-HEK293A cells and representative western blot **(L)**.

GlaOC and/or GluOC can activate CASR and to investigate the effect of the GlaOC/GluOC-CASR activation on pERK/ERK and β-catenin signaling (n=4). In presence of 1.5 mM $[Ca^{2+}]_o$, increasing concentrations of both GlaOC and GluOC significantly inhibited basal pERK/ERK levels (Figures 5G–I), resembling the inhibitory effect observed in PAds-derived cells and suggesting that it is likely mediated by OC-stimulated CASR. Unlike what happened in PAds-derived cells, both GlaOC and GluOC did not exert any significant change in the basal active β-catenin levels in CASR-HEK293 cells (Figures 5J–L).

Effects of CASR silencing on GlaOC and GluOC stimulated intracellular signaling pathways in PAds-derived cells

To define the specific role of OC-activated CASR, experiments modulating intracellular signaling pathways were repeated in PAds-derived cell preparations (n=6) with transiently silenced *CASR*. CASR expression resulted to be reduced of at least 50% in the total protein extracts from all cell preparations (Figure 6A), while GPRC6A protein expression levels were unaffected by CASR silencing (Figure 6B). Immunoblots of GPRC6A were faint in 2 out 6 primary cell cultures, in line with the highly variable expression observed in IHC sections, therefore, the cell cultures were excluded from the analysis. In PAds expressing GPRC6A and CASR, reduction of CASR expression, blunted the inhibitions of pERK/ERK levels induced by GlaOC and GluOC (80 ng/mL) (Figure 6C). At variance, GlaOC and GluOC-induced increases in active β-catenin levels were unaffected by CASR silencing (Figure 6D), suggesting that β-catenin may be mainly modulated by GPRC6A activation.

Effects of GlaOC and GluOC stimulation on apoptosis in PAds-derived cells, GPRC6A-HEK293A, and CASR-HEK293A cells

Finally, considering the inhibitory effect of GlaOC and GluOC in PAds-derived cells on the expression of *TP73*, which is a master of apoptotic pathways (28), we tested the effect of GlaOC and GluOC on staurosporin-induced caspase 3/7 activity, known to have executioner roles for apoptosis (29). In PAds-derived cells (n=4), both GlaOC and GluOC significantly reduced the staurosporin-induced caspase 3/7 activities of about 40% of the basal levels, after 5 hours incubation (Figure 7A). Though HEK293A cells were less sensitive to the staurosporin apoptotic stimulus after 5 hours than PAds-derived cells, in GPRC6A-HEK293A cells (n=3) (Figure 7B) as well as in CASR-HEK293A cells (n=3) (Figure 7C), staurosporin-induced caspase 3/7 activities were reduced of about 25% by treatments with 80 ng/mL of GlaOC and GluOC, similarly to the effect detected in PAds-derived cells. These observations suggest that the OC antiapoptotic effect may be mediated by both GPRC6A and CASR.

Discussion

The present study firstly provides evidence suggesting that the bone-derived OC may modulate parathyroid tumor cell function in PHPT-related parathyroid adenomas. Osteocalcin, which is variably γ-carboxylated to three glutamic residues (3) and is released by osteoblasts, recently received researchers' attention, who defined its hormonal function. Besides the role in bone matrix mineralization (30), OC modulates, through the activation of the class C G-protein coupled receptor GPRC6A, the function of β cells of pancreatic islets, skeletal muscle fibers, adipose tissue, brain, and testes (31). In different cell models, OC modulates intracellular ERK, AKT, and β-catenin pathways through activation of GPRC6A (18, 25, 26).

Previous studies described the important role of the MAPK/ERK pathway in parathyroid cell function, and its dysregulation in parathyroid adenomas, where *HRAS*, *ARAF*, and *MEK1* genes are up-regulated (32) and ERK is hyperactivated (19, 33, 34). For these reasons, we investigated the effect of OC modulation on ERK pathway in PAds-derived cells. We demonstrated that GlaOC and GluOC inhibited basal pERK/ERK levels. Of note, OC exerts an opposite effect with respect to the stimulation induced by $[Ca^{2+}]_o$-activated CASR on intracellular pERK/ERK levels (19, 33, 34).

Though AKT and β-catenin signaling has been poorly investigated in parathyroid tumor cell biology so far, the PI3K/AKT/mTOR pathway was impaired in about one fifth of the parathyroid cancers (35, 36), suggesting a role of the AKT pathway in parathyroid cell pathophysiology. Similarly, data about the nuclear β-catenin accumulation in parathyroid tumors are controversial; nonetheless, the WNT/β-catenin pathway can play a role in parathyroid cell biology as its activation by lithium chloride inhibited the expression of the embryonic transcription factor TBX1 (37) and increased the aberrant expression of miR-372 in PAds-derived cells (38). Present data suggest that pAKT/AKT pathway is poorly modulated by OC in PAds-derived cells, while GlaOC and GluOC significantly increased active β-catenin levels.

Furthermore, the two OC isoforms not only modulate intracellular signaling, but also affect the expression of parathyroid specific genes. PAds-derived cells responded to both GlaOC and GluOC stimulations by increasing the expression levels of the parathyroid specific gene *PTH*. The observed increase of *PTH* gene expression is consistent with the inhibitory effect of GlaOC and GluOC on pERK/ERK levels. It has been demonstrated that abrogation of the ERK pathway abolishes the inhibitory effect of 1.5 mM $[Ca^{2+}]_o$ on PTH release from normal parathyroid cells supporting the role of MAPK in the modulation of the PTH secretion (39). Similarly, inhibition of the ERK pathway by FGF23 stimulates the release of PTH in rats with secondary hyperparathyroidism (40). Considering that PTH itself stimulates the release of OC by osteoblasts (4), the detected PTH stimulation by both GlaOC and GluOC suggests the existence of a self-regulatory positive feedback loop between PTH and OC.

GlaOC, but not GluOC, also increased the expression of the genes *CCND1* and *CASR*, and decreased the expression of *CDKN1B* and *TP73*, showing a heterogeneous response to GlaOC and GluOC

10.3389/fendo.2023.1129930

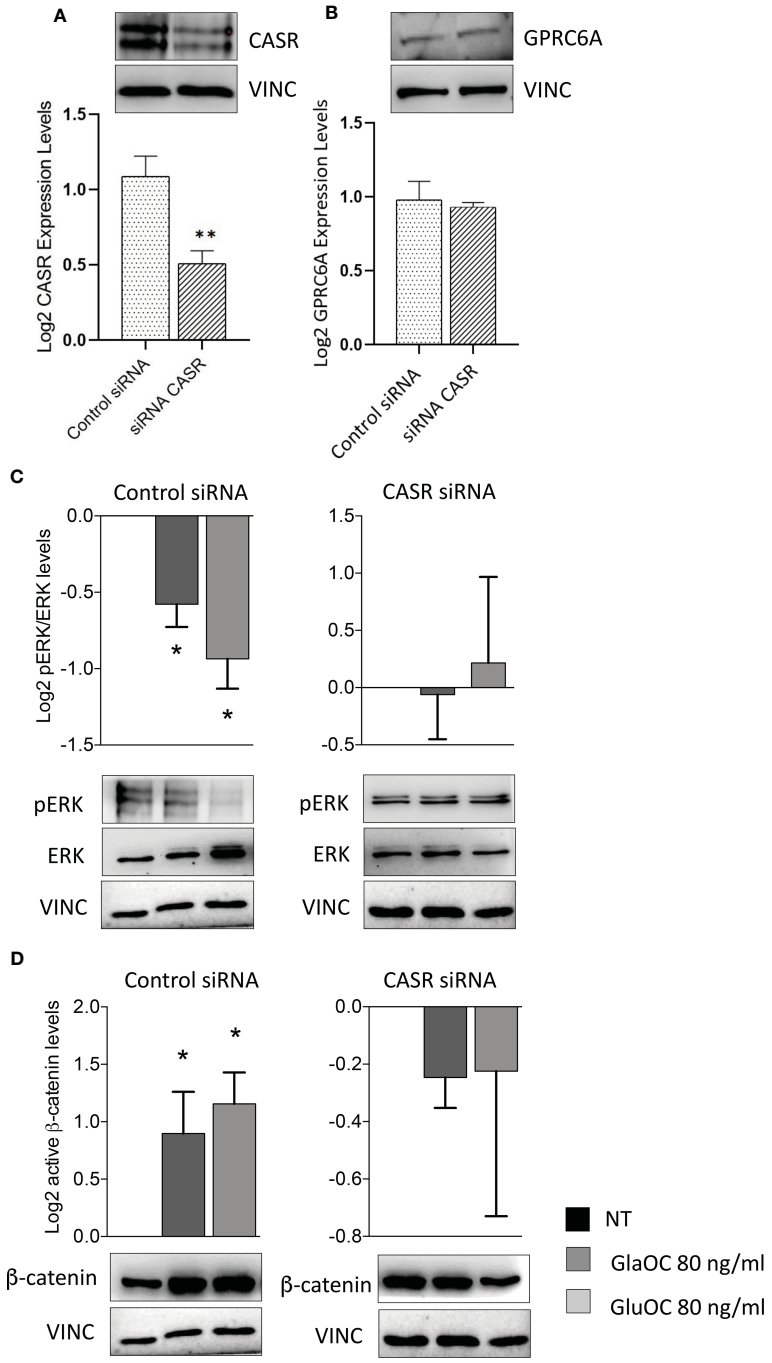

FIGURE 6
Effect of CASR silencing on the GlaOC/GluOC-activated signaling in PAds-derived cells. **(A)** Effect of the *CASR* silencing on CASR protein expression (**, P=0.0043). **(B)** Effect of the *CASR* silencing on GPRC6A protein levels; expression levels are presented as fold changes versus untreated conditions incubated with control siRNA, and log2 transformed. **(C)** Effects of GlaOC (dark grey columns) and GluOC (light grey columns) stimulation in PAds-derived cell preparations treated with control siRNA and with CASR siRNA on pERK/ERK levels (*, P<0.05). **(D)** Effects of GlaOC (dark grey columns) and GluOC (light grey columns) stimulation in PAds-derived cell preparations treated with control siRNA and with CASR siRNA on active β-catenin levels (*, P<0.05). Densitometric data were log2 transformed and presented as mean±SEM. A representative western blot is shown for each experimental condition.

in terms of PAds gene modulation. Of note, CCND1 has been previously shown to be stimulated by CASR activation (41). In line with this view, GluOC, but not GlaOC, inhibited the expression of the tumor suppressor gene *MEN1*. The effects observed on *CCND1* and *MEN1* suggested a possible modulation of the parathyroid tumor cell proliferation.

Admittedly, the modulation of the parathyroid genes' expression is of modest entity: it may be related to the extremely variable expression of both CASR and GPRC6A detected in the different PAds.

IHC revealed GPRC6A specific staining in both normal and adenomatous parathyroid glands with intensity even more

10.3389/fendo.2023.1129930

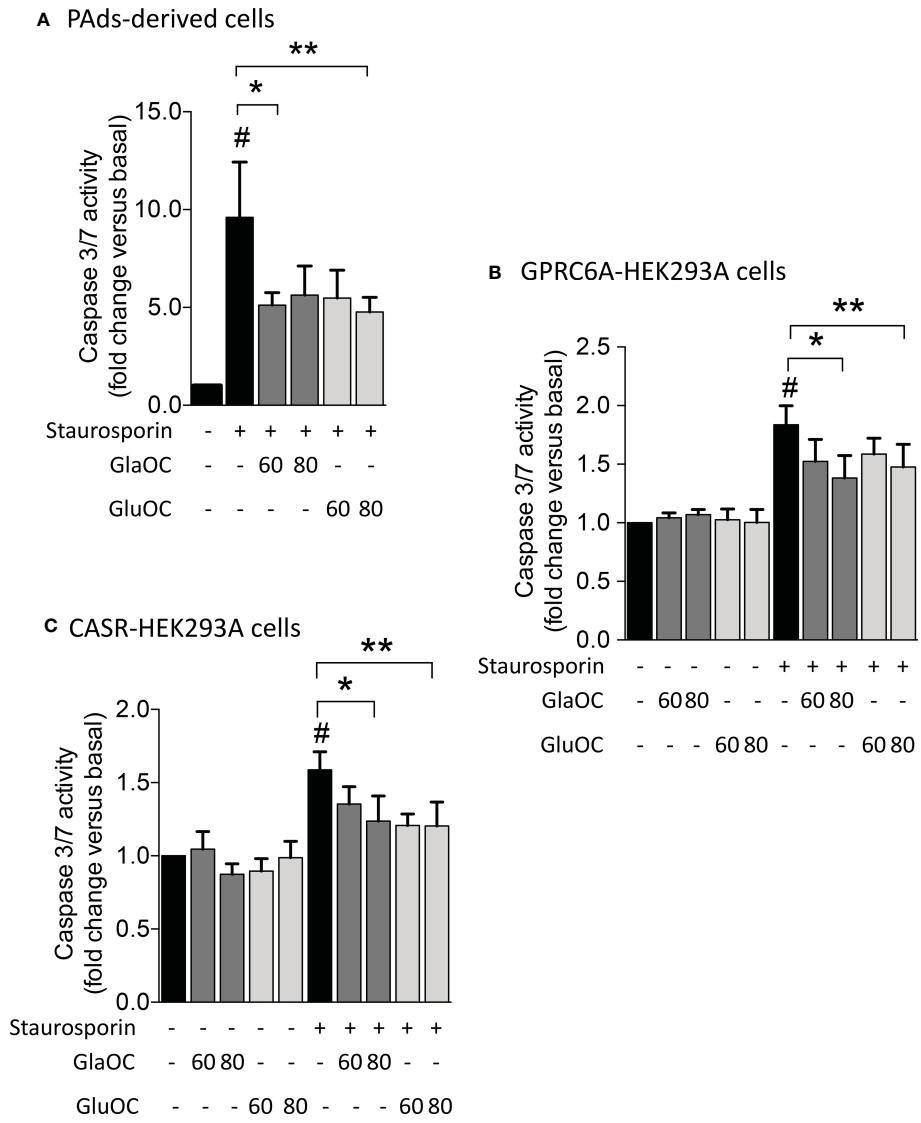

FIGURE 7
Effects of GlaOC and GluOC stimulation on staurosporin-induced apoptosis. **(A)** Effects of 60-80 ng/mL GlaOC (dark grey columns) and GluOC (light grey columns) on staurosporin-induced apoptosis in PAds-derived cells (#, P=0.022 versus basal levels; *, P=0.050 vs staurosporin treated cells; **, P=0.045 vs staurosporin treated cells). **(B)** Effects of 60-80 ng/mL GlaOC and GluOC on staurosporin-induced apoptosis in GPRC6A-HEK293A cells (#, P=0.036 vs basal levels; *, P=0.013 vs staurosporin treated cells; **, P=0.087 vs staurosporin treated cells). **(C)** Effects of 60-80 ng/mL GlaOC and GluOC on staurosporin-induced apoptosis in CASR-HEK293A cells (#, P=0.042 vs basal levels; *, P=0.010 vs staurosporin treated cells; **, P=0.040 versus staurosporin treated cells).

consistent compared with that detected in human testicular Leydig cells (42). GPRC6A was expressed by the endocrine parathyroid cells co-expressing PTH and the specific parathyroid transcription factor GCM2. Furthermore, the GPRC6A expression was heterogeneous in the single parathyroid tumor: intensively positive cells were scattered through cells with weak membrane positive staining. Similarly, CASR, which is highly homolog with GPRC6A, was heterogeneously expressed in PAds, in agreement with previous reports (39). Of note, the expression levels of the two receptors showed a positive correlation and were positively correlated with the circulating levels of ionized calcium and PTH in PHPT patients, suggesting that also GPRC6A may be involved in modulating PTH secretion and in determining the clinical presentation of PHPT. Therefore, the effects determined by GlaOC and GluOC through the activation of GPRC6A or CASR, on pERK/ERK and β-catenin signaling, were dissected using HEK293A cells transiently transfected with the human GPRC6A or with the human CASR, as experimental models.

In GPRC6A-HEK293A cells, GlaOC and GluOC increased basal pERK/ERK levels exerting opposite effects with respect to those detected in PAds-derived cells. GPRC6A is mainly coupled to G protein q/11 in HEK293 cells (43), and our data may suggest Gq/11 coupling mediating GlaOC and GluOC-stimulated ERK signalling.

Interestingly, in CASR-HEK293A cells, GlaOC and GluOC inhibited basal pERK/ERK levels, suggesting that GlaOC and GluOC in PAds likely act through the activation of CASR. In line with this observation, the reduction of CASR expression in PAds-

derived cells blunted the pERK inhibition induced by GlaOC and GluOC, confirming that in parathyroid tumor cells pERK/ERK modulation by GlaOC and GluOC is mainly mediated by CASR activation.

Resembling what detected in PAds-derived cells, in GPRC6A-HEK293A cells GlaOC increased the basal levels of active β-catenin. In silenced PAds-derived cells, the reduction of CASR expression abolished the increases in active β-catenin levels, suggesting that also β-catenin is mainly modulated by GlaOC- and GluOC-activated CASR.

Finally, GlaOC and GluOC had protective effects on induction of apoptosis in PAds-derived cells as well as in GPRC6A-HEK293A and CASR-HEK293A cells. In contrast with what previously described in other studies (44, 45), not only GluOC but also GlaOC partially prevented apoptosis acting through GPRC6A and CASR.

Interestingly, at variance with data reported in mouse models, where GluOC showed endocrine function (46), our data obtained both in human primary tumor cell and in human cell line cultures, indicated GlaOC as the bioactive molecule able to more consistently elicit modulation of intracellular signaling pathways and of gene expression. Differences observed between mice, where the hormone function is evident for GluOC, and humans, where GlaOC may act as modulator of the parathyroid function in adenomatous glands and of the skeletal muscle (47), may be related to the different carboxylation status: OC is γ-carboxylated on glutamic acids (Glu) 13, 17 and 20 of protein in mouse, and on Glu 17, 21 and 24 in humans (48).

Finally, according to previously published studies, average circulating levels of total OC range between 9 and 42 ng/mL, in adult women (https://www.mayocliniclabs.com/test-catalog/overview/80579#Clinical-and-Interpretive). To our knowledge, no data are available from PHPT patients. We tested in the *in vitro* experiments OC concentrations sensibly higher, i.e., supraphysiological, than the circulating ones in humans. This might appear as a simplification, or a limitation of the study; however, it should be considered that PAds-derived cells rapidly develop reduced sensitivity to $[Ca^{2+}]_o$ due to CASR downregulation implying the need to stimulate cells with supraphysiological $[Ca^{2+}]_o$ (2.5-5.0 mM) (39) and, since the hypothesized CASR-mediated effects of OCs, the use of supraphysiological doses was acknowledged. Moreover, the OCs concentrations used are in line with doses already reported in other *in vitro* models derived from different species (18, 21).

In conclusion, GlaOC and GluOC released from bone matrix may affect parathyroid tumor cell function, apoptosis, and indirectly proliferation (Figure 8). They may contribute to defining the heterogeneity of the biochemical phenotype associated with parathyroid adenomas in PHPT patients, promoting development of autonomous PTH secretion. It is tempting to speculate that persistent high bone turnover with release of GlaOC and GluOC, as occurs in postmenopausal bone demineralization, may desensitize parathyroid cells towards $[Ca^{2+}]_o$, and it may also promote parathyroid cell proliferation, and protect parathyroid cells from apoptotic stimuli, ultimately contributing to parathyroid hyperplasia. Parathyroid hyperplasia associated with high circulating GlaOC and GluOC concentrations might benefit of antiresorptive agents as inhibition of the bone turnover and consequent decrease in GlaOC and GluOC release may improve parathyroid cells sensitivity to $[Ca^{2+}]_o$. However, further studies aimed to elucidate the role of GlaOC and GluOC in modulating the mineral metabolism and the clinical effects should be conceived.

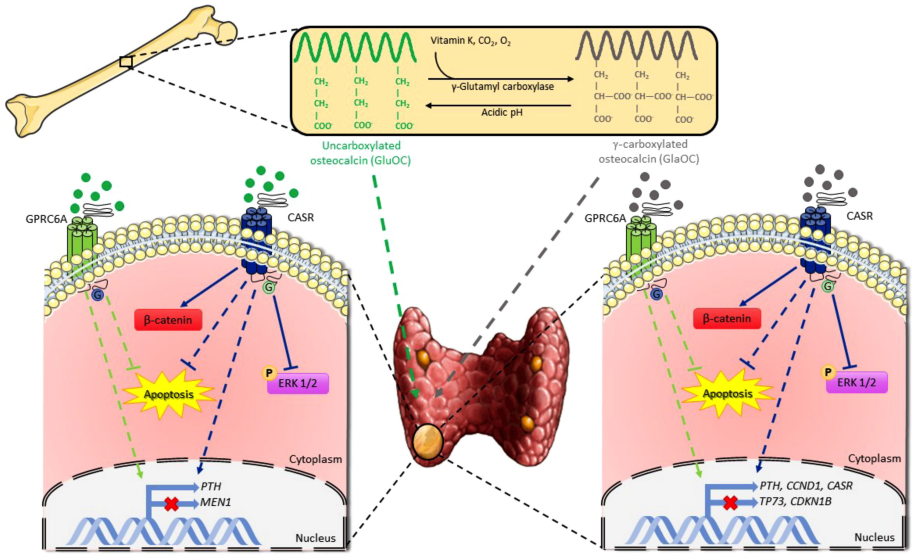

FIGURE 8
Schematic representation of osteocalcin effects on parathyroid tumor cell signaling pathways. GlaOC and GluOC, activating GPRC6A and CASR, modulate parathyroid gene expression and partially prevent apoptosis. GlaOC also reduces ERK phosphorylation and increases β-catenin mainly acting through CASR. Part of this figure was created using images from Servier Medical Art, licensed under a Creative Commons Attribution 3.0 Unported License (https://smart.servier.com).

Data availability statement

The datasets presented in this study can be found in online repositories. The names of the repository/repositories and accession number(s) can be found below: https://doi.org/10.5281/zenodo.5069796.

Ethics statement

The studies involving human participants were reviewed and approved by Ospedale San Raffaele Ethical Committee, protocol no. GPRC6A PARA, 07/03/2019; CE40/2019. The patients/participants provided their written informed consent to participate in this study.

Author contributions

CV and GT contributed equally to this work. Conceptualization, CV and SC; methodology, CV, GT, IF, validation, CV, GT; formal analysis, CV, GT; investigation, CV,GT, IF, VV, RM, LV, PD, FP; resources GL, SC; data curation, SC; writing – original draft preparation, SC; writing – review and editing, CV, GT and SC; supervision, SC; project administration, SC; funding acquisition, SC. All authors contributed to the article and approved the submitted version.

Funding

This work was supported by "Bando SIOMMMS 2018 Giovani Ricercatori" for the project "Expanding the crosstalk between bone and parathyroids: analysis of the osteocalcin receptor GPRC6A and of the potential interaction with the calcium sensing receptor in human parathyroid cells" to CV, by "Bando CARIPLO sulla ricerca biomedica legata alle malattie dell'invecchiamento 2018" for the project OSTMARK (no.2018-0458) to SC and GL, and by Italian Ministry of Health.

Conflict of interest

The authors declare that the research was conducted in the absence of any commercial or financial relationships that could be construed as a potential conflict of interest.

Publisher's note

Supplementary material

The Supplementary Material for this article can be found online at: https://www.frontiersin.org/articles/10.3389/fendo.2023.1129930/full#supplementary-material

SUPPLEMENTARY FIGURE 1
Functional characterization of the GPRC6A-HEK293A cells and CASR-HEK293A cells. **(A)** Western blot detection of GPRC6A protein in GPRC6A-HEK293A cells as a band of 105 kDa. **(B)** Increases of the basal pERK/ERK levels after stimulation with 20 and 30 mM L-arginine of GPRC6A-HEK293A cells transiently transfected with different amount of GPRC6A plasmid (2 and 4 µg). **(C)** Densitometric analysis of the western blot shown in b. **(D)** Western blot detection of CASR protein in CASR-HEK293A cells as two bands of 100 and 150 kDa. **(E)** Significant increases of the basal pERK/ERK levels after stimulation of CASR-HEK293A cells with increasing concentrations of $[Ca^{2+}]_o$ (1.0, 3.0 and 5.0 mM). **(F)** Densitometric analysis of the western blot shown in e. **(G)** Basal pERK/ERK level increases after stimulation with different concentrations (50 and 100 nM, 0.5 and 5.0 µM) of the potent CASR agonist R568 (Cayman Chemical Company; Ann Arbor, Michigan, USA). **(H)** Densitometric analysis of the western blot shown in g.

SUPPLEMENTARY FIGURE 2
(A) Representative western blot analysis of the GPRC6A and CASR proteins' expression in membrane protein fractions from 2 PAds (TBP ab51841, Abcam, Cambridge, UK). **(B)** Exemplificative western blots obtained in a GPRC6A-expressing PAd transfected with Control siRNA and with CASR siRNA.

SUPPLEMENTARY TABLE 1
Clinical and biochemical features of PHPT patients, whose surgically removed PAds were analyzed for CASR and GPRC6A membrane expression. Patient ID, identification corresponding to that used in; age, PHPT patient age at diagnosis; BMI, body mass index; Ca^{2+}, plasma ionized calcium; SCa, serum total calcium; PTH, plasma parathormone; creat, serum creatinine; tumor size, maximal diameter of the surgically removed parathyroid adenoma; kidney, diagnosis of kidney stones symptomatic disease and asymptomatic stones detected by imaging); bone, diagnosis of osteopenia/osteoporosis according WHO criteria (49).

References

1. Bandeira L, Bilezikian J. Primary hyperparathyroidism. *F1000Res* (2016) 5:F1000. doi: 10.12688/f1000research.7039.1

2. Makras P, Anastasilakis AD. Bone disease in primary hyperparathyroidism. *Metabolism* (2018) 80:57–65. doi: 10.1016/j.metabol.2017.10.003

3. Ferron M, Lacombe J, Germain A, Oury F, Karsenty G. GGCX and VKORC1 inhibit osteocalcin endocrine functions. *J Cell Biol* (2015) 208(6):761–76. doi: 10.1083/jcb.201409111

4. Diaz–Franco MC, Franco–Diaz de Leon R, Villafan–Bernal JR. Osteocalcin –GPRC6A: An update of its clinical and biological multi–organic interactions (Review). *Mol Med Rep* (2019) 19(1):15–22. doi: 10.3892/mmr.2018.9627

5. Cristiani A, Maset F, Toni LD, Guidolin D, Sabbadin D, Strapazzon G, et al. Carboxylation-dependent conformational changes of human osteocalcin. *Front Biosci (Lendmark Ed)* (2014) 19(7):1105–16. doi: 10.2741/4270

6. Komori T. Functions of osteocalcin in bone, pancreas, testis, and muscle. *Int J Mol Sci* (2020) 21(20):7513. doi: 10.3390/ijms21207513

7. Kapoor K, Pi M, Nishimoto SK, Quarles LD, Baudry J, Smith JC. The carboxylation status of osteocalcin has important consequences for its structure and dynamics. *Biochim Biophysi Acta Gen Subj* (2021) 1865(3):129809. doi: 10.1016/j.bbagen.2020.129809

8. Verdelli C, Tavanti GS, Corbetta S. Intratumor heterogeneity in human parathyroid tumors. *Histol Histopathol* (2020) 35(11):1213–28. doi: 10.14670/HH-18-230

9. Silver J, Levi R. Regulation of PTH synthesis and secretion relevant to the management of secondary hyperparathyroidism in chronic kidney disease. *Kidney Int Suppl* (2005) 95):S8–12. doi: 10.1111/j.1523-1755.2005.09501.x

10. Gianotti L, Piovesan A, Croce CG, Pellegrino M, Baffoni C, Cesario F, et al. Interplay between serum osteocalcin and insulin sensitivity in primary hyperparathyroidism. *Calcif Tissue Int* (2011) 88(3):231–7. doi: 10.1007/s00223-010-9453-1

11. Mendonça ML, Batista SL, Nogueira-Barbosa MH, Salmon CE, Paula FJ. Primary hyperparathyroidism: The influence of bone marrow adipose tissue on bone loss and of osteocalcin on insulin resistance. *Clinics* (2016) 71(8):464–9. doi: 10.6061/clinics/2016(08)09

12. Maser RE, Lenhard MJ, Pohlig RT, Balagopal PB, Abdel-Misih R. Effect of parathyroidectomy on osteopontin and undercarboxylated osteocalcin in patients with primary hyperparathyroidism. *Endocr Res* (2018) 43(1):21–8. doi: 10.1080/07435800.2017.1369432

13. Thier M, Daudi S, Bergenfelz A, Almquist M. Predictors of multiglandular disease in primary hyperparathyroidism. *Langenbeck's Arch Surg* (2018) 403(1):103–9. doi: 10.1007/s00423-017-1647-9

14. Clemmensen C, Smajilovic S, Wellendorph P, Bräuner-Osborne H. The GPCR, class c, group 6, subtype a (GPRC6A) receptor: From cloning to physiological function. *Br J Pharmacol* (2014) 171(5):1129–41. doi: 10.1111/bph.12365

15. Pi M, Nishimoto SK, Quarles LD. GPRC6A: Jack of all metabolism (or master of none). *Mol Metab* (2016) 6(2):185–93. doi: 10.1016/j.molmet.2016.12.006

16. Leach K, Hannan FM, Josephs TM, Keller AN, Møller TC, Ward DT, et al. International union of basic and clinical pharmacology. CVIII. calcium-sensing receptor nomenclature, pharmacology, and function. *Pharmacol Rev* (2020) 72 (3):558–604. doi: 10.1124/pr.119.018531

17. Leach K, Gregory KJ. Molecular insights into allosteric modulation of class c G protein-coupled receptors. *Pharmacol Res* (2017) 116:105–18. doi: 10.1016/j.phrs.2016.12.006

18. Pi M, Kapoor K, Ye R, Nishimoto SK, Smith JC, Baudry J, et al. Evidence for osteocalcin binding and activation of GPRC6A in β-cells. *Endocrinology* (2016) 157 (5):1866–80. doi: 10.1210/en.2015-2010

19. Terranegra A, Ferraretto A, Dogliotti E, Scarpellini M, Corbetta S, Barbieri AM, et al. Calcimimetic r-568 effects on activity of R990G polymorphism of calcium-sensing receptor. *J Mol Endocrinol* (2010) 45:245–56. doi: 10.1677/JME-10-0034

20. Zoch ML, Clemens TL, Riddle RC. New insights into the biology of osteocalcin. *Bone* (2016) 82:42–9. doi: 10.1016/j.bone.2015.05.046

21. Pi M, Wu Y, Quarles LD. GPRC6A mediates responses to osteocalcin in β-cells. *In Vitro pancreas vivo. J Bone Miner Res* (2011) 26(7):1680–3. doi: 10.1002/jbmr.390

22. Pi M, Quarles LD. GPRC6A regulates prostate cancer progression. *Prostate* (2012) 72(4):399–409. doi: 10.1002/pros.21442

23. Otani T, Mizokami A, Hayashi Y, Gao J, Mori Y, Nakamura S, et al. Signaling pathway for adiponectin expression in adipocytes by osteocalcin. *Cell Signal* (2015) 27:532–44. doi: 10.1016/j.cellsig.2014.12.018

24. Fujiwara T, Kanazawa S, Ichibori R, Tanigawa T, Magome T, Shingaki K, et al. L-arginine stimulates fibroblast proliferation through the GPRC6A-ERK1/2 and PI3K/Akt pathway. *PLoS One* (2014) 9(3):e92168. doi: 10.1371/journal.pone.0092168

25. Liu S, Gao F, Wen L, Ouyang M, Wang Y, Wang Q, et al. Osteocalcin induces proliferation *via* positive activation of the PI3K/Akt, P38 MAPK pathways and promotes differentiation through activation of the GPRC6A-ERK1/2 pathway in C2C12 myoblast cells. *Cell Physiol Biochem* (2017) 43(3):1100–12. doi: 10.1159/000481752

26. Zhang J, Ma Z, Yan K, Wang Y, Yang Y, Wu X. Matrix gla protein promotes the bone formation by up-regulating wnt/β-catenin signaling pathway. *Front Endocrinol* (2019) 10:891. doi: 10.3389/fendo.2019.00891

27. Conigrave AD, Hampson DR. Broad-spectrum amino acid-sensing class c G-protein coupled receptors: Molecular mechanisms, physiological significance and options for drug development. *Pharmacol Ther* (2010) 127(3):252–60. doi: 10.1016/j.pharmthera.2010.04.007

28. Dobbelstein M, Strano S, Roth J, Blandino G. p73-induced apoptosis: A question of compartments and cooperation. *Biochem Biophys Res Commun* (2005) 331(3):688–93. doi: 10.1016/j.bbrc.2005.03.155

29. Brentnall M, Rodriguez-Menocal L, De Guevara RL, Cepero E, Boise LH. Caspase-9, caspase-3 and caspase-7 have distinct roles during intrinsic apoptosis. *BMC Cell Biol* (2013) 14:32. doi: 10.1186/1471-2121-14-32

30. Zhang M, Xuan S, Bouxsein ML, von SD, Akeno N, MC F, et al. Osteoblast-specific knockout of the insulin-like growth factor (IGF) receptor gene reveals an essential role of IGF signaling in bone matrix mineralization. *J Biol Chem* (2002) 277 (46):44005–12. doi: 10.1074/jbc.M208265200

31. Zofkova I. Involvement of bone in systemic endocrine regulation. *Physiol Res* (2018) 67(5):669–77. doi: 10.33549/physiolres.933843

32. Arya AK, Singh P, Saikia UN, Sachdeva N, Dahiya D, Behera A, et al. Dysregulated mitogen-activated protein kinase pathway mediated cell cycle disruption in sporadic parathyroid tumors. *J Endocrinol Invest* (2020) 43(2):247–53. doi: 10.1007/s40618-019-01098-3

33. Corbetta S, Lania A, Filopanti M, Vicentini L, Ballaré E, Spada A. Mitogen-activated protein kinase cascade in human normal and tumoral parathyroid cells. *J Clin Endocrinol Metab* (2002) 87(5):2201–5. doi: 10.1210/jcem.87.5.8492

34. Kifor O, Kifor I, Moore FDJr, Butters RRJr, Cantor T, Gao P, et al. Decreased expression of caveolin-1 and altered regulation of mitogen-activated protein kinase in cultured bovine parathyroid cells and human parathyroid adenomas. *J Clinl Endocrinol Metab* (2003) 88(9):4455–64. doi: 10.1210/jc.2002-021427

35. Pandya C, Uzilov AV, Bellizzi J, Lau CY, Moe AS, Strahl M, et al. Genomic profiling reveals mutational landscape in parathyroid carcinomas. *JCI Insight* (2017) 2 (6):e92061. doi: 10.1172/jci.insight.92061

36. Cui M, Hu Y, Bi Y, Wang W, Wang M, Zhang X, et al. Preliminary exploration of potential molecular therapeutic targets in recurrent and metastatic parathyroid carcinomas. *Int J Cancer* (2019) 144(3):525–32. doi: 10.1002/ijc.31948

37. Verdelli C, Avagliano L, Guarnieri V, Cetani F, Ferrero S, Vicentini L, et al. Expression, function, and regulation of the embryonic transcription factor TBX1 in parathyroid tumors. *Lab Invest* (2017) 97(12):1488–99. doi: 10.1038/labinvest.2017.88

38. Verdelli C, Forno I, Morotti A, Creo P, Guarnieri V, Scillitani A, et al. The aberrantly expressed miR-372 partly impairs sensitivity to apoptosis in parathyroid tumor cells. *Endocr Relat Cancer* (2018) 25(7):761–71. doi: 10.1530/ERC-17-0204

39. Corbetta S, Mantovani G, Lania A, Borgato S, Vicentini L, Beretta E, et al. Calcium-sensing receptor expression and signalling in human parathyroid adenomas and primary hyperplasia. *Clin Endocrinol* (2000) 52(3):339–48. doi: 10.1046/j.1365-2265.2000.00933.x

40. Chen XJ, Chen X, Wu WJ, Zhou Q, Gong XH, Shi BM. Effects of FGF-23-mediated ERK/MAPK signaling pathway on parathyroid hormone secretion of parathyroid cells in rats with secondary hyperparathyroidism. *J Cell Physiol* (2018) 233(9):7092–102. doi: 10.1002/jcp.26525

41. Corbetta S, Eller-Vainicher C, Vicentini L, Lania A, Mantovani G, Beck-Peccoz P, et al. Modulation of cyclin D1 expression in human tumoral parathyroid cells: Effects of growth factors and calcium sensing receptor activation. *Cancer Lett* (2007) 255 (1):34–41. doi: 10.1016/j.canlet.2007.03.014

42. De Toni L, De Filippis V, Tescari S, Ferigo M, Ferlin A, Scattolini V, et al. Uncarboxylated osteocalcin stimulates 25-hydroxy vitamin d production in leydig cell line through a GPRC6a-dependent pathway. *Endocrinology* (2014) 155(11):4266–74. doi: 10.1210/en.2014-1283

43. Jørgensen CV, Bräuner-Osborne H. Pharmacology and physiological function of the orphan GPRC6A receptor. *Basic Clin Pharmacol Toxicol* (2020) 126(Suppl6):77–87. doi: 10.1111/bcpt.13397

44. Jung CH, Lee WJ, Hwang JY, Lee MJ, Seol SM, Kim YM, et al. The preventive effect of uncarboxylated osteocalcin against free fatty acid-induced endothelial apoptosis through the activation of phosphatidylinositol 3-kinase/Akt signaling pathway. *Metabolism* (2013) 62(9):1250–7. doi: 10.1016/j.metabol.2013.03.005

45. Obri A, Khrimian L, Karsenty G, Oury F. Osteocalcin in the brain: From embryonic development to age-related decline in cognition. *Nat Rev Endocrinol* (2018) 14(3):174–82. doi: 10.1038/nrendo.2017.181

46. Rossi M, Battafarano G, Pepe J, Minisola S, Del Fattore A. The endocrine function of osteocalcin regulated by bone resorption: A lesson from reduced and increased bone mass diseases. *Int J Mol Sci* (2019) 20(18):4502. doi: 10.3390/ijms20184502

47. Vitale JA, Sansoni V, Faraldi M, Messina C, Verdelli C, Lombardi G, et al. Circulating carboxylated osteocalcin correlates with skeletal muscle mass and risk of fall in postmenopausal osteoporotic women. *Front Endocrinol* (2021) 12:669704. doi: 10.3389/fendo.2021.669704

48. Hauschka PV, Lian JB, Cole DE, Gundberg CM. Osteocalcin and matrix gla protein: vitamin K-dependent proteins in bone. *Physiol Rev* (1989) 69(3):990–1047. doi: 10.1152/physrev.1989.69.3.990

49. Kanis JA, Melton LJ3rd, Christiansen C, Johnston CC, Khaltaev N. The diagnosis of osteoporosis. *J Bone Miner Res* (1994) 9(8):1137–41. doi: 10.1002/jbmr.5650090802

frontiers | Frontiers in Endocrinology

TYPE Original Research
PUBLISHED 17 May 2023
DOI 10.3389/fendo.2023.1191501

OPEN ACCESS

EDITED BY
Helen Knowles,
University of Oxford, United Kingdom

REVIEWED BY
Anna Kęska,
Józef Piłsudski University of Physical Education in Warsaw, Poland
Ruijie Xie,
German Cancer Research Center (DKFZ), Germany
Mingjiang Liu,
University of South China, China

*CORRESPONDENCE
Lin Xie
xielin@njucm.edu.cn

RECEIVED 22 March 2023
ACCEPTED 03 May 2023
PUBLISHED 17 May 2023

CITATION
Wang X, Yang S, He G and Xie L (2023) The association between weight-adjusted-waist index and total bone mineral density in adolescents: NHANES 2011–2018. *Front. Endocrinol.* 14:1191501. doi: 10.3389/fendo.2023.1191501

The association between weight-adjusted-waist index and total bone mineral density in adolescents: NHANES 2011–2018

Xiaohua Wang, Shuo Yang, Gansheng He and Lin Xie*

Department of Spine Surgery, Affiliated Hospital of Integrated Traditional Chinese and Western Medicine, Nanjing University of Chinese Medicine, Nanjing, China

Introduction: The weight-adjusted waist index (WWI) serves as an innovative obesity measure, seemingly surpassing body mass index (BMI) and waist circumference (WC) in evaluating lean and fat mass. This study aimed to explore the relationship between WWI and total bone mineral density (BMD) in US adolescents.

Methods: This population-based study investigated adolescents aged 8–19 years with comprehensive WWI and total BMD data from the National Health and Nutrition Examination Survey (NHANES) 2011–2018. WWI was computed by dividing WC by the square root of body weight. Weighted multivariate linear regression and smoothed curve fitting were employed to examine linear and non-linear associations. Threshold effects were determined using a two-part linear regression model. Additionally, subgroup analyses and interaction tests were conducted.

Results: Multivariate linear regression analysis revealed a significant negative association between WWI and total BMD in 6,923 US adolescents aged 8–19 years [β = -0.03, 95% CI: (-0.03, -0.03)]. This negative correlation remained consistent across all subcategories, with the exception of age, encompassing gender,ethnicity, and diabetes status subgroups. Furthermore, a non-linear relationship and saturation effect between WWI and total BMD were identified, with an inflection point at 9.88 cm/$\sqrt{}$kg.

Conclusions: Our research demonstrated a notable negative relationship and saturation effect between WWI and total BMD among US adolescents.

KEYWORDS

bone mineral density, NHANES, obese, osteoporosis, weight-adjusted-waist index, adolescent

Abbreviations: WWI, weight-adjusted waist index; BMI, body mass index; WC, waist circumference; BMD, bone mineral density; OP, osteoporosis; PBM, peak bone mass; NHANES, National Health and Nutrition Examination Survey; ALP, alkaline phosphatase; AST, aspartate aminotransferase; HDL-C, high-density lipoprotein cholesterol; LDL-C, low-density lipoprotein cholesterol; PIR, ratio of family income to poverty; BUN, blood urea nitrogen; NCHS, National Center for Health Statistics.

1 Background

Osteoporosis (OP) is a systemic degenerative bone disorder characterized by diminished bone density and compromised bone microarchitecture, resulting in bone fragility and fractures (1–3). A global epidemiological investigation estimated that roughly 200 million individuals suffer from OP worldwide, with this number increasing annually (4). Childhood and adolescence represent critical phases for bone development, with bone mass typically peaking in late adolescence (5, 6). Numerous studies have shown that bone mineral density (BMD) is traceable from childhood to adolescence and into adulthood (7, 8). Consequently, bone metabolism during childhood and adolescence plays a vital role in preventing OP in later life (9).

Obesity is defined by abnormal or excessive body fat, which negatively impacts health and is closely associated with the development of various chronic diseases (10). Childhood obesity is a major concern in the United States, affecting an estimated 14.4 million children and adolescents (11). While body mass index (BMI) and waist circumference (WC) are the predominant measures of obesity, the obesity paradox has cast doubt on the utility of BMI. It has been proposed that BMI fails to distinguish between lean and fat mass and is subject to influence by factors such as age, gender, and ethnic differences (12, 13). In contrast, WC is considered a superior indicator of body fat for predicting obesity-related diseases compared to BMI, as it demonstrates a strong correlation with abdominal fat accumulation (14, 15). However, the substantial correlation between WC and BMI constrains the utility of WC as an independent obesity marker. Consequently, in 2018, Park et al. proposed a new obesity index, the weight-adjusted waist index (WWI), which standardizes WC and body weight, rendering it easy to measure (16). Furthermore, WWI highlights the

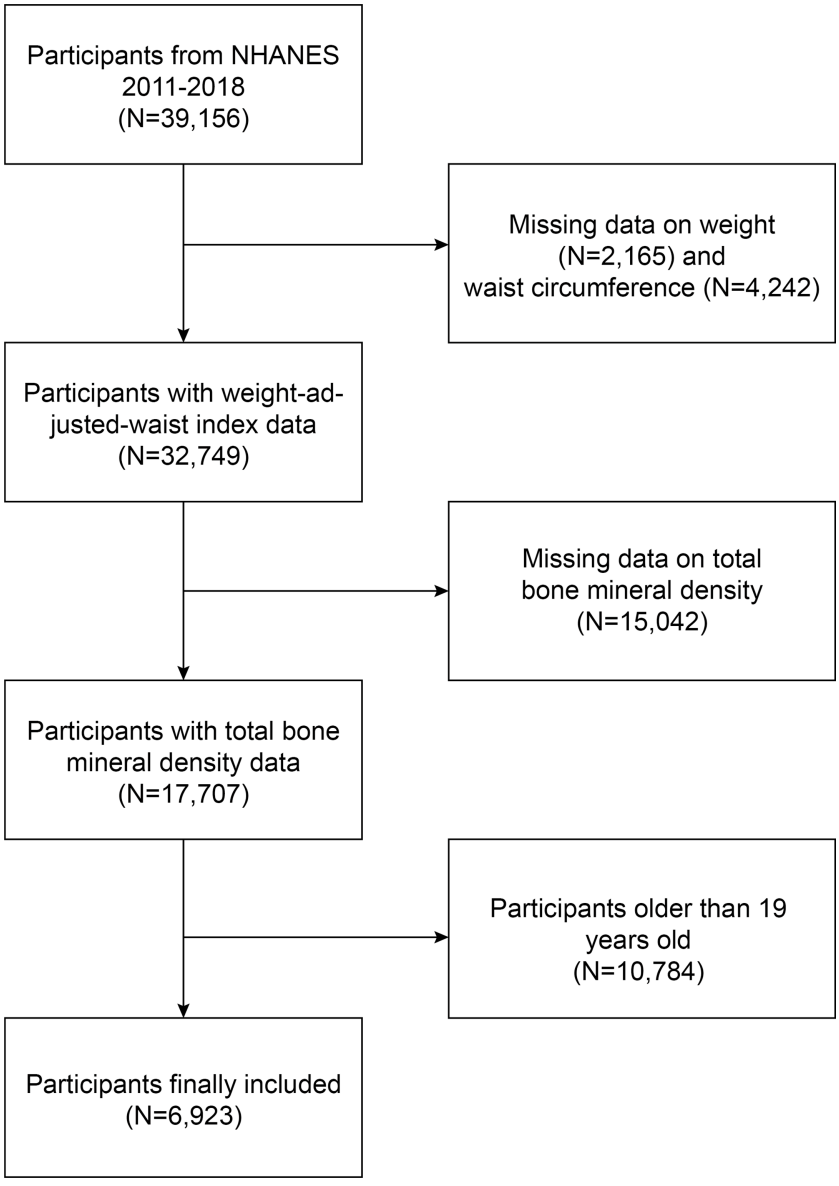

FIGURE 1
Baseline characteristics of participants.

advantages of WC and reduces the correlation between WC and BMI by primarily reflecting weight-independent central obesity. Numerous studies have demonstrated a positive relationship between WWI and the onset of hypertension, diabetes, and even all-cause and cardiovascular mortality (17–19).

As ongoing research progresses, scholars observed a potential correlation between body fat composition and bone tissue development. Consequently, tracking this development through easily quantifiable obesity indicators proves valuable. To date, no studies have established a connection between WWI and total BMD. The objective of this investigation was to examine the relationship between WWI and total BMD in US adolescents aged 8–19 years, utilizing data from the National Health and Nutrition Examination Survey (NHANES).

2 Methods

2.1 Data source and study population

NHANES is a comprehensive cross-sectional survey carried out in the United States to furnish impartial statistics regarding health concerns and population health issues (20–22). This study employed NHANES data from 2011 to 2018; out of 39,156 eligible participants, 2,165 lacked weight data, 4,242 lacked WC data, 15,042 lacked total BMD data, and 10,784 individuals aged over 19 were excluded. Ultimately, 6,923 adolescents were enrolled in the study (Figure 1).

2.2 Ethics statement

The NHANES protocol received approval from the National Research Ethics Committee on Health Statistics, and signed consent forms were obtained. Once anonymized, the NHANES data were made publicly available, enabling researchers to transform the data into a research-appropriate format. We adhered to research data usage guidelines, ensuring that data were employed solely for statistical analysis and that all experiments conformed to current standards and regulations. The authors did not access any information capable of identifying individual participants during or after data collection.

2.3 Study variables

In this study, the dependent variable is total BMD, with the expected independent variable being WWI. WWI (cm/√kg) is computed by dividing WC (cm) by the square root of body weight (kg). To guarantee data reliability, outliers were inspected as needed. Age, weight, and gender were employed to confirm data accuracy, and any erroneous data were eliminated. Total BMD was calculated using dual-energy X-ray absorptiometry results. Covariates included age, sex, race, ratio of family income to poverty (PIR), diabetes status, uric acid, albumin, alanine aminotransferase (ALT), direct high-density lipoprotein cholesterol (HDL-C), weight, alkaline phosphatase (ALP), 25OHD2 + 25OHD3, BMI, WC, aspartate aminotransferase (AST), blood urea nitrogen (BUN), glycated hemoglobin, creatinine, triglycerides, total cholesterol, total calcium, low-density lipoprotein cholesterol (LDL-C), phosphorus, and serum glucose. For additional information on confounding factors, visit http://www.cdc.gov/nchs/nhanes/.

2.4 Statistical analysis

Statistical evaluations in this investigation were executed using R (http://www.r-project.org) and EmpowerStats (http://www.empowerstats.com), adopting a significance threshold of $p<0.05$. As NHANES aims to generate data representative of the non-institutionalized civilian population within the United States, all estimates were computed utilizing sample weights in line with NCHS analytical guidelines (23, 24). Weighted multiple linear regression analysis was implemented to explore the linear relationship between WWI and total BMD, while smoothing curve fitting and threshold effects evaluation were applied to assess the non-linear association between WWI and total BMD. The study incorporated three models: Model 1 entailed no variable adjustments; Model 2 accounted for age, gender, and race; and Model 3 adjusted for all the covariates listed in Table 1 except BMI, WC, and weight. Subgroup analyses were additionally performed.

3 Results

3.1 Baseline characteristics

After applying inclusion and exclusion criteria, 6,923 participants, with a mean age of 13.03 ± 3.45 years, were included in the study. The sample comprised 51.86% boys and 48.14% girls, along with 20.05% non-Hispanic white people, 24.38% non-Hispanic black people, 20.99% Mexican-American people, 10.63% other Hispanic people, and 16.94% individuals from other racial backgrounds. The average (SD) values of WWI and total BMD were 10.50 (0.86) cm/√kg and 0.94 (0.16) g/cm^2, respectively. Table 1 outlines the clinical characteristics of the participants, with columns displaying stratified groups based on WWI quartiles. Relative to the bottom quartile, those in the top WWI quartile were more likely to be female and younger, have a higher proportion of Mexican Americans and other Hispanics, exhibit a higher prevalence of diabetes, and show increased levels of ALT, ALP, serum glucose, uric acid, glycohemoglobin, total cholesterol, triglyceride, LDL-C, BMI, and WC. Conversely, they demonstrated lower levels of PIR, albumin, AST, 25OHD2 + 25OHD3, BUN, total calcium, creatinine, direct HDL-C, weight, and total BMD ($p < 0.05$) (Table 1).

10.3389/fendo.2023.1191501

TABLE 1 Basic characteristics of participants by weight-adjusted waist index quartile.

Characteristics	Weight-adjusted waist index (cm/√kg)				p-value
	Q1 (8.04–10.43) N=1,730	Q2 (10.43–11.00) N=1,731	Q3 (11.01–11.59) N=1,731	Q4 (11.59–15.21) N=1,731	
Age (years)	15.49 ± 2.34	14.10 ± 2.99	12.55 ± 3.33	11.18 ± 3.27	<0.0001
Sex (%)					<0.0001
Male	72.26	41.15	44.51	49.14	
Female	27.74	58.85	55.49	50.86	
Race/ethnicity (%)					<0.0001
Mexican American	8.96	13.58	17.67	23.22	
Other Hispanic	6.06	7.11	8.82	9.58	
Non-Hispanic White	52.94	56.95	53.01	50.97	
Non-Hispanic Black	21.89	12.72	10.32	7.64	
Other Race	10.16	9.63	10.18	8.59	
Diabetes (%)					<0.001
Yes	0.09	0.49	0.55	0.52	
No	99.76	99.22	99.01	98.46	
Borderline	0.15	0.29	0.44	1.02	
PIR	2.65 ± 1.64	2.63 ± 1.65	2.43 ± 1.62	2.13 ± 1.50	<0.0001
Albumin (g/dl)	4.52 ± 0.31	4.48 ± 0.31	4.41 ± 0.29	4.32 ± 0.28	<0.0001
ALT (U/L)	17.50 ± 13.04	17.77 ± 12.93	20.02 ± 16.20	23.78 ± 15.28	<0.0001
AST (U/L)	23.80 ± 11.89	22.84 ± 12.64	22.47 ± 8.36	23.57 ± 7.67	0.0304
ALP (IU/L)	143.50 ± 98.84	132.49 ± 94.96	132.09 ± 88.21	144.24 ± 91.42	0.0039
vitamin D (nmol/L)	65.77 ± 22.50	65.76 ± 23.58	63.12 ± 20.03	62.85 ± 18.67	<0.0001
BUN (mg/dl)	11.89 ± 3.46	11.07 ± 3.34	11.02 ± 3.69	10.48 ± 3.06	<0.0001
Total calcium (mg/dl)	9.62 ± 0.30	9.59 ± 0.29	9.58 ± 0.31	9.54 ± 0.32	<0.0001
Creatinine (mg/dl)	0.80 ± 0.16	0.70 ± 0.15	0.68 ± 0.15	0.64 ± 0.16	<0.0001
Serum glucose (mg/dl)	87.27 ± 10.27	88.87 ± 9.24	91.04 ± 15.17	89.90 ± 11.90	<0.0001
Phosphorus (mg/dl)	4.33 ± 0.67	4.31 ± 0.63	4.29 ± 0.69	4.29 ± 0.72	0.4666
Uric acid (mg/dl)	5.18 ± 1.13	4.82 ± 1.18	5.08 ± 1.31	5.36 ± 1.27	<0.0001
Glycohemoglobin (%)	5.21 ± 0.33	5.21 ± 0.36	5.23 ± 0.40	5.31 ± 0.47	<0.0001
Total cholesterol (mg/dl)	150.21 ± 26.44	157.59 ± 27.76	158.96 ± 29.01	161.99 ± 28.96	<0.0001
Triglyceride (mg/dl)	65.27 ± 41.15	77.71 ± 48.81	81.72 ± 51.48	100.09 ± 52.53	<0.0001
LDL-C (mg/dl)	81.83 ± 23.61	90.14 ± 25.02	91.42 ± 26.30	93.95 ± 26.99	<0.0001
Direct HDL-C (mg/dl)	54.15 ± 11.53	54.48 ± 12.25	52.56 ± 12.96	49.87 ± 12.27	<0.0001
Weight (kg)	61.41 ± 13.44	56.50 ± 18.35	54.88 ± 24.59	54.58 ± 26.89	<0.0001
BMI (kg/m^2)	21.22 ± 3.48	21.71 ± 4.88	22.62 ± 6.64	24.30 ± 7.72	<0.0001
Waist circumference (cm)	73.55 ± 7.90	75.45 ± 12.17	77.74 ± 17.19	83.59 ± 20.55	<0.0001
WWI (cm/√kg)	9.45 ± 0.30	10.17 ± 0.16	10.75 ± 0.18	11.63 ± 0.44	<0.0001
Total BMD (g/cm^2)	1.06 ± 0.13	0.97 ± 0.13	0.91 ± 0.15	0.85 ± 0.14	<0.0001

Mean ± SD for continuous variables: the p-value was calculated by the weighted linear regression model. (%) for categorical variables: the p-value was calculated by the weighted chi-square test. Q, quartile; PIR, ratio of family income to poverty; BMI, body mass index; LDL-C, low-density lipoprotein cholesterol; BMD, bone mineral density; HDL-C, high-density lipoprotein cholesterol; AST, aspartate aminotransferase; ALT, alanine aminotransferase; ALP, alkaline phosphatase; BUN, blood urea nitrogen; vitamin D, 25OHD2 + 25OHD3.

TABLE 2 Association between weight-adjusted waist index (cm/$\sqrt{kg}$) and total bone mineral density (g/cm^2).

Exposure	Model 1 [β (95% CI)]	Model 2 [β (95% CI)]	Model 3 [β (95% CI)]
WWI (continuous)	−0.09 (−0.10, −0.09)	−0.02 (−0.03, −0.02)	−0.03 (−0.03, −0.03)
WWI (quartile)			
Quartile 1	Reference	Reference	Reference
Quartile 2	−0.09 (−0.10, −0.08)	−0.03 (−0.04, −0.02)	−0.03 (−0.03, −0.02)
Quartile 3	−0.15 (−0.16, −0.14)	−0.04 (−0.05, −0.04)	−0.05 (−0.05, −0.04)
Quartile 4	−0.21 (−0.22, −0.20)	−0.05 (−0.05, −0.04)	−0.06 (−0.06, −0.05)
p for trend	<0.001	<0.001	<0.001

Model 1: no covariates were adjusted. Model 2: age, gender, and race were adjusted. Model 3: age, gender, race, diabetes, PIR, albumin, ALT, AST, ALP, vitamin D, BUN, total calcium, creatinine, serum glucose, phosphorus, uric acid, glycohemoglobin, total cholesterol, triglyceride, LDL-C, and direct HDL-C were adjusted.
PIR, ratio of family income to poverty; LDL-C, low-density lipoproteincholesterol; HDL-C, high-density lipoprotein cholesterol; AST, aspartate aminotransferase; ALT, alanine aminotransferase; ALP, alkaline phosphatase; BUN, blood urea nitrogen; vitamin D, 25OHD2 + 25OHD3.

TABLE 3 Association between weight-adjusted waist index (cm/$\sqrt{kg}$) and total bone mineral density (g/cm^2).

	β (95% CI)	*p* for interaction
Stratified by gender		0.3371
Male	1.20 (1.07, 1.35)	
Female	1.12 (1.03, 1.21)	
Stratified by race		0.6982
Mexican American	−0.03 (−0.04, −0.02)	
Other Hispanic	−0.03 (−0.04, −0.02)	
Non-Hispanic White	−0.03 (−0.03, −0.03)	
Non-Hispanic Black	−0.02 (−0.03, −0.02)	
Other Race	−0.03 (−0.04, −0.02)	
Stratified by age		<0.0001
8–9 years old	−0.01 (−0.02, −0.00)	
10–11 years old	−0.02 (−0.02, −0.01)	
12–13 years old	−0.03 (−0.03, −0.02)	
14–15 years old	−0.02 (−0.02, −0.01)	
16–17 years old	−0.02 (−0.02, −0.01)	
18–19 years old	−0.03 (−0.04, −0.02)	
Stratified by PIR		0.2997
<1.3	−0.03 (−0.03, −0.02)	
1.3–3.5	−0.03 (−0.03, −0.02)	
>3.5	−0.03 (−0.04, −0.03)	
Stratified by diabetes		0.9309
Yes	−0.01 (−0.11, 0.08)	
No	−0.03 (−0.03, −0.03)	
Borderline	−0.03 (−0.11, 0.04)	

In subgroup analyses stratified by sex, race, age, and diabetes status. The model adjusted for covariates such as age, sex, race, diabetes, PIR, albumin, ALT, AST, ALP, vitamin D, BUN, total calcium, creatinine, serum glucose, phosphorus, uric acid, glycohemoglobin, total cholesterol, triglycerides, LDL-C, and direct HDL-C, but the model did not adjust for the stratification variables themselves.
PIR, ratio of family income to poverty; LDL-C, low-density lipoproteincholesterol; HDL-C, high-density lipoprotein cholesterol; AST, aspartate aminotransferase; ALT, alanine aminotransferase; ALP, alkaline phosphatase; BUN, blood urea nitrogen; vitamin D, 25OHD2 + 25OHD3.

3.2 Association between WWI and total BMD

Table 2 presents the connection between WWI and total BMD. All models exhibited an inverse association between WWI and total BMD. Upon adjusting for all confounding variables, a one-unit increment in WWI was significantly linked to a 0.03 g/cm^2 reduction in total BMD (Model 3: β = −0.03, 95% CI: −0.03, −0.03). This correlation persisted as statistically significant when categorizing WWI into quartiles: a one-unit rise in WWI corresponded to a 0.06-unit larger decrease in total BMD for cipants in the top WWI quartile compared to those in the bottom WWI quartile (β = -0.06, 95% CI: −0.06, −0.05; p for trend < 0.001).

3.3 Subgroup analysis

A subgroup analysis was conducted to evaluate the stability of the relationship between WWI and total BMD across different demographic contexts. The results indicated that the influence of factors other than age stratification on the relationship between WWI and total BMD was not significant. As illustrated in Table 3, the inverse association between WWI and total BMD was not significantly affected by any of the remaining strata, including gender, ethnicity, diabetes status, and the ratio of family income to poverty, except for the age stratum (p > 0.05 for all interactions). However, in the age-stratified subgroup analyses, the absolute effect values for 8–11-year-olds were significantly smaller than those for 12–19-year-olds. This implies that each unit increase in WWI for 8–11-year-olds was associated with a 0.01 cm/√kg decrease in total BMD, while each unit increase in WWI for 12–19-year-olds corresponded to a 0.03 cm/√kg decrease in total BMD. Furthermore, the results of the WWI quartile subgroup analysis demonstrated a dose–response relationship between WWI and total BMD (Table 3).

3.4 Non-linearity and saturation effect analysis between WWI and total BMD

Smooth curve fitting was implemented to delineate the non-linear association and saturation phenomenon between WWI and total BMD (Figure 2). The results uncovered that the saturation effect value for the WWI–total BMD relationship was 9.88 cm/√kg for all participants (Table 4). When WWI was below 9.88 cm/√kg, the effect value registered at −0.06; on the other hand, when WWI surpassed 9.88 cm/√kg, the effect value transitioned to −0.02. All participants were segregated into three groups with 2-year age intervals. Smooth curves and saturation effect evaluation were applied to ascertain WWI saturation values for total BMD within each age bracket (Table 4; Figure 3).

4 Discussion

Our cross-sectional investigation uncovered a notable negative correlation between WWI and total BMD among adolescents. Subgroup analyses and interaction evaluations revealed that this negative correlation remained consistent across all subcategories, with the exception of age, encompassing gender, ethnicity, and diabetes status subgroups. Notably, we discerned an L-shaped association between WWI and total BMD, exhibiting an inflection point at 9.98 cm/√kg.

To the best of our knowledge, this constitutes the first cross-sectional investigation exploring the relationship between WWI and total BMD. Globally, recognized standards for defining obesity include BMI and WC (14, 25–27). Numerous studies have reported a positive correlation between BMI, WC, and BMD (28, 29). Leonard, et al. concluded that childhood and adolescent obesity is linked to increased BMD by analyzing data from 182 children and adolescents aged 4–20 years, gathered from the Nutrition and

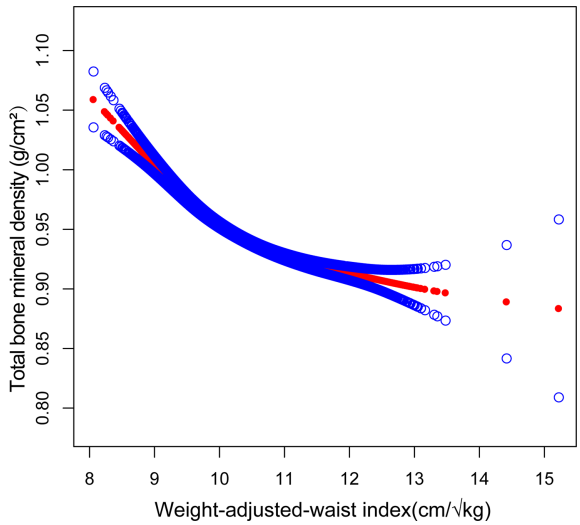

FIGURE 2
Association between WWI and total bone mineral density (The solid red line represents the smooth curve fit between variables. Blue bands represent the 95% confidence interval from the fit).

10.3389/fendo.2023.1191501

TABLE 4 Saturation effect analysis of WWI (cm/$\sqrt{kg}$) on total BMD (g/cm^2).

Total bone mineral density	Model: saturation effect analysis [β (95% CI) P value]
WWI turning point (K)	9.88
<K, effect1	−0.06(−0.07, −0.05) <0.0001
>K, effect2	−0.02(−0.03, −0.02) <0.0001
Log-likelihood ratio	<0.001
Subgroup analysis stratified by age	
WWI turning point for 8–9 years old (K)	10.55
<K, effect1	−0.04 (−0.07, −0.02) 0.0003
>K, effect2	−0.01 (−0.01, −0.00) 0.0477
Log-likelihood ratio	0.006
WWI turning point for 10–11 years old (K)	11.3
<K, effect1	−0.02 (−0.03, −0.02) <0.0001
>K, effect2	−0.00 (−0.02, 0.01) 0.5770
Log-likelihood ratio	0.057
WWI turning point for 12–13 years old (K)	9.91
<K, effect1	−0.06 (−0.09, −0.04) <0.0001
>K, effect2	−0.02 (−0.03, −0.01) 0.0004
Log-likelihood ratio	0.002
WWI turning point for 14–15 years old (K)	9.87
<K, effect1	−0.06 (−0.08, −0.03) <0.0001
>K, effect2	0.00 (−0.01, 0.02) 0.4910
Log-likelihood ratio	<0.001
WWI turning point for 16–17 years old (K)	9.51
<K, effect1	−0.07 (−0.10, −0.03) <0.0001
>K, effect2	−0.01 (−0.02, 0.00) 0.1501
Log-likelihood ratio	0.001
WWI turning point for 18–19 years old (K)	10.00
<K, effect1	−0.07 (−0.09, −0.04) <0.0001
>K, effect2	0.00 (−0.01, 0.01) 0.9354
Log-likelihood ratio	<0.001

Age, gender, race, diabetes status, albumin, ALT, AST, ALP, BMI, vitamin D, BUN, total cholesterol, total calcium, creatinine, phosphorus, glycohemoglobin, triglyceride, LDL-C, direct HDL-C, uric acid, serum glucose, refrigerated serum, and PIR were adjusted.
PIR, ratio of family income to poverty; LDL-C, low-density lipoproteincholesterol; HDL-C, high-density lipoprotein cholesterol; AST, aspartate aminotransferase; ALT, alanine aminotransferase; ALP, alkaline phosphatase; BUN, blood urea nitrogen; vitamin D, 25OHD2 + 25OHD3.

Growth Laboratory at the Children's Hospital of Philadelphia, and categorizing them into obese and non-obese groups based on BMI and WC (30). However, due to the limited sample size in this study, additional research with a larger sample is warranted. Ouyang et al. incorporated data from 6,143 adolescents aged 8–19 from the 2011–2020 NHANES and utilized smooth curve fitting and threshold effect analysis for statistical evaluation. The smooth curve fitting results revealed a significant positive association between BMI and BMD. Threshold effect analysis determined that maintaining BMI at saturation (21.5kg/m^2) could minimize other adverse consequences and optimize BMD (31). Wang et al. evaluated the association between BMI, WC, and BMD by incorporating data from 4,056 US adolescents aged 8–19 years from the 2011–2018 NHANES. They concluded that both BMI and WC were positively associated with total BMD and that a saturation effect of BMD could be achieved by maintaining BMI at 22 kg/m^2 and WC at 70.5 cm (32). However, as research has progressed, some scholars have discovered an obesity paradox when using BMI and WC as obesity measures. The obesity paradox suggests that obesity does not necessarily shorten patients' expected survival time and that

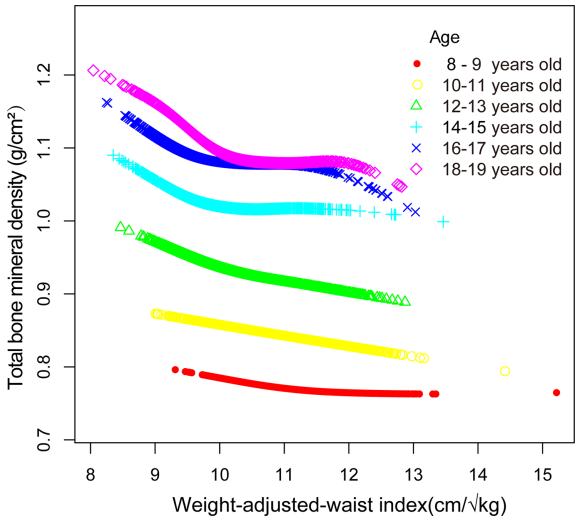

FIGURE 3
Association between WWI and total bone mineral density stratified by age.

overweight individuals may have a slightly lower risk of death compared to those with normal weight and may even exhibit beneficial effects in some cases. The existence of the obesity paradox raises questions about the validity of BMI and WC as obesity measures among researchers (33–36). Consequently, identifying an obesity index that eliminates the obesity paradox is essential; WWI is a recently devised anthropometric index that has gained recognition as a reliable obesity measure alongside BMI and WC, attributed to its straightforward calculation and capacity to discern between lean and fat masses (37, 38). Contemporary research has substantiated WWI's ability to differentiate muscle mass from fat mass, and its application has extended to various fields, including cardiovascular disease and obesity (39). Numerous studies have demonstrated that WWI is a distinct anthropometric index positively associated with heart failure incidence and mortality rates (40, 41). Remarkably, the obesity paradox observed in the relationship between BMI and mortality is absent in the association between WWI and mortality (42). Moreover, some researchers contend that the obesity paradox might not exist at all, potentially due to BMI's limitations in differentiating between muscle mass and fat mass (43, 44). Our findings diverge from prior studies. While earlier research has indicated positive correlations between BMI, WC, and total BMD, our investigation identified a negative association between WWI and total BMD.

At present, the potential mechanisms underpinning the observed negative association between WWI and total BMD are not well elucidated. Several mechanisms might be involved (32). First, excessive body fat accumulation and elevated obesity levels result in increased static mechanical compliance, imposing various static mechanical stresses on bones and inducing alterations in bone structure (45–47). Subsequently, research has indicated that obesity augments the population of adipocytes within the bone marrow while concurrently modifying their metabolic function. The bone marrow houses bone mesenchymal stem cells (BMSCs), which possess the capacity to differentiate into both osteoblasts and adipocytes (48, 49). The presence of obesity has been demonstrated to promote the differentiation of BMSCs towards adipocytes, culminating in a heightened presence of adipocytes within the bone marrow and a concomitant reduction in the osteoblast population (50). Excessive fat cell accumulation within the bone marrow results in an imbalance in osteocyte activity and diminished bone turnover, predisposing individuals to surgical intervention at a younger age (51). Moreover, obesity is associated with an increased susceptibility to inflammation (52). The expansion of adipocytes in the bone marrow microenvironment not only stimulates osteoclastogenesis and activation but also restricts osteoprotegerin secretion, inhibits osteoblast differentiation, and expedites the release of inflammatory and immunomodulatory factors that facilitate osteoclast formation (53, 54).

The conclusions drawn from this study warrant careful consideration, given several constraints. Primarily, the study's cross-sectional framework hinders the establishment of a causal link between WWI and total BMD. Additionally, database restrictions precluded the collection of information regarding lifestyle, dietary habits, bone metabolism parameters, and calcium and vitamin D intake for all participants, which may have impacted total BMD. Lastly, the unavailability of youth fracture data due to database limitations rendered it infeasible to ascertain whether the fracture incidence was elevated in young individuals with higher WWI compared to the general population. Notwithstanding the aforementioned constraints, the merits of this investigation warrant recognition. Primarily, employing a nationally representative cohort ensured that the results encapsulated the heterogeneity of the youth demographic across the United States. Additionally, the substantial sample size facilitated subgroup analyses by segregating participants aged 8–19 into distinct age categories.

5 Conclusion

This investigation's outcomes reveal an inverse association and saturation phenomenon between WWI and total BMD among American adolescents. The implications suggest that maintaining WWI within the optimal range could be vital for effectively managing bone metabolic health during this developmental stage. Nonetheless, to corroborate these conclusions, additional longitudinal research with more extensive cohorts is required.

Data availability statement

Publicly available datasets were analyzed in this study. This data can be found here: https://www.cdc.gov/nchs/nhanes/index.htm.

Ethics statement

The studies involving human participants were reviewed and approved by The National Research Ethics Committee. Written informed consent to participate in this study was provided by the participants' legal guardian/next of kin.

Author contributions

XW and LX designed the research. XW, SY, and GH collected and analyzed the data. XW drafted the manuscript. LX revised the manuscript. All authors contributed to the article and approved the submitted version.

Funding

The current research was funded by Jiangsu Provincial Traditional Chinese Medicine Science and Technology Development Plan Project (2020 ZD202008), Science and Technology Projects in Jiangsu Province (2019 BE2019765), and Natural Science Foundation of Jiangsu Province (BK20221420).

Conflict of interest

The authors declare that the research was conducted in the absence of any commercial or financial relationships that could be construed as a potential conflict of interest.

Publisher's note

References

1. Fassio A, Idolazzi L, Rossini M, Gatti D, Adami G, Giollo A, et al. The obesity paradox and osteoporosis. *Eat Weight Disord* (2018) 23:293–302. doi: 10.1007/s40519-018-0505-2

2. Bliuc D, Nguyen ND, Milch VE, Nguyen TV, Eisman JA, Center JR. Mortality risk associated with low-trauma osteoporotic fracture and subsequent fracture in men and women. *Jama* (2009) 301:513–21. doi: 10.1001/jama.2009.50

3. Barrett-Connor E, Siris ES, Wehren LE, Miller PD, Abbott TA, Berger ML, et al. Osteoporosis and fracture risk in women of different ethnic groups. *J Bone Miner Res* (2005) 20:185–94. doi: 10.1359/JBMR.041007

4. Qaseem A, Forciea MA, McLean RM, Denberg TD, Barry MJ, Cooke M, et al. Treatment of low bone density or osteoporosis to prevent fractures in men and women: a clinical practice guideline update from the American college of physicians. *Ann Intern Med* (2017) 166:818–39. doi: 10.7326/M15-1361

5. Baxter-Jones AD, Faulkner RA, Forwood MR, Mirwald RL, Bailey DA. Bone mineral accrual from 8 to 30 years of age: an estimation of peak bone mass. *J Bone Miner Res* (2011) 26:1729–39. doi: 10.1002/jbmr.412

6. Pan K, Zhang C, Yao X, Zhu Z. Association between dietary calcium intake and BMD in children and adolescents. *Endocr Connect* (2020) 9:194–200. doi: 10.1530/EC-19-0534

7. Yang Y, Wu F, Winzenberg T, Jones G. Tracking of areal bone mineral density from age eight to young adulthood and factors associated with deviation from tracking: a 17-year prospective cohort study. *J Bone Miner Res* (2018) 33:832–9. doi: 10.1002/jbmr.3361

8. Foley S, Quinn S, Jones G. Tracking of bone mass from childhood to adolescence and factors that predict deviation from tracking. *Bone* (2009) 44:752–7. doi: 10.1016/j.bone.2008.11.009

9. Ma CM, Lu N, Zhang MM, Kong FS, Lu Q, Yin FZ, et al. The relationship between obesity and bone mineral density in children and adolescents: analysis of the national health and nutrition examination survey. *Arch Osteoporos* (2023) 18:25. doi: 10.1007/s11657-022-01208-4

10. Rinonapoli G, Pace V, Ruggiero C, Ceccarini P, Bisaccia M, Meccariello L, et al. Obesity and bone: a complex relationship. *Int J Mol Sci* (2021) 22:24. doi: 10.3390/ijms222413662

11. Skinner AC, Ravanbakht SN, Skelton JA, Perrin EM, Armstrong SC. Prevalence of obesity and severe obesity in US children, 1999-2016. *Pediatr* (2018) 141(3): e20173459. doi: 10.1542/peds.2017-3459

12. Jackson AS, Stanforth PR, Gagnon J, Rankinen T, Leon AS, Rao DC, et al. The effect of sex, age and race on estimating percentage body fat from body mass index: the heritage family study. *Int J Obes Relat Metab Disord* (2002) 26:789–96. doi: 10.1038/sj.ijo.0802006

13. Lam BC, Koh GC, Chen C, Wong MT, Fallows SJ. Comparison of body mass index (BMI), body adiposity index (BAI), waist circumference (WC), waist-To-Hip ratio (WHR) and waist-To-Height ratio (WHtR) as predictors of cardiovascular disease risk factors in an adult population in Singapore. *PloS One* (2015) 10:e0122985. doi: 10.1371/journal.pone.0122985

14. Cornier MA, Després JP, Davis N, Grossniklaus DA, Klein S, Lamarche B, et al. Assessing adiposity: a scientific statement from the American heart association. *Circulation* (2011) 124:1996–2019. doi: 10.1161/CIR.0b013e318233bc6a

15. Pischon T, Boeing H, Hoffmann K, Bergmann M, Schulze MB, Overvad K, et al. General and abdominal adiposity and risk of death in Europe. *N Engl J Med* (2008) 359:2105–20. doi: 10.1056/NEJMoa0801891

16. Park Y, Kim NH, Kwon TY, Kim SG. A novel adiposity index as an integrated predictor of cardiometabolic disease morbidity and mortality. *Sci Rep* (2018) 8:16753. doi: 10.1038/s41598-018-35073-4

17. Li Q, Qie R, Qin P, Zhang D, Guo C, Zhou Q, et al. Association of weight-adjusted-waist index with incident hypertension: the rural Chinese cohort study. *Nutr Metab Cardiovasc Dis* (2020) 30:1732–41. doi: 10.1016/j.numecd.2020.05.033

18. Ding C, Shi Y, Li J, Li M, Hu L, Rao J, et al. Association of weight-adjusted-waist index with all-cause and cardiovascular mortality in China: a prospective cohort study. *Nutr Metab Cardiovasc Dis* (2022) 32:1210–7. doi: 10.1016/j.numecd.2022.01.033

19. Liu Y, Liu X, Zhang S, Zhu Q, Fu X, Chen H, et al. Association of anthropometric indices with the development of diabetes among hypertensive patients in China: a cohort study. *Front Endocrinol (Lausanne)* (2021) 12:736077. doi: 10.3389/fendo.2021.736077

20. Curtin LR, Mohadjer LK, Dohrmann SM, Kruszon-Moran D, Mirel LB, Carroll MD, et al. National health and nutrition examination survey: sample design, 2007-2010. *Vital Health Stat* (2013) 2:1–23.

21. Xie R, Zhang Y. Is assessing the degree of hepatic steatosis and fibrosis based on index calculations the best choice for epidemiological studies? *Environ pollut* (2023) 317:120783. doi: 10.1016/j.envpol.2022.120783

22. Xie R, Zhang Y. Association between 19 dietary fatty acids intake and rheumatoid arthritis: results of a nationwide survey. *Prostaglandins Leukot Essent Fatty Acids* (2023) 188:102530. doi: 10.1016/j.plefa.2022.102530

23. Xie R, Zhang Y. Associations between dietary flavonoid intake with hepatic steatosis and fibrosis quantified by VCTE: evidence from NHANES and FNDDS. *Nutr Metab Cardiovasc Dis* (2023) S0939–4753(23)00090-X. doi: 10.1016/j.numecd.2023.03.005

24. Xie R, Liu Y, Wang J, Zhang C, Xiao M, Liu M, et al. Race and gender differences in the associations between cadmium exposure and bone mineral density in US adults. *Biol Trace Elem Res* (2022). doi: 10.1007/s12011-022-03521-y

25. Browning LM, Hsieh SD, Ashwell M. A systematic review of waist-to-height ratio as a screening tool for the prediction of cardiovascular disease and diabetes: 0·5 could be a suitable global boundary value. *Nutr Res Rev* (2010) 23:247–69. doi: 10.1017/S0954422410000144

26. Nguyen NT, Magno CP, Lane KT, Hinojosa MW, Lane JS. Association of hypertension, diabetes, dyslipidemia, and metabolic syndrome with obesity: findings from the national health and nutrition examination survey, 1999 to 2004. *J Am Coll Surg* (2008) 207:928–34. doi: 10.1016/j.jamcollsurg.2008.08.022

27. Wilson PW, D'Agostino RB, Sullivan L, Parise H, Kannel WB. Overweight and obesity as determinants of cardiovascular risk: the framingham experience. *Arch Intern Med* (2002) 162:1867–72. doi: 10.1001/archinte.162.16.1867

28. Julian V, O'Malley G, Metz L, Weghuber D, Courteix D, Fillon A, et al. Does the severity of obesity influence bone density, geometry and strength in adolescents? *Pediatr Obes* (2021) 16:e12826. doi: 10.1111/ijpo.12826

29. Zhang L, Li H, Zhang Y, Kong Z, Zhang T, Zhang Z. Association of body compositions and bone mineral density in chinese children and adolescents: compositional data analysis. *BioMed Res Int* (2021) 2021:1904343. doi: 10.1155/2021/1904343

30. Leonard MB, Shults J, Wilson BA, Tershakovec AM, Zemel BS. Obesity during childhood and adolescence augments bone mass and bone dimensions. *Am J Clin Nutr* (2004) 80:514–23. doi: 10.1093/ajcn/80.2.514

31. Ouyang Y, Quan Y, Guo C, Xie S, Liu C, Huang X, et al. Saturation effect of body mass index on bone mineral density in adolescents of different ages: a population-based study. *Front Endocrinol (Lausanne)* (2022) 13:922903. doi: 10.3389/fendo.2022.922903

32. Wang GX, Fang ZB, Li HL, Liu DL, Chu SF, Zhao HX. Effect of obesity status on adolescent bone mineral density and saturation effect: a cross-sectional study. *Front Endocrinol (Lausanne)* (2022) 13:994406. doi: 10.3389/fendo.2022.994406

33. Mesinovic J, Jansons P, Zengin A, de Courten B, Rodriguez AJ, Daly RM, et al. Exercise attenuates bone mineral density loss during diet-induced weight loss in adults with overweight and obesity: a systematic review and meta-analysis. *J Sport Health Sci* (2021) 10:550–9. doi: 10.1016/j.jshs.2021.05.001

34. Aparisi Gómez MP, Ayuso Benavent C, Simoni P, Aparisi F, Guglielmi G, Bazzocchi A. Fat and bone: the multiperspective analysis of a close relationship. *Quant Imaging Med Surg* (2020) 10:1614–35. doi: 10.21037/qims.2020.01.11

35. Chin KY, Wong SK, Ekeuku SO, Pang KL. Relationship between metabolic syndrome and bone health - an evaluation of epidemiological studies and mechanisms involved. *Diabetes Metab Syndr Obes* (2020) 13:3667–90. doi: 10.2147/DMSO.S275560

36. Jensen VFH, Mølck AM, Dalgaard M, McGuigan FE, Akesson KE. Changes in bone mass associated with obesity and weight loss in humans: applicability of animal models. *Bone* (2021) 145:115781. doi: 10.1016/j.bone.2020.115781

37. Kim JY, Choi J, Vella CA, Criqui MH, Allison MA, Kim NH. Associations between weight-adjusted waist index and abdominal fat and muscle mass: multi-ethnic study of atherosclerosis. *Diabetes Metab J* (2022) 46:747–55. doi: 10.4093/dmj.2021.0294

38. Wu L, Zhu W, Qiao Q, Huang L, Li Y, Chen L. Novel and traditional anthropometric indices for identifying metabolic syndrome in non-overweight/obese adults. *Nutr Metab (Lond)* (2021) 18:3. doi: 10.1186/s12986-020-00536-x

39. Kim JE, Choi J, Kim M, Won CW. Assessment of existing anthropometric indices for screening sarcopenic obesity in older adults. *Br J Nutr* (2023) 129:875–87. doi: 10.1017/S0007114522001817

40. Zhang D, Shi W, Ding Z, Park J, Wu S, Zhang J. Association between weight-adjusted-waist index and heart failure: results from national health and nutrition examination survey 1999-2018. *Front Cardiovasc Med* (2022) 9:1069146. doi: 10.3389/fcvm.2022.1069146

41. Cai S, Zhu T, Ding Y, Cheng B, Zhang A, Bao Q, et al. The relationship between the weight-adjusted-waist index and left ventricular hypertrophy in Chinese hypertension adults. *Hypertens Res* (2023) 46:253–60. doi: 10.1038/s41440-022-01075-z

42. Kim NH, Park Y, Kim NH, Kim SG. Weight-adjusted waist index reflects fat and muscle mass in the opposite direction in older adults. *Age Ageing* (2021) 50:780–6. doi: 10.1093/ageing/afaa208

43. Antonopoulos AS, Oikonomou EK, Antoniades C, Tousoulis D. From the BMI paradox to the obesity paradox: the obesity-mortality association in coronary heart disease. *Obes Rev* (2016) 17:989–1000. doi: 10.1111/obr.12440

44. Standl E, Erbach M, Schnell O. Defending the con side: obesity paradox does not exist. *Diabetes Care* (2013) 36 Suppl 2:S282–6. doi: 10.2337/dcS13-2040

45. Lanyon LE. Control of bone architecture by functional load bearing. *J Bone Miner Res* (1992) 7 Suppl 2:S369–75. doi: 10.1002/jbmr.5650071403

46. Hla MM, Davis JW, Ross PD, Wasnich RD, Yates AJ, Ravn P, et al. A multicenter study of the influence of fat and lean mass on bone mineral content: evidence for differences in their relative influence at major fracture sites. *Early Postmenopausal Intervention Cohort (EPIC) Study Group Am J Clin Nutr* (1996) 64:354–60. doi: 10.1093/ajcn/64.3.345

47. Dakanalis A, Mentzelou M, Papadopoulou SK, Papandreou D, Spanoudaki M, Vasios GK, et al. The association of emotional eating with overweight/obesity, depression, anxiety/stress, and dietary patterns: a review of the current clinical evidence. *Nutrients* (2023) 15:5. doi: 10.3390/nu15051173

48. Zong Q, Bundkirchen K, Neunaber C, Noack S. Are the properties of bone marrow-derived mesenchymal stem cells influenced by overweight and obesity? *Int J Mol Sci* (2023) 24:5. doi: 10.3390/ijms24054831

49. Vanhie JJ, Kim W, Ek Orloff L, Ngu M, Collao N, De Lisio M. The role of exercise-and high fat diet-induced bone marrow extracellular vesicles in stress hematopoiesis. *Front Physiol* (2022) 13:1054463. doi: 10.3389/fphys.2022.1054463

50. Khan AU, Qu R, Fan T, Ouyang J, Dai J. A glance on the role of actin in osteogenic and adipogenic differentiation of mesenchymal stem cells. *Stem Cell Res Ther* (2020) 11:283. doi: 10.1186/s13287-020-01789-2

51. Fintini D, Cianfarani S, Cofini M, Andreoletti A, Ubertini GM, Cappa M, et al. The bones of children with obesity. *Front Endocrinol (Lausanne)* (2020) 11:200. doi: 10.3389/fendo.2020.00200

52. Guerrero-Romero F, Castellanos-Juárez FX, Salas-Pacheco JM, Morales-Gurrola FG, Salas-Leal AC, Simental-Mendía LE. Association between the expression of TLR4, TLR2, and MyD88 with low-grade chronic inflammation in individuals with metabolically healthy obesity. *Mol Biol Rep* (2023) 50(5):4723–8. doi: 10.1007/s11033-023-08338-z

53. Segar AH, Fairbank JCT, Urban J. Leptin and the intervertebral disc: a biochemical link exists between obesity, intervertebral disc degeneration and low back pain-an *in vitro* study in a bovine model. *Eur Spine J* (2019) 28:214–23. doi: 10.1007/s00586-018-5778-7

54. Forte YS, Renovato-Martins M, Barja-Fidalgo C. Cellular and molecular mechanisms associating obesity to bone loss. *Cells* (2023) 12(4):521. doi: 10.3390/cells12040521

frontiers | Frontiers in Endocrinology

TYPE Original Research
PUBLISHED 12 June 2023
DOI 10.3389/fendo.2023.1127536

OPEN ACCESS

EDITED BY
Michela Rossi,
Bambino Gesù Children's Hospital (IRCCS), Italy

REVIEWED BY
Xiaofang Wang,
Texas A&M University Baylor College of Dentistry, United States
Akiko Suzuki,
University of Missouri–Kansas City, United States

*CORRESPONDENCE
Dalit Sela-Donenfeld
dalit.seladon@mail.huji.ac.il
Efrat Monsonego-Ornan
efrat.mo@mail.huji.ac.il

RECEIVED 19 December 2022
ACCEPTED 21 February 2023
PUBLISHED 12 June 2023

CITATION
Janssen JN, Kalev-Altman R, Shalit T, Sela-Donenfeld D and Monsonego-Ornan E (2023) Differential gene expression in the calvarial and cortical bone of juvenile female mice.
Front. Endocrinol. 14:1127536.
doi: 10.3389/fendo.2023.1127536

Differential gene expression in the calvarial and cortical bone of juvenile female mice

Jerome Nicolas Janssen[1], Rotem Kalev-Altman[1,2], Tali Shalit[3], Dalit Sela-Donenfeld[2*] and Efrat Monsonego-Ornan[1*]

[1]The Institute of Biochemistry, Food Science and Nutrition, The Faculty of Agriculture, Food and Environment, The Hebrew University of Jerusalem, Rehovot, Israel, [2]The Koret School of Veterinary Medicine, The Faculty of Agriculture, Food and Environment, The Hebrew University of Jerusalem, Rehovot, Israel, [3]The Ilana and Pascal Mantoux Institute for Bioinformatics, The Nancy and Stephen Grand Israel National Center for Personalized Medicine, Weizmann Institute of Science, Rehovot, Israel

Introduction: Both the calvarial and the cortical bones develop through intramembranous ossification, yet they have very different structures and functions. The calvaria enables the rapid while protected growth of the brain, whereas the cortical bone takes part in locomotion. Both types of bones undergo extensive modeling during embryonic and post-natal growth, while bone remodeling is the most dominant process in adults. Their shared formation mechanism and their highly distinct functions raise the fundamental question of how similar or diverse the molecular pathways that act in each bone type are.

Methods: To answer this question, we aimed to compare the transcriptomes of calvaria and cortices from 21-day old mice by bulk RNA-Seq analysis.

Results: The results revealed clear differences in expression levels of genes related to bone pathologies, craniosynostosis, mechanical loading and bone-relevant signaling pathways like WNT and IHH, emphasizing the functional differences between these bones. We further discussed the less expected candidate genes and gene sets in the context of bone. Finally, we compared differences between juvenile and mature bone, highlighting commonalities and dissimilarities of gene expression between calvaria and cortices during post-natal bone growth and adult bone remodeling.

Discussion: Altogether, this study revealed significant differences between the transcriptome of calvaria and cortical bones in juvenile female mice, highlighting the most important pathway mediators for the development and function of two different bone types that originate both through intramembranous ossification.

KEYWORDS

juvenile, development, mouse, cortical, calvarial, transcriptome, locomotion

Introduction

The calvaria, the upper structure of the skull, allows fast and protected brain growth without heavy load bearing. Conversely, the cortical bone, which is the external layer of long bones, is crucial for locomotion and is constantly remodeled under the influence of weight loading. Despite differences in structure and function, both bones develop through the mechanism of intramembranous ossification, which initiates in the embryo and extensively progresses in neonates (1). The shared mode of formation of the cortical and calvarial bone, coupled with their distinct structures and functions, raises the fundamental question of how similar or diverged the molecular pathways that control their post-natal growth are. Investigating these mechanisms will enable a better understanding of the fundamental connection between shape and function and unravel the origin of specific bone-type diseases.

The process of intramembranous ossification is initiated by the condensation of mesenchymal cells in the flat bones of the skull and in the cortices of long bones. Following the differentiation of these mesenchymal cells into osteoblast (2, 3), a collagen-proteoglycan matrix becomes deposited, which enables the binding of calcium salts for the calcification of the bone matrix. Once embedded into the calcified bone matrix, osteoblasts differentiate into osteocytes regulating the mass and shape of the various types of bone (1).

In mice, the calvaria is formed by several skull bones connected through cranial sutures derived from the cranial neural crest and head mesoderm (4). Calvarial growth is the most intense during the first 9 post-natal days, but parameters like calvaria width still increase up to 25 post-natal days (5). The time for the fusion of the posterior frontal suture has been reported to end between 13 and 45 post-natal days (6, 7). However, sutures like the lambdoid suture remain unfused throughout life in mice (8).

On the other hand, the femoral cortical bone originates from the porous bone collar formed by osteoblasts, which derives from the lateral plate mesoderm during the early stages of bone development (9). In C57BL/6J mice, the cortical area increases nonlinearly between birth and 112 post-natal days. In contrast, the cortical thickness increases linearly from 14 to 112 post-natal days, indicating the switch from primarily bone formation to bone remodeling (10). Furthermore, the cortical bone grows by forming alternating struts and woven bone rings before becoming remodeled into a dense lamellar structure after birth (11). It matures during the process of secondary mineralization characterized by collagen compaction and changes in osteocyte gene expression (12).

Despite the shared process of intramembranous bone formation at early stages, differences between the extra-cellular matrix (ECM) of long bones and calvaria were observed in mature mice. For example, collagen was found to be more abundant in the calvaria and suggested to be less crosslinked. Contrary to this, the collagenous matrix of the long bones is more mineralized, probably providing an increased strength to the long bone that is necessary for weight bearing (13).

The growth and homeostasis of the cortical and calvarial bones are regulated by various signaling pathways, hence mutations in several signaling pathway mediators lead to distinct skeletal diseases that are shared between human and mice, making the latter a useful model for research (14). Other gene mutations or diseases are known to only affect one type of bone but not the other. For instance, the prevalent disease osteoporosis affects intensively the cortical bone, while the calvaria bone appear to be osteoporosis resistant (15). Yet, these studies focused on specific genes and diseases, hence systematic comparative studies are needed to fully uncover the shared or distinct molecular pathways in the two bone types at different stages.

Previous studies on adult mice, rats and macaques have compared gene expression between cortical and calvaria bones (16, 17). Both studies reported differential expression of genes related to body patterning and the WNT signaling pathway. However, these studies were done in mature bones undergoing remodeling rather than during their development and modeling. Moreover, both studies were performed on bone after the removal of periosteum and sutures, despite the suggested involvement of these tissues in intramembranous ossification (18). Hence, comprehensive knowledge regarding differential gene expression during the development and modeling of calvarial and cortical bones is missing.

This study focused on the post-natal developmental period by investigating juvenile cortical and calvarial bones. We used bulk RNA-Sequencing to analyze the transcriptome of 7 calvaria and 7 femoral cortical samples of 21 days old juvenile female mice to identify commonalities and differences in the expression level of genes associated with bone development, disease, weight loading and homeostasis. We further highlight differences between the juvenile and mature bone as well as differences in bone relevant signaling pathways observed between the juvenile murine calvaria and cortices.

Material and methods

Animals and RNA-sequencing

As described in Kalev-Altman et al. (19), female wild-type (WT) C57BL/6J (RRID: IMSR_JAX:000664) mice were purchased from Jackson laboratories (Rehovot, Israel). Mice were maintained at the Hebrew University Specific Pathogen Free animal facility according to animal care regulations. All procedures were approved by the Hebrew University Animal Care Committee (license number 21-16657-3). For growth analyses (n>10 for each weight measurement and n=7-12 for other measurements), animals were weighed weekly from P0 to 4 weeks of age and then biweekly. Body length was measured from nose to end of the sacral bone at P0 using the μCT software (Bruker, Kontich, Belgium) or from nose to tail at all other groups of age using a standard office ruler. Their skull and femur were dissected and cleaned from adjacent tissues. The femur length as well as all measurements of skull bones and long bones of P0 animals were all measured using the Amira software 3D measuring tool.

For RNA-Sequencing, mice were euthanized with CO2 at three weeks (P21). Cortical samples (n=7) were cleaned from all adjacent tissues (muscle, tendon and ligaments) and the diaphyseal bone marrow was removed by washing it out with ultra-pure water, using a small needle and syringe. Periosteum and endosteum were not removed. The left or right frontal bone was taken for the calvaria samples (n=7) without removing the periosteum or adjacent suture mesenchyme. The samples were individually flash-frozen in liquid nitrogen and were subjected to manual pulverization. Total RNA was extracted as previously described (20, 21). Each freshly frozen RNA sample had a RIN>5.6. Libraries were prepared by the Nancy and Stephen Grand Israel National Center for Personalized Medicine (G-INCPM) research facility, Weizmann Institute of Science, Rehovot, Israel; using INCPM-mRNA-seq, which is based on the Transeq protocol (22, 23). Sequencing was done on an Illumina NovaSeqmachine, using SP (100 cycles) protocol. The output was ~9.5 million single-end 100bp reads per sample. The RNA-Seq datasets are available at NCBI Gene Expression Omnibus (GEO), GEO accession: GSE223750.

Bioinformatical analysis

Bioinformatical analysis was performed as previously described (20) with the following modifications: The EndToEnd option was used and outFilterMismatchNoverLmax was set to 0.05. Expression levels for each gene were quantified using htseq-count (version 0.11.2) (24) and using the gene annotations downloaded from Ensemble (release 102). Non-annotated genes were excluded. Differentially expressed genes were determined by a p.adj of <0.05, absolute fold changes >=1.5 and max counts >=15. PCA and PERMANOVA were performed based on the 1000 most variable genes, using R 4.2.0 and the vegan package (2.6-2). GOrilla website application (25) was used with default parameters using the list of DEGs and all genes detected having max counts >=15 as the background list. Gene set enrichment analysis (GSEA) was conducted using R packages clusterProfiler (3.18.1) and Org.Mm.eg.db (3.12.0) with FDR correction. Figures were created using DOSE (3.16.0) and PathView (1.30.1) (26).

Results

Gene set introduction

The calvarial and femoral cortical bone transcriptome data subset of 21 days old female C57BL/6J WT mice from Kalev-Altman et al. (19) was used and re-analyzed. This age is equivalent to ~6 months for humans, considering the average weaning period for mice and humans (27). Figure 1 shows the assessment of weight, body length, skull length and femur length from P0 to 3M, demonstrating that calvaria and cortices of 21 days old mice are still subject to major bone growth and modeling (Figures 1A–D, respectively).

PCA analysis of the 1000 most variable genes revealed a clustering of the calvarial and cortical bone samples, without overlapping samples from the different tissues (Figure 2A). PERMANOVA on the clusters' centroids showed a significant difference between the samples from cortices and calvaria. The list of the top 100 expressed genes by transcript number for both tissues is shown in TabS1. As expected, bone-related genes such as *Collagen type I alpha 1* (*Col1a1*), *Col1a2*, *Serpin family F member 1* (*Serpinf1*), *Bone gamma-carboxyglutamate protein 1* (*Bglap1*), *Bglap2*, *Prolyl 4-hydroxylase subunit beta* (*P4hb*), *Osteonectin* (*Sparc*) (13) were detected in both bones. Furthermore, the expression of genes related to bone development and osteochondrogenic signaling pathways, such as bone morphogenetic protein (BMP), wingless-related integration site (WNT) and hedgehog (HH) (29) is shown in Table S2 and provides an overview of the bone relevant pathways present in each type of bone.

Moreover, from the 10569 genes found, 602 differentially expressed genes (DEGs) were detected between the calvaria and the cortices. Of these 140 DEGs were higher expressed and 462 were lower expressed in the cortical bone compared to the calvaria (Figure 2B; Table S3). The expression of the top 100 DEGs by $\log_2$ fold change indicated two clusters of genes (Figure 2C). The upper cluster shows higher expression of DEGs in the cortical bone including several members of the *Homeobox* (*Hox*) family of transcription factors, while in the bottom cluster DEGs, such as the BMP inhibitor *Noggin* (*Nog*), were higher expressed in the calvaria.

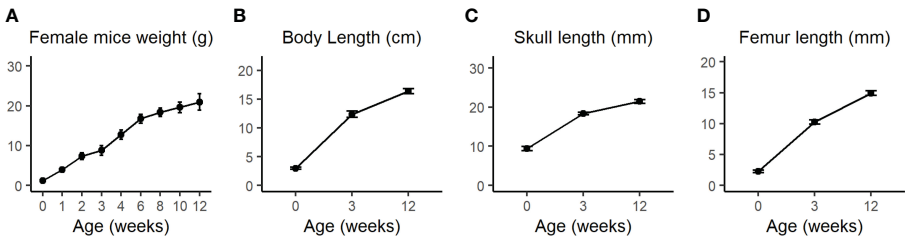

FIGURE 1
(A) Body weight of WT female mice was measured once a week from birth until 4 weeks (w) and then every two weeks until the age of 12w. **(B)** Total body length from nose to the end of the sacral bone at P0 as measured by the Amira software or from nose to tail at 3w and 12w as measured by a standard office ruler. **(C)** Total skull length measured by the Amira software 3D measuring tool. **(D)** Femur length was measured by the CTAn software. Values are expressed as the mean ± SD; n>10 for each weight measurement and n=7-12 for other measurements. Modified from Kalev-Altman et al. (19).

10.3389/fendo.2023.1127536

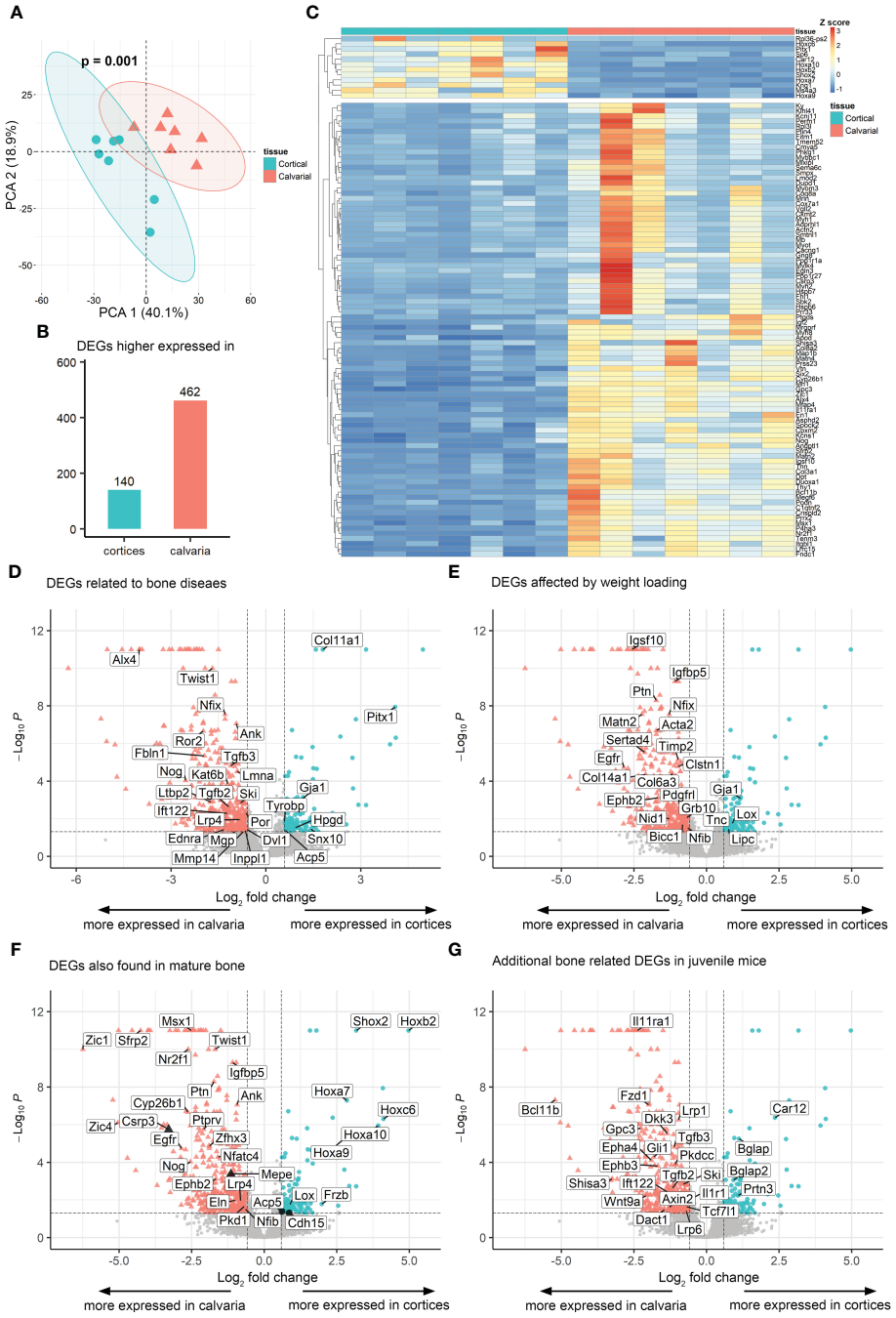

FIGURE 2
Transcriptome of cortical and calvarial bone of juvenile mice. **(A)** PCA analysis and PERMANOVA on centroids demonstrated that samples clustered according to tissue. 95% confidence ellipses of centroids are indicated. **(B)** Heatmap displaying the Z score of the 100 most variable differentially expressed genes (DEGs) between cortical and calvarial bone clustered according to the tissue of origin. **(C)** Total number of DEGs found to be higher expressed in either the cortices or the calvaria. **(D–G)** Volcano plots indicate the distribution of DEGs in cortical and calvarial bone. Annotated DEGs related to **(D)** diseases (14), **(E)** weight loading (28) and **(F)** DEGs that were also found to be differentially expressed between mature calvaria and cortices by Rawlinson et al. (17) or Wang et al. (16). DEGs with inverted expression levels compared to Rawlinson et al. (17) are colored in black. **(G)** Additional bone–associated DEGs in juvenile mice that are not differentially expressed in mature animals. DEGs were defined by total fold change >= 1.5, p.adj < 0.05 and maximal transcript number in at least one sample >=15.

Differential expression of disease related genes in cortices and calvaria

As the first step of identifying DEGs that are highly relevant for bone formation, we compared our list of DEGs with the review of Brommage and Ohlsson (14), which summarized 441 genes related to human skeletal diseases including aggrecanopathies, channelopathies, ciliopathies, cohesinopathies, laminopathies, linkeropathies, lysosomal storage diseases, protein-folding and RNA splicing defects and ribosomopathies. Despite the lack of

10.3389/fendo.2023.1127536

studies on several of these genes in mice, their subsequent literature search found 249 genes mimicking the human phenotype in mice. The expression of these conserved genes must be tightly regulated to prevent the occurrence of skeletal diseases. Therefore, a difference in their gene expression level between the cortical and calvarial bones may indicate an important role in site-specific bone development. We found 28 disease related DEGs including patterning and differentiation related transcriptions factors such as Paired-like homeodomain transcription factor 1 (Pitx1) and Twist basic helix-loop-helix transcription factor 1 (Twist1), the epigenetic regulator RUNX2 interacting histone lysine acetyltransferase 6B (Kat6b), general constituents of the bone matrix including Matrix gla protein (Mgp) and Col11a1, the osteoclast marker Acid phosphatase 5 tartrate resistant (Acp5), the WNT signaling associated Lipoprotein receptor-related protein 4 (Lrp4) and the ECM remodeling associated Matrix metallopeptidase (Mmp14) (14) (Figure 2D; Table 1). The difference in expression levels of disease related genes associated with bone cell differentiation, bone matrix composition and remodeling between calvarial and cortical bone are likely relevant for the bones' diverging function, e.g., resisting heavy loading of the cortices for locomotion (30) or providing a permanent and robust protection of the brain by the calvarial bone matrix.

TABLE 1 Bone pathology associated DEGs as reported by Brommage and Ohlsson (14).

Gene ID	Gene name	log2FC (Cortical/Calvarial)	p.adj
ENSMUSG00000021506	Pitx1	4.09	1.15E-08
ENSMUSG00000027966	Col11a1	1.80	0.00E+00
ENSMUSG00000038301	Snx10	1.42	3.54E-02
ENSMUSG00000050953	Gja1	1.17	8.40E-04
ENSMUSG00000031613	Hpgd	0.93	3.10E-02
ENSMUSG00000001348	Acp5	0.62	4.09E-02
ENSMUSG00000030579	Tyrobp	0.59	1.35E-02
ENSMUSG00000029071	Dvl1	-0.59	3.76E-02
ENSMUSG00000005514	Por	-0.63	5.07E-03
ENSMUSG00000032737	Inppl1	-0.65	4.32E-02
ENSMUSG00000000957	Mmp14	-0.71	4.91E-02
ENSMUSG00000029050	Ski	-0.81	1.49E-03
ENSMUSG00000027253	Lrp4	-0.82	1.12E-02
ENSMUSG00000028063	Lmna	-0.91	3.03E-05
ENSMUSG00000022265	Ank	-0.94	8.85E-08
ENSMUSG00000030218	Mgp	-0.97	4.89E-02
ENSMUSG00000021253	Tgfb3	-1.11	1.54E-05
ENSMUSG00000039239	Tgfb2	-1.17	2.38E-03
ENSMUSG00000021767	Kat6b	-1.21	1.39E-04
ENSMUSG00000030323	Ift122	-1.21	5.20E-03
ENSMUSG00000001911	Nfix	-1.29	2.89E-08
ENSMUSG00000031616	Ednra	-1.32	3.76E-02
ENSMUSG00000035799	Twist1	-1.69	1.00E-10
ENSMUSG00000002020	Ltbp2	-1.74	1.31E-03
ENSMUSG00000006369	Fbln1	-1.94	4.56E-06
ENSMUSG00000021464	Ror2	-1.98	2.18E-07
ENSMUSG00000048616	Nog	-2.54	9.25E-05
ENSMUSG00000040310	Alx4	-4.01	0.00E+00

Mechanical loading-associated genes are upregulated in the calvaria

Mechanical loading is a major effector in the modeling and remodeling of bones (30). Thus, we expected significant differences in the expression of mechanical load-associated genes between the load-bearing cortices and non-load-bearing calvaria. Accordingly, we compared our list of DEGs to the list of loading-associated genes reported by Xing et al. (28), which studied the tibia of 10-week-old female mice. 22 of our DEGs were associated with mechanical loading. Four genes were higher expressed in the cortical bone. These include the Lysyl oxidase (Lox), whose crosslinking activity has been proposed to give collagen fibers more stiffness that may be necessary for locomotion (13) and the WNT-related Gap junction protein alpha 1 (Gja1). However, the majority of 18 genes were higher expressed in the calvaria, including the Growth factor receptor bound protein 10 (Grb10), other genes involved in ECM cell signaling as reported for Nidogen 1 (Nid1), ECM constituents like Col14a1 and the tissue inhibitor of metalloproteinase 2 (Timp2) that could play a role in preventing matrix degradation due to a lack of weight loading in the skull (Figure 2E; Table 2).

Commonalities and differences between juvenile and mature calvaria and cortices

Juvenile and adolescent bone differ in various processes, such as bone elongation. Hence, we sought to investigate if the DEGs found between the juvenile calvaria and cortices overlap with DEGs found between adult calvaria and cortices. We compared our list of DEGs obtained from 21 days old female mice to the combined 225 DEGs found by Wang et al. (16), who analyzed calvaria and tibia osteocytes in 4-month old mice, 6-month old rats and 6-year old macaque using RNA-Seq and Rawlinson et al. (17), who compared skull and limb bones of rats as well as of mature mice by microarray. Our study included bones with adjacent suture tissue, periosteum and endosteum, as these tissues are involved in intramembranous ossification (18). It should be considered that both studies on mature animals removed suture tissue and periosteum, therefore impeding the comparison with these studies. From 225 DEGs reported in their studies, 135 genes were also detected in our RNA-Seq.

First, we found several DEGs with a higher expression level in the calvaria as compared to the cortical bone in juvenile animals,

TABLE 2 DEGs associated with mechanical loading as reported by Xing et al. (28).

Gene ID	Gene name	log2FC (Cortical/Calvarial)	p.adj
ENSMUSG00000050953	Gja1	1.17	8.40E-04
ENSMUSG00000024529	Lox	0.89	1.79E-02
ENSMUSG00000032207	Lipc	0.76	3.60E-02
ENSMUSG00000028364	Tnc	0.70	2.55E-02
ENSMUSG00000008575	Nfib	-0.65	3.06E-02
ENSMUSG00000020176	Grb10	-0.68	9.01E-03
ENSMUSG00000014329	Bicc1	-0.83	2.01E-02
ENSMUSG00000031595	Pdgfrl	-0.91	2.29E-03
ENSMUSG00000017466	Timp2	-0.98	7.23E-06
ENSMUSG00000039953	Clstn1	-0.99	1.69E-05
ENSMUSG00000026185	Igfbp5	-1.09	5.00E-10
ENSMUSG00000048126	Col6a3	-1.17	4.06E-05
ENSMUSG00000005397	Nid1	-1.27	1.02E-02
ENSMUSG00000001911	Nfix	-1.29	2.89E-08
ENSMUSG00000028664	Ephb2	-1.66	7.67E-04
ENSMUSG00000029838	Ptn	-1.73	5.20E-09
ENSMUSG00000035783	Acta2	-1.73	2.07E-07
ENSMUSG00000022371	Col14a1	-2.10	4.42E-05
ENSMUSG00000016262	Sertad4	-2.13	2.96E-06
ENSMUSG00000022324	Matn2	-2.22	2.82E-08
ENSMUSG00000036334	Igsf10	-2.57	0.00E+00
ENSMUSG00000020122	Egfr	-2.85	1.85E-05

which was also reported for mature animals. These include, among others, Insulin-like growth factor binding protein 5 (Igfbp5), Lrp4, Msh homeobox 1 (Msx1) and Nog (Figure 2F; Table S4). Additionally, Rawlinson et al. (17), found a significantly higher expression level of several DEGs in the skull compared to the limb, such as Lrp5 and Sclerostin (Sost). However, we observed only a non-significant elevated expression of these genes in our study, which may also result from differences in study design that will be elaborated on in the discussion.

Next, to further address commonalities between adolescent and mature bone, we focused on genes with a higher expression level in the cortical bone as compared to the calvaria. In agreement with the studies mentioned above on mature bone, we found DEGs such as Frizzled-related protein (Frzb), Short stature homeobox 2 (Shox2) and several HOX genes having a significantly higher expression level in the juvenile cortical bone compared to the calvaria. Furthermore, our analysis of juvenile bone revealed only a non-significant higher expression level of genes such as Cartilage oligomeric matrix protein (Comp) and Catenin beta 1 (Ctnnb1) in the cortical bone compared to the calvaria. Their expression levels were found to be significantly higher in Wang et al. (16) and Rawlinson et al. (17) studies on mature animals contrary to our study on juvenile mice.

At variance with the expression levels observed by Rawlinson et al. (17) investigating mature bone, we detected higher expression levels of the osteogenic marker Matrix extra-cellular phosphoglycoprotein (Mepe) and cardiomyopathy related Cysteine and glycine-rich protein 3 (Csrp3) in the calvaria compared to the cortical bone. Hitherto, no reports on Csrp3 function in bone cells exist, but as seen for their role in the heart, a function in mechanical sensing is possible (31). Additionally, we detected lower expression levels of the osteoclast marker Acp5 and skeletal muscle marker Cadherin 15 (Cdh15) in the juvenile calvarial bone compared to the cortical bone. It was previously shown that C2C12 myoblasts which undergo osteogenic differentiation following BMP2 treatment suppress CDH15 protein level (32). However, it should be considered that our whole tissue RNA-Seq approach may not be sensitive enough to detect differences in low abundant cell populations like osteoclasts. Single cell RNA-Seq may overcome this limitation, although it has recently been described as not yet sensitive enough for low abundant bone cells (33). In total, several DEGs between cortical and calvarial bone exhibited the same expression pattern in juvenile and in mature bone, while only 4 DEGs between the cortical and calvarial bone had opposing expression levels comparing juvenile and mature bone.

Moreover, we detected additional bone or ECM related DEGs that were not detected or categorized as being differentially expressed by Wang et al. (16) and Rawlinson et al. (17). Some of these DEGs may be related to the non-removal of the periosteum and sutures. Amongst others Bglap, Bglap2 (13), Carbonic anhydrase 12 (Car12) (34) and Proteinase 3 (Prtn3) (35) exhibited a higher expression level in the cortical bone compared to the calvaria (Figure 2G; Table 3). Moreover, the calvaria demonstrated higher expression levels compared to the cortical bone of several mediators linked to the BMP, WNT and HH signaling pathways that have been associated with bone development (29). These differences in expression level of their mediators may play an important role in fine-tuning bone growth according to their function. For example, Transforming growth factor beta 2 (Tgfb2) and Tgfb3 are both linked to skeletal diseases (14). Next, the WNT-associated Shisa3 has been reported by Murakami et al. (44) to be expressed in calvarial osteoblasts, although no phenotype was reported after Shisa3 knockout. Dickkopf 3 (Dkk3) has been previously proposed to inhibit endochondral bone formation (42), but as with WNT related Transcription factor 7 like 1 (Tcf7l1) (39) and Dishevelled-binding antagonist of beta-catenin 1 (Dact1) (43), no study investigated its role in calvaria or cortical bone development in juvenile mice. The HH pathway mediators GLI family zinc finger 1 (Gli1) that promotes osteoblast differentiation (48), Intraflagellar transport 122 (Ift122) that was linked to cranioectodermal dysplasia in humans and protein kinase domain containing cytoplasmic (Pkdcc), which regulates craniofacial and long bone development (46) demonstrated higher expression levels in the calvaria compared to cortices. Finally, additional genes associated with craniosynostosis were strongly expressed in the calvaria compared to the cortical bone, such as Axin2 (6), B cell leukemia/lymphoma 11B (Bcl11b) (49), Interleukin 11 receptor alpha chain 1 (Il11ra1) and Ski sarcoma viral oncogene homolog (Ski) (4), as well as the ephrin receptors Epha4 and Ephb3.

In summary, we found over 600 DEGs between calvaria and cortical bone of femur in juvenile female mice, including DEGs that were detected in previous studies that focused on adult animals and differed in experimental procedures. Many of our bone related DEGs, like several WNT signaling mediators, were not categorized as DEGs in these studies, and many DEGs reported in these studies were not confirmed by us in juvenile animals.

Enrichment of bone-relevant gene ontology terms in juvenile murine bone

Next, to check for enriched gene ontology (GO) Biological Process terms, we used GOrilla on the DEGs detected in this study. The resulting top 20 terms ranked by the enrichment score are shown in Table 4, including bone relevant terms related to protein kinase C activity (50), response to Vitamin K (51), forelimb morphogenesis, cartilage condensation and WNT signaling (52) (Table 4). DEGs that were associated with these gene sets include Epidermal growth factor receptor (Egfr), Receptor tyrosine kinase like orphan receptor 2 (Ror2), Bglap2, Twist1, Alx4, Wnt9a, Msx1, Lrp6, Ift122, Polycystin 1 (Pkd1) and Tgfb2, which exhibited a higher expression level in the calvaria compared to the cortical bone as well as Shox2, Hoxa9 and Col11a1, which exhibited a higher expression level in the cortical bone compared to the calvaria (Figures 2D–G). Our results indicate that multiple gene sets are responsible for the differential development of the juvenile murine calvarial and cortical bone.

10.3389/fendo.2023.1127536

TABLE 3 Additional bone related DEGs found comparing juvenile murine cortices and calvaria.

Category	Gene ID	Gene name	log2FoldChange (Cortical/ Calvarial)	p.adj	References
Uncategorized	ENSMUSG00000032373	Car12	2.36	4.30E-07	Liu et al. (34)
	ENSMUSG00000074483	Bglap	1.12	5.58E-06	van den Bos et al. (13)
	ENSMUSG00000057729	Prtn3	1.09	5.95E-03	Shao et al. (35)
	ENSMUSG00000074486	Bglap2	0.93	8.84E-04	van den Bos et al. (13)
	ENSMUSG00000026072	Il1r1	-0.85	1.67E-02	Matsuda et al., 2010 (36)
BMP signaling	ENSMUSG00000021253	Tgfb3	-1.11	1.54E-05	Guasto and Cormier-Daire, (29)
	ENSMUSG00000039239	Tgfb2	-1.17	2.38E-03	Guasto and Cormier-Daire, (29)
	ENSMUSG00000055653	Gpc3	-2.26	1.52E-06	Dwivedi et al. (37); Kolluri and Ho, 2019 (38)
WNT signaling	ENSMUSG00000055799	Tcf7l1	-0.69	2.27E-02	Velasco et al. (39)
	ENSMUSG00000030201	Lrp6	-0.70	3.82E-02	Maupin et al. (40)
	ENSMUSG00000040249	Lrp1	-0.96	5.54E-07	Lu et al. (41)
	ENSMUSG00000030772	Dkk3	-1.35	2.96E-06	Aslan et al., 2006, (42); Maupin et al. (40)
	ENSMUSG00000044548	Dact1	-1.44	3.31E-02	Esposito et al. (43)
	ENSMUSG00000044674	Fzd1	-1.99	8.85E-08	Maupin et al. (40)
	ENSMUSG00000000126	Wnt9a	-2.08	5.92E-03	Maupin et al. (40)
	ENSMUSG00000050010	Shisa3	-3.25	7.54E-04	Murakami et al. (44)
HH signaling	ENSMUSG00000032855	Pkd1	-0.69	2.22E-02	Qiu et al. (45)
	ENSMUSG00000024247	Pkdcc	-1.08	1.30E-04	Maridas et al. (46)
	ENSMUSG00000030323	Ift122	-1.21	5.20E-03	Moosa et al., 2016 (47)
	ENSMUSG00000025407	Gli1	-1.82	5.33E-05	Ohba (48)
Craniosynostosis	ENSMUSG00000000142	Axin2	-1.29	2.47E-02	Behr et al. (6)
	ENSMUSG00000005958	Ephb3	-1.67	1.57E-04	Ishii et al. (4)
	ENSMUSG00000026235	Epha4	-1.90	7.72E-05	Ishii et al. (4)
	ENSMUSG00000073889	Il11ra1	-2.39	0.00E +00	Ishii et al. (4)
	ENSMUSG00000048251	Bcl11b	-5.22	4.91E-08	Holmes et al. (49)

Enrichment of KEGG gene sets in the juvenile murine calvaria and cortices

In the next step, we performed GSEA using the KEGG database to identify enriched data sets by ranking all detected genes, including DEGs (Figure 3; Table S5). In total, 26 enriched gene sets were found, including 14 with a positive normalized enrichment score and 12 with a negative normalized enrichment score in the cortical bone compared to the calvaria.

Gene sets positively enriched in the cortical bone focused on cellular pathways and included nucleotide metabolism, homologous recombination, DNA replication, mismatch repair, spliceosome and ribosome-related terms. Moreover, the calvaria demonstrated a positive enrichment for terms focusing on signaling pathways such as calcium, Hedgehog, MAPK and WNT signaling as well as related terms like ECM-receptor interaction and Focal adhesion.

For instance, Figure S1 shows the enriched gene sets of WNT/HH signaling, Ribosome and ECM-receptor interaction. Canonical and non-canonical WNT signaling pathways contained genes with higher and lower expression levels between the calvaria and cortices. Therefore no conclusion could be drawn as to which specific WNT pathway may be more activated in cortical bone or the calvaria (Figure S1A). Additionally, Figure S1B shows the increased expression of several HH mediators in the calvaria. The HH signaling gene set has been linked to craniofacial development and our list of DEGs contained the HH pathway mediators Gli1, Ift122, Pkd1 that effects Gli2 expression (45), and Pkdcc. All four genes were linked to the primary cilium (53–56), an organ that is involved in mechanosensing (57, 58), indicating another connection between the HH and WNT pathways regulating bone development (52). Furthermore, Figures S1C, D show the increased expression levels of ribosome-related genes in the cortical bone. These gene sets

10.3389/fendo.2023.1127536

TABLE 4 Enriched terms by Gorilla.

GO Biological Process Term	Description	p.value	FDR q-value	Enrichment Score	Genes
GO:1900020	positive regulation of protein kinase C activity	2.70E-04	2.25E-02	15.44	Agt - angiotensinogen (serpin peptidase inhibitor, clade a, member 8), Egfr - epidermal growth factor receptor, Ror2 - receptor tyrosine kinase-like orphan receptor 2
GO:1900019	regulation of protein kinase C activity	2.70E-04	2.24E-02	15.44	Agt - angiotensinogen (serpin peptidase inhibitor, clade a, member 8), Egfr - epidermal growth factor receptor, Ror2 - receptor tyrosine kinase-like orphan receptor 2
GO:1990048	anterograde neuronal dense core vesicle transport	2.70E-04	2.23E-02	15.44	Kif1c - kinesin family member 1c, Kif1b - kinesin family member 1b, Sybu - syntabulin (syntaxin-interacting)
GO:0060371	regulation of atrial cardiac muscle cell membrane depolarization	2.70E-04	2.21E-02	15.44	Cacna1g - calcium channel, voltage-dependent, t type, alpha 1g subunit, Scn1b - sodium channel, voltage-gated, type i, beta, Gja1 - gap junction protein, alpha 1
GO:0032571	response to vitamin K	8.27E-05	8.50E-03	12.35	Gas6 - growth arrest specific 6, Bglap - bone gamma carboxyglutamate protein, Bglap2 - bone gamma-carboxyglutamate protein 2, Postn - periostin, osteoblast specific factor
GO:0014820	tonic smooth muscle contraction	8.27E-05	8.44E-03	12.35	Mylk - myosin, light polypeptide kinase, Ednra - endothelin receptor type a, Cacna1g - calcium channel, voltage-dependent, t type, alpha 1g subunit, Agt - angiotensinogen (serpin peptidase inhibitor, clade a, member 8)
GO:0062042	regulation of cardiac epithelial to mesenchymal transition	5.21E-04	3.76E-02	8.82	Twist1 - twist basic helix-loop-helix transcription factor 1, Tgfb2 - transforming growth factor, beta 2, Nog - noggin, Eng - endoglin
GO:0014829	vascular smooth muscle contraction	5.21E-04	3.74E-02	8.82	Ednra - endothelin receptor type a, Acta2 - actin, alpha 2, smooth muscle, aorta, Cacna1g - calcium channel, voltage-dependent, t type, alpha 1g subunit, Agt - angiotensinogen (serpin peptidase inhibitor, clade a, member 8)
GO:0003071	renal system process involved in regulation of systemic arterial blood pressure	5.21E-04	3.72E-02	8.82	Gas6 - growth arrest specific 6, Emp2 - epithelial membrane protein 2, Agt - angiotensinogen (serpin peptidase inhibitor, clade a, member 8), Gja1 - gap junction protein, alpha 1
GO:0060312	regulation of blood vessel remodeling	5.21E-04	3.70E-02	8.82	Tmbim1 - transmembrane bax inhibitor motif containing 1, Flt4 - fms-like tyrosine kinase 4, Erg - avian erythroblastosis virus e-26 (v-ets) oncogene related, Gja1 - gap junction protein, alpha 1
GO:0035115	embryonic forelimb morphogenesis	2.87E-07	9.06E-05	8.17	En1 - engrailed 1, Msx1 - msh homeobox 1, Alx4 - aristaless-like homeobox 4, Wnt9a - wingless-type mmtv integration site 9a, Twist1 - twist basic helix-loop-helix transcription factor 1, Shox2 - short stature homeobox 2, Hoxa9 - homeobox a9, Lrp6 - low density lipoprotein receptor-related protein 6, Ift122 - intraflagellar transport 122
GO:0048251	elastic fiber assembly	2.15E-04	1.86E-02	7.72	Fbln5 - fibulin 5, Ltbp4 - latent transforming growth factor beta binding protein 4, Mfap4 - microfibrillar-associated protein 4, Lox - lysyl oxidase, Thsd4 - thrombospondin, type i, domain containing 4
GO:0033622	integrin activation	9.88E-04	5.99E-02	7.72	Cx3cl1 - chemokine (c-x3-c motif) ligand 1, Cxcl12 - chemokine (c-x-c motif) ligand 12, Fermt2 - fermitin family homolog 2 (drosophila), Col16a1 - collagen, type xvi, alpha 1
GO:0060065	uterus development	9.88E-04	5.96E-02	7.72	Hoxa10 - homeobox a10, Hoxa9 - homeobox a9, Rbp4 - retinol binding protein 4, plasma, Tgfb2 - transforming growth factor, beta 2
GO:0098743	cell aggregation	8.34E-05	8.45E-03	7.13	Thra - thyroid hormone receptor alpha, Mpz - myelin protein zero, Pkd1 - polycystic kidney disease 1 homolog, Tgfb2 - transforming growth factor, beta 2, Ror2 - receptor tyrosine kinase-like orphan receptor 2, Col11a1 - collagen, type xi, alpha 1
GO:0033273	response to vitamin	8.34E-05	8.39E-03	7.13	Gas6 - growth arrest specific 6, Ada - adenosine deaminase, Bglap - bone gamma carboxyglutamate protein, Bglap2 - bone gamma-carboxyglutamate protein 2, Lrp6 -

(Continued)

10.3389/fendo.2023.1127536

TABLE 4 Continued

GO Biological Process Term	Description	p.value	FDR q-value	Enrichment Score	Genes
					low density lipoprotein receptor-related protein 6, Postn - periostin, osteoblast specific factor
GO:2000095	regulation of Wnt signaling pathway, planar cell polarity pathway	3.73E-04	2.88E-02	7.02	Nkd1 - naked cuticle 1 homolog (drosophila), Gpc3 - glypican 3, Sfrp2 - secreted frizzled-related protein 2, Lrp6 - low density lipoprotein receptor-related protein 6, Dact1 - dapper homolog 1, antagonist of beta-catenin (xenopus)
GO:0035136	forelimb morphogenesis	1.66E-06	3.76E-04	6.95	En1 - engrailed 1, Msx1 - msh homeobox 1, Alx4 - aristaless-like homeobox 4, Wnt9a - wingless-type mmtv integration site 9a, Twist1 - twist basic helix-loop-helix transcription factor 1, Shox2 - short stature homeobox 2, Hoxa9 - homeobox a9, Lrp6 - low density lipoprotein receptor-related protein 6, Ift122 - intraflagellar transport 122
GO:0001502	cartilage condensation	6.06E-04	4.22E-02	6.43	Thra - thyroid hormone receptor alpha, Pkd1 - polycystic kidney disease 1 homolog, Tgfb2 - transforming growth factor, beta 2, Ror2 - receptor tyrosine kinase-like orphan receptor 2, Col11a1 - collagen, type xi, alpha 1
GO:0060004	reflex	6.06E-04	4.20E-02	6.43	Auts2 - autism susceptibility candidate 2, Npnt - nephronectin, Shank1 - sh3/ankyrin domain gene 1, Pmp22 - peripheral myelin protein 22, Gja1 - gap junction protein, alpha 1

include the genes EMG1 N1-specific pseudouridine methyltransferase (Emg1), which is associated with the Bowen-Conradi syndrome (59), Treacle (Tcof1), which is associated with Treacher Collins syndrome as well as the Diamond-Blackfan anemia associated Ribosomal protein L11 (Rpl11), Rpl35a, Ribosomal protein S17 (Rps17) and Rps24 (60). Several integrins as well as ECM molecules like collagens and osteopontin were differentially expressed between cortices and calvaria (Figure S1E). For instance, we observed elevated Integrin alpha 5 (Itga5) and Integrin beta 1 (Itgb1) expression levels in the calvaria, and a decreased expression of these integrins was linked to apoptosis in unloaded rat osteoblasts (61). Furthermore, in agreement with the finding that αVβ3 integrins are highly abundant in osteoclasts (62), we observed an increased Itgav/Itgb3 integrins expression level in the cortical bone. Therefore, the enrichment of the ECM receptor gene set could indicate differences in osteoblast and osteoclast activity.

The MAPK signaling gene set was positively enriched in the calvaria and has been linked to osteogenesis (63) and WNT signaling (64). Although our list of DEGs did not contain the most abundant MAPK signaling mediators, it did include some distant mediators of the KEGG MAPK gene set such as Egfr, Interleukin 1 receptor type I (Il1r1), Tgfb2 and Tgfb3. Interestingly, MAPK is further related to the calvaria-enriched calcium signaling gene set. Moreover, Eapen et al. (65) reported that calcium signaling activates the p38 MAPK pathway, eventually inducing Runt-related transcription factor 2 (Runx2) expression and calvarial osteoblast differentiation *in vitro*. Finally, the calvaria showed a positive enrichment for gene sets related to cardiovascular-related terms compared to the cortices. This is not surprising as the enriched gene sets included integrins as well as DEGs like Lamin A/C (Lmna) (66) and Tenascin C (Tnc) (67), both taking part in bone formation as well as cardiovascular related gene sets.

Discussion

In this study, we compared the transcriptome of two different bones, the skull calvaria and the femoral cortical bone. While both bones develop through intramembranous ossification, each is structurally and functionally different. The skull bone protects the brain, whereas the cortical bone is involved in locomotion and load-bearing. Moreover, each bone is affected by different diseases. Hence, the question regarding their similar or divergent molecular signature arises. Previous studies focused on embryological development (4, 11) and the mature state of these bones at various mammalian species (16, 17). Here, we used a high number of biological replicates to provide new insights into the juvenile murine bone, which still undergoes modeling processes. A limitation of this study was the analysis of only juvenile female mice. However, the sexual maturation for C57BL/6 mice has been reported to begin after P25 (68) and therefore, only minor differences to male mice can be expected. Notably, the bulk RNA-Seq was conducted on RNA extracted directly from bone tissue to remain as close as possible to the native tissue since isolation and cultivation of osteogenic cells *in-vitro* before RNA-Seq analysis was reported to affect gene expression levels (33). First, we scanned our list of DEG for genes that have been linked to bone disease, development and homeostasis in the literature. The GO analysis of all 602 DEGs showed expected results, e.g., biologically relevant terms related to limb development that match the higher expression levels of pattern-associated *Hox* genes in the cortices compared to the calvaria as reported for mature animals as well (16, 17). The detected DEGs are involved in various processes from epigenetic regulation up to matrix remodeling, rather than only one process, indicating that every step of bone modeling in calvaria and cortices can vary between both bones. Subsequently, we performed GSEA to identify enriched KEGG pathways in the cortical bone and calvaria.

10.3389/fendo.2023.1127536

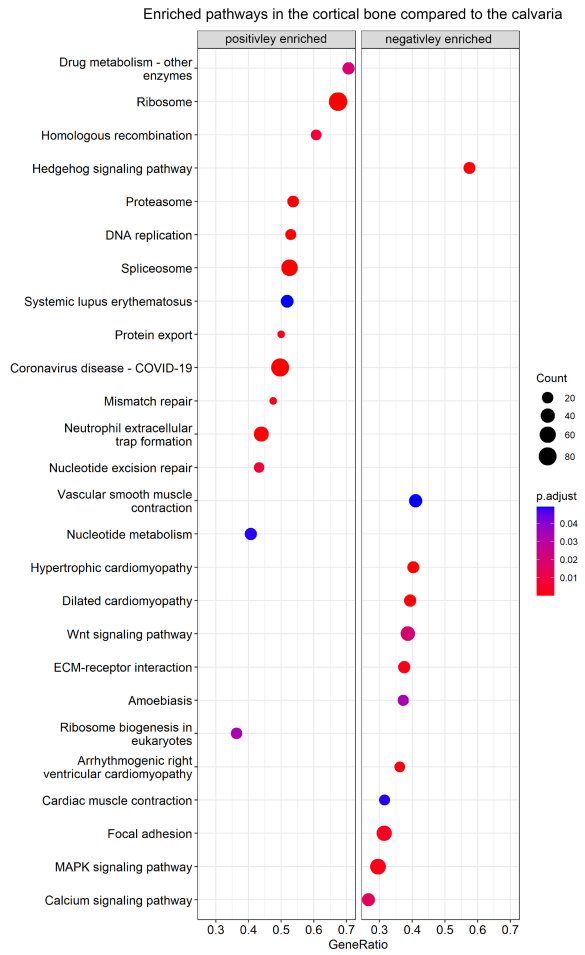

FIGURE 3
GSEA of enriched KEGG pathways between cortical and calvarial bone. The cortical bone displayed a positive enrichment for gene sets related to DNA replication, whereas the calvaria displayed a positive enrichment of gene sets related to signaling pathways. P–values were adjusted using FDR correction. Gene ratio is defined as the number of enriched genes in the gene set/total number of genes in the gene set and the enriched gene number per gene set is represented by count size.

Several key bone markers are not differentially expressed between the calvaria and cortical bone of juvenile mice

Our study provided general oversight of the expression level of several genes related to bone development and homeostasis. We were not able to detect significant differences in the expression level of major bone genes between calvaria and cortical bones, such as Alkaline phosphatase (Alpl), Col1a1, Col1a2, Dentin matrix protein 1 (Dmp), Integrin binding sialoprotein (Ibsp), Runx1, Runx2, Runx3, Osterix (Sp7), Serpinf1 or Sparc. It seems likely that the expression levels of these universal bone markers are bone type independent and bone-specific differences occur in the subsequent processes, such as posttranscriptional regulation. At variance from the classical bone genes described above, many genes displayed significant differences in expression level between both bone types. For instance, the expression level of Lox was significantly higher in the cortical bone compared to the skull. This finding is in line with the increased cross-linked collagen in the cortical bone reported by van den Bos et al. (13). Furthermore, our observation of increased expression levels of the calcification associated genes Bglap, Bglap2 (13), Car12 (34) and Prtn3 (35) in the cortical bone compared to the calvaria supports the assumption that increased calcification occurs in locomotion-participating bones (13).

High expression of synostosis-related genes in the calvaria

The calvaria originates, contrary to the cortical bone, from several bones bound together by cranial sutures to enable rapid while protected brain growth. Cranial sutures of mice remain mostly unfused. Our list of DEGs from juvenile mice contained several craniosynostosis-related genes whose expression was higher in the calvaria than in the cortical bone. The different sample preparation, including the removal of sutures as performed by Wang et al. (16) and Rawlinson et al. (17) on mature animals impedes the comparison of craniosynostosis relevant DEGs that were detected in their studies and the DEGs reported here, such as Axin2, Aristaless-like homeobox 4 (Alx4), Zic family member 1 (Zic1), the Glycoprotein glypican 3 (Gpc3) and ephrin receptors. Axin2 knockout lead to a reduction in hypertrophic chondrocytes and enhanced cranial suture mineralization and ossification, possibly by aberrant activation of WNT signaling (40). Alx4 interacts with BMPs as well as WNT-family proteins (69), whereas Zic1 is thought to induce engrailed (En) expression *via* WNT signaling (70). Gpc3 has been reported to modulate WNT and HH signaling in liver cancer (38) and interestingly, GPC3 was previously found to interact with BMP2, like the not differentially expressed GPC1, to regulate suture fusion. Yet, contrary to single knockouts, only a combined knockout of Gpc1 and Gpc3 led to a skull phenotype (37). This redundant function suggests that Gpc3 is only a minor regulator of bone development through fine-tuning of BMP signaling. Altogether, many craniosynostosis-related genes that are upregulated in the calvaria act *via* modulation of signaling pathways like the BMP and WNT signaling pathways. These pathways regulate osteogenic and chondrogenic differentiation events, which delay suture fusion until the growth of the brain is completed and ossification of the sutures, except for the lambdoid suture, takes place. The role of other craniosynostosis-related genes in the calvaria has not been completely understood yet. For example, Ephb3 has been reported to be present in the embryonic and adult calvaria sutures and an Ephb3 knockout increased calvaria bone tissue volume (71). Ephb2 was suggested to be involved in embryonic skull development; however, Ephb2 knockout mice did not show any calvaria phenotype (72). Therefore, Ephb2 may work together with Ephb3 as seen during palate formation (73) but downstream of Ephb3 during craniosynostosis. It has been suggested that adult calvarial sutures may act as reservoirs of Ephb3 osteoblastic stem cells responding upon brain injury. Thus, some detected DEGs might function in calvarial bone repair rather than calvarial bone formation.

WNT signaling in the calvaria and the response to mechanical loading

Maupin et al. (40) reviewed the effects of mutations in WNT signaling genes on general bone development in human and mice, which included several of our DEGs, such as *Lrp4*, whose expression has been linked to increased bone mineral content and density. We found additional WNT signaling mediators with a significantly higher expression level in the calvaria, such as *Lrp1*, that is expressed in osteoblast regulating osteoclast activity (74). The osteoclast-specific loss of *Lrp1* increased osteoclastogenesis and bone resorption in mice (41). Therefore, the higher expression of *Lrp1* in the calvaria may have a pivotal role in preventing calvaria bone loss. The expression of WNT genes may not be limited to cells residing in the bone, as it was shown that periosteal stem cells express WNT genes during the growth phase (18), indicating an essential role of the periosteum in site-specific bone formation.

The WNT signaling pathway is not just crucial for bone development but also connects mechanical loading with bone remodeling. Surprisingly, most DEGs associated with mechanical loading had a higher expression level in the non-load-bearing calvaria than in the load-bearing cortical bone. In the cortical bone, mechanical loading leads to the expression of bone anabolic genes and prevents bone loss. This feedback mechanism cannot be applied to the non-load-bearing skull. Therefore, we suggest that at least a subset of these genes responsive to mechanical loading in the cortical bone is also involved in regulating bone homeostasis in the calvaria. This subset of genes including e.g., *Timp2* is constantly expressed by WNT signaling to prevent calvaria bone loss in juvenile mice. In addition, other load-inducible genes being highly expressed in the calvaria of mature animals, as demonstrated by Rawlinson et al. (17) may explain how the senescent skull does not suffer from osteoporosis (15).

We highlight the WNT pathway's role in juvenile mice in osteogenic differentiation and subsequent bone mineralization during craniosynostosis, as well as WNT signaling as a response to mechanical loading and inhibiting bone loss in the calvaria. The gene expression data presented here identified WNT signaling as the most significant pathway to establish the differences in bone structure and function observed between the juvenile calvaria and cortical bone. While this study focused on differential expression of WNT pathway members and effectors, more research on the posttranscriptional level is necessary to fully comprehend how differences between the juvenile calvarial and cortical bone are established.

DNA handling and ribosomal composition may specify cortical and calvarial bone development in juvenile mice

The cortical bone showed a positive enrichment for gene sets related to DNA including its replication, homologous recombination, mismatch repair as well as nucleotide excision repair and metabolism. Wang and Li, (75) summarized how the expression of DNA damage and cell cycle associated genes regulate *Sp7* during osteoblast differentiation, further suggesting that as only osteoblasts express *Sp7*, this connection was not observed in other cell types. Moreover, the low bone mass associated diseases Werner's syndrome and Hutchinson Gilford Progeria syndrome are caused respectively by loss of the DNA repair enzyme *WRN RecQ like helicase* (*Wrn*) or the nuclear matrix protein *Lmna* (76). Considering the enrichment of several DNA related gene sets between cortices and calvaria as well as that most bone inhabiting cells are post-mitotic osteocytes (77), further studies on intramembranous bones should elucidate the relevance of the cell cycle genes during bone modeling.

Finally, the cortical bone exhibited a positive enrichment for gene sets associated with ribosome biogenesis in the GSEA. The occurrence of site-specific bone diseases related to ribosome associated genes suggests that despite the universality of ribosomes, different bone tissues have a ribosome machinery of diverging composition fitting the tissue's function (78). For example, RPL10 has been detected in several regions of the developing bovine femur, mostly in cells that are poised to produce a mineralized matrix and its expression diminishing when the mineralization complex has been established. RPL10 was found in the perichondrium and periosteum surrounding the growth plate but not in osteocytes (79). This indicates that the non-removal of the periosteum could have affected the differential enrichment of the ribosome gene set in this study. The site-specific ribosomal function during bone formation could be mediated by various interaction partners such as the osteogenic master regulator RUNX2 (60). Furthermore, Treacher-Collins syndrome, a disease affecting only the cranial bone formation but not the rest of the skeleton, is caused by mutations in the ribosomal DNA transcription regulator *Tcof1*, despite the universal expression of *Tcof1* in embryonic and adult tissues (80). Other studies link the processes of ribosome biogenesis, cell cycle arrest, increased cell death and reduced proliferation and migration of neural crest cells, a cell population strongly involved in cranial bone formation (81, 82). Deletion of *Tcof1* in murine neuroblastoma cell line changed the expression pattern of genes associated with various processes, such as cell cycle and development, beyond ribosomal DNA regulation (83). We hypothesize that the differential enrichment of KEGG gene sets related to cell cycle, DNA damage and ribosome biogenesis suggest a precise mechanism for diverging bone development despite the universal expression of, e.g., cell cycle-associated genes. Furthermore, the differential enrichment of these pathway terms indicates the involvement of the cranial neural crest as an origin for the observed differences in gene expression between both bones. In the first step, the involvement of the cranial neural crest already specifies the developmental program of the calvaria, despite both calvaria and cortical bone develop through the mechanism of intramembranous ossification. Subsequently, the modulation of signaling pathways like WNT according to the bones origin participate in forming bone-specific differences.

The comparison between juvenile and mature calvaria and cortices reveals a continuous developmental program

We investigated age-related changes of differential gene expression between cortical bone and calvaria by comparing our list of DEGs from juvenile mice and the DEGs reported by Wang et al. (16) and Rawlinson et al. (17) from mature animals. First, we found a high number of bone-associated DEGs having the same expression pattern in juvenile mice and mature animals, such as genes related to patterning, WNT signaling and craniosynostosis. Several other genes classified as DEGs in adult bones by Wang et al. (2020) (16) and Rawlinson et al. (17), such as *Wnt16*, *Fibroblast growth factor 1* (*Fgf1*), *Dkk1*, *Sost* and a few *Hox* genes were not found to be differentially expressed in juvenile bones in our study. In addition to the age differences, this may be attributed to our samples' origin from female mice compared to male rats being investigated by Rawlinson et al. (17). Moreover, contrary to Wang et al. (16), we collected the samples from the femur, not from the tibia, and we did not remove the periosteum and cranial sutures. As discussed earlier, this may significantly affect DEG detection, considering these tissues' functions of harboring stem cell populations and expressing signaling molecules (18). DEGs detected only in this study and have not been found by Wang et al. (16) and Rawlinson et al. (17), therefore, this can only indicate a juvenile specific gene set, but still needs to be verified in subsequent studies. However, it is unlikely that non-removal of sutures and periosteum affects the differential expression analysis of bone cell restricted genes such as *Bglap* (84). Considering the younger age of our mice, processes such as bone growth (12) and the expression level of associated genes will therefore differ from mature animals. However, we cannot exclude that some of the DEGs that were only found in our study on juvenile animals, would also be considered differentially expressed by Wang et al. (16), if the same threshold was applied and their analysis was limited to DEGs between murine calvaria and tibia samples (n=2) instead of only including DEGs showing the same trend between calvaria and tibia in mice, rats and macaques.

We suggest that during the juvenile and mature phase, differences in bone (re)modeling of cortical and calvarial bone could primarily be mediated by a key gene set related to pathways like BMP, HH and WNT signaling. Many additional genes related to these pathways only show a differential expression between the cortices and calvaria either in juvenile animals during bone modeling or mature animals during remodeling. In line with this is our finding of only four genes *Mepe*, *Acp5*, *Cspr3* and *Cdh15* showing an opposing expression pattern between juvenile mice and mature animals.

In conclusion, a high number of DEGs detected between juvenile murine calvaria and cortices were also found in mature animals, whereas only four genes showed an opposing expression pattern between juvenile and mature samples. This indicates a DEG key set, that is independent of age is constantly differentially expressed between the cortical and calvarial bone. Thus, determining the character of both bones' structure and function. For example, the high expression levels of *Lox* in the cortical bone provide the bone's stiffness for locomotion in juvenile and mature mice, as locomotion is essential age-independently. This is complemented by age-dependent DEGs as demonstrated in this study or reported by Wang et al. (16) and Rawlinson et al. (17). For example, the calcification associated gene *Bglap* was only differentially expressed in juvenile mice. Many other age-dependent DEGs are related to signaling pathways and future studies will help to reveal how their expression is linked to the development of bone-site specific differences.

Bone-site specific phenotype development

The prediction how differential gene expression affects bone development in this and other published studies is strongly deterred by the bone-site specific function of genes. For example, *Msx1* exhibited a significantly higher expression level in the calvaria compared to the cortices of juvenile and adult mice (17), and it's expression has been linked to directional craniofacial bone growth. *Msx1* affects the mandibular trabecular and mandibular cortical bone in a different manner (85). Murine *Msx1* overexpression using a Col1a promoter showed a higher collagenous bone matrix volume in the trabecular mandibles that was less mineralized because of limited osteocyte differentiation in the skull. Contrary to this, the overexpression of *Msx1* led to increased apoptosis in the cortical mandibles, suggesting site-specific effects of *Msx1*.

Next, contrary to the study of Wang et al. (16) on adult animals, in our study *Mepe* expression level was higher in the juvenile calvaria compared to the cortices. A knock out of *Mepe* was reported to decrease calvarial bone mineralization (86) and on the other hand to increase osteoblast number and trabecular bone mass *in vivo* as well as to increase mineralized nodules in osteoblast cell culture (87). Since both studies performed a *Mepe* knock out and did not investigate a decreased *Mepe* expression level, it is difficult to transfer their insights to Wang et al. (16) and to our study. In line with Gullard et al. (86) and Gowen et al. (87), the higher expression of *Mepe* in juvenile mice undergoing bone modeling as demonstrated in our study could indicate a site-specific effect of Mepe allowing for quick calvarial mineralization and long bone osteoblast proliferation. In the adult animal, a lower expression level of *Mepe* in the calvaria may inhibit ectopic calcification whereas the higher expression level of *Mepe* in the long bone decreases osteoblast numbers to a minimum that is sufficient for bone remodeling.

It should be considered that additional bone related DEGs may exhibit such a site-specific effect between the calvaria and the long bones, adding another regulatory level of bone development and highlighting the importance of subsequent experiments to clarify the genes function in each bone site.

Conclusion

This study, based on a high number of biological replicates from freshly isolated tissue, compared the transcriptome of two bone types that share a similar developmental ontogeny of membranous ossification but display a highly different shape and function. Our

data revealed for the first-time significant differences between the transcriptome of the calvaria and cortical bone in juvenile female mice. Our results differed from previous studies about calvarial and cortical bone homeostasis in adult animals, highlighting the most crucial pathway mediators for juvenile skeletal development. However, a core set of DEGs was found in juvenile mice and mature animals. The differentially expressed genes detected in our study were related to bone diseases, craniosynostosis and weight loading. Intriguingly the expression level of most weight-loading associated genes was higher in the calvaria than in the cortical bone. This could be related to a mechanism preventing bone loss in the non-weight-bearing calvaria. Moreover, we confirmed the widely known importance of signaling pathways like WNT and HH for bone development while identifying new potential candidates participating in site-specific regulation of bone development. Using GSEA, we demonstrated that the calvaria exhibited a positive enrichment for signaling pathways. In contrast, the cortical bone was positively enriched for gene sets related to DNA replication, cell cycle and ribosome.

Data availability statement

The datasets presented in this study can be found in online repositories. The names of the repository/repositories and accession number(s) can be found below: https://www.ncbi.nlm.nih.gov/geo/query/acc.cgi?acc=GSE223750.

Ethics statement

The animal study was reviewed and approved by the Hebrew University Animal Care Committee (license number 21-16657-3).

Author contributions

JJ, RK-A, DS-D and EM-O contributed to conception and design of the study. JJ and TS organized the database. JJ and TS performed the statistical analysis. JJ wrote the first draft of the manuscript. JJ and RK-A wrote sections of the manuscript. All authors contributed to the article and approved the submitted version.

Acknowledgments

We acknowledge Astar Shitrit for technical assistance. This research was supported by the ISRAEL SCIENCE FOUNDATION (grant No. 1252/19). RK-A fellowship was supported by the Einstein Kaye Foundation.

Conflict of interest

The authors declare that the research was conducted in the absence of any commercial or financial relationships that could be construed as a potential conflict of interest.

Publisher's note

Supplementary material

The Supplementary Material for this article can be found online at: https://www.frontiersin.org/articles/10.3389/fendo.2023.1127536/full#supplementary-material

SUPPLEMENTARY MATERIAL FIGURE 1
Enriched KEGG gene sets determined by GSEA clusterProfiler and PathView. **(A)** Wntsignaling pathway, **(B)** Hedgehog signaling pathway, **(C)** Ribosome, **(D)** Ribosome biogenesis in eukaryotes and **(E)** ECM-receptor interaction. Colors indicate normalized gene expression change value between cortices (1) and calvaria (-1).

References

1. Moreira CA, Dempster DW, Baron R. Anatomy and ultrastructure of bone – histogenesis, growth and remodeling. *Endotext*. South Dartmouth (MA: MDText.com, Inc. (2000). Available at: http://www.ncbi.nlm.nih.gov/books/NBK279149/.

2. Eames BF, de la Fuente L, Helms JA. Molecular ontogeny of the skeleton. *Birth Defects Res Part C Embryo Today Rev* (2003) 69(2):93–101. doi: 10.1002/bdrc.10016

3. Karsenty G. Minireview: transcriptional control of osteoblast differentiation. *Endocrinology* (2001) 142(7):2731–3. doi: 10.1210/endo.142.7.8306

4. Ishii M, Sun J, Ting MC, Maxson RE. Chapter six – the development of the calvarial bones and sutures and the pathophysiology of craniosynostosis. In: Chai Y, editor. *Current topics in developmental biology*, vol. 115. Elsevier Inc: Academic Press (2015). p. 131–56. Available at: https://www.sciencedirect.com/science/article/pii/S007021531500040X.

5. Sahar DE, Longaker MT, Quarto N. Sox9 neural crest determinant gene controls patterning and closure of the posterior frontal cranial suture. *Dev Biol* (2005) 280 (2):344–61. doi: 10.1016/j.ydbio.2005.01.022

6. Behr B, Longaker MT, Quarto N. Absence of endochondral ossification and craniosynostosis in posterior frontal cranial sutures of Axin2–/– mice. *PloS One* (2013) 8(8):e70240. doi: 10.1371/journal.pone.0070240

7. Warren SM, Greenwald JA, Spector JA, Bouletreau P, Mehrara BJ, Longaker MT. New developments in cranial suture research. *Plast Reconstr Surg* (2001) 107(2):523–40. doi: 10.1097/00006534-200102000-00034

8. Rice DPC, Connor EC, Veltmaat JM, Lana–Elola E, Veistinen L, Tanimoto Y, et al. Gli3Xt–J/Xt–J mice exhibit lambdoid suture craniosynostosis which results from altered osteoprogenitor proliferation and differentiation. *Hum Mol Genet* (2010) 19 (17):3457–67. doi: 10.1093/hmg/ddq258

9. Nakashima K, Crombrugghe B. Transcriptional mechanisms in osteoblast differentiation and bone formation. *Trends Genet* (2003) 19(8):458–66. doi: 10.1016/S0168-9525(03)00176-8

10. Price C, Herman BC, Lufkin T, Goldman HM, Jepsen KJ. Genetic variation in bone growth patterns defines adult mouse bone fragility. *J Bone Miner Res Off J Am Soc Bone Miner Res* (2005) 20(11):1983–91. doi: 10.1359/JBMR.050707

11. Isojima T, Sims NA. Cortical bone development, maintenance and porosity: genetic alterations in humans and mice influencing chondrocytes, osteoclasts, osteoblasts and osteocytes. *Cell Mol Life Sci CMLS.* (2021) 78(15):5755–73. doi: 10.1007/s00018-021-03884-w

12. Blank M, Sims NA. Cellular processes by which osteoblasts and osteocytes control bone mineral deposition and maturation revealed by stage–specific EphrinB2 knockdown. *Curr Osteoporos Rep* (2019) 17(5):270–80. doi: 10.1007/s11914-019-00524-y

13. van den Bos T, Speijer D, Bank RA, Brömme D, Everts V. Differences in matrix composition between calvaria and long bone in mice suggest differences in biomechanical properties and resorption: Special emphasis on collagen. *Bone* (2008) 43(3):459–68. doi: 10.1016/j.bone.2008.05.009

14. Brommage R, Ohlsson C. High fidelity of mouse models mimicking human genetic skeletal disorders. *Front Endocrinol* (2020) 10:934. doi: 10.3389/fendo.2019.00934

15. Warriner AH, Patkar NM, Curtis JR, Delzell E, Gary L, Kilgore M, et al. Which fractures are most attributable to osteoporosis? *J Clin Epidemiol* (2011) 64(1):46–53. doi: 10.1016/j.jclinepi.2010.07.007

16. Wang N, Niger C, Li N, Richards GO, Skerry TM. Cross–species RNA–seq study comparing transcriptomes of enriched osteocyte populations in the tibia and skull. *Front Endocrinol* (2020) 11:581002. doi: 10.3389/fendo.2020.581002

17. Rawlinson SCF, McKay IJ, Ghuman M, Wellmann C, Ryan P, Prajaneh S, et al. Adult rat bones maintain distinct regionalized expression of markers associated with their development. *PloS One* (2009) 4(12):e8358. doi: 10.1371/journal.pone.0008358

18. Debnath S, Yallowitz AR, McCormick J, Lalani S, Zhang T, Xu R, et al. Discovery of a periosteal stem cell mediating intramembranous bone formation. *Nature* (2018) 562(7725):133–9. doi: 10.1038/s41586-018-0554-8

19. Kalev–Altman R, Janssen JN, Ben–Haim N, Levy T, Shitrit–Tovli A, Milgram J, et al. The gelatinases, matrix metalloproteinases 2 and 9, play individual roles in skeleton development. *Matrix Biol J Int Soc Matrix Biol* (2022), S0945–053X(22)00124–X. doi: 10.1016/j.matbio.2022.10.002

20. Rozner R, Vernikov J, Griess–Fishheimer S, Travinsky T, Penn S, Schwartz B, et al. The role of omega–3 polyunsaturated fatty acids from different sources in bone development. *Nutrients* (2020) 12(11):1–22. doi: 10.3390/nu12113494

21. Zaretsky J, Griess–Fishheimer S, Carmi A, Travinsky Shmul T, Ofer L, Sinai T, et al. Ultra–processed food targets bone quality *via* endochondral ossification. *Bone Res* (2021) 9(1):14. doi: 10.1038/s41413-020-00127-9

22. Jaitin DA, Kenigsberg E, Keren–Shaul H, Elefant N, Paul F, Zaretsky I, et al. Massively parallel single–cell RNA–seq for marker–free decomposition of tissues into cell types. *Science* (2014) 343(6172):776–9. doi: 10.1126/science.1247651

23. Keren–Shaul H, Kenigsberg E, Jaitin DA, David E, Paul F, Tanay A, et al. MARS–seq2.0: an experimental and analytical pipeline for indexed sorting combined with single–cell RNA sequencing. *Nat Protoc* (2019) 14(6):1841–62.

24. Anders S, Pyl PT, Huber W. HTSeq–a Python framework to work with high–throughput sequencing data. *Bioinforma Oxf Engl* (2015) 31(2):166–9. doi: 10.1093/bioinformatics/btu638

25. Eden E, Navon R, Steinfeld I, Lipson D, Yakhini Z. GOrilla: a tool for discovery and visualization of enriched GO terms in ranked gene lists. *BMC Bioinf* (2009) 10:48. doi: 10.1186/1471-2105-10-48

26. Luo W, Brouwer C. Pathview: an R/Bioconductor package for pathway–based data integration and visualization. *Bioinforma Oxf Engl* (2013) 29(14):1830–1. doi: 10.1093/bioinformatics/btt285

27. Dutta S, Sengupta P. Men and mice: Relating their ages. *Life Sci* (2016) 152:244–8. doi: 10.1016/j.lfs.2015.10.025

28. Xing W, Baylink D, Kesavan C, Hu Y, Kapoor S, Chadwick RB, et al. Global gene expression analysis in the bones reveals involvement of several novel genes and pathways in mediating an anabolic response of mechanical loading in mice. *J Cell Biochem* (2005) 96(5):1049–60. doi: 10.1002/jcb.20606

29. Guasto A, Cormier–Daire V. Signaling pathways in bone development and their related skeletal dysplasia. *Int J Mol Sci* (2021) 22(9):4321. doi: 10.3390/ijms22094321

30. Berendsen AD, Olsen BR. Bone development. *Bone* (2015) 80:14–8. doi: 10.1016/j.bone.2015.04.035

31. Knöll R, Hoshijima M, Hoffman HM, Person V, Lorenzen–Schmidt I, Bang ML, et al. The cardiac mechanical stretch sensor machinery involves a z disc complex that is defective in a subset of human dilated cardiomyopathy. *Cell* (2002) 111(7):943–55. doi: 10.1016/S0092-8674(02)01226-6

32. Kawaguchi J, Kii I, Sugiyama Y, Takeshita S, Kudo A. The transition of cadherin expression in osteoblast differentiation from mesenchymal cells: Consistent expression of cadherin–11 in osteoblast lineage. *J Bone Miner Res* (2001) 16(2):260–9. doi: 10.1359/jbmr.2001.16.2.260

33. Ayturk UM, Scollan JP, Ayturk DG, Suh ES, Vesprey A, Jacobsen CM, et al. SINGLE CELL RNA SEQUENCING OF CALVARIAL AND LONG BONE ENDOCORTICAL CELLS. *J Bone Miner Res Off J Am Soc Bone Miner Res* (2020) 35 (10):1981–91. doi: 10.1002/jbmr.4052

34. Liu S, Tang W, Fang J, Ren J, Li H, Xiao Z, et al. Novel regulators of Fgf23 expression and mineralization in hyp bone. *Mol Endocrinol Baltim Md.* (2009) 23 (9):1505–18. doi: 10.1210/me.2009-0085

35. Shao J, Yu M, Jiang L, Wu F, Liu X. Sequencing and bioinformatics analysis of the differentially expressed genes in herniated discs with or without calcification. *Int J Mol Med* (2017) 39(1):81–90. doi: 10.3892/ijmm.2016.2821

36. Matsuda T, Kondo A, Tsunashima Y, Togari A. Inhibitory effect of vitamin K(2) on interleukin-1beta-stimulated proliferation of human osteoblasts. *Biol Pharm Bull* (2010) 33(5):804–8. doi: 10.1248/bpb.33.804

37. Dwivedi PP, Grose RH, Filmus J, Hii CST, Xian CJ, Anderson PJ, et al. Regulation of bone morphogenetic protein signalling and cranial osteogenesis by Gpc1 and Gpc3. *Bone* (2013) 55(2):367–76. doi: 10.1016/j.bone.2013.04.013

38. Kolluri A, Ho M. The role of glypican–3 in regulating wnt, YAP, and hedgehog in liver cancer. *Front Oncol* (2019) 9:708. doi: 10.3389/fonc.2019.00708

39. Velasco J, Zarrabeitia MT, Prieto JR, Perez–Castrillon JL, Perez–Aguilar MD, Perez–Nuñez MI, et al. Wnt pathway genes in osteoporosis and osteoarthritis: differential expression and genetic association study. *Osteoporos Int J Establ Result Coop Eur Found Osteoporos Natl Osteoporos Found USA* (2010) 21(1):109–18. doi: 10.1007/s00198-009-0931-0

40. Maupin KA, Droscha CJ, Williams BO. A comprehensive overview of skeletal phenotypes associated with alterations in wnt/β–catenin signaling in humans and mice. *Bone Res* (2013) 1(1):27–71. doi: 10.4248/BR201301004

41. Lu D, Li J, Liu H, Foxa GE, Weaver K, Li J, et al. LRP1 suppresses bone resorption in mice by inhibiting the RANKL–stimulated NF–κB and p38 pathways during osteoclastogenesis. *J Bone Miner Res* (2018) 33(10):1773–84. doi: 10.1002/jbmr.3469

42. Aslan H, Ravid–Amir O, Clancy BM, Rezvankhah S, Pittman D, Pelled G, et al. Advanced molecular profiling in vivo detects novel function of dickkopf–3 in the regulation of bone formation. *J Bone Miner Res* (2006) 21(12):1935–45. doi: 10.1359/jbmr.060819

43. Esposito M, Fang C, Cook KC, Park N, Wei Y, Spadazzi C, et al. TGF–β–induced DACT1 biomolecular condensates repress wnt signalling to promote bone metastasis. *Nat Cell Biol* (2021) 23(3):257–67. doi: 10.1038/s41556-021-00641-w

44. Murakami K, Zhifeng H, Suzuki T, Kobayashi Y, Nakamura Y. The Shisa3 knockout mouse exhibits normal bone phenotype. *J Bone Miner Me* (019) 37(6):967–75. doi: 10.1007/s00774-019-01014-y

45. Qiu N, Cao L, David V, Quarles LD, Xiao Z. Kif3a deficiency reverses the skeletal abnormalities in Pkd1 deficient mice by restoring the balance between osteogenesis and adipogenesis. *PloS One* (2010) 5(12):e15240. doi: 10.1371/journal.pone.0015240

46. Maridas DE, Gamer L, Moore ER, Doedens AM, Yu Y, Ionescu A, et al. Loss of vlk in Prx1+ cells delays the initial steps of endochondral bone formation and fracture repair in the limb. *J Bone Miner Res Off J Am Soc Bone Miner Res* (2022) 37(4):764–75. doi: 10.1002/jbmr.4514

47. Moosa S, Obregon MG, Altmüller J, Thiele H, Nürnberg P, Fano V, et al. Novel IFT122 mutations in three Argentinian patients with cranioectodermal dysplasia: Expanding the mutational spectrum. *Am J Med Genet A* (2016) 170A(5):1295–301. doi: 10.1002/ajmg.a.37570

48. Ohba S. Hedgehog signaling in skeletal development: Roles of Indian hedgehog and the mode of its action. *Int J Mol Sci* (2020) 21(18):6665. doi: 10.3390/ijms21186665

49. Holmes G, van Bakel H, Zhou X, Losic B, Jabs EW. BCL11B expression in intramembranous osteogenesis during murine craniofacial suture development. *Gene Expr Patterns GEP* (2015) 17(1):16–25. doi: 10.1016/j.gep.2014.12.001

50. Galea GL, Meakin LB, Williams CM, Hulin–Curtis SL, Lanyon LE, Poole AW, et al. Protein kinase cα (PKCα) regulates bone architecture and osteoblast activity. *J Biol Chem* (2014) 289(37):25509–22. doi: 10.1074/jbc.M114.580365

51. Stock M, Schett G. Vitamin K–dependent proteins in skeletal development and disease. *Int J Mol Sci* (2021) 22(17):9328. doi: 10.3390/ijms22179328

52. Baron R, Rawadi G, Roman–Roman S. Wnt signaling: a key regulator of bone mass. *Curr Top Dev Biol* (2006) 76:103–27. doi: 10.1016/S0070-2153(06)76004-5

53. Kim JM, Han H, Bahn M, Hur Y, Yeo CY, Kim DW. Secreted tyrosine kinase vlk negatively regulates hedgehog signaling by inducing lysosomal degradation of smoothened. *Biochem J* (2020) 477(1):121–36. doi: 10.1042/BCJ20190784

54. Martín–Guerrero E, Tirado–Cabrera I, Buendía I, Alonso V, Gortázar AR, Ardura JA. Primary cilia mediate parathyroid hormone receptor type 1 osteogenic actions in osteocytes and osteoblasts *via* gli activation. *J Cell Physiol* (2020) 235 (10):7356–69. doi: 10.1002/jcp.29636

55. Patel A. The primary cilium calcium channels and their role in flow sensing. *Pflugers Arch* (2015) 467(1):157–65. doi: 10.1007/s00424-014-1516-0

56. Walczak–Sztulpa J, Eggenschwiler J, Osborn D, Brown DA, Emma F, Klingenberg C, et al. Cranioectodermal dysplasia, sensenbrenner syndrome, is a ciliopathy caused by mutations in the IFT122 gene. *Am J Hum Genet* (2010) 86 (6):949–56. doi: 10.1016/j.ajhg.2010.04.012

57. Muhammad H, Rais Y, Miosge N, Ornan EM. The primary cilium as a dual sensor of mechanochemical signals in chondrocytes. *Cell Mol Life Sci CMLS.* (2012) 69 (13):2101–7. doi: 10.1007/s00018-011-0911-3

58. Rais Y, Reich A, Simsa–Maziel S, Moshe M, Idelevich A, Kfir T, et al. The growth plate's response to load is partially mediated by mechano–sensing *via* the chondrocytic primary cilium. *Cell Mol Life Sci CMLS.* (2015) 72(3):597–615. doi: 10.1007/s00018-014-1690-4

59. Ross AP, Zarbalis KS. The emerging roles of ribosome biogenesis in craniofacial development. *Front Physiol* (2014) 5:26. doi: 10.3389/fphys.2014.00026

60. Trainor PA, Merrill AE. Ribosome biogenesis in skeletal development and the pathogenesis of skeletal disorders. *Biochim Biophys Acta BBA – Mol Basis Dis* (2014) 1842(6):769–78. doi: 10.1016/j.bbadis.2013.11.010

61. Dufour C, Holy X, Marie PJ. Skeletal unloading induces osteoblast apoptosis and targets α5β1–PI3K–Bcl–2 signaling in rat bone. *Exp Cell Res* (2007) 313(2):394–403. doi: 10.1016/j.yexcr.2006.10.021

62. Brunner M, Jurdic P, Tuckerman JP, Block MR, Bouvard D. New insights into adhesion signaling in bone formation. *Int Rev Cell Mol Biol* (2013) 305:1–68. doi: 10.1016/B978-0-12-407695-2.00001-9

63. Rodríguez–Carballo E, Gámez B, Ventura F. p38 MAPK signaling in osteoblast differentiation. *Front Cell Dev Biol* (2016) 4:40. doi: 10.3389/fcell.2016.00040

64. Caverzasio J, Manen D. Essential role of Wnt3a–mediated activation of mitogen–activated protein kinase p38 for the stimulation of alkaline phosphatase activity and matrix mineralization in C3H10T1/2 mesenchymal cells. *Endocrinology* (2007) 148(11):5323–30. doi: 10.1210/en.2007-0520

65. Eapen A, Sundivakkam P, Song Y, Ravindran S, Ramachandran A, Tiruppathi C, et al. Calcium-mediated stress kinase activation by DMP1 promotes osteoblast differentiation. *J Biol Chem* (2010) 285(47):36339–51. doi: 10.1074/jbc.M110.145607

66. Renou L, Stora S, Yaou RB, Volk M, Sinkovec M, Demay L, et al. Heart–hand syndrome of Slovenian type: a new kind of laminopathy. *J Med Genet* (2008) 45 (10):666–71. doi: 10.1136/jmg.2008.060020

67. Morgan JM, Wong A, Yellowley CE, Genetos DC. Regulation of tenascin expression in bone. *J Cell Biochem* (2011) 112(11):3354–63. doi: 10.1002/jcb.23265

68. Nelson JF, Karelus K, Felicio LS, Johnson TE. Genetic influences on the timing of puberty in mice. *Biol Reprod* (1990) 42(4):649–55. doi: 10.1095/biolreprod42.4.649

69. Yagnik G, Ghuman A, Kim S, Stevens CG, Kimonis V, Stoler J, et al. ALX4 gain–of–function mutations in nonsyndromic craniosynostosis. *Hum Mutat* (2012) 33 (12):1626–9. doi: 10.1002/humu.22166

70. Twigg SRF, Forecki J, Goos JAC, Richardson ICA, Hoogeboom AJM, van den Ouweland AMW, et al. Gain–of–Function mutations in ZIC1 are associated with coronal craniosynostosis and learning disability. *Am J Hum Genet* (2015) 97(3):378–88. doi: 10.1016/j.ajhg.2015.07.007

71. Kamath RAD, Benson MD. EphB3 as a potential mediator of developmental and reparative osteogenesis. *Cells Tissues Organs* (2021). doi: 10.1159/000520369

72. Benson MD, Opperman LA, Westerlund J, Fernandez CR, San Miguel S, Henkemeyer M, et al. Ephrin–b stimulation of calvarial bone formation. *Dev Dyn.* (2012) 241(12):1901–10. doi: 10.1002/dvdy.23874

73. Orioli D, Henkemeyer M, Lemke G, Klein R, Pawson T. Sek4 and nuk receptors cooperate in guidance of commissural axons and in palate formation. *EMBO J* (1996) 15(22):6035–49. doi: 10.1002/j.1460-2075.1996.tb00992.x

74. Bartelt A, BJ F, tB F, K T, M B, S T, et al. Lrp1 in osteoblasts controls osteoclast activity and protects against osteoporosis by limiting PDGF–RANKL signaling. *Bone Res* (2018) 6. doi: 10.1038/s41413-017-0006-3

75. Wang X, Li B. Genetic studies of bone diseases: Evidence for involvement of DNA damage response proteins in bone remodeling. *Int J BioMed Sci IJBS.* (2007) 3 (4):217–28.

76. Jilka RL. The relevance of mouse models for investigating age–related bone loss in humans. *J Gerontol A Biol Sci Med Sci* (2013) 68(10):1209–17. doi: 10.1093/gerona/glt046

77. Guo D, Bonewald LF. Advancing our understanding of osteocyte cell biology. *Ther Adv Musculoskelet Dis* (2009) 1(2):87–96. doi: 10.1177/1759720X09341484

78. Slavov N, Semrau S, Airoldi E, Budnik B, van Oudenaarden A. Differential stoichiometry among core ribosomal proteins. *Cell Rep* (2015) 13(5):865–73. doi: 10.1016/j.celrep.2015.09.056

79. Green H, Canfield AE, Hillarby MC, Grant ME, Boot–Handford RP, Freemont AJ, et al. The ribosomal protein QM is expressed differentially during vertebrate endochondral bone development. *J Bone Miner Res* (2000) 15(6):1066–75. doi: 10.1359/jbmr.2000.15.6.1066

80. Paznekas WA, Zhang N, Gridley T, Jabs EW. Mouse TCOF1 is expressed widely, has motifs conserved in nucleolar phosphoproteins, and maps to chromosome 18. *Biochem Biophys Res Commun* (1997) 238(1):1–6. doi: 10.1006/bbrc.1997.7229

81. Jones NC, Lynn ML, Gaudenz K, Sakai D, Aoto K, Rey JP, et al. Prevention of the neurocristopathy treacher Collins syndrome through inhibition of p53 function. *Nat Med* (2008) 14(2):125–33. doi: 10.1038/nm1725

82. Dixon J, Jones NC, Sandell LL, Jayasinghe SM, Crane J, Rey JP, et al. Tcof1/Treacle is required for neural crest cell formation and proliferation deficiencies that cause craniofacial abnormalities. *Proc Natl Acad Sci U S A.* (2006) 103(36):13403–8. doi: 10.1073/pnas.0603730103

83. Mogass M, York TP, Li L, Rujirabanjerd S, Shiang R. Genomewide analysis of gene expression associated with Tcof1 in mouse neuroblastoma. *Biochem Biophys Res Commun* (2004) 325(1):124–32. doi: 10.1016/j.bbrc.2004.10.004

84. Komori T. Functions of osteocalcin in bone, pancreas, testis, and muscle. *Int J Mol Sci* (2020) 21(20):7513. doi: 10.3390/ijms21207513

85. Nassif A, Senussi I, Meary F, Loiodice S, Hotton D, Robert B, et al. Msx1 role in craniofacial bone morphogenesis. *Bone* (2014), 66:96–104. doi: 10.1016/j.bone.2014.06.003

86. Gullard A, Gluhak–Heinrich J, Papagerakis S, Sohn P, Unterbrink A, Chen S, et al. MEPE localization in the craniofacial complex and function in tooth dentin formation. *J Histochem Cytochem* (2016) 64(4):224–36. doi: 10.1369/0022155416635569

87. Gowen LC, Petersen DN, Mansolf AL, Qi H, Stock JL, Tkalcevic GT, et al. Targeted disruption of the Osteoblast/Osteocyte factor 45 gene (OF45) results in increased bone formation and bone mass *. *J Biol Chem* (2003) 278(3):1998–2007. doi: 10.1074/jbc.M203250200

frontiers | Frontiers in Endocrinology

TYPE Original Research
PUBLISHED 09 August 2023
DOI 10.3389/fendo.2023.1215790

OPEN ACCESS

EDITED BY
Michela Rossi,
Bambino Gesù Children's Hospital (IRCCS), Italy

REVIEWED BY
Atika Dhar,
National Institutes of Health (NIH), United States
Stefano Ciardullo,
University of Milano Bicocca, Italy

*CORRESPONDENCE
Yan Zhuang
zhuangyan2512@163.com
Pengfei Wang
pengfei_wang@163.com
Xing Wei
92871360@163.com

†These authors have contributed equally to this work

RECEIVED 02 May 2023
ACCEPTED 19 July 2023
PUBLISHED 09 August 2023

CITATION
Cui A, Xiao P, Fan Z, Lei J, Han S, Zhang D, Wei X, Wang P and Zhuang Y (2023) Causal association of NAFLD with osteoporosis, fracture and falling risk: a bidirectional Mendelian randomization study. *Front. Endocrinol.* 14:1215790. doi: 10.3389/fendo.2023.1215790

Causal association of NAFLD with osteoporosis, fracture and falling risk: a bidirectional Mendelian randomization study

Aiyong Cui[1†], Peilun Xiao[2†], Zhiqiang Fan[1†], Jinlai Lei[1], Shuang Han[1], Danlong Zhang[1], Xing Wei[1*], Pengfei Wang[1*] and Yan Zhuang[1*]

[1]Department of Orthopaedics, Honghui Hospital, Xi'an Jiao Tong University, Xi'an, China, [2]Department of Orthopaedics, The Fifth Affiliated Hospital of Sun Yat-Sen University, Zhuhai, Guangdong, China

Introduction: The causal association between non-alcoholic fatty liver disease (NAFLD) and osteoporosis remains controversial in previous epidemiological studies. We employed a bidirectional two-sample Mendelian analysis to explore the causal relationship between NAFLD and osteoporosis.

Method: The NAFLD instrumental variables (IVs) were obtained from a large Genome-wide association study (GWAS) meta-analysis dataset of European descent. Two-sample Mendelian randomization (MR) analyses were used to estimate the causal effect of NAFLD on osteoporosis, fracture, and fall. Reverse Mendelian randomization analysis was conducted to estimate the causal effect of osteoporosis on NAFLD. The inverse-variance weighted (IVW) method was the primary analysis in this analysis. We used the MR-Egger method to determine horizontal pleiotropic. The heterogeneity effect of IVs was detected by MR-Egger and IVW analyses.

Results: Five SNPs (rs2980854, rs429358, rs1040196, rs738409, and rs5764430) were chosen as IVs for NAFLD. In forward MR analysis, the IVW-random effect indicated the causal effect of NAFLD on osteoporosis (OR= 1.0021, 95% CI: 1.0006-1.0037, *P*= 0.007) but not on fracture (OR= 1.0016, 95% CI: 0.998-1.0053, *P*= 0.389) and fall (OR= 0.9912, 95% CI: 0.9412-1.0440, *P*= 0.740). Furthermore, the reverse Mendelian randomization did not support a causal effect of osteoporosis on NAFLD (OR= 1.0002, 95% CI: 0.9997-1.0007, *P*= 0.231). No horizontal pleiotropic was detected in all MR analyses.

Conclusions: The results of this study indicate a causal association between NAFLD and osteoporosis. NAFLD patients have a higher risk of osteoporosis but not fracture and falling risk. In addition, our results do not support a causal effect of osteoporosis on NAFLD.

KEYWORDS

NAFLD, osteoporosis, fracture, Mendelian randomization, genome-wide association study

Introduction

Osteoporosis (OP) is a bone disorder featured by low bone mass density (BMD) and impaired microarchitecture, leading to a higher fragility fracture risk for the old (1). In a meta-analysis, the global prevalence of osteoporosis in people aged 50-59, 60-69, and 70-79 was 11.4%, 24.8, and 37.6%, respectively (2). In 2013, twenty-two million females and 5.5 million males in European Union (EU) countries suffered from osteoporosis, leading to 3.5 million fragility fractures annually (3). Osteoporosis is a multifactorial disease involving clinical, nutritional, behavioral, medical, and genetic factors in their occurrence (4). Imbalance in bone formation and resorption due to various reasons, such as reduced estrogen levels in postmenopausal women or advanced age, will lead to osteoporosis (5). Previously, gender, age, family osteoporosis history, alcohol consumption, smoking, hormone use, some diseases, and others were considered possible risk factors for osteoporosis (6, 7).

Non-alcoholic fatty liver disease (NAFLD) has become the most common chronic liver disease, threatening about 25% population worldwide (8). With the epidemic of the western diet, sedentary lifestyle, and obesity, the prevalence of NAFLD in the general population has been increasing in recent years (9). NAFLD spectrum includes non-alcoholic fatty liver (NAFL), non-alcoholic steatohepatitis (NASH), and NASH-related end-stage liver disease, such as cirrhosis. Insulin resistance, type 2 diabetes (T2D), hyperlipidemia, hypertension, and metabolic syndrome may play an essential role in the development of NAFLD (10). In previous studies, a large number of studies have demonstrated the possible role of NAFLD in the development of osteoporosis. Studies showed that the prevalence of osteoporosis in NAFLD patients is higher than in patients without NAFLD (11). NAFLD may affect osteoporosis or osteoporotic fractures in several ways, including the changes in bone metabolic transforming factors, vitamin D levels, the chronic inflammatory state of the liver, degree of hepatic fibrosis, and disturbances in lipid metabolism, and others. However, previous observational studies investigating the association between NAFLD and osteoporosis have consistently yielded inconsistent results. Some studies have shown that NAFLD is associated with lower BMD or higher fracture risk in adolescents or adults (12–14), while others have shown no significant correlation or even opposite results (15–17). These observational studies have obvious limitations like unmeasured or imprecisely measured confounders such as gender, age, menstrual status, and others, which inevitably lead to some biases.

Mendelian randomization (MR) is a novel genetic variation method to assess the causal relationship between exposure and outcome (18). It could avoid confounding factors and infer causality since the alleles of exposure genetic variants are randomly assigned (19). Thus, we employed an MR analysis to explore the causal effect of NAFLD on osteoporosis, fracture, and falling risk. A reverse MR analysis was also used to explore the causal effect of osteoporosis on NAFLD.

Materials and methods

Study design

The MR analyses conform to three assumptions: 1. Selected SNPs should be strongly correlated with exposure. 2. Selected SNPs are not related to the outcome through confounders. 3. Selected SNPs are supposed to affect outcomes *via* exposure, but not the direct association (Figure 1). All information in this study was obtained from public databases or existing publications, which did not need additional ethical approval.

Data sources for NAFLD

The sources of NAFLD were obtained from large GWASs by Ghodsian et al. (20). The GWASs meta-analysis included summary statistics from the FinnGen cohorts eMERGE, the latest GWAS

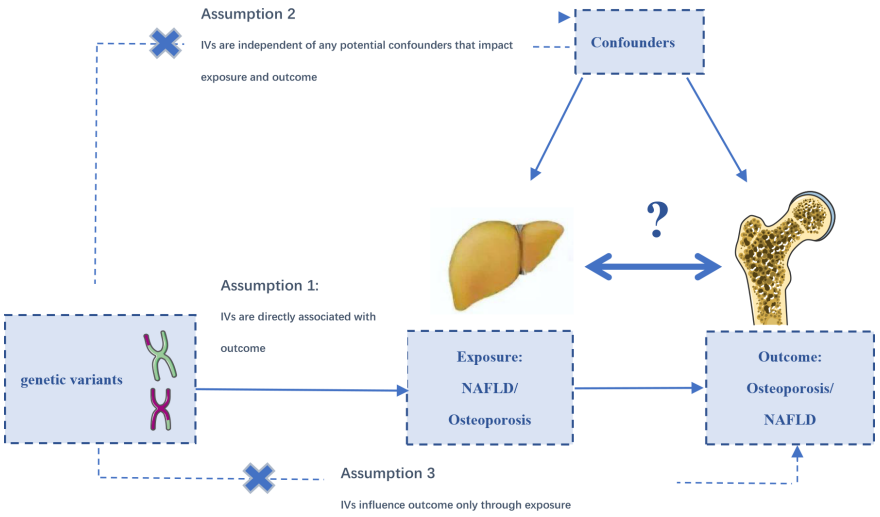

FIGURE 1
The designs and assumptions for the bidirectional Mendelian randomization study of the causal association of NAFLD and osteoporosis, fracture, and falling risk.

conducted by the Estonian Biobank (4,119 cases and 190,120 controls), and a new NAFLD GWAS from the UK Biobank (2,558 cases and 395,241 controls), with a total of 8,434 NAFLD cases and 770,180 controls. In this GWAS meta-analysis, the associations were conducted by adjusting for gender, age, and ten main ancestry-based principal components and genotyping (20). The electronic health record documented NAFLD with participants of European ancestry with hepatic steatosis, NASH, or liver fibrosis (LF). Finally, five SNPs (rs2980854, rs429358, rs10401969, rs738409, rs5764430) closely associated with NAFLD ($p< 5\times10^{-08}$) without linkage were chosen as alternative instruments for NAFLD ($R^2<0.001$, window size =10,000 kb).

Data sources for osteoporosis, fractures, and fall

Summary-level genetic data on osteoporosis were collected from the UK Biobank (UK Biobank: 20002#1309), including 7,547 osteoporosis samples and 455,386 control samples. The genetic associations with fracture risk were revealed in a large GWAS meta-analysis combining 23andMe cohorts and the UK Biobank, with a total of 1.2 million subjects (21). The fracture diagnosis was defined as a break in bone continuity at any site in the past five years, except for fractures at hands, feet, skull, or pathological fractures due to malignancy, infection, and others (21). GWAS data for falling susceptibility were collected from a UK Biobank study, involving 89,076 fall cases and 362,103 controls (22). A "fall" is defined when the subject gives an affirmative answer to the following question: "Have you fallen in the last year?

Statistical analysis

The bidirectional MR approach was conducted to estimate the causality between NAFLD and osteoporosis, fracture, and fall. Relevant SNPs were selected when genome-wide significance was less than $p< 5\times10^{-8}$. SNPs were excluded when detecting linkage disequilibrium (LD) ($R^2 > 0.001$ or clump distance< 10,000 kb). Five methods were employed to examine the causal association, including inverse-variance weighted (IVW), MR-Egger, weighted mode, weighted median, and simple model, among which IVW was the primary method (23). Random-effects IVW was performed to assess the genetic predictions between them. The MR-Egger method was used to test its horizontal pleiotropic. Outlier SNPs were detected by MR-PRESSO packages and then deleted. Cochran's Q statistic was applied to examine the heterogeneity of individual SNPs in IVW and MR-Egger tests. We additionally performed sensitivity analysis by removing single SNP one by one. To evaluate the weak instrument bias, we calculated the F statistics using the formula $F = (\frac{N-K-1}{K})(\frac{R^2}{1-R^2})$, where N is the sample size, K is the number of IVs, and R^2 is the proportion of the variability of the exposure explained by IVs. All data were analyzed by package "TwoSampleMR" of the R language.

Results

Genetical prediction of NAFLD on osteoporosis

Five SNPs (rs2980854 in/near TRIB1, rs429358 in/near APOE, rs10401969 in/near SUGP1, rs738409 in/near PNPLA3, rs5764430 in/near SAMM50) were chosen as IVs for NAFLD (Supplementary Table 1). The SNP was larger than the empirical threshold 10 of the F statistics, indicating a weak bias of the IVs. The causal association of NAFLD variants with osteoporosis was shown in Table 1 and Figure 2. The IVW results found a positive effect of NAFLD on osteoporosis (OR= 1.0021, 95% CI: 1.0006-1.0037, *P*= 0.007). The consistent result was also found in MR Egger (OR= 1.0041, 95% CI: 1.0003-1.0087, *P*= 0.012), weighted median (OR= 1.0022, 95% CI: 1.0004-1.0040, *P*= 0.015), and weighted mode (OR= 1.0023, 95% CI: 1.0002-1.0045, *P*= 0.024). The Cochran's Q statistic of MR-Egger (*P*= 0.972) and IVW methods (*P*= 0.831) indicated no significant heterogeneity between IVs. No horizontal pleiotropy was detected in MR–Egger intercept (*P*= 0.346). In the leave-one-

TABLE 1 Causal effect of NAFLD on osteoporosis using genetic variant randomization in different MR methods.

Exposure	Outcome	Method	No. of SNP	OR (95% CI)	95% CI	*P*
NAFLD	Osteoporosis	IVW	5	1.0021	1.0006-1.0037	0.007
		MR Egger	5	1.0041	1.0003-1.0087	0.012
		Weighted median	5	1.0022	1.0004-1.0040	0.015
		Simple mode	5	1.0014	0.9987-1.0041	0.375
		Weighted mode	5	1.0023	1.0002-1.0045	0.024
MR Egger: Cochran's Q= 0.234, *P*= 0.972						
IVW: Cochran's Q= 1.476, *P*= 0.831						
MR-Egger intercept= -0.0004, *P*= 0.346						
MR-PRESSO global test= 0.868						

No outlier was observed in the MR-PRESSO analysis in MR analysis in NAFLD and osteoporosis. CI, confidence interval; MR, Mendelian randomization; IVW, inverse-variance weighted; NAFLD, non-alcoholic fatty liver disease.

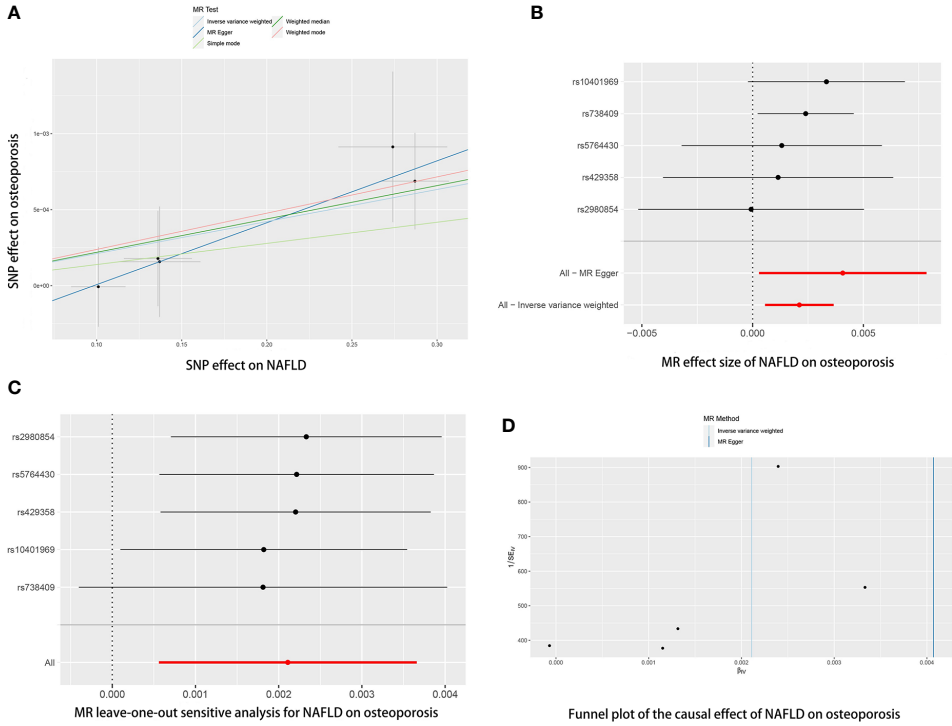

FIGURE 2
The causal effects of NAFLD on osteoporosis in different MR methods. **(A)** Scatter plot. The slopes of each line represent the causal association for each method. **(B)** Forrest plot. **(C)** Leave-one-out analysis. **(D)** Funnel plot.

out sensitive analyses, we found rs738409 strongly drove the overall effect of NAFLD on osteoporosis (Figure 2C). Furthermore, the MR-PRESSO test did not identify any potential SNP outliers.

Genetical prediction of NAFLD on fracture risk

The causal association of NAFLD variants with fracture was shown in Table 2 and Figure 3. MR analysis by the IVW method showed that there was no causal effect of NAFLD on fracture (OR= 1.0016, 95% CI: 0.998-1.0053, *P*= 0.389). The consistent result was also found in MR Egger (OR= 1.0057, 95% CI: 0.9969-1.0147, *P*= 0.295), weighted median (OR= 1.0012, 95% CI: 0.9970-1.0055, *P*= 0.581), simple mode (OR= 1.0029, 95% CI: 0.9961-1.0098, *P*= 0.448) and weighted mode (OR= 1.0013, 95% CI: 0.9963-1.0064, *P*= 0.632). The Cochran's Q statistic of MR-Egger (*P*= 0.396) and IVW methods (*P*= 0.411) indicated no significant heterogeneity between IVs. No horizontal pleiotropy was detected in MR–Egger intercept (*P*= 0.391). In addition, the result remains no significant after excluding a single SNP (Figure 3C). MR-PRESSO test did not identify any potential SNP outliers.

TABLE 2 Causal effect of NAFLD on fracture risk using genetic variant randomization in different MR methods.

Exposure	Outcome	Method	No. of SNP	OR (95% CI)	95% CI	*P*
NAFLD	Fracture	IVW	5	1.0016	0.998-1.0053	0.389
		MR Egger	5	1.0057	0.9969-1.0147	0.295
		Weighted median	5	1.0012	0.9970-1.0055	0.581
		Simple mode	5	1.0029	0.9961-1.0098	0.448
		Weighted mode	5	1.0013	0.9963-1.0064	0.632
MR Egger: Cochran's Q= 2.967, *P*= 0.396						
IVW: Cochran's Q= 3.965, P= 0.411						
MR-Egger intercept= -0.0008, *P*= 0.391						
MR-PRESSO global test= 0.517						

No outlier was observed in the MR-PRESSO analysis in MR analysis in NAFLD and fractures. CI, confidence interval; MR, Mendelian randomization; IVW, inverse-variance weighted; NAFLD, non-alcoholic fatty liver disease.

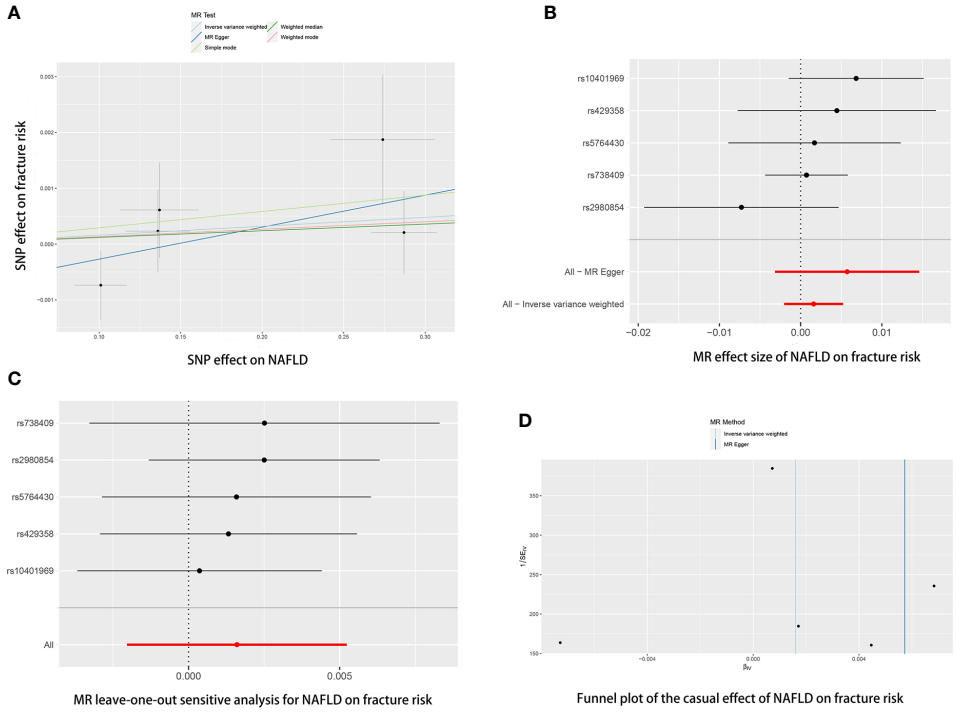

FIGURE 3
The causal effects of NAFLD on fracture risk in different MR methods. **(A)** Scatter plot. The slopes of each line represent the causal association for each method. **(B)** Forrest plot. **(C)** Leave-one-out analysis. **(D)** Funnel plot.

Genetical prediction of NAFLD on falling risk

The causal association of NAFLD variants with fracture was shown in Table 3 and Figure 4. MR analysis by the IVW method showed that there was no causal effect of NAFLD on falling risk (OR= 0.9912, 95% CI: 0.9412-1.0440, *P*= 0.740). The consistent result was also found in MR Egger (OR= 1.0211, 95% CI: 0.8865-1.1763, *P*= 0.791), weighted median (OR= 0.9987, 95% CI: 0.9681-1.0301, *P*= 0.932), simple mode (OR= 0.9949, 95% CI: 0.9521-1.0396, *P*= 0.831) and weighted mode (OR= 0.9964, 95% CI: 0.9613-1.0327, *P*= 0.852). The Cochran's Q statistic of MR-Egger (*P*= 0.002) and IVW methods (*P*= 0.004) indicated significant heterogeneity between IVs, suggesting the use of the random effect model of IVW. No horizontal pleiotropy was detected in MR–Egger intercept (*P*= 0.682). The result remains no significant in leave-one-out sensitive analyses (Figure 4C). MR-PRESSO did not identify any potential SNP outliers.

Reverse Mendelian randomization analysis

Reverse MR analyses were then conducted to assess the causal effect of osteoporosis on NAFLD. Sixteen SNPs without linkage were chosen as the IVs for osteoporosis (Supplementary Table 2). Our study found no causal effect of osteoporosis on NAFLD (OR= 0.9759, 95% CI: 0.9246-1.3000, *P*= 0.375) (Table 4 and Figure 5). The F-statistic for IVs was 60.2 > 10. The consistent results were also found in other MR methods. The Cochran's Q statistic of MR-Egger (*P*= 0.869) and IVW methods (*P*= 0.847) indicated no significant heterogeneity between IVs. The result remains no significant in leave-one-out sensitive analyses (Figure 5C). No horizontal pleiotropy was detected in MR–Egger intercept (*P*= 0.296). MR-PRESSO also did not identify any potential SNP outliers.

Discussion

Although much work has explored the potential link between NAFLD and osteoporosis, the results are hardly convincing because of the nature of observational studies that cannot overcome the confounding factors. To our knowledge, this is the first MR study to assess the causal association between NAFLD and osteoporosis. Our studies indicated that genetic prediction of NAFLD was associated with a higher risk of osteoporosis. However, our findings did not support a causal association of NAFLD variants with fractures and falling risk. Moreover, the reverse MR analysis showed no genetic prediction of NAFLD on osteoporosis. In this study, five variations (rs2980854, rs429358, rs10401969, rs738409, rs5764430) at the APOE, SUGP1, TRIB1, SAMM50, and PNPLA3 loci linked to NAFLD was chosen for analysis. There are two known susceptibility loci for NAFLD (SAMM50, PNPLA3) and three potentially new candidate genetic regions for a clinical NAFLD diagnosis (APOE, SUGP1, TRIB1) (20).

10.3389/fendo.2023.1215790

TABLE 3 Causal effect of NAFLD on falling risk using genetic variant randomization in different MR methods.

Exposure	Outcome	Method	No. of SNP	OR (95% CI)	95% CI	*P*
NAFLD	Falling risk	IVW	5	0.9912	0.9412-1.0440	0.740
		MR Egger	5	1.0211	0.8865-1.1763	0.791
		Weighted median	5	0.9987	0.9681-1.0301	0.932
		Simple mode	5	0.9949	0.9521-1.0396	0.831
		Weighted mode	5	0.9964	0.9613-1.0327	0.852
MR Egger: Cochran's Q= 14.341, *P*= 0.002						
IVW: Cochran's Q= 15.315, *P*= 0.004						
MR-Egger intercept= -0.006, *P*= 0.682						
MR-PRESSO global test= 0.756						

No outlier was observed in the MR-PRESSO analysis in MR analysis in NAFLD and fractures. CI, confidence interval; MR, Mendelian randomization; IVW, inverse-variance weighted; NAFLD, non-alcoholic fatty liver disease.

Previously, several potential mechanisms behind NAFLD in osteoporosis have been widely discussed, including vitamin D deficiency, increased cytokines from the inflamed liver, limited physical activity, and others. In NAFLD, chronic production of pro-inflammatory cytokines like tumor necrosis factor (TNF)-a, interleukin (IL)-1, IL-6, and IL-7. TNF-a may be an important cytokine that mediates bone loss in NAFLD patients. Several studies have reported increased levels of circulating TNF-a in patients with NAFLD (24, 25). Studies showed that increased levels of TNF-α lead to increased osteoclast production and inhibit osteoblast activation (26). In addition, studies have indicated that serum TNF-a level was negatively associated with vitamin D levels (27). Osteocalcin (OCN) is a non-collagen protein expressed by osteoblasts, works as a marker of bone formation, and involves calcium homeostasis. Fernández-Real et al. (28) reported that serum OCN level was negatively associated with the blood markers of liver diseases, such as alanine transaminase (ALT) and aspartate transaminase (AST). In a cohort of 47 subjects, Szalay et al. (29) reported a decreased serum OCN level in NAFLD patients (29). At the same time, OCN may play a role in postmenopausal

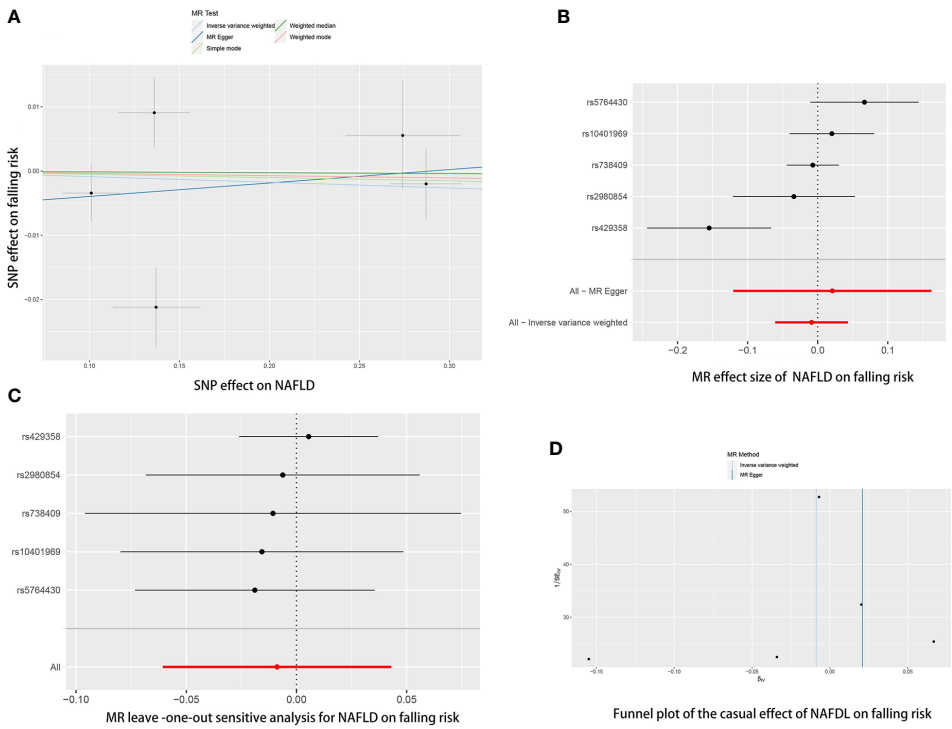

FIGURE 4
The causal effects of NAFLD on falling risk in different MR methods. **(A)** Scatter plot. The slopes of each line represent the causal association for each method. **(B)** Forrest plot. **(C)** Leave-one-out analysis. **(D)** Funnel plot.

10.3389/fendo.2023.1215790

TABLE 4 Causal effect of osteoporosis on NAFLD using genetic variant randomization in different MR methods.

Exposure	Outcome	Method	No. of SNP	OR (95% CI)	95% CI	*P*
Osteoporosis	NAFLD	IVW	16	0.9759	0.9246-1.3000	0.375
		MR Egger	16	0.8410	0.6393-1.1062	0.235
		Weighted median	16	0.9834	0.9143-1.0578	0.653
		Simple mode	16	0.9898	0.8753-1.1192	0.872
		Weighted mode	16	0.9897	0.8818-1.1101	0.864
MR Egger: Cochran's Q=8.365, *P*= 0.869						
IVW: Cochran's Q= 9.542, P= 0.847						
MR-Egger intercept= 0.0003, *P*= 0.296						
MR-PRESSO global test= 0.856						

No outlier was observed in the MR-PRESSO analysis in MR analysis in osteoporosis and NAFLD. CI, confidence interval; MR, Mendelian randomization; IVW, inverse-variance weighted; NAFLD, non-alcoholic fatty liver disease.

osteoporosis (30). In a recent study by Xu et al. (31), decreased OCN was associated with bone turn markers and osteopenia, and osteoporosis. Thus, decreased OCN in NAFLD patients could be a potential factor leading to osteoporosis. Osteopontin (OPN) is another multi-functional protein in our body, which is regarded as another factor that may mediate low BMD in NAFLD. Syn et al. (32) demonstrated that OPN was overexpressed in NAFLD patients. They found that the level of OPN is also linked with fibrosis progression in NASH in transgenic mice. On the other hand, higher OPN is also known as a risk of osteoporosis (33, 34). In an animal study, Chiang et al. showed that OPN-deficient mice could resist ovariectomy-induced osteoporosis (33). Another human study by Chang et al. (34) showed the same conclusion. They found a higher serum OPN levels (>14.7 ng/ml) are an essential risk factor for menopausal osteoporosis. Studies have shown that OPN may regulate the function of osteoblasts and osteoclasts by inhibiting the growth of mineral crystals (35). Vitamin D deficiency in NAFLD patients may provide another

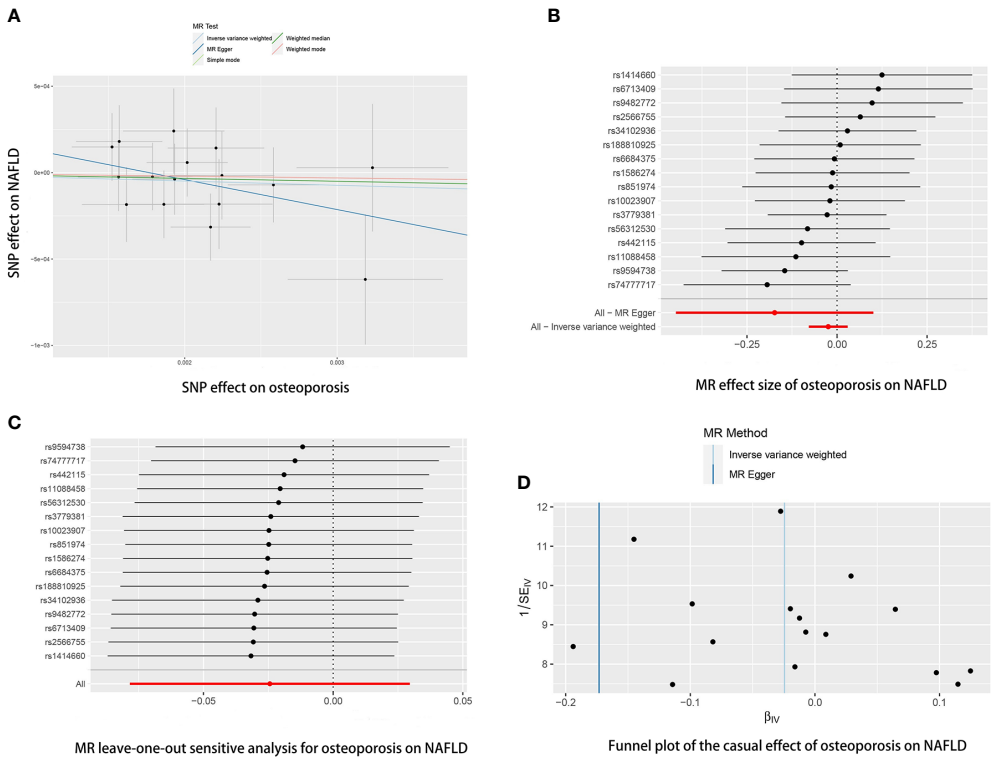

FIGURE 5
The causal effects of osteoporosis on NAFLD in different MR methods. **(A)** Scatter plot. The slopes of each line represent the causal association for each method. **(B)** Forrest plot. **(C)** Leave-one-out analysis. **(D)** Funnel plot.

explanation for osteoporosis tendency. Targher et al. (36) found that NAFLD patients have a lower serum vitamin D level than the control group, and the level of vitamin D decrease was closely related to the histological severity of hepatic steatosis. In a recent study, Ciardullo et al. (37) found an inverse relationship between vitamin D status and NAFLD and fibrosis. The evidence suggests that vitamin D deficiency may play a role in NAFLD occurrence and progression. Furthermore, insufficient physical activity is also an essential factor in developing NAFLD. Physical activity is considered an important treatment to prevent NAFLD and reduce fat accumulation in the liver. At the same time, much clinical evidence has shown that limited physical inactivity is essential to osteoporosis in the elderly. Thus, insufficient physical activity could be an important lifestyle link to NAFLD with osteoporosis.

All in all, much evidence supports the tendency of osteoporosis in NAFLD patients *in vivo* and *in vitro* experiments. However, the previous results in clinical observational studies on their association were always controversial. In a retrospective cross-sectional study including 3,739 postmenopausal women, Lee et al. (38) indicated a significant negative association between NAFLD and BMD after adjusting potential confounders. A recent meta-analysis encompassing 7 observational studies showed a similar conclusion (12). In the analysis, Pan et al. showed that NAFLD patients have a higher risk of osteoporosis (OR = 1.33, 95%CI:1.24-1.44) and osteoporotic fractures (OR = 1.57, 95%CI:1.08-2.29) (12). However, after parameter adjustment, the significant association was only found in men but not in women (12). In a recent NHANES study, Xie et al. (39) found a negative association between NAFLD and osteoporosis. However, the association correlation becomes insignificant after adjusting for a large range of covariates, including gender, age, race, poverty income ratio (PIR), body mass index (BMI), and others. In another NAHENS study of 1784 subjects older than 50, Ciardullo et al. (40) shown the same findings. After adjusting for confounders, they found no association between NAFLD and femoral BMD and osteoporosis. These conflicting findings may result from the confounding factor in observational studies. For example, obesity may be an important mediator of the relationship between NAFLD and osteoporosis. In an early study by Li et al. (41), they found a positive association between NAFLD and osteoporosis in multivariable-adjusted models. However, after additionally adjusting visceral adipose tissue and BMI, they found NAFLD was negatively associated with vertebral BMD.

These epidemiological studies are prone to generate biased results because of the residual confounding and reverse causation (42). We first use MR analysis to reveal a causal association between NAFLD and osteoporosis risk. However, although the IVW method showed that NAFLD may increase fracture risk, the results were not statistically significant. Our results do not support that NAFLD increases the risk of fracture. Fracture is influenced by many factors. Our results show that NAFLD only slightly increased osteoporosis risk, so NAFLD may not cause a significantly increased fracture risk. In addition, our results also do not support that NAFLD increases the falling risk. Our study has several advantages. First, MR analysis was designed to reduce confounding and reverse causality using a genetic variation, as SNPs are randomly assigned at conception. Second, we used a large sample of the GWAS meta-analysis dataset (8,434 NAFLD cases and 770,180 controls) to conduct this MR analysis. Large F-statistic values indicated five IVs were closely related to NAFLD. Third, we also performed a reverse MR analysis to explore the causal effect of osteoporosis on NAFLD, which facilitates our better understanding of the interconnection between these two diseases. However, some potential limitations could not be avoided. First, some heterogeneity is found between NAFLD and fracture, which could be led by the choice of some instrumental variables. Second, this MR study reveals the potential causal effect of NAFLD on osteoporosis, but no causal association is observed between NAFLD and fracture and falling risk. The inconsistent result remains elusive and needs further investigation. Third, due to the limitations of GWAS, we did not perform MR analysis by age and sex. Fourth, another thing worth mentioning is that although we found a higher osteoporosis risk in NAFLD patients, this increase was small, and the OR was quite low. So, the conclusion should be interpreted more cautiously. Fifth, these findings should be interpreted cautiously, as the study sample was from a European population. Whether the results can be generalized to other populations will need to be further investigated.

Conclusions

The results of this study indicate a causal association between NAFLD and osteoporosis. NAFLD patients have a higher risk of osteoporosis but not fractures and falling risk. In addition, our results do not support a causal effect of osteoporosis on NAFLD.

Data availability statement

The original contributions presented in the study are included in the article/Supplementary Material. Further inquiries can be directed to the corresponding authors.

Ethics statement

Ethical review and approval was not required for the study on human participants in accordance with the local legislation and institutional requirements. Written informed consent for participation was not required for this study in accordance with the national legislation and the institutional requirements.

Author contributions

Conceptualization: AC, PX, PW. Data curation: ZF, XW, and YZ. Formal analysis, XW and YZ. Investigation: AC, PX, and ZF. Methodology: AC, PX, ZF, JL, SH, and DZ. Project administration: AC, PX, and PW. Software: AC, PX, and ZF. Visualization: HW and YZ. Writing – original draft: AC, PX, ZF, DZ, XW, PW, and YZ.

Writing – review & editing, AC, PX, and ZF. All authors contributed to the article and approved the submitted version.

Acknowledgments

We acknowledge the investigators of the original GWAS studies for sharing summary data used in this study.

Conflict of interest

The authors declare that the research was conducted in the absence of any commercial or financial relationships that could be construed as a potential conflict of interest.

Publisher's note

Supplementary material

The Supplementary Material for this article can be found online at: https://www.frontiersin.org/articles/10.3389/fendo.2023.1215790/full#supplementary-material

References

1. Styrkarsdottir U, Thorleifsson G, Gudjonsson SA, Sigurdsson A, Center JR, Lee SH, et al. Sequence variants in the PTCH1 gene associate with spine bone mineral density and osteoporotic fractures. *Nat Commun* (2016) 7:10129. doi: 10.1038/ncomms10129

2. Xiao PL, Cui AY, Hsu CJ, Peng R, Jiang N, Xu XH, et al. Global, regional prevalence, and risk factors of osteoporosis according to the World Health Organization diagnostic criteria: a systematic review and meta-analysis. *Osteoporos Int* (2022) 33(10):2137–53. doi: 10.1007/s00198-022-06454-3

3. Hernlund E, Svedbom A, Ivergård M, Compston J, Cooper C, Stenmark J, et al. Osteoporosis in the European Union: medical management, epidemiology and economic burden. A report prepared in collaboration with the International Osteoporosis Foundation (IOF) and the European Federation of Pharmaceutical Industry Associations (EFPIA). *Arch Osteoporos* (2013) 8:136. doi: 10.1007/s11657-013-0136-1

4. Compston JE, McClung MR, Leslie WD. Osteoporosis. *Lancet* (2019) 393:364–76. doi: 10.1016/S0140-6736(18)32112-3

5. Demontiero O, Vidal C, Duque G. Aging and bone loss: new insights for the clinician. *Ther Adv Musculoskelet Dis* (2012) 4:61–76. doi: 10.1177/1759720X11430858

6. Osteoporosis and activity. *Lancet* (1983) 1:1365–6.

7. Gao Y, Shi L. Mindfulness, physical activity and avoidance of secondhand smoke: A study of college students in shanghai. *Int J Environ Res Public Health* (2015) 12:10106–16. doi: 10.3390/ijerph120810106

8. Fan JG, Kim SU, Wong VW. New trends on obesity and NAFLD in Asia. *J Hepatol* (2017) 67:862–73. doi: 10.1016/j.jhep.2017.06.003

9. Younossi ZM, Koenig AB, Abdelatif D, Fazel Y, Henry L, Wymer M. Global epidemiology of nonalcoholic fatty liver disease-Meta-analytic assessment of prevalence, incidence, and outcomes. *Hepatology* (2016) 64:73–84. doi: 10.1002/hep.28431

10. Ye Q, Zou B, Yeo YH, Li J, Huang DQ, Wu Y, et al. Global prevalence, incidence, and outcomes of non-obese or lean non-alcoholic fatty liver disease: a systematic review and meta-analysis. *Lancet Gastroenterol Hepatol* (2020) 5:739–52. doi: 10.1016/S2468-1253(20)30077-7

11. Yang YJ, Kim DJ. An overview of the molecular mechanisms contributing to musculoskeletal disorders in chronic liver disease: osteoporosis, sarcopenia, and osteoporotic sarcopenia. *Int J Mol Sci* (2021) 22(5):2604. doi: 10.3390/ijms22052604

12. Pan B, Cai J, Zhao P, Liu J, Fu S, Jing G, et al. Relationship between prevalence and risk of osteoporosis or osteoporotic fracture with non-alcoholic fatty liver disease: A systematic review and meta-analysis. *Osteoporos Int* (2022) 33:2275–86. doi: 10.1007/s00198-022-06459-y

13. Loosen SH, Roderburg C, Demir M, Qvartskhava N, Keitel V, Kostev K, et al. Non-alcoholic fatty liver disease (NAFLD) is associated with an increased incidence of osteoporosis and bone fractures. *Z Gastroenterol* (2022) 60:1221–7. doi: 10.1055/a-1482-9236

14. Mantovani A, Dauriz M, Gatti D, Viapiana O, Zoppini G, Lippi G, et al. Systematic review with meta-analysis: non-alcoholic fatty liver disease is associated with a history of osteoporotic fractures but not with low bone mineral density. *Aliment Pharmacol Ther* (2019) 49:375–88. doi: 10.1111/apt.15087

15. Bhatt SP, Nigam P, Misra A, Guleria R, Qadar Pasha MA. Independent associations of low 25 hydroxy vitamin D and high parathyroid hormonal levels with nonalcoholic fatty liver disease in Asian Indians residing in north India. *Atherosclerosis* (2013) 230:157–63. doi: 10.1016/j.atherosclerosis.2013.07.006

16. Lee SH, Yun JM, Kim SH, Seo YG, Min H, Chung E, et al. Association between bone mineral density and nonalcoholic fatty liver disease in Korean adults. *J Endocrinol Invest* (2016) 39:1329–36. doi: 10.1007/s40618-016-0528-3

17. Kaya M, Işık D, Beştaş R, Evliyaoğlu O, Akpolat V, Büyükbayram H, et al. Increased bone mineral density in patients with non-alcoholic steatohepatitis. *World J Hepatol* (2013) 5:627–34. doi: 10.4254/wjh.v5.i11.627

18. Sekula P, Del Greco MF, Pattaro C, Köttgen A. Mendelian randomization as an approach to assess causality using observational data. *J Am Soc Nephrol* (2016) 27:3253–65. doi: 10.1681/ASN.2016010098

19. Guo Q, Burgess S, Turman C, Bolla MK, Wang Q, Lush M, et al. Body mass index and breast cancer survival: a Mendelian randomization analysis. *Int J Epidemiol* (2017) 46:1814–22. doi: 10.1093/ije/dyx131

20. Ghodsian N, Abner E, Emdin CA, Gobeil É, Taba N, Haas ME, et al. Electronic health record-based genome-wide meta-analysis provides insights on the genetic architecture of non-alcoholic fatty liver disease. *Cell Rep Med* (2021) 2:100437. doi: 10.1016/j.xcrm.2021.100437

21. Morris JA, Kemp JP, Youlten SE, Laurent L, Logan JG, Chai RC, et al. An atlas of genetic influences on osteoporosis in humans and mice. *Nat Genet* (2019) 51:258–66. doi: 10.1038/s41588-018-0302-x

22. Trajanoska K, Seppala LJ, Medina-Gomez C, Hsu YH, Zhou S, van Schoor NM, et al. Genetic basis of falling risk susceptibility in the UK Biobank Study. *Commun Biol* (2020) 3:543. doi: 10.1038/s42003-020-01256-x

23. Burgess S, Butterworth A, Thompson SG. Mendelian randomization analysis with multiple genetic variants using summarized data. *Genet Epidemiol* (2013) 37:658–65. doi: 10.1002/gepi.21758

24. Aigner E, Theurl I, Theurl M, Lederer D, Haufe H, Dietze O, et al. Pathways underlying iron accumulation in human nonalcoholic fatty liver disease. *Am J Clin Nutr* (2008) 87:1374–83. doi: 10.1093/ajcn/87.5.1374

25. Chu CJ, Lu RH, Wang SS, Chang FY, Wu SL, Lu CL, et al. Risk factors associated with non-alcoholic fatty liver disease in Chinese patients and the role of tumor necrosis factor-alpha. *Hepatogastroenterology* (2007) 54:2099–102.

26. Zou W, Hakim I, Tschoep K, Endres S, Bar-Shavit Z. Tumor necrosis factor-alpha mediates RANK ligand stimulation of osteoclast differentiation by an autocrine mechanism. *J Cell Biochem* (2001) 83:70–83. doi: 10.1002/jcb.1202

27. Peterson CA, Heffernan ME. Serum tumor necrosis factor-alpha concentrations are negatively correlated with serum 25(OH)D concentrations in healthy women. *J Inflammation (Lond)* (2008) 5:10. doi: 10.1186/1476-9255-5-10

28. Fernández-Real JM, Ortega F, Gómez-Ambrosi J, Salvador J, Frühbeck G, Ricart W. Circulating osteocalcin concentrations are associated with parameters of liver fat infiltration and increase in parallel to decreased liver enzymes after weight loss. *Osteoporos Int* (2010) 21:2101–7. doi: 10.1007/s00198-010-1174-9

29. Szalay F, Lakatos P, Németh J, Abonyi M, Büki B, Tarján G, et al. [Decreased serum osteocalcin level in non-alcoholic and alcoholic chronic liver diseases]. *Orv Hetil* (1991) 132:1301–5.

30. Pietschmann P, Resch H, Krexner E, Woloszczuk W, Willvonseder R. Decreased serum osteocalcin levels in patients with postmenopausal osteoporosis. *Acta Med Austriaca* (1991) 18:114–6.

31. Xu Y, Shen L, Liu L, Zhang Z, Hu W. Undercarboxylated osteocalcin and its associations with bone mineral density, bone turnover markers, and prevalence of osteopenia and osteoporosis in chinese population: A cross-sectional study. *Front Endocrinol (Lausanne)* (2022) 13:843912. doi: 10.3389/fendo.2022.843912

32. Syn WK, Choi SS, Liaskou E, Karaca GF, Agboola KM, Oo YH, et al. Osteopontin is induced by hedgehog pathway activation and promotes fibrosis progression in nonalcoholic steatohepatitis. *Hepatology* (2011) 53:106–15. doi: 10.1002/hep.23998

33. Chiang TI, Chang IC, Lee HS, Lee H, Huang CH, Cheng YW. Osteopontin regulates anabolic effect in human menopausal osteoporosis with intermittent parathyroid hormone treatment. *Osteoporos Int* (2011) 22:577–85. doi: 10.1007/s00198-010-1327-x

34. Chang IC, Chiang TI, Yeh KT, Lee H, Cheng YW. Increased serum osteopontin is a risk factor for osteoporosis in menopausal women. *Osteoporos Int* (2010) 21:1401–9. doi: 10.1007/s00198-009-1107-7

35. Ishijima M, Rittling SR, Yamashita T, Tsuji K, Kurosawa H, Nifuji A, et al. Enhancement of osteoclastic bone resorption and suppression of osteoblastic bone formation in response to reduced mechanical stress do not occur in the absence of osteopontin. *J Exp Med* (2001) 193:399–404. doi: 10.1084/jem.193.3.399

36. Targher G, Bertolini L, Scala L, Cigolini M, Zenari L, Falezza G, et al. Associations between serum 25-hydroxyvitamin D3 concentrations and liver histology in patients with non-alcoholic fatty liver disease. *Nutr Metab Cardiovasc Dis* (2007) 17:517–24. doi: 10.1016/j.numecd.2006.04.002

37. Ciardullo S, Muraca E, Cannistraci R, Perra S, Lattuada G, Perseghin G. Low 25 (OH) vitamin D levels are associated with increased prevalence of nonalcoholic fatty liver disease and significant liver fibrosis. *Diabetes Metab Res Rev* (2023) 39:e3628. doi: 10.1002/dmrr.3628

38. Lee DY, Park JK, Hur KY, Um SH. Association between nonalcoholic fatty liver disease and bone mineral density in postmenopausal women. *Climacteric* (2018) 21:498–501. doi: 10.1080/13697137.2018.1481380

39. Xie R, Liu M. Relationship between non-alcoholic fatty liver disease and degree of hepatic steatosis and bone mineral density. *Front Endocrinol (Lausanne)* (2022) 13:857110. doi: 10.3389/fendo.2022.857110

40. Ciardullo S, Muraca E, Zerbini F, Manzoni G, Perseghin G. NAFLD and liver fibrosis are not associated with reduced femoral bone mineral density in the general US population. *J Clin Endocrinol Metab* (2021) 106:e2856–65. doi: 10.1210/clinem/dgab262

41. Li BT, Simon TG, Wang N, Chung RT, Corey KE, Dichtel LE, et al. Association between liver fat and bone density is confounded by general and visceral adiposity in a community-based cohort. *Obes (Silver Spring)* (2021) 29:595–600. doi: 10.1002/oby.23100

42. Davey Smith G, Hemani G. Mendelian randomization: genetic anchors for causal inference in epidemiological studies. *Hum Mol Genet* (2014) 23:R89–98. doi: 10.1093/hmg/ddu328

frontiers | Frontiers in Endocrinology

TYPE Review
PUBLISHED 24 August 2023
DOI 10.3389/fendo.2023.1231580

OPEN ACCESS

EDITED BY
Andrea Del Fattore,
IRCCS, Italy

REVIEWED BY
Mara Boschetti,
University of Genoa, Italy
Marianna Cacciapuoti,
San Giovanni di Dio Hospital, Italy

*CORRESPONDENCE
Fiammetta Romano
fromano.med@gmail.com

RECEIVED 30 May 2023
ACCEPTED 10 August 2023
PUBLISHED 24 August 2023

CITATION
Romano F, Serpico D, Cantelli M, Di Sarno A, Dalia C, Arianna R, Lavorgna M, Colao A and Di Somma C (2023) Osteoporosis and dermatoporosis: a review on the role of vitamin D. *Front. Endocrinol.* 14:1231580. doi: 10.3389/fendo.2023.1231580

Osteoporosis and dermatoporosis: a review on the role of vitamin D

Fiammetta Romano[1*], Domenico Serpico[1], Mariateresa Cantelli[2], Antonella Di Sarno[1], Carmine Dalia[3], Rossana Arianna[1], Mariarosaria Lavorgna[1], Annamaria Colao[1,4] and Carolina Di Somma[1,4]

[1]Endocrinology Diabetology and Andrology Unit, Department of Clinical Medicine and Surgery, University of Naples "Federico II", Naples, Italy, [2]Dermatology Unit, Department of Clinical Medicine and Surgery, University of Naples "Federico II", Naples, Italy, [3]Internal Medicine S. Maria Della Pietà Hospital Nola, Nola, Italy, [4]UNESCO Chair "Education for Health and Sustainable Development", University of Naples "Federico II", Naples, Italy

Osteoporosis (OP) and Dermatoporosis (DP) are expressions of the aging process at the skin and bone levels, respectively. Both conditions are associated with increased morbidity for elderly people, and this requires necessary interventions. They share many common risk factors; among these, vitamin D (VD) deficiency appears to have a role. VD is involved in either disease with many mechanisms, among which immunomodulation. VD deficiency has been linked to OP because it inhibits the body's capacity to absorb calcium and maintain optimal bone health. Available evidence suggests that proper vitaminosis D also appears to be vital in preventing skin age-related issues. DP is often seen in elderly individuals, particularly those with long-term sun exposure and a history of chronic sun damage. VD deficiency can be linked to DP, since its involvement in collagen production, epidermal barrier function, inflammation regulation, wound healing, and sun protection. Aim of this review is to summarize the most updated existing evidence on the role of VD in the development of fragility syndromes such as DP and OP and the possible benefits of VD supplementation as a simple and harmful weapon against aging.

KEYWORDS

dermatoporosis, osteoporosis, skin, skin aging, aging, glucocorticoids, vitamin D

Abbreviations: DP, Dermatoporosis; OP, Osteoporosis; VD, Vitamin D; 25(OH)D3, 25 hydroxyvitamin d; 1,25(OH)2D3, 1,25 dihydroxyvitamin d; 7-DHC, 7-dehydrocholesterol; BMD, Bone mineral density; TNF-alpha, Tumor necrosis factor-alpha; RANKL, Receptor activator of nuclear factor-Kappa B Ligand; OPG, Osteoprotegerin; ECM, Extracellular matrix; HA, Hyaluronic acid; MMP, Metalloproteinases; DHH, Deep dissecting hematomas; PTH, Parathyroid hormone; FGF-23, Fibroblast growth factor-23; IGF-1, Insulin-like growth factor-1; VDPB, Vitamin D Binding Protein; VDR, Nuclear receptor of VD; APC, Antigen presenting cells; ROR, Retinoic acid-related orphan receptors.

1 Introduction

The most frequent metabolic bone disorder is osteoporosis (OP). It is distinguished by low bone mineral density (BMD) and decreased bone strength, which increases the risk of fragility fractures. OP is the leading cause of bone fractures in the elderly, making it a substantial public health issue with a large impact on health systems (1). Kaya and Saurat created the term dermatoporosis (DP) to describe an excessive cutaneous fragility induced by increasing loss of the skin's protective mechanical function with age. The word DP derives its name from the similarities to OP-induced bone fragility (2): just as in OP we witness a decline in the mass and quality of skeletal tissue, so in DP the structural elements of the skin barrier are lost (3). OP and DP share many common risk factors, such as aging, sex and corticosteroid use. Among these, a lack of vitamin D (VD) could have a role. The VD impact on skeletal health is well known and it is universally recognised the importance of its supplementation in elderly patients suffering from bone loss (4), however VD actions are involved in many tissues and skin is one of them. In fact, when there is adequate UV-B irradiation, this organ is capable of producing itself the active form of VD which is 1,25(OH)2D. The latter 1,25(OH)2D has crucial roles such as the control of epidermal barrier integrity (5). Recent findings indicate that VD regulates aging in various tissues, including the skin (6). Our review sought to investigate the links between OP and DP, as well as the available information on the function of VD in the onset of these conditions and the possible therapeutic use of VD supplements.

2 Osteoporosis in elderly

2.1 Definition and epidemiology

OP is a systemic skeletal illness marked by low bone mass, micro-architectural degeneration of bone tissue, bone fragility, and an increase in fracture risk (especially of vertebrae, femur, humerus, wrist and ankle bones) due to even minimal trauma (7). The epidemiological impact is very high: nowadays it is believed that in Italy around 5 million elderly people are affected by OP and a greater increase in its incidence is expected in the next future, since the proportion of the Italian community of over 65 years is going to rise by 25% in the next 20 years. Osteoporotic fractures raise the relative risk of mortality, particularly for femur fractures: it is 5-8 times greater in the first 3 months after the occurrence, decreases in the next 2 years, but stays high even after a 10-year follow-up. Furthermore, 50% of women with hip fractures had a significant loss in self-sufficiency which involves long-term institutionalization in about 20% of cases. The economic burden of such a widespread pathology is therefore very high (8, 9). The World Health Organization operationally defines OP as the presence of a bone mineral density (BMD) of 2.5 SDs under the average of young white adult women (1). OP is classed as 'primary' when it is not caused by medical conditions, and secondary' when it arises as a result of particular, well-defined clinical diseases or drug use (10).

2.2 Elderly osteoporosis: pathogenesis

Under physiological conditions, skeletal homeostasis is guaranteed by an appropriate ratio between formation and resorption of bone tissue. Skeletal homeostasis is maintained under physiological settings by a balance of bone production and bone resorption. This adjustment is altered in pathological circumstances in favor of osteoclast-mediated bone resorption (5).

This bone regeneration cycle decoupling is exactly what happens in elderly people: the decreased osteoblast activity determine a longer time required to fill resorption cavities and there is a low-grade systemic inflammation, especially involving pro-inflammatory cytokines [tumor necrosis factor-alpha (TNF-alpha), IL-1, and IL-6)] which determine an increase in the amount and functioning of osteoclasts. As a result, in older persons there is an overall decline in bone with time. A negative calcium balance resulting from decreased dietary intake, reduced absorption and the compromise of kidney function, reduces the activation of VD and the calcium absorption from the gut (11). Osteoclasts indeed must resorb calcium in order to fill this void (4). Estrogen deficiency is of course another critical factor responsible for the increased bone resorption both in men and women. For either sex, bone loss occurs right after attaining maximal bone mass; nevertheless, this process accelerates after menopause in women and after the age of 70 in men (12). Estrogens are well known for regulating the synthesis of bone. They have a bone-protective role by limiting bone resorption and sustaining bone formation (13). As a result, estrogen deprivation causes OP, which is associated with an increase in bone resorption due to a boost in the number and activity of osteoclasts, as well as osteocyte death. A growing body of information suggests that OP related with estrogen loss of estrogen is also due to the increase in oxidative stress and changes in immune system homeostasis and inflammatory pathways, which are accentuated by the aging process. Specific T-cell subsets, such as T helper cells, can be activated, supporting the production of IL-17, Receptor activator of nuclear factor-Kappa B Ligand (RANKL), IL-1, TNF, and IL-6. These factors are able to stimulate osteoclast maturation and activity by preventing the differentiation of osteoblast, increasing apoptotic osteocytes, and raising RANKL expression and the RANKL/Osteoprotegerin (OPG)-ratio (14).

2.3 Elderly osteoporosis: clinical features

OP is asymptomatic for the majority of its clinical history; approximately one-third of fracture occurrences are silent, while the remainder present in pain. Osteoporotic fractures are fragility fractures, meaning they occur spontaneously or as a result of little trauma. In order of frequency, the most commonly affected sites are vertebra, femur, major non-vertebral/non-femoral fractures (pelvis, radial tip, proximal tibia, humerus, 3 or more ribs, etc.), minor fractures followed by pain. Vertebral compression fractures (VCFs) are the hallmark clinical presentation of OP. Unlike major posttraumatic VCFs, which are invariably symptomatic, those

caused by moderate trauma are frequently misunderstood and thus go undiagnosed. They are typically asymptomatic or present with symptoms such as back or low back pain that responds to analgesic therapy (15, 16). They primarily impact the dorsolumbar junction (T12-L1), followed by the mid-dorsal tract (T7-T8) and other locations (17). The Genant classification, which takes into account the level of vertebral body involvement by a semi-quantitative evaluation of its deformity, is used to categorize the severity of vertebral fractures (18). The reduction in the patient's height, which can be partly attributed to antalgic posture and partially to the accentuation of the thoracic kyphosis, is the evident and immediately observable result of vertebral collapse. The latter causes a number of issues, including sleep disturbances caused by adopting analgesic positions, limitations on daily activities, respiratory (modest reduction of respiratory volumes due to reduction of rib cage support) and gastrointestinal (early satiety due to abdominal distension) disturbances. Neurological deficits occur rarely, even when they cause compression of the spinal cord (by sliding) (19). Hip fracture is a severe injury that necessitates hospitalization and immediate medical surgery (20). Such fractures account for a small percentage of fractures caused by OP (about 15%), but they have a greater impact on health expenditure (21) because they are associated with a higher rate of morbidity and mortality, particularly in the first three months after the fracture; numerous complications are in fact associated with this event: embolism, pulmonary disease, infections, sepsis, heart attack, and cardio-pulmonary problems in general (22). Hip fracture risk increases with age, and so does mortality (by 5-8 times): this connects with both BMD decline and an increase in the chance of falling (which accounts for around 90% of fractures in the elderly) (21). Colles fracture, or fractures of the distal epiphysis of the radius, are more common in persons with a higher performance level because they are more active and hence at a higher risk of falling. Its prevalence rises gradually after menopause, then levels out at the age of 65. In contrast, wrist fractures are uncommon in men, regardless of age (M:F 1:6-1:10 at 65 years) (21). This disparity is related to the male skeleton's bigger cortex and lower endocortical resorption (23). Other types of fractures (humerus, pelvis, proximal radius, or distal femur) are more uncommon. Although the association with age is indisputable due to the loss in BMD, it is relatively weak for rib fractures and more meaningful for pelvic fractures (21).

3 Dermatoporosis

3.1 Definition and epidemiology

Skin aging is not just an aesthetic problem. In fact, its effects also weaken the skin on a functional level, reducing the crucial protective properties of the skin. Since this growing knowledge in recent years, it has been necessary to coniate a term as DP that could focus the attention of clinicians on the urgency of preventing and treating this condition as well as OP.

DP is a clinical entity that includes the whole broad spectrum of skin alterations due to aging, including complications that can cause severe morbidity for the affected elderly person, taking the form of a real chronic skin frailty syndrome (2). People with dermatoporosis have particularly thin and fragile skin. This results in a poor tolerance to friction and shear forces, and consequent susceptibility to skin tears and more or less serious hematomas. DP also tends to delay the healing of wounds once they have formed. Additionally, skin failure leads to loss of temperature regulation combined with the incapacity of keeping the core body temperature. In more severe cases, it may result in percutaneous loss of fluid with electrolytes and protein, as well as an increased susceptibility to infection (24). For this reason, severe DP is a cause of death in intensive care units (25). Similarly to OP, DP is classified as 'primary" and 'secondary'. Primary DP is caused by chronological aging along with long-term, unprotected sun exposure. Although data on genes associated in DP pathogenesis are limited, genetic variables are known to play a substantial role in the regulation and loss of extracellular matrix (ECM) components, in the viscoelastic characteristics of the skin, and hence could be involved in DP susceptibility. Chronic use of topical and systemic corticosteroids causes the secondary type. These iatrogenic forms may appear earlier and be more severe in people predisposed to primary DP. Corticosteroids are known to affect the expression of genes encoding collagens I, III, IV, V, decorin, elastin, metalloproteinases (MMPs) 1, 2, 3, tenascin, and MMP 1 and 2 tissue inhibitors (2).

Data on the prevalence of the disease are currently scarce, however they show the high frequency among the elderly and especially in women. The frequency of dermatoporosis is 32%, based on a study of 202 hospitalized participants aged 60 to 80 years. DP was found in approximately 22% of females and 38% of males (26). Another French study evaluated 533 people over the age of 65 who went to see a dermatologist, resulting in an overall prevalence of dermatoporosis of 37.5%, which was prevalent in women (27). Finally, in a prospective analysis of 176 patients aged 60 years or more, Kluger et al. discovered DP in 30.7% of patients, mostly in the upper extremities (94%) (28).

3.2 Dermatoporosis: pathogenesis

There are many factors implicated in the development of DP. First of all, the decline with aging in dermal hyaluronic acid (HA). In the elderly there is a thinning of the skin, which loses its resistance to mechanical forces. The firmness of "healthy" skin is provided by the ECM, whose major constituent is HA, a non-sulfated glycosaminoglycan that is mostly produced by fibroblasts. HA is a very hydrophilic material that decreases friction between collagen fibers and provides shear force resistance. Yet, as people age, fibroblasts lose their ability to make HA; as a result, the ECM loses volume and consequently is protective mechanical function, determining skin laceration from minimal trauma (2). The lack of interaction between HA and the cell surface receptor CD44, which normally increases keratinocyte proliferation, is a second mechanism hypothesized. In mice models, the selective suppression of keratinocyte CD44 determines skin atrophy (29). This observation has served as the foundation for DP research: it

has been shown that dermatoporotic skin has lower CD44 levels than "healthy" skin from young persons (30). Expression of CD44 is also decreased by UVA and UVB exposure (31) and topical corticosteroid application (30–32). Corticosteroids can also cause dermatoporotic alterations by modifying collagen I, collagen III, collagen IV, and matrix MMP gene expression (33). With age, the overexpression of MMP 1, 2, and 3 and the downregulation of the tissue inhibitor of MMP 1 leads to the degradation of collagen and elastin in the dermis (34). The malfunction of the hyalurosome, a multimeric macromolecule complex comprising of components involved in HA metabolism and cell signaling in keratinocytes such as CD44, heparin binding epidermal growth factor, and its receptor erbB, appears to be the most critical aspect of DP (35).

3.3 Dermatoporosis: clinical features

Clinical manifestation is variable and includes morphological and functional alteration of the skin. Skin atrophy, senile purpura, and stellate pseudoscars are morphological signs of skin fragility. Sun-exposed areas of skin atrophy include the pretibial zones, the back of the forearms, the dorsum of the hands, the presternal area, and the scalp. Dermatoporotic skin is clinically very thin and transparent, with many wrinkles, senile purpura, and pseudoscars as compared to younger skin. There is a significant reduction in skin thickness, demonstrated by ultrasound (1.4-1.5 mm "healthy" skin thickness vs 0.7-0.8 mm in dermatoporotic skin). The dermis, which contains the majority of the subcutaneous fat, shows substantial elastosis, while the epidermis displays linearization with lack of rete ridges (2). Senile purpura, also known as Bateman purpura, is a benign superficial hemorrhagic lesion caused by repeated spontaneous or minor trauma. Histologically, it is distinguished by erythrocyte extravasation and enhanced vascular fragility as a result of connective tissue injury and atrophy in the dermis. These dermal bleedings are not associated with any coagulation disorders (3). Senile purpura is very common in up to 10% of the elderly population between the ages of 70 and 90 and in 90% of cases it is associated with pseudoscars. As these purpuric plaques fade, a dark brownish pigmentation that resembles hemosiderin pigment is left behind (36). Vitamin C, whose protective role on blood vessels is well known, is often deficient in elderly people with dermatoporosis, leading to dermal hematomas; so acid ascorbic replacement therapy should be considered in this pattern (2). Stellate Pseudoscar is a superficial lesion of the skin with a star shape, deriving from spontaneous dermal laceration caused by minimal trauma. These lesions have a hypocellular dermal zone in a background of fibrosis and elastotic collagen fibers covered by an atrophic epidermis. As the senile purpura, Stellate Pseudoscar appears on the backs of elderly people's hands and forearms and they show as pale lesions on medical inspection. Pseudoscars are classified into three kinds based on their shape: star-shaped, linear, and plaque (36).

Functional manifestations of DP are skin lacerations, delayed wound healing, and subcutaneous bleeding with the development of deep dissecting hematomas (DHH) and in the most serious cases even large areas of necrosis (3). DHH is the most serious DP complication. It occurs as a result of extensive bleeding between subcutaneous fat and muscle fascia following a small injury (37). DHH typically occurs in elderly patients with dermatoporosis who underwent anticoagulation therapy or topical or systemic corticosteroid therapy (33). Histologically, there is exposure of deep skin vessels to the skin surface in the context of significant skin thinning. Unlike the other clinical signs of DP, DHH occurs mostly in the lower limbs of elderly adults with severe DP (M/F ratio: 1/5) (38). Necrosis is caused by large hematomas that cut off the blood flow to the skin. As soon as possible to prevent severe skin damage in this situation, the bleeding area and necrotic tissue should be surgically removed. It may be essential to make large and deep incisions that reach the muscular tissue, determining a significant loss of skin surface (39). The exact mechanism causing the delay in wound healing in elderly is still unclear. Tissue deterioration is caused by a reduction in the ability of keratinocytes and fibroblasts to proliferate, a surplus of matrix MMPs, which delay the production of renewed ECM (40).

4 Osteoporosis and dermatoporosis: common risk factors

OP and DP share many common risk factors (Figure 1). The major risk factor for both illnesses is advancing age. Aging exponentially raises the likelihood of osteoporotic fractures, only partially due to the observed reduction in BMD, but also due to many other factors accompanying aging, namely alterations in bone

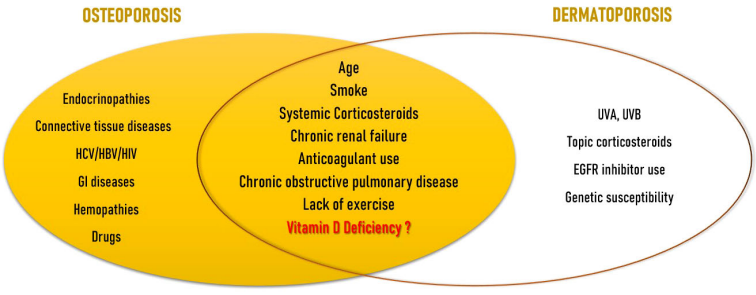

FIGURE 1
Dermatoporosis and Osteoporosis: common risk factors.

quality, a rise in the number of falls, and a slowing of defensive reactions. In fact, fracture risk can be higher in elderly than young patients even if in presence of similar BMD (8). Clinical signs of DP appear from the age of 60, and are more noticeable at between 70 and 90 years of age (41). Observational studies on subjects attending dermatology units aged 60 or older (28, 42) or on geriatric rehabilitation patients (43) showed that age was an independent risk factor for the development of DP. Another well recognised risk factor is smoke. Tobacco use is an independent risk factor for both vertebral and limb fractures (8). Current smokers exhibit a weaker inverse relationship between PTH and serum VD levels compared to nonsmokers. They also lose more BMD over time, particularly at the femoral site, and are more likely to experience fragility fractures (44). Smoking was found to be significantly associated also with DP (43). Use of systemic corticosteroids represent the main form of secondary OP and is distinguished by a qualitative change in the skeleton as well as in the macro and bone microarchitecture (45). As seen above, corticosteroids are involved in the regulation of the expression of genes that encode collagens I, III, IV, V, decorin, elastin, MMPs 1, 2, 3, tenascin and tissue inhibitors of MMPs 1 and 2 (33). Kluger et al. discovered that use of both topical and systemic corticosteroids was strongly linked with DP in a Finnish observational research (28). Chronic renal failure causes the condition named as "Chronic Kidney Disease-Mineral and Bone Disorder" (CKD-MBD) which is characterized by a group of alterations in calcium-phosphorus metabolism, changes in hormones involved in bone homeostasis such as parathyroid hormone (PTH), VD and fibroblast growth factor-23 (FGF-23), anomalies in bone turnover and mineralization, and vascular calcification. The risk of fracture and vascular disease increases as a result of all these factors (46). Dermatoporosis and chronic renal failure have also been linked in a strong, age-independent way (28, 42). Chronic renal failure was revealed to be the only age-independent factor that significantly increased the incidence of DP more than five times by multivariate analysis in the cross-sectional observational investigation by Mengeaud et al. (26). Hyperpigmentation and haematomas, which are seen in most advanced stages of DP, are frequently documented in patients with end-stage renal disease; however, there is no convincing understanding for the link between severe chronic renal disease and DP. Anticoagulant use has shown the most important association for the development of DP in observational studies (27, 42, 43); anticoagulant use and chronic renal disease seems to act as additional cofactors (28). The prevalence of OP in individuals with chronic obstructive pulmonary disease (COPD) ranges from 9 to 69% (47). In this setting, OP-related fractures are associated with several adverse health outcomes, including an increase in hospitalization and mortality rates, in lung function, and poor quality of life (48). In a cross-sectional analysis of individuals 65 and older, Reszke et al. found that those with COPD were at higher risk to demonstrate senile purpura, although it could be a consequence of systemic corticosteroid use (49). Lack of exercise is seen as a moderate risk factor for OP and fragility fractures (8), as well as for DP (50). Since the observation that DP and OP share many common risk factors, Villeneuve et al. proposed that DP could be a sign of underlying bone fragility. In their prospective, observational, cross-sectional, multicenter study on patients of 50 years or older, they found a link between DP and a history of significant osteoporotic fracture, regardless of age or gender (51). Not much research has been done on the role of VD insufficiency as a risk factor that both diseases share. However, there is evidence that VD is involved in both skin (52) and bone health (53).

5 Vitamin D

5.1 Metabolism

Besides being a lipid-soluble vitamin, VD is a steroid hormone. Humans obtain VD from either sunlight exposure to UVB rays or minimally from the introduction with plant or animal foods, dietary foods and supplements, as VD2 (or ergocalciferol) or VD3 (or cholecalciferol) (54). VD is produced in the skin via 7-dehydrocholesterol (7-DHC) present in keratinocytes; UVB rays mediate a photochemical reaction that converts 7-DHC in vitamin D3 (55). The latter is transported to the liver binded to a type of alpha-globulin called Vitamin D Binding Protein (VDPB), where it undergoes the first hydroxylation and is released in the form of 25 (OH)D3. Finally, VD3 is activated with a second hydroxylation at the kidney level. The proximal tubule is the primary site of action for this mechanism, and it is vulnerable to both negative and positive feedback processes mediated by 1,25(OH)2D3, phosphorus, calcium, and FGF-23 (56). The 1,25(OH)2D3 acts through activation of the nuclear receptor of VD (VDR), a transcription factor and part of the steroid receptor family, with which VD has a high affinity. Although the primary function of VD, which is the control of calcium-phosphorus metabolism and the balance of bone mineral reserves, is well understood (57, 58), there is also ample evidence of its numerous other activities in extra-skeletal tissues (59, 60). In reality, the VDR is expressed everywhere (61), and VD is essential for the immune system's physiology (62), for controlling the activity of other hormones like IGF-1 (63), in the prevention of many types of neoplasms (64), in the maintenance of a solid skeletal muscle (65), participates in carbohydrate metabolism (66), of the cardiovascular (67) and reproductive systems (68), of the neuro cognitive (69) and cell proliferation (70, 71). As we will see in more detail later, it is relevant also in the constitution of the skin (72). VD seems to act either directly on organs such as bone and skin, and indirectly through influencing the immune system and, in turn, inflammatory processes, which is a major factor in the development of many diseases like OP and skin aging. All immune system cells have VDR, and antigen-presenting cells (APC) can create 1,25(OH)2D3 in response to immunological stimuli by using the same enzyme that is produced in the kidney (62).

Both innate and acquired immunity are affected by 1,25(OH) 2D3. VD and its metabolites influence innate immunity by promoting macrophage development and activation, which results in the production of defensins including cathelicidin and 2-defensin (73). Mice on a diet lacking in vitamin D produced less IL-6, TNF-, and IL-1, and their antibacterial activity was weak (74). The primary inhibitory effects of VD on acquired immunity result in a

phenotypic shift in T cells from an effector phenotype, which is involved in autoimmune disorders, to a regulating and protecting one (75).

5.2 Vitamin D deficiency: definition and epidemiology

The interpretation of serum 25(OH)D has to take into account many factors, as levels can vary widely in different life periods, based on degree of exposure to sunshine (period of the year, latitude), phototype, and nutritional status (76). There is also a large variability in its dosage between different laboratories. In fact, there is still no unanimous consensus among scientific societies for the definition of the deficiency of VD, except for the condition of serious deficiency represented by values of 25(OH)D <10 ng/mL which are linked with higher risk of rickets and osteomalacia. Since the observation that in the general population there is a relationship between values of serum 25(OH)D < 20 ng/mL and increased risk of fracture (77), the Italian Society for Osteoporosis, Mineral Metabolism and Bone Diseases (SIOMMMS) suggests to consider these cutoffs: "deficient" means a 25(OH)D level of 10 ng/mL; "insufficient" means a level of 20 ng/mL; and "optimal" means a level of 20-50 ng/mL (76). In patients with OP, especially those who necessitate a treatment with OP drugs and subjects at risk of hypovitaminosis D, an "optimal" level of at least 30 ng/mL is instead indicated. This value is related with a considerable reduction in the incidence of hip fractures in institutionalized women and a 4.5 times better response in bisphosphonate-treated patients (78). Globally, there are many people who have mild or severe VD deficiencies. Around 7% of the world's population has severe VD deficit (serum 25(OH)D concentrations below 25/30 nmol/l (10/12 ng/ml)), while 37% has mild VD deficiency (serum 25 (OH)D concentrations below 50 nmol/l (20 ng/ml)) (79).

5.3 Vitamin D and bone health

5.3.1 Effects on bone homeostasis

VD is required to increase the active intestinal absorption of calcium by 30-80% which, later, becomes available for multiple physiological processes and for the mineralization of the skeleton. Additionally, it promotes calcium reabsorption in the kidney's distal tubule. By encouraging osteoblast development and regulation as well as the generation of proteins including collagen, alkaline phosphatase, osteocalcin, and RANKL, 1.25 (OH)2D3 also has direct effects on bone. It controls both bone formation and resorption (80). Intestinal calcium and phosphate absorption significantly decreases when serum 25(OH)D is less than 30 ng/mL. The blood ionized calcium concentration is lowered as a result, which leads to secondary hyperparathyroidism. Increased osteoclast activity is caused by preosteoclast differentiation into mature osteoclasts, which is induced by elevated PTH levels. Increased bone resorption, loss of bone matrix, and resultant reduced bone mass are the outcomes of this. Due to the PTH-induced increase in osteoclast activity and quantity, VD-deficient osteons exhibit broader Haversian canals and greater lacunae. This increases porosity. Additionally, osteoid mineralization is defective when compared to that of normal bone (53). Clinical manifestations of VD deficiency reflect all these functions. Severe deficiency leads to an insufficient calcium-phosphate product: the result is broadly deficient osteoid mineralizations. Rickets, which manifests as poor mineralization throughout the developing skeleton, and osteomalacia, which results from impaired skeletal mineralization after the fusion of epiphyseal plates in adults, are the clinical consequences (81). 25(OH)D levels in rickets and osteomalacia patients typically fall below 15 ng/mL (82).

5.3.2 Vitamin D and osteoporosis

Less severe degrees of deficiency may also produce skeletal disease. In fact, long-standing VD deficiency/insufficiency (serum 25(OH)D level lower than 30 ng/mL) is considered a risk factor of OP because of the mechanisms that increase resorption seen above (53). Epidemiologic studies show that VD deficiency is associated with lower BMD and fractures. In the Longitudinal Aging Study Amsterdam (83) 25(OH)D levels and BMD of lumbar spine and hip of 1319 subjects (643 men and 676 women) between the ages of 65 and 88 yr were correlated. It was found a threshold around the serum 25(OH)D level of 50 nmol/liter for the relationship between serum 25(OH)D and BMD of total hip and femoral trochanter. Kuchuk and colleagues also found an association between VD deficiency and fractures. Serum 25(OH)D levels below or equal to 30 nmol/L were associated with an increased fracture risk in persons aged 65 to 75 years (83). Also longer follow-up studies show a similar increase in fracture among subjects with the lowest VD status (84). Besides epidemiologic observations, contradictory findings have been obtained from the numerous intervention trials conducted in elderly individuals to determine if VD supplementation alone or with calcium can reduce the risk of fractures (85). VD's anti-fracture impact has mostly only been observed for femoral fractures and non-vertebral fractures, not vertebral ones. It also appears to be mediated by the reported decline in the risk of falling (86). Data on elderly people indicate very clearly that the skeletal benefits of the VD supplementation are seen in those who are severely VD and not if they have mild or no VD deficit (87, 88). In the New Zealand Vitamin D Assessment (ViDA) study of older community-resident men and women treated with monthly dosing of 100,000 IU VD for 2 years, clinically significant reductions in bone loss at the spine and femoral neck, were found only in participants with a baseline serum 25(OH)D < 30 nmol/L (87). Subsequently, in the Aberdeen study (88), authors aimed to verify if the baseline 25(OH)D threshold of <30 nmol/L was confirmed. 305 postmenopausal were randomized to receive either VD 400 IU/day or 1000 IU/day, or placebo over 1 year. Results of a *post-hoc* analysis confirmed the usefulness in terms of increasing BMD of the VD supplementation only in the group with a baseline level of 25 (OH)D ≤ 30 nmol/L (88). Benefits of VD supplementation seem to be enhanced when combined with calcium, a non surprising observation since it is well known that elderly people are often at high risk of contemporary VD and calcium deficiency (89). In the 2019 meta-analysis by Yao and colleagues, VD reduced the risk of

any fracture by 6% and of hip fracture by 16% but only when supplementation consisted also in calcium (90). In any case, an adequate intake of calcium and VD is the prerequisite for any specific drug treatment since calcium and/or VD shortage is one of the most frequent reasons for failure or a poor response to osteoporosis medication (91, 92). This could obviously enhance the risk of future further fracture (93). As discussed earlier, OP may have also an inflammatory etiology (14); it is possible, given the immunoregulatory effects of VD (62), that its benefits on fracture risk may at least be partially mediated, at least in part, by an influence of VD on cytokine concentration. In the research conducted by Inanir et al., 70 post-menopausal women diagnosed as osteoporotic were randomized to receive calcium and calcitriol or calcium alone. At baseline and six months into the course of treatment, measurements of BMD and serum levels of IL-1, IL-6, and tumor necrosis factor-alpha (TNF-alpha) were made. According to study findings, taking 20 IU of calcitriol every day for six months enhanced BMD and lowered IL-1 and TNF-a concentrations (94).

5.4 Vitamin D and skin

5.4.1 Effects on skin

Skin and VD have a special relationship: skin is in fact the only organ that can produce VD and its metabolites, also being at the same time a major target for this hormone as well (95). Keratinocytes express all enzymes of the VD metabolic pathway and can produce hormonal 1,25(OH)2D3 when exposed to enough UV-B irradiation. Thusly produced 1,25(OH)2D3 acts in many ways at the skin level, with three most important actions: regulation of keratinocyte proliferation and differentiation, control of epidermal barrier integrity (5), and modulation of the immune skin system (96). Different receptors in the skin have varied affinities for VD and its CYP11A1-derived hydroxyderivatives, which allows them to exert a variety of partially overlapping actions. The binding to the nuclear VDR plays a significant role in mediating the biological consequences (97). A non-genomic, membrane-associated approach based on a different ligand-binding site (98) or the action on the 1,25D3-MARRS receptor (99) can also be used by the activated VDR to cause rapid response signaling. Retinoic acid-related orphan receptors (ROR) α and γ, which are expressed in the skin, are two additional nuclear receptors that VD metabolites can use to control some skin activities (100). Last but not least, the traditional 1,25(OH)2D3 and CYP11A1 derivatives can bind to the liver X receptors (LXR) and aryl hydrocarbon receptors (AhR) and operate as agonists (101, 102). Through intracrine, autocrine, and paracrine effects, 1.25(OH)2D3 produced in keratinocytes controls their own development, differentiation, and death (103). Specifically, VD causes in vitro keratinocyte growth to be stimulated at low doses and inhibited at higher concentrations (108 M) (104). Additionally, it preserves the integrity of the epidermal barrier by promoting the synthesis of ceramides, key players in the control of the skin's water-holding capacity and homeostasis (105). In a feedback loop, ceramide boosts the pro-differentiating effect of calcitriol on keratinocytes when VD stimulates the neutral Mg2+-dependent sphingomyelinase (106). Physiological levels of calcitriol inhibit the effects of pro-apoptotic ceramides, UV radiation, and TNF-α, whilst pharmaceutical doses cause keratinocytes and other epidermal cells to undergo apoptosis (107).

As previously reported, the presence of VDRs in almost all immune cells suggests that they are one of vitamin D's primary targets, and various immunological indicators are controlled by VDRs action (108). This happens also in the skin, where VD and its metabolites exert multiple actions on T-cells, dendritic cells, keratinocytes and myeloid cells (109, 110).

Overall, VD has an immunomodulatory effect on T cells (52). VD inhibits proinflammatory Th1/Th17/Th9-Lym T-cells activation (111), as well as the generation of inflammatory cytokines (interferon gamma, TNF-α, IL-2, IL-17/21) (111–113), while increasing the levels of anti-inflammatory IL-10 and IL-4 (114, 115). As a consequence, VD increases the production of CD25 +/CD4+ regulatory T cells, shifting the Th1 inflammatory response towards the more tolerogenic Th2 response (116). Following antigen stimulation, VD directly controls the expression of the antimicrobial peptide (AMP) gene in innate immune cells, promoting tolerance and inhibiting immunity (117, 118). VD causes the surface of T-cells to express the CCR10 receptor, which enables them to migrate from dermal blood arteries to epidermal keratinocytes (119).

5.4.2 Vitamin D and dermatoporosis

Several studies on VD receptor mutant mice have put the basis for the knowledge of VD relevance in controlling aging in skin and many other tissues, as these mice developed typical phenotypic traits of premature aging such as skin and overall body atrophy as well as OP. By normalizing mineral VD, these phenotypic traits can be reversed (6, 120–122). Surprisingly, the aging phenotypes of mice with hypovitaminosis D (VDR–/– and CYP27B1–/– mice) are strikingly comparable to those of mice with hypervitaminosis D (including FGF-23–/– and Klotho–/– mice) (6, 121). Keisala et al.'s study used VDR "Tokyo" knockout (KO) mice to examine growth, skin and cerebellar morphology, as well as general motor function. They discovered that the phenotype of old VDR KO mice was comparable to old hypervitaminosis D3 mouse models, indicating that VDR genetic ablation accelerates early mouse aging (121). Therefore, vitamin D deficiencies, both mild and severe, may speed up aging. According to VD status, aging actually appears to follow a U-shaped curve, making adequate levels of VD important regulators of the physiological aging process and essential for avoiding premature aging (120).

Aside from its potential application in the treatment of skin aging for aesthetic purposes, there is evidence that VD can also play a role in the prevention and management of DP and its severe repercussions. Here we summarize some key ways in which VD influences skin health and its potential impact on DP.

First of all, in DP there is an impairment of the collagen component of the skin (2). As discussed above, collagen, a protein responsible for skin strength and elasticity (123), tends to decrease with age, contributing to the thinning and fragility of the skin (2). VD has been found to stimulate collagen synthesis, promoting skin thickness and resilience (124). By enhancing

collagen production, VD may help counteract the effects of DP and support overall skin health. A second aspect is the regulation of epidermal barrier function. The latter is vital for maintaining skin hydration and protection against external stressors (125). VD affects the expression of genes that contribute to skin barrier development and maintenance. It helps strengthen the protective layer of the skin, reducing water loss and improving the skin's ability to defend against environmental factors that contribute to DP (126). Anti-inflammatory effects are of course involved. Chronic inflammation is a key contributor to skin aging and DP. An immunological change and an imbalance between pro- and anti-inflammatory mechanisms cause a chronic low-grade inflammation state known as "inflammaging" (127, 128), which is brought on by both persistent oxidative stress and chronic antigen stimulation (129, 130). With advancing age, skin immune system presents a deep remodeling, resulting in a decrease in its capacity for adaptation (131, 132). As deeply discussed before, VD possesses anti-inflammatory properties, modulating the immune response in the skin and reducing inflammation (52). By mitigating inflammation, VD may help alleviate the symptoms associated with dermatoporosis and promote healthier, more resilient skin.

Impaired wound healing is a common characteristic of dermatoporotic skin (2). VD has been demonstrated to improve wound healing by encouraging cell proliferation and migration and facilitating collagen synthesis (133). By supporting the healing process, VD may help improve the recovery time of wounds and minimize the risk of complications in dermatoporotic skin.

Finally, VD is involved in protection against harmful UV radiation. DP skin is more vulnerable to sun damage and should be shielded from excessive sun exposure (134). The idea that 1,25(OH)2D3 has a cytoprotective effect against the harmful impacts of UV and other agents, that may aid in preventing premature skin aging, is strongly supported by a number of in vitro investigations (135–138). Oral administration of high-dose vitamin D3 immediately following exposure to UVB light reversed photo-induced cutaneous injury quickly in a double-blinded, placebo-controlled interventional trial on 20 healthy adults by reducing inflammation and inducing the epidermal barrier's repair mechanisms (139).

Only one MR trial has looked at vitamin D status and skin phenotype. Higher observed serum 25OHD concentrations were linked to perceived age, skin wrinkling, and pigmented spots, according to research by Noordam et al. on facial skin aging features in about 4500 Dutch individuals. However, according to genetic predictions, serum 25OHD was not linked to these skin characteristics. This seems to suggest that the cause of skin aging is exposure to UV-B light rather than serum 25OHD concentrations (140).

5.5 Vitamin D deficiency: therapy

Everyone in the aging population, regardless of bone health status, should get enough VD (together with an adequate calcium intake of 800-1000 mg/day as well) (4). The Bone Health and Osteoporosis Foundation (BHOF) advises 800 to 1000 international units (IU) of VD per day for persons over the age of 50, while the Institute of Medicine (IOM) recommends 600 IU per day till the age of 70 and 800 IU per day for adults over the age of 71. It is however very common that older individuals develop VD deficiency, which is caused mostly by being institutionalized or chronically ill with inadequate sun exposure, absorption problems, chronic renal illness. If enough and non-hazardous solar exposure is insufficient to obtain the necessary amounts of VD for skeletal occurrences (fractures and falls), oral supplements should be used. Treatment must be personalized. Cholecalciferol is the first line therapy in most patients. No one who requires supplementing will respond to a single set dose; instead, a dose between 800 and 2000 IU per day should be taken into consideration (141). The daily method of supplementing is the most physiological; however, from a pharmacological perspective, the use of similar weekly or monthly doses is recommended in order to increase adherence to therapy. In individuals who require quick vitamin D level normalization (symptomatic osteomalacia or zoledronic acid or denosumab initiators) it is recommended to use a initial loading dose of either cholecalciferol in a single dosage of 60,000 to 150,000 IU, followed by a maintenance dose, or 3,000–10,000 IU/day (mean 5,000 IU/day) for 1–2 months (142). As an alternative, it is feasible to utilize calcifediol for 20 to 30 days before moving to cholecalciferol for maintenance dose. Since its pharmacokinetics are different from the cholecalciferol's one because it has a lower volume of distribution, calcifediol causes a 25(OH)D level increase more quickly. In obese subjects it is suggested to use either cholecalciferol at a dosage increased by approximately 30% of the usual dose or calcifediol. The latter can also be indicated in other conditions of 25-hydroxylation deficiency which are often observed in older people, such as severe liver failure, male hypogonadism or intestinal malabsorption (79). Chronic renal disease is another ailment that is typically common in aged persons. In this setting it is recommended to use cholecalciferol and to restrict the administration of active vitamin D compounds (calcitriol or synthetic analogues) to dialysis patients or those in the G4-G5 phase with severe and progressive hyperparathyroidism (143).

6 Conclusions

Aging is marked by the continuous and progressive decline in organic functions and the increase of prevalence of chronic degenerative disease. OP and DP are expressions of this process at the bone and skin levels, respectively. Both conditions are associated with increased morbidity for elderly people, and this makes preventive interventions necessary. A first conclusion of our study is that since DP is a frequently observed condition by dermatologists, its presence might serve as a straightforward clinical indicator of bone frailty, encouraging healthcare providers to recognize and treat underlying OP. Furthermore, the two conditions share many risk factors, some not always editable such as corticosteroid use, others on which it is possible to intervene as VD deficiency. VD is involved in either disease with many mechanisms, among which immunomodulation (Figure 2). VD deficiency has been linked to OP because it inhibits the body's capacity to absorb calcium and maintain optimal bone health.

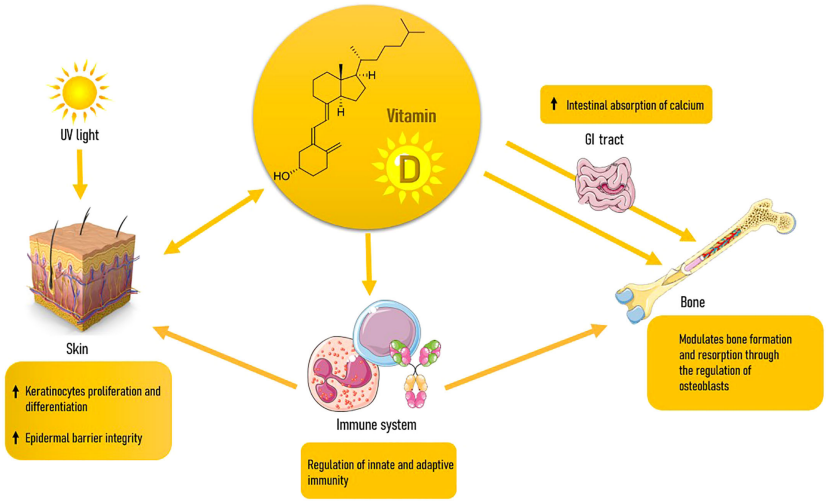

FIGURE 2
Interplays between Vitamin D, skin, bone and immune system.

When it comes to skin, VD is involved in the formation, growth, and repair of skin cells. Both hypo and hypervitaminosis D appear to accelerate skin aging, with a U-shaped response curve to VD status. As a result, proper vitaminosis D appears to be vital in preventing age-related issues. DP is often seen in elderly individuals, particularly those with long-term sun exposure and a history of chronic sun damage. VD deficiency can be linked to DP, as it affects the quality and the composition of the skin. Although further research is needed to establish a definitive link between VD and DP, the existing evidence suggests its potential benefits in supporting skin health and mitigating the effects of this age-related condition. VD's role in collagen production, epidermal barrier function, inflammation regulation, wound healing, and sun protection makes it a promising avenue for addressing DP.

More research with rigorous and reproducible evaluation is required to better understand the role of VD in the development of fragility syndromes as DP and OP, but since now it is advisable to maintain adequate levels of VD to prevent these conditions, as VD deficiency is a simply avoidable and curable condition with major health effects.

Author contributions

FR and CDS contributed to ideation, drafting, and revising of the manuscript. FR, DS, CMT, AS, DAC, RA, ML and CDS, contributed to the literature search and drafting of the manuscript. AC contributed to ideation and revising of the manuscript. All authors have revised and accepted the final version of the manuscript.

Funding

The authors declare that no financial support was received for the research, authorship, and/or publication of this article.

Conflict of interest

The authors declare that the research was conducted in the absence of any commercial or financial relationships that could be construed as a potential conflict of interest.

Publisher's note

All claims expressed in this article are solely those of the authors and do not necessarily represent those of their affiliated organizations, or those of the publisher, the editors and the reviewers. Any product that may be evaluated in this article, or claim that may be made by its manufacturer, is not guaranteed or endorsed by the publisher.

References

1. NIH Consensus Development Panel on Osteoporosis Prevention, Diagnosis, and Therapy. Osteoporosis prevention, diagnosis, and therapy. *JAMA*. (2001) 285:785–95. doi: 10.1001/jama.285.6.785

2. Kaya G, Saurat J-H. Dermatoporosis: a chronic cutaneous insufficiency/fragility syndrome. Clinicopathological features, mechanisms, prevention and potential treatments. *Dermatology* (2007) 215(4):284–94. doi: 10.1159/000107621

3. Kaya G. New therapeutic targets in dermatoporosis. *J Nutr Health Aging* (2012) 16 (4):285–8. doi: 10.1007/s12603-012-0041-0

4. Khandelwal S, Lane NE. Osteoporosis: review of etiology, mechanisms, and approach to management in the aging population. *Endocrinol Metab Clin North Am* (2022) 52(2):259–75. doi: 10.1016/j.ecl.2022.10.009

5. Sirufo MM, De Pietro F, Bassino EM, Ginaldi L, De Martinis M. Osteoporosis in skin diseases. *Int J Mol Sci* (2020) 21(13):4749. doi: 10.3390/ijms21134749

6. Tuohimaa P. Vitamin D and aging. *J Steroid Biochem Mol Biol* (2008) 114(1-2):78–84. doi: 10.1016/j.jsbmb.2008.12.020

7. Kanis JA, Cooper C, Rizzoli R, Reginster JY. European guidance for the diagnosis and management of osteoporosis in postmenopausal women. *Osteoporos Int* (2019) 30 (1):3–44. doi: 10.1007/s00198-018-4704-5

8. Commissione Intersocietaria per l'Osteoporosi (SIE, SIGG, SIMFER, SIMG, SIMI, SIOMMMS, SIR, SIOT). Linee Guida sulla gestione dell'Osteoporosi e delle Fratture da fragilità. (2021) Available at: https://siommms.it/commissione-intersocietaria-per-losteoporosi/.

9. Khandelwal S, Lane NE. Osteoporosis: review of etiology, mechanisms, and approach to management in the aging population. *Endocrinol Metab Clin North Am* (2023) 52(2):259–75. doi: 10.1016/j.ecl.2022.10.009

10. Mirza F, Canalis E. MANAGEMENT OF ENDOCRINE DISEASE: Secondary osteoporosis: pathophysiology and management. *Eur J Endocrinol* (2015) Volume 173, Issue 3:R131–51. doi: 10.1530/EJE-15-0118

11. Bullamore JR, Wilkinson R, Gallagher JC, Nordin BE, Marshall DH. Effect of age on calcium absorption. *Lancet* (1970) 2(7672):535–7. doi: 10.1016/S0140-6736(70) 91344-9

12. Cummings SR, Nevitt MC, Browner WS, Stone K, Fox KM, Ensrud KE. Risk factors for hip fracture in white women. Study of Osteoporotic Fractures Research Group. *N Engl J Med* (1995) 332:767–73. doi: 10.1056/NEJM199503233321202

13. Khosla S, Oursler MJ, Monroe DG. Estrogen and the skeleton. Trends endocrinol. *Metab* (2012) 23:576–81. doi: 10.1016/j.tem.2012.03.008

14. Iantomasi T, Romagnoli C, Palmini G, Donati S, Falsetti I, Miglietta F, et al. Oxidative stress and inflammation in osteoporosis: molecular mechanisms involved and the relationship with microRNAs. *Int J Mol Sci* (2023) 24(4):3772. doi: 10.3390/ijms24043772

15. Silverman SL. *Clin consequences vertebral compression fracture. Bone*. The clinical consequences of vertebral compression fracture. (1992) 13 Suppl 2:S27–31. doi: 10.1016/8756-3282(92)90193-z

16. Gehlbach SH, Bigelow C, Heimisdottir M, May S, Walker M, Kirkwood JR. Recognition of vertebral fracture in a clinical setting. *Osteoporos. Int* (2000) 11(7):577–82. doi: 10.1007/s001980070078

17. Ismail AA, Cooper C, Felsenberg D, Varlow J, Kanis JA, Silman AJ, et al. Number and type of vertebral deformities: epidemiological characteristics and relation to back pain and height loss. European Vertebral Osteoporosis Study Group. *Osteoporos. Int* (1999) 9(3):206–13. doi: 10.1007/s001980050138

18. Grados F, Roux C, de Vernejoul MC, Utard G, Sebert JL, Fardellone P. Comparison of four morphometric definitions and a semiquantitative consensus reading for assessing prevalent vertebral fractures. *Osteoporos. Int* (2001) 12(9):716–22. doi: 10.1007/s001980170046

19. Lee YL, Yip KM. The osteoporotic spine. *Clin Orthop Relat Res* (1996) 1996 (323):91–7. doi: 10.1097/00003086-199602000-00012

20. Cummings SR, Melton LJ. Epidemiology and outcomes of osteoporotic fractures. *Lance* (2002) 359(9319):1761–7. doi: 10.1016/S0140-6736(02)08657-9

21. Ensrud KE. Epidemiology of fracture risk with advancing age. *Journals Gerontology: Ser A* (2013) 68(10):1236–42. doi: 10.1093/gerona/glt092

22. Haentjens P, Rivista J, Colón-Emeric CS, Vanderschueren D, Milsen K, Velkeniers B, et al. Meta-analysis: excess mortality after hip fracture among older women and men. *Ann Intern Med* (2010) 152(6):380–90. doi: 10.7326/0003-4819-152-6-201003160-00008

23. Vanderschueren D, Boonen S, Bouillon R. Osteoporosis and osteoporotic fractures in men: a clinical perspective. *Baillieres Best Pract Res Clin Endocrinol Metab* (2000) 14(2):299–315. doi: 10.1053/beem.2000.0075

24. Irvine C. 'Skin failure'–a real entity: discussion paper. *J R Soc Med* (1991) 84 (7):412–3. doi: 10.1177/014107689108400711

25. Wollina U, Lotti T, Vojvotic A, Nowak A. Dermatoporosis – the chronic cutaneous fragility syndrome. *J Med Sci* (2019) 7(18):3046–9. doi: 10.3889/oamjms.2019.766

26. Mengeaud V, Dautezac-Vieu C, Josse G, Vellas B, Schmitt AM. Prevalence of dermatoporosis in elderly French hospital in-patients: a cross-sectional study. *Br J Dermatol* (2012) 166:442–3. doi: 10.1111/j.1365-2133.2011.10534.x

27. Saurat JH, Mengeaud V, Georgescu V, Coutanceau G, Ezzedine K, Taïeb C. A simple self-diagnosis tool to assess the prevalence of dermatoporosis in France. *J Eur Acad Dermatol Venereol* (2017) 31(8):1380–6. doi: 10.1111/jdv.14240

28. Kluger N, Impivaara S. Prevalence of and risk factors for dermatoporosis: a prospective observational study of dermatology outpatients in a Finnish tertiary care hospital. *J Eur Acad Dermatol Venereol* (2019) 33(2):447–50. doi: 10.1111/jdv.15240

29. Kaya G, Rodriguez I, Jorcano JL, Vassalli P, Stamenkovic I. Selective suppression of CD44 in keratinocytes of mice bearing an antisense CD44 transgene driven by a tissue-specific promoter disrupts hyaluronate metabolism in the skin and impairs keratinocyte proliferation. *Genes Dev* (1997) 11(8):996–1007. doi: 10.1101/gad.11.8.996

30. Kaya G, Tran C, Sorg O, Hotz R, Grand D, Carraux ,P, et al. Hyaluronate fragments reverse skin atrophy by a CD44-dependent mechanism. *PloS Med* (2006) 3 (12):e493. doi: 10.1371/journal.pmed.0030493

31. Calikoglu E, Sorg O, Tran C, Grand D, Carraux P, Saurat JH, et al. UVA and UVB decrease expression of CD44 and hyaluronate in mouse epidermis which is counteracted by topical retinoids. *Photochem Photobiol* (2006) 82(5):1342–7. doi: 10.1562/2006-02-10-RA-801

32. Barnes L, Ino F, Jaunin F, Saurat JH, Kaya G. Inhibition of putative hyalurosome platform in keratinocytes as a mechanism for corticosteroid-induced epidermal atrophy. *J Invest Dermatol* (2012) 133(4):1017–26. doi: 10.1038/jid.2012.439

33. Schoepe S, Schäcke H, May E, Asadullah K. Glucocorticoid therapy-induced skin atrophy. *Exp Dermatol* (2006) 15(6):406–20. doi: 10.1111/j.0906-6705.2006.00435.x

34. Hornebeck W.). Down-regulation of tissue inhibitor of matrix metalloproteinase-1 (TIMP-1) in aged human skin contributes to matrix degradation and impaired cell growth and survival. *Pathol Biol* (2003) 51(10):569–73. doi: 10.1016/j.patbio.2003.09.003

35. Kaya G, Kaya A, Sauratb JH. Induction of hyalurosome by topical hyaluronate fragments results in superficial filling of the skin complementary to hyaluronate filler injections. *Dermatopathology (Basel).* (2019) 6(2):45–9. doi: 10.1159/000500493

36. Colomb D. Stellate spontaneous pseudoscars. Senile and presenile forms: especially those forms caused by prolonged corticoid therapy. *Arch Dermatol* (1972) 105(4):551–4. doi: 10.1001/archderm.1972.01620070023008

37. Kaya G, Jacobs F, Prins C, Viero D, Kaya A, Saurat JH. Deep dissecting hematoma: An emerging severe complication of dermatoporosis. *Arch Dermatol* (2008) 144:1303–8. doi: 10.1001/archderm.144.10.1303

38. Toutous-Trellu L, Weiss L, Tarteaut MH, Kaya A, Cheretakis A, Kaya G. Deep dissecting hematoma: a plaidoyer for an early and specialized management. *Eur Geriatr Med* (2010) 1:228–30. doi: 10.1016/j.eurger.2010.07.001

39. Prins C. L'insuffisance cutanée. *Méd Hyg* (2004) 2472:478–80.

40. Tomic-Canic M, Brem H. Gene array technology and pathogenesis of chronic wounds. *Am J Surg* (2004) 188(1A suppl):67–72. doi: 10.1016/S0002-9610(03)00293-9

41. Kaya G, Kaya A, Sorg O, Saurat JH. Dermatoporosis: a further step to recognition. *J Eur Acad Dermatol Venereol* (2018) 32:189–91. doi: 10.1111/jdv.14777

42. Castillo-Cruz UDR, Cortés-García JD, Castanedo-Cázares JP, Hernández-Blanco DP, Torres-Álvarez B. Factors associated with dermatoporosis in a sample of geriatric patients in Mexico. *Gac Med Mex* (2023) 159(1):49–54. doi: 10.24875/GMM.M22000737

43. Chanca L, Fontaine J, Kerever S, Feneche Y, Forasassi C, Meaume S, et al. Prevalence and risk factors of dermatoporosis in older adults in a rehabilitation hospital. *J Am Geriatr Soc* (2022) 70(4):1252–6. doi: 10.1111/jgs.17618

44. Trevisan C, Alessi A, Girotti G, Zanforlini BM, Bertocco A, Mazzochin M. The impact of smoking on bone metabolism, bone mineral density and vertebral fractures in postmenopausal women. *J Clin Densitometry* (2021) 23(3):381–9. doi: 10.1016/j.jocd.2019.07.007

45. Hardy RS, Zhou H, Seibel JS, Cooper MS. Glucocorticoids and bone: consequences of endogenous and exogenous excess and replacement therapy. *Endocr Rev* (2018) 39(5):519–48. doi: 10.1210/er.2018-00097

46. Bellorin-Font E, Rojas E, Martin KJ. Bone disease in chronic kidney disease and kidney transplant. *Nutrients* (2022) 15(1):167. doi: 10.3390/nu15010167

47. Graat-Verboom L, Wouters EF, Smeenk FW, van den Borne BE, Lunde R, Spruit MA. Current status of research on osteoporosis in COPD: a systematic review. *Eur Respir J* (2009) 34(1):209–18. doi: 10.1183/09031936.50130408

48. Chen YW, Ramsook AH, Coxson HO, Bon J, Reid WD. Prevalence and risk factors for osteoporosis in individuals with COPD: A systematic review and meta-analysis. *Chest* (2019) 156:1092–110. doi: 10.1016/j.chest.2019.06.036

49. Reszke R, Pełka D, Walasek A, Machaj Z, Reich A. Skin disorders in elderly subjects. *Int J Dermatol* (2015) 54(9):e332–8. doi: 10.1111/ijd.12832

50. Whitmore SE, Levine MA. Risk factors for reduced skin thickness and bone density: possible clues regarding pathophysiology, prevention, and treatment. *J Am Acad Dermatol* (1998) 38(2 Pt1):248–55. doi: 10.1016/s0190-9622(98)70600-0

51. Villeneuve D, Lidove O, Chazerain P, Ziza J-M, Sené T. Association between dermatoporosis and history of major osteoporotic fractures: A French prospective observational study in a general practice population. *Jt. Bone Spine.* (2020) 2020:1297. doi: 10.1016/j.jbspin.2020.04.004

52. Bocheva G, Slominski RM, Slominski AT. The impact of vitamin D on skin aging. *Int J Mol Sci* (2021) 22(16):9097. doi: 10.3390/ijms22169097

53. Charoenngam N, Shirvani A, Holick MF. Vitamin D for skeletal and non-skeletal health: What we should know. *J Clin Orthop Trauma* (2019) 10(6):1082–93. doi: 10.1016/j.jcot.2019.07.004

54. Webb AR, Pilbeam C, Hanafin N, Holick MF. An evaluation of the relative contributions of exposure to sunlight and of diet to the circulating concentrations of 25-hydroxyvitamin D in an elderly nursing home population in Boston. *Am J Clin Nutr* (1990) 51:1075–81. doi: 10.1093/ajcn/51.6.1075

55. MacLaughlin J, Holick MF. Aging decreases the capacity of human skin to produce vitamin D3. *J Clin Invest* (1985) 76:1536–8. doi: 10.1172/JCI112134

56. Merke J, Milde P, Lewicka S, Hugel U, Klaus G, Mangelsdorf DJ, et al. Identification and regulation of 1,25-dihydrox- vitamin D3 receptor activity and

biosynthesis of 1,25-dihy- droxyvitamin D3. Studies in cultured bovine aortic endothelial cells and human dermal capillaries. *J Clin Invest* (1989) 83:1903–15. doi: 10.1172/JCI114097

57. Nuzzo V, Zuccoli A, de Terlizzi F, Colao A, Tauchmanova L. Low 25-hydroxyvitamin D levels and low bone density assessed by quantitative ultrasonometry in a cohort of postmenopausal Italian nuns. *J Clin Densitom* (2013) 16(3):308–12. doi: 10.1016/j.jocd.2012.05.009

58. Di Monaco M, Castiglioni C, Tappero R. Parathyroid hormone response to severe vitamin D deficiency is associated with femoral neck bone mineral density: an observational study of 405 women with hip-fracture. *Hormones (Athens)* (2016) 15 (4):527–33. doi: 10.14310/horm.2002.1709

59. Muscogiuri G, Altieri B, Annweiler C, Balercia G, Pal HB, Boucher BJ, et al. Vitamin D and chronic diseases: the current state of the art. *Arch Toxicol* (2017) 91 (1):97–107. doi: 10.1007/s00204-016-1804-x

60. Muscogiuri G, Mitri J, Mathieu C, Badenhoop K, Tamer G, Orio F, et al. Mechanisms in endocrinology: vitamin D as a potential contributor in endocrine health and disease. *Eur J Endocrinol* (2014) 171(3):R101– 10. doi: 10.1530/EJE-14-0158

61. Bouillon R, Carmeliet G, Verlinden L, van Etten E, Luderer HF, Verstuyf A, et al. Vitamin D and human health: lessons from vitamin D receptor null mice. *Endocr Rev* (2008) 29:726–76. doi: 10.1210/er.2008-0004

62. Overbergh L, Stoffels K, Waer M, Verstuyf A, Bouillon R, Mathieu C. Immune regulation of 25-hydroxyvitamin D-1alpha-hydroxylase in human monocytic THP1 cells: mechanisms of interferon-gamma-mediated induction. *J Clin Endocrinol Metab* (2006) 91:3566–74. doi: 10.1210/jc.2006-0678

63. Ameri P, Giusti A, Boschetti M, Murialdo G, Minuto F, Ferone D. Interactions between vitamin D and IGF-I: from physiology to clinical practice. *Clin Endocrinol (Oxf)* (2013) 79(4):457–63. doi: 10.1111/cen.12268

64. Vuolo L, Di Somma C, Faggiano A, Colao A. Vitamin D and cancer. *Front Endocrinol (Lausanne)* (2012) 3:58. doi: 10.3389/fendo.2012.00058

65. Antinozzi C, Corinaldesi C, Giordano C, Pisano A, Cerbelli B, Migliaccio S, et al. Potential role for the VDR agonist elocalcitol in metabolic control: Evidences in human skeletal muscle cells. *J Steroid Biochem Mol Biol Mar* (2016) 167:169–81. doi: 10.1016/j.jsbmb.2016.12.010

66. Savastano S, Di Somma C, Colao A. Vitamin-D & prediabetes: a promising ménage in the Indian Scenario. *Indian J Med Res* (2013) 138(6):829–30.

67. Muscogiuri G, Barrea L, Altieri B, Di Somma C, Bhattoa HP, Laudisio D, et al. Calcium and vitamin D supplementation. Myths and realities with regard to cardiovascular risk. *Curr Vasc Pharmacol* (2019) 17(6):610–7. doi: 10.2174/1570161117666190408165805

68. Foresta C, Strapazzon G, De Toni L, Perilli L, Di Mambro A, Muciaccia B, et al. Bone mineral density and testicular failure: evidence for a role of vitamin D 25-hydroxylase in human testis. *J Clin Endocrinol Metab* (2011) 96(4):E646–52. doi: 10.1210/jc.2010-1628

69. ROmano F, Muscogiuri G, Di Benedetto E, Zhukouskaya VV, Barrea L, Savastano S, et al. Vitamin D and sleep regulation: is there a role for vitamin D? *Curr Pharm Des* (2020) 26(21):2492–6. doi: 10.2174/1381612826666200310145935

70. Jensen SS, Madsen MW, Lukas J, Binderup L, Bartek J. Inhibitory effects of 1alpha,25-dihydroxyvitamin D(3) on the G(1)-S phase-controlling machinery. *Mol Endocrinol* (2001) 15:1370–80. doi: 10.1210/mend.15.8.0673

71. Santoro D, Sebekova K, Teta D, De Nicola L. Extraskeletal functions of vitamin D. *BioMed Res Int* (2015) 2015:2. doi: 10.1155/2015/294719

72. Barrea L, Savanelli MC, Di Somma C, Napolitano M, Megna M, Colao A, et al. Vitamin D and its role in psoriasis: An overview of the dermatologist and nutritionist. *Rev Endocr Metab Disord* (2017) 18(2):195–205. doi: 10.1007/s11154-017-9411-6

73. Amado Diago CA, Garcia-Unzueta MT, Farinas MD, Amado JA. Calcitriol-modulated human antibiotics: new pathophysiological aspects of vitamin D. *Endocrinol Nutr* (2006) 63:87–94. doi: 10.1016/j.endonu.2015.09.005

74. Kankova M, Luini W, Pedrazzoni M, Riganti F, Sironi M, Bottazzi B, et al. Impairment of cytokine production in mice fed a vitamin D3-deficient diet. *Immunology* (1991) 73:466–71.

75. Bouillon R, Lieben L, Mathieu C, Verstuyf A, Carmeliet G. Vitamin D action: lessons from VDR and Cyp27b1 null mice. *Pediatr Endocrinol Rev* (2013) 10(Suppl 2):354–66.

76. Bertoldo F, Cianferotti L, Di Monaco M, Falchetti A, Fassio A, Gatti D, et al. Definition, assessment, and management of vitamin D inadequacy: suggestions, recommendations, and warnings from the italian society for osteoporosis, mineral metabolism and bone diseases (SIOMMMS). *Nutrients*. (2022) 14(19):4148. doi: 10.3390/nu14194148

77. Holvik K, Ahmed LA, Forsmo S, Gjesdal CG, Grimnes G, Samuelsen SO, et al. Low serum levels of 25-hydroxyvitamin D predict hip fracture in the elderly: A NOREPOS study. *J Clin Endocrinol Metab* (2013) 98:3341–50. doi: 10.1210/jc.2013-1468

78. Bischoff-Ferrari HA, Willett WC, Wong JB, Giovannucci E, Dietrich T, Dawson-Hugheset B. Fracture prevention with vitamin D supplementation: A meta-analysis of randomized controlled trials. *JAMA* (2005) 293:2257–64. doi: 10.1001/jama.293.18.2257

79. Cesareo R, Attanasio R, Caputo M, Castello R, Chiodini I, Falchetti A, et al. Italian association of clinical endocrinologists (AME) and italian chapter of the american association of clinical endocrinologists (AACE) position statement: clinical management of vitamin D deficiency in adults. *Nutrients* (2018) 10(5):546. doi: 10.3390/nu10050546

80. Bikle DD, Feingold KR, Anawalt B, Blackman MR, Boyce A, Chrousos G, et al. Vitamin D: production, metabolism and mechanisms of action, in: *Endotext* (2017) (Accessed 11 August 2017).

81. Sahay M, Sahay R. Rickets-vitamin D deficiency and dependency. *Indian J Endocrinol Metabol* (2012) 16(2):164e176. doi: 10.4103/2230-8210.93732

82. Holick MF. Resurrection of vitamin D deficiency and rickets. *J Clin Invest.* (. (2006) 116(8):2062e2072. doi: 10.1172/JCI29449

83. Kuchuk NO, Pluijm SM, van Schoor NM, LoOman CW, Smit JH, Lips P. Relationships of serum 25-hydroxyvitamin D to bone mineral density and serum parathyroid hormone and markers of bone turnover in older persons. *J Clin Endocrinol Metab* (2009) 94(4):1244–50. doi: 10.1210/jc.2008-1832

84. Bouillon R, Van Schoor NM, Gielen E, Boonen S, Mathieu C, Vanderschueren D, et al. Optimal vitamin D status: a critical analysis on the basis of evidence-based medicine. *J Clin Endocrinol Metab* (2013) 98(8):E1283–304. doi: 10.1210/jc.2013-1195

85. Lips P, van Schoor NM. The effect of vitamin D on bone and osteoporosis. *Best Pract Res Clin Endocrinol Metab* (2011) 25(4):585–91. doi: 10.1016/j.beem.2011.05.002

86. Bouillon R, Marcocci C, Carmeliet G, Bikle D, White JH, Dawson-Hughes B. Skeletal and extraskeletal actions of vitamin D: current evidence and outstanding questions. *Endocr Rev* (2019) 40(4):1109–51. doi: 10.1210/er.2018-00126

87. Reid IR, Horne AM, Mihov B, Gamble GD, Al-Abuwsi F, Singh M, et al. Effect of monthly high-dose vitamin D on bone density in community-dwelling older adults substudy of a randomized controlled trial. *J Intern Med* (2017) 282:452–60. doi: 10.1111/joim.12651

88. Macdonald HM, Reid IR, Gamble GD, Fraser WD, Tang JC, Wood AD. 25-Hydroxyvitamin D threshold for the effects of vitamin D supplements on bone density: secondary analysis of a randomized controlled trial. *J Bone Miner. Res* (2018) 33:1464–9. doi: 10.1002/jbmr.3442

89. Weaver CM, Alexander DD, Boushey CJ, Dawson-Hughes B, Lappe JM, LeBoff MS, et al. Calcium plus vitamin D supplementation and risk of fractures: an updated meta-analysis from the National Osteoporosis Foundation. *Osteoporos. Int* (2016) 27:367–76. doi: 10.1007/s00198-015-3386-5

90. Yao P, Bennett D, Mafham M, Lin X, Chen Z, Armitage J, et al. Vitamin D and calcium for the prevention of fracture: a systematic review and meta-analysis. *JAMA Netw Open* (2019) 2:e1917789. doi: 10.1001/jamanetworkopen.2019.17789

91. Adami S, Giannini S, Bianchi G, Sinigaglia L, Di Munno O, Fiore CE, et al. Vitamin D status and response to treatment in post-menopausal osteoporosis. *Osteoporos. Int* (2009) 20:239–44. doi: 10.1007/s00198-008-0650-y

92. Degli Esposti L, Girardi A, Saragoni S, Sella S, Andretta M, Rossini M, et al. Use of anti osteoporotic drugs and calcium/vitamin D in patients with fragility fractures: Impact on re-fracture and mortality risk. *Endocrine* (2019) 64:367–77. doi: 10.1007/s12020-018-1824-9

93. Neer RM, Arnaud CD, Zanchetta JR, Prince R, Gaich GA, Reginster JY, et al. Effect of parathyroid hormone (1-34) on fractures and bone mineral density in postmenopausal women with osteoporosis. *N Engl J Med* (2001) 344:1434–41. doi: 10.1056/NEJM200105103441904

94. Inanir A, Ozoran K, Tutkak H, Mermerci B. The effects of calcitriol therapy on serum interleukin-1, interleukin-6 and tumor necrosis factor-alpha concentrations in post-menopausal patients with osteoporosis. *J Int Med Res* (2004) 32(6):570–82. doi: 10.1177/147323000403200602

95. Bikle DD. Vitamin D metabolism and function in the skin. *Mol Cell Endocrinol* (2011) 347(1-2):80–9. doi: 10.1016/j.mce.2011.05.017

96. Wadhwa B, Relhan V, Goel K, Kochhar AM, Garg VK. Vitamin D and skin diseases: A review. *Indian J Dermatol Venereol Leprol.* (2015) 81(4):344–55. doi: 10.4103/0378-6323.159928

97. Zmijewski MA, Carlberg C. Vitamin D receptor(s): In the nucleus but also at membranes? *Exp Dermatol* (2020) 29:876–84. doi: 10.1111/exd.14147

98. Mizwicki MT, Keidel D, Bula CM, Bishop JE, Zanello LP, Wurtz JM, et al. Identification of an alternative ligand-binding pocket in the nuclear vitamin D receptor and its functional importance in 1alpha,25(OH)2-vitamin D3 signaling. *Proc Natl Acad Sci USA* (2004) 101:12876–81. doi: 10.1073/pnas.0403606101

99. Nemere I, Garbi N, Hammerling G, Hintze KJ. Role of the 1,25D3-MARRS receptor in the 1,25(OH)2D3-stimulated uptake of calcium and phosphate in intestinal cells. *Steroids* (2012) 77:897–902. doi: 10.1016/j.steroids.2012.04.002

100. Slominski AT, Kim TK, Takeda Y, Janjetovic Z, Brozyna AA, Skobowiat C, et al. RORα and ROR γ are expressed in human skin and serve as receptors for endogenously produced noncalcemic 20-hydroxy- and 20,23-dihydroxyvitamin D. *FASEB J* (2014) 28:2775–89. doi: 10.1096/fj.13-242040

101. Slominski AT, Kim TK, Janjetovic Z, Brożyna AA, Żmijewski MA, Xu H, et al. Differential and overlapping effects of 20,23(OH)2D3 and 1,25(OH)2D3 on gene expression in human epidermal keratinocytes: identification of ahR as an alternative receptor for 20,23(OH)2D3. *Int J Mol Sci* (2018) 19:3072. doi: 10.3390/ijms19103072

102. Slominski AT, Kim TK, Qayyum S, Song Y, Janjetovic Z, Oak ASW, et al. Vitamin D and lumisterol derivatives can act on liver X receptors (LXRs). *Sci Rep* (2021) 11:8002. doi: 10.1038/s41598-021-87061-w

103. Segaert S, Bouillon R. Epidermal keratinocytes as source and target cells for vitamin D. In: Norman AW, Bouillon R, Thomasset M, editors. *Vitamin D endocrine system: structural, biological, genetic and clinical aspects. Proceedings of the eleventh workshop on vitamin D*. Nashville, TN, USA: University of Calif (2000).

104. Gniadecki R. Stimulation versus inhibition of keratinocytes growth by 1,25-dihydroxy vitamin D3: Dependence on cell culture conditions. *J Invest Dermatol* (1996) 106:510–6. doi: 10.1111/1523-1747.ep12343866

105. Choi MJ, Maibach HI. Role of ceramides in barrier function of healthy and diseased skin. *Am J Clin Dermatol* (2005) 6(4):215–23. doi: 10.2165/00128071-200506040-00002

106. Beilawaska A, Linardic CM, Hannun YA. Modulation of cell growth and differentiation by ceramide. *FEBS Lett* (1992) 307:211–4. doi: 10.1016/0014-5793(92)80769-D

107. Geilen CC, Bektas M, Weider T, Orfanos CR. 1α, 25-dihydroxy vitamin D3 induces sphingomyelin hydrolysis in Ha Ca T cells via tumor necrotic factor α. *J Biol Chem* (1997) 272:8997–9001. doi: 10.1074/jbc.272.14.8997

108. Teymoori-Rad M, Shokri F, Salimi V, Mahdi Marashi S. The interplay between vitamin D and viral infections. *Rev Med Virol* (2019) 29(2):e2032. doi: 10.1002/rmv.2032

109. Chun RF, Liu PT, Modlin RL, Adams JS, Hewison M. Impact of vitamin D on immune function: Lessons learned from genome-wide analysis. *Front Physiol* (2014) 5:151. doi: 10.3389/fphys.2014.00151

110. Wobke TK, Sorg BL, Steinhilber D. Vitamin D in inflammatory diseases. *Front Physiol* (2014) 5:244. doi: 10.3389/fphys.2014.00244

111. Skrobot A, Demkow U, Wachowska M.). Immunomodulatory role of vitamin D: A review. *Adv Exp Med Biol* (2018) 1108:13–23. doi: 10.1007/5584_2018_246

112. Gorman S, Geldenhuys S, Weeden CE, Grimbaldeston MA, Hart PH. Investigating the roles of regulatory T cells, mast cells and interleukin-9 in the control of skin inflammation by vitamin D. *Arch Dermatol Res* (2018) 310:221–30. doi: 10.1007/s00403-018-1814-z

113. Lemire JM, Archer DC, Beck L, Spiegelberg HL. Immunosuppressive actions of 1,25-dihydroxyvitamin D3: Preferential inhibition of Th1 functions. *J Nutr* (1995) 6 (Suppl. S36):1704S–8S. doi: 10.1016/0960-0760(95)00106-A

114. Fisher SA, Rahimzadeh M, Brierley C, Gration B, Doree C, Kimber CE, et al. The role of vitamin D in increasing circulating T regulatory cell numbers and modulating T regulatory cell phenotypes in patients with inflammatory disease or in healthy volunteers: A systematic review. *PloS One* (2019) 14:e0222313. doi: 10.1371/journal.pone.0222313

115. Cantorna MT, Snyder L, Lin YD, Yang L. Vitamin D and 1,25(OH)2D regulation of T cells. *Nutrients* (2015) 7:3011–21. doi: 10.3390/nu7043011

116. Sassi F, Tamone C, D'Amelio P. Vitamin D: nutrient, hormone, and immunomodulator. *Nutrients* (2018) 10:1656. doi: 10.3390/nu10111656

117. Wang TT, Nestel FP, Bourdeau V, Nagai Y, Wang Q, Liao J, et al. Cutting edge: 1,25-dihydroxyvitamin D3 is a direct inducer of antimicrobial peptide gene expression. *J Immunol* (2004) 173:2909–12. doi: 10.4049/jimmunol.173.5.2909

118. Svensson D, Nebel D, Nilsson BO. Vitamin D3 modulates the innate immune response through regulation of the hCAP-18/LL-37 gene expression and cytokine production. *Inflamm Res* (2016) 65:25–32. doi: 10.1007/s00011-015-0884-z

119. Van Etten E, Decallone B, Verlinden L, Verstuyf A, Bouillon R, Mathieu C, et al. Analogs of 1α,25-dihydroxy vitamin D3 as pluripotent immunomodulators. *J Cell Biochem* (2003) 88:223–6. doi: 10.1002/jcb.10329

120. Tuohimaa P, Keisala T, Minasyan A, Cachat J, Kalueff A. Vitamin D, nervous system and aging. *Psychoneuroendocrinology* (2009) 34(Suppl 1):S278–86. doi: 10.1016/j.psyneuen.2009.07.003

121. Keisala T, Minasyan A, Lou YR, Zou J, Kalueff AV, Pyykkö I, et al. Premature aging in vitamin D receptor mutant mice. *J Steroid Biochem Mol Biol* (2009) 115:91–7. doi: 10.1016/j.jsbmb.2009.03.007

122. Haussler MR, Haussler CA, Whitfield GK, Hsieh JC, Thompson PD, Barthel TK, et al. The nuclear vitamin D receptor controls the expression of genes encoding factors which feed the "Fountain of Youth" to mediate healthful aging. *J Steroid Biochem Mol Biol* (2010) 121:88–97. doi: 10.1016/j.jsbmb.2010.03.019

123. Bolke L, Schlippe G, Gerß J, Voss W. A collagen supplement improves skin hydration, elasticity, roughness, and density: results of a randomized, placebo-controlled, blind study. *Nutrients.* (2019) 11(10):2494. doi: 10.3390/nu11102494

124. Gniadecki R. Stimulation versus inhibition of keratinocyte growth by 1,25-Dihydroxyvitamin D3: dependence on cell culture conditions. *J Invest Dermatol* (1996) 106(3):510–6. doi: 10.1111/1523-1747

125. Lefèvre-Utile A, Braun C, Haftek M, Aubin F. Five functional aspects of the epidermal barrier. *Int J Mol Sci 2021* (2021) 22(21):11676. doi: 10.3390/ijms222111676

126. Roider E, Ruzicka T, Schauber J. Vitamin D, the cutaneous barrier, antimicrobial peptides and allergies: is there a link? *Allergy Asthma Immunol Res* (2013) 5(3):119–28. doi: 10.4168/aair.2013.5.3.119

127. Cevenini E, Monti D, Franceschi C. Inflamm-ageing. *Curr Opin Clin Nutr Metab Care* (2013) 16:14–20. doi: 10.1097/MCO.0b013e32835ada13

128. Pilkington SM, Bulfone-Paus S, Griffiths CEM, Watson REB. Inflammaging and the skin. *J Investig Dermatol* (2021) 141:1087–95. doi: 10.1016/j.jid.2020.11.006

129. Lee YI, Choi S, Roh WS, Lee JH, Kim TG. Cellular senescence and inflammaging in the skin microenvironment. *Int J Mol Sci* (2021) 22:3849. doi: 10.3390/ijms22083849

130. Arck PC, Overall R, Spatz K, Liezman C, Handjiski B, Klapp BF, et al. Towards a "free radical theory of graying": Melanocyte apoptosis in the aging human hair follicle is an indicator of oxidative stress induced tissue damage. *FASEB J* (2006) 20:1567–9. doi: 10.1096/fj.05-4039fje

131. Sunderkötter C, Kalden H, Luger TA. Aging and the skin immune system. *Arch Dermatol* (1997) 133:1256–62. doi: 10.1001/archderm.1997.03890460078009

132. Nguyen AV, Soulika AM. The dynamics of the skin's immune system. *Int J Mol Sci* (2019) 20:1811. doi: 10.3390/ijms20081811

133. Bikle DD. Role of vitamin D and calcium signaling in epidermal wound healing. *J Endocrinol Invest* (2023) 46(2):205–12. doi: 10.1007/s40618-022-01893-5

134. Dyer JM, Miller RA. Chronic skin fragility of aging: current concepts in the pathogenesis, recognition, and management of dermatoporosis. *J Clin Aesthet Dermatol* (2018) 11(1):13–8.

135. Trémezaygues L, Seifert M, Tilgen W, Reichrath J. 1,25-dihydroxyvitamin D(3) protects human keratinocytes against UV-B-induced damage: In vitro analysis of cell viability/proliferation, DNA-damage and -repair. *Dermatoendocrinol* (2009) 1:239–45. doi: 10.4161/derm.1.4.9705

136. De Haes P, Garmyn M, Verstuyf A, De Clercq P, Vandewalle M, Degreef H, et al. 1,25(OH)2D3 and analogues protect primary human keatinocytes against UVB-induced DNA damage. *J Photochem Photobiol* (2005) 78:141–8. doi: 10.1016/j.jphotobiol.2004.09.010

137. Lee JH, Youn JI. The photoprotective effect of 1,25-dihydroxyvitamin D3 on ultraviolet light B-induced damage in keratinocyte and its mechanism of action. *J Dermatol Sci* (1998) 18:11–8. doi: 10.1016/S0923-1811(98)00015-2

138. De Haes P, Garmyn M, Verstuyf A, De Clercq P, Vandewalle M, Vantieghem K, et al. Two 14-epi analogues of 1,25-dihydroxyvitamin D3 protect human keratinocytes against the effects of UVB. *Arch Dermatol Res* (2004) 295:527–34. doi: 10.1007/s00403-004-0451-x

139. Scott JF, Das LM, Ahsanuddin S, Qiu Y, Binko AM, Traylor ZP, et al. Oral vitamin D rapidly attenuates inflammation from sunburn: an interventional study. *J Investig Dermatol* (2017) 137:2078–86. doi: 10.1016/j.jid.2017.04.040

140. Noordam R, Hamer MA, Pardo LM, van der Nat T, Kiefte-de Jong JC, Kayser M, et al. No causal association between 25-hydroxyvitamin D and features of skin aging: evidence from a bidirectional mendelian randomization study. *Invest Dermatol* (2017) 137(11):2291–7. doi: 10.1016/j.jid.2017.07.817

141. Minisola S, Pepe J, Donato P, Vigna E, Occhiuto M, Ferrone F. Replenishment of vitamin D status: theoretical and practical considerations. *Hormones (Athens)* (2019) 18(1):3–5. doi: 10.1007/s42000-018-0040-6

142. van Groningen L, Opdenoordt S, van Sorge A, Telting D, Giesen A, de Boer H. Cholecalciferol loading dose guideline for vitamin D deficient adults. *Eur J Endocrinol* (2010) 162:805–11. doi: 10.1530/EJE-09-0932

143. Ketteler M, Block GA, Evenepoel P, Fukagawa M, Herzog CA, McCann L. Diagnosis, evaluation, prevention, and treatment of chronic kidney disease-mineral and bone disorder: synopsis of the kidney disease: improving global outcomes 2017 clinical practice guideline update. *Ann Intern Med* (2017) 168:422–30. doi: 10.7326/M17-2640

frontiers | Frontiers in Endocrinology

TYPE Original Research
PUBLISHED 04 January 2024
DOI 10.3389/fendo.2023.1280429

OPEN ACCESS

EDITED BY
Michela Rossi,
Bambino Gesù Children's Hospital (IRCCS), Italy

REVIEWED BY
Hao Zhang,
Shanghai Jiao Tong University, China
Nattapon Panupinthu,
Mahidol University, Thailand

*CORRESPONDENCE
Chuanglong Xu
mqxcl@163.com
Dezhi Tang
dztang@shutcm.edu.cn
Yongjun Wang
wangyongjun@shutcm.edu.cn

†These authors have contributed equally to this work

RECEIVED 20 August 2023
ACCEPTED 09 October 2023
PUBLISHED 04 January 2024

CITATION
Zhang H, Shi B, Yuan C, Huang C, Huang T, Liao Z, Zhu W, Zhong W, Xu H, Ji J, Cai F, Chen Y, Sun P, Zeng X, Yang Z, Wang J, Shu B, Liang Q, Shi Q, Xu C, Tang D and Wang Y (2024) Correlation between the non-use of cooking oil fume extractors and bone mineral density in population aged 45 years and older in China: a cross-sectional study. *Front. Endocrinol.* 14:1280429. doi: 10.3389/fendo.2023.1280429

Correlation between the non-use of cooking oil fume extractors and bone mineral density in population aged 45 years and older in China: a cross-sectional study

Haitao Zhang[1,2,3†], Binhao Shi[1,2,4†], Chunchun Yuan[1,2,3†], Chen Huang[1,2,3], Tingrui Huang[1,2,3], Zhangyu Liao[5], Wenhao Zhu[1,2,3], Wei Zhong[5], Hongbin Xu[1,2,3], Jiangxun Ji[1,2,3], Feihong Cai[1,2,3], Yue Chen[1,2,3], Pan Sun[1,2,4], Xianhui Zeng[5], Zhiwu Yang[5], Jing Wang[1,4,6], Bing Shu[2,3,4], Qianqian Liang[1,2,4], Qi Shi[1,2,4], Chuanglong Xu[7]*, Dezhi Tang[1,2,4]* and Yongjun Wang[1,2,3,4]*

[1]Longhua Hospital, Shanghai University of Traditional Chinese Medicine, Shanghai, China, [2]Spine Institute, Shanghai Academy of Traditional Chinese Medicine, Shanghai, China, [3]Shanghai University of Traditional Chinese Medicine, Shanghai, China, [4]Key Laboratory of Theory and Therapy of Muscles and Bones, Ministry of Education, Shanghai, China, [5]Ganzhou Nankang District Traditional Chinese Medicine Hospital, Ganzhou, China, [6]Shanghai Geriatric Institute of Chinese Medicine, Shanghai, China, [7]Ningxia Hospital of Traditional Chinese Medicine and Chinese Medicine Research Institute, Yinchuan, China

Introduction: The correlation between the non-use of cooking oil fumes (COFs) extractors and bone mineral density (BMD) have not been clarified. Consequently, this study attempted to explore the impact of non-use COFs extractors on BMD in population aged 45 years and older based on a cross-sectional study.

Methods: This study was a cross-sectional study within the framework of an ongoing prospective population-based cohort study in China. The multivariate linear regression models were used to evaluate the correlation between the non-use of fume extractors in family cooking and total lumbar spine (LS), femoral neck (FN), total hip BMD and levels of bone metabolism markers.

Results: A total of 3433 participants were included in the final analyses, of which 2607 (75.93%) participants used fume extractors. The results of models indicated that there were significant correlations of the non-use of fume extractors on total LS BMD (β = -0.024, 95% CI, -0.036, -0.012, $p < 0.001$), PINP (β = 4.363, 95% CI, 2.371, 6.356, $p < 0.001$) and ALP (β = 4.555, 95% CI, 2.593, 6.517, $p < 0.001$) levels.

Conclusions: This study verified that the use of fume extractors is an efficacious measure to prevent LS bone loss. For the sake of public bone health, people should install a fume extractor in the kitchen and use it routinely when cooking.

KEYWORDS

bone mineral density, fume extractors, cross-sectional study, correlation, population

Introduction

Osteoporosis (OP) is one of the common orthopedic metabolic diseases characterized by decreased bone mass, damage of bone tissue microstructure, and increased bone fragility (1, 2). OP has attracted widespread attention due to its high incidence and associated fracture risk in the middle-aged and elderly population. According to statistics, the incidence of OP and low bone mineral density (BMD) among those over 50 years old in the United States is 11% and 46%, respectively (3). Correspondingly, the direct medical cost caused by OP exceeds $20 billion annually, which is still increasing (4). China has a large population, and the incidence of osteoporosis in males and females over 50 years old is 10-20% and 30-40%, respectively (5). With the aging of the population, it can be predicted that the incidence of OP will continue to rise, resulting in multiple adverse effects such as pain, depression, and low quality of life. Hence, it is vital to systematically understand the risk factors of OP and carry out early prevention, diagnosis, and intervention.

A great deal of cooking oil fumes (COFs) produced are an essential source of household indoor air pollutants (6). Chinese cuisine is more likely to produce COFs. There are two paramount reasons. On the one hand, Chinese people generally cook by stir-frying. On the other hand, it is customary to wait until the oil is heated to smoke, and then add food and ingredients. Recently, several studies have confirmed that COFs increase the risk of various diseases, such as respiratory diseases, cardiovascular diseases, diabetes, cancer, and poor sleep quality (7–10). COFs contain particulate matter (PM), polycyclic aromatic hydrocarbons (PAHs), organic carbon (OC), volatile organic compounds (VOCs) and carbonyl compounds, etc (11–13). The particulate matter derived from COFs are predominantly of a diameter ≤ 2.5μm ($PM_{2.5}$) (14–16). Previous studies have shown that air pollutants such as PAHs and $PM_{2.5}$ can stimulate bone growth and inhibit bone resorption (17, 18). Cohort studies have also confirmed a potential relationship between long-term exposure to air pollution and OP (19, 20). The use of COFs extractor can effectively reduce the degree of indoor air pollution caused by COFs (21). Studies by Chen et al. presented that use of COFs extractors can significantly reduce the risk of lung cancer (22). It was reasonable to suspect that there was a potential relationship between long-term use of COFs extractors and BMD.

Consequently, this study attempted to explore the impact of non-use COFs extractors on BMD in population aged 45 years and older based on a prospective cross-sectional study in China. We hypothesized that using COFs extractors is an effective measure to prevent bone mass loss in the human body.

Materials and methods

Study design

This present study was a cross-sectional study within the framework of an ongoing prospective China Community-based Cohort of Osteoporosis (CCCO) (Clinical trials. gov., NCT02958020) (23, 24). Additionally, our research scheme has been approved by the Institutional Review Committee of Longhua Hospital, Shanghai University of Traditional Chinese Medicine (No. 2016LCSY065). This study was conducted in strict accordance with the Declaration of Helsinki, and all participants signed informed consent.

Selection of study population

The screening of the study population was shown in Figure 1. The study population came from residents of Jiangxi province, China. Initially, 5275 participants were enrolled from January 2020 to September 2022. It is worth explaining that an age threshold of ≥ 45 years old selected to mitigate potential confounding influences, align with clinical practice relevance, and taking data availability into account. Thus, participants with under 45 years (n = 218) were excluded. Subsequently, participants with missing records on the use of COFs extractors (n =1421), missing bone metabolic indexes data (n = 83), missing BMD data (n = 60), missing data on other variables, taking hormone or antiosteoporosis drugs and fracture or implants in the lumber spine (LS) or hip (n = 60) were excluded in turn. Finally, 3433 participants were included in the analysis.

Variable data

The independent variables of this study were whether participants used a COFs extractor. All participants were asked whether used a COFs extractor when cooking at home (yes/no). If yes, was it used on a long-term basis (≥ 3 years)? The individuals' information about frequencies cooking at home (≥ once a day or < once a day), the type of cooking fuel used (clean fuel or solid fuel),

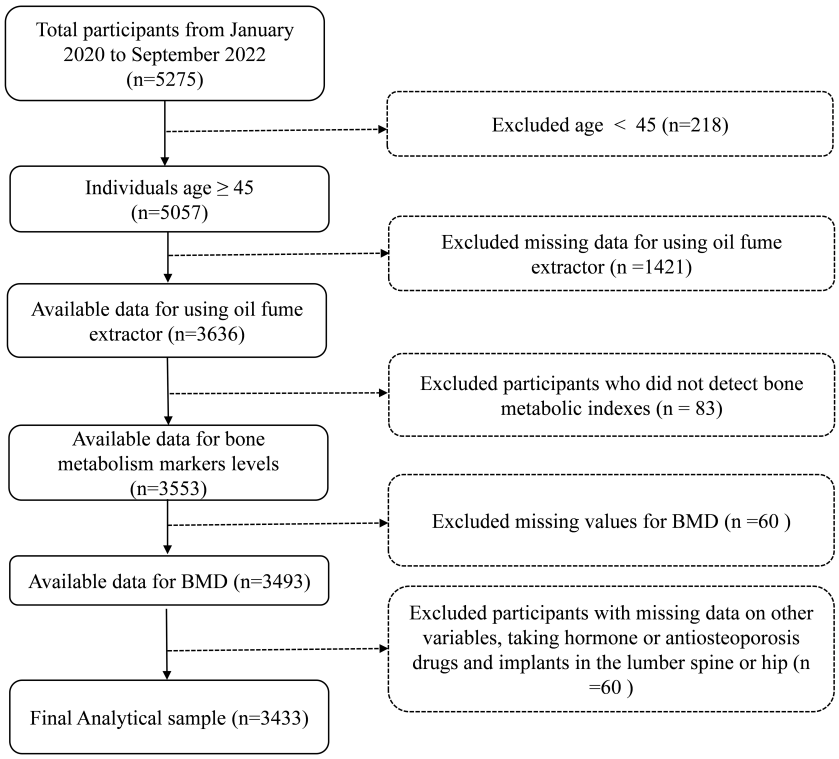

FIGURE 1
The study participant's selection flow chart.

and preference for frying food (yes or no) were also documented. All the aforementioned culinary-related data were obtained through a questionnaire.

The outcome variables were BMD (primary outcome) and bone metabolism markers (secondary outcome). The BMDs of each lumbar vertebra (L1, L2, L3, and L4), total LS, femoral neck (FN) and left hip (FN, trochanter, and intertrochanteric region combined with BMD) in all participants were quantified using dual energy X-ray absorptiometry (DXA, Hologic Discovery CI, Bedford, MA, USA). Calibration procedures routinely performed and calibration blocks provided to minimize measurement errors before each use of DXA.

Routine collection of fasting 5 ml venous blood from the median elbow vein of participants. The serum was isolated by centrifugation at the speed of 3,000 rpm for 15 minutes to detect the biochemical indexes of bone metabolism. Serum alkaline phosphatase (ALP) level was measured by continuous monitoring technique. The serum levels of osteocalcin (OST), N-terminal propeptide of type I collagen (PINP), and β-C-terminal telopeptide of type I collagen (β-CTX) were detected by electrochemiluminescence immunoassay. Serum creatinine content was determined by the creatinase method. The serum contents of calcium (Ca), phosphorus (P), and magnesium (Mg) were determined by the o-cresolphthalein-complex one method, phosphomolybdate ultraviolet colorimetry, and complex indicator method, respectively.

All participants were required to complete a paper questionnaire on OP under the guidance of trained professional clinicians. The contents of the questionnaire included baseline data, past medical history, family genetic history, living habits, eating habits, physical activity, and other modules. In this study, we extracted the required covariates according to the International Osteoporosis Foundation's suggestion (25), including age, gender, and body mass index (BMI), self-reported marital status, smoking behavior, drinking behavior, history of parental osteoporosis, history of hypertension, history of hyperlipidemia, history of diabetes, history of knee osteoarthritis, history of gout, history of chronic obstructive pulmonary disease, history of chronic pharyngitis, and physical activity.

Statistical analysis

Continuous variables were demonstrated as mean ± standard deviation and categorical variables were demonstrated as a percentage. The Mann-Whitney test and the Chi-square test were used to analyze the differences between the continuous variables and categorical variables, respectively. The multivariate linear regression models were used to evaluate the correlations of the non-use of fume extractors in family cooking with total LS, single LS, FN, hip BMD, and bone metabolism index level. The association between cooking frequency and total LS BMD was also further examined. In conformity with the Strengthening the Reporting of Observational Studies in Epidemiology (STROBE) statement guidelines published in 2007 (26), we have constructed the following three models: model 1, no covariates were adjusted; model 2, age, gender, and BMI were adjusted; model 3, age, gender, BMI, marital status, smoking behavior, drinking behavior,

10.3389/fendo.2023.1280429

history of the parental OP, hypertension, hyperlipidemia, diabetes, knee osteoarthritis, gout, and physical activity were adjusted. Subsequently, subgroup analyses stratified by age, gender, smoking and drinking behavior were conducted, respectively. Furthermore, linear regression models were used to assess the independent relationship between cooking fuel type, food frying and total BMD of LS in participants using fume extractors.

All data were analyzed using R software (http://www.R-project.org, The R Foundation) and EmpowerStats software (http://empowwerstats.com/, X&Y Solutions, Inc., Boston, MA). $P < 0.05$ was considered statistically significant.

Results

Baseline characteristics of the study population

A total of 3433 participants were included in the final analyses, of which 2607 (75.93%) participants used fume extractors for home cooking on a long-term basis (group A) and 826 (24.06%) participants did not use fume extractors for home cooking (group B). There were significant differences in age, sex, marital status, smoking behavior, hypertension, and chronic obstructive pulmonary disease between the two groups ($P < 0.05$). The BMDs of L1, L2, L3, L4, total LS, and total hip in group A were higher than those in group B (all $P < 0.05$). However, the BMD of FN showed no significant difference between the two groups. Serum creatinine, PINP, β-CTX, and ALP levels were statistically significant between the two groups (all $P < 0.05$). In contrast, serum levels of OST, Serum P, Mg, and Ca were not significantly different between the two groups. Detailed baseline data for participants was shown in Table 1.

Association of non-use of fume extractors with BMD

The results of the linear regression model for the non-use of COFs extractors with total LS, total hip, and FN BMD showed that there was a significant negative correlation between the non-use of COFs extractors and total LS BMD (model 3: β = -0.024, 95% CI, -0.036, -0.012, $p < 0.001$). Nevertheless, there was no correlation between the non-use of fume extractors and FN BMD (model 3: β = -0.014, 95% CI: -0.014, 0.019, $p = 0.762$) and the total BMD of the hip (model 3: β = -0.004, 95% CI: -0.018, 0.010, $p = 0.591$) (Table 2).

The results of the multivariate linear regression model between the non-use of COFs extractors and single LS BMD presented that the non-use of fume extractor was negatively correlated with L2 (model 3: β = -0.023, 95% CI: -0.038, -0.008, $p = 0.002$), L3 (model 3: β = -0.028, 95% CI: -0.042, -0.015, $p < 0.001$), L4 (model 3: β = -0.026, 95% CI: -0.043, 0.010, $p = 0.002$) BMD. However, the non-use of the fume extractor was not associated with L1 BMD (model 3: β = -0.003, 95% CI: -0.018, -0.012, $p = 0.672$) (Table 3).

TABLE 1 Characteristics of the participants in a cross-sectional study.

Variables	Group A (n =2607)	Group B (n =826)	*P* value
Age, mean ± SD, year	61.44 ± 9.54	65.92 ± 9.05	< **0.001**
Age, n (%)			< **0.001**
45-60	1219(46.76%)	217 (26.27%)	
60-75	1155 (44.30%)	470 (56.90%)	
≥75	233 (8.94%)	139 (16.83%)	
Gender			< **0.001**
male	563 (21.60%)	266 (32.20%)	
female	2044 (78.40%)	560 (67.80%)	
BMI, mean ± SD, m^2/kg	23.28 ± 3.17	23.07 ± 3.60	0.103
Marital status, n (%)			**0.007**
Married	2473 (94.86%)	763 (92.37%)	
Others	134 (5.14%)	63 (7.63%)	
History of parental OP, n (%)			0.115
No	2526 (96.89%)	809 (97.94%)	
Yes	81 (3.11%)	17 (2.06%)	
Smoking behavior, n (%)			**0.015**
Never	2336(89.61%)	715 (86.56%)	
Current or past	271 (10.40%)	111 (13.44%)	
Drinking behavior, n (%)			0.994
Never	2228 (85.46%)	706 (85.47%)	
Current or past	379 (14.54%)	120 (14.53%)	
Hyperlipidemia, n (%)			0.162
No	2265 (86.88%)	733 (88.74%)	
Yes	342 (13.12%)	93 (11.25%)	
Hypertension, n (%)			**0.001**
No	1760 (67.51%)	508 (61.50%)	
Yes	847 (32.49%)	318 (38.50%)	
Knee osteoarthritis, n (%)			0.190
No	2319 (88.95%)	721 (87.29%)	
Yes	288 (11.05%)	105 (12.71%)	
Gout, n (%)			0.107
No	2548 (97.74%)	799 (96.73%)	
Yes	59 (2.26%)	27 (3.27%)	
Diabetes, n (%)			0.913
No	2367 (90.79%)	751 (90.92%)	
Yes	240 (9.21%)	75 (9.08%)	

(Continued)

10.3389/fendo.2023.1280429

TABLE 1 Continued

Variables	Group A (n =2607)	Group B (n =826)	*P* value
Chronic pharyngitis, n (%)			
No	2343 (97.26%)	66 (2.74%)	0.184
Yes	66 (2.74%)	66 (2.74%)	
Chronic obstructive pulmonary disease, n (%)			0.006
No	2348 (97.55%)	59 (2.45%)	
Yes	59 (2.45%)	33 (4.39%)	
Physical activity, n (%)			0.050
Hardly any or mild exercise	694 (26.62%)	256 (30.99%)	
Moderate activities	794 (30.46%)	238 (28.81%)	
Vigorous activity	1119 (42.92%)	332 (40.19%)	
Frequencies of cooking, n (%)			0.093
≥once a day	1915 (73.46%)	631 (76.39%)	
< once a day	692 (26.54%)	195 (23.61%)	
L1 BMD, g/cm^2	0.737 ± 0.167	0.713 ± 0.200	< **0.001**
L2 BMD, g/cm^2	0.762 ± 0.186	0.722 ± 0.258	< **0.001**
L3 BMD, g/cm^2	0.796 ± 0.192	0.749 ± 0.185	< **0.001**
L4 BMD, g/cm^2	0.820 ± 0.231	0.780 ± 0.198	< **0.001**
Total LS BMD, g/cm^2	0.783 ± 0.181	0.742 ± 0.165	< **0.001**
Total hip BMD, g/cm^2	0.761 ± 0.173	0.741 ± 0.230	**0.010**
FN BMD, g/cm^2	0.675 ± 0.195	0.665 ± 0.271	0.260
β-CTX, ng/ml	0.283 ± 0.163	0.269 ± 0.160	**0.037**
OST, ng/ml	15.614 ± 7.382	15.870 ± 7.103	0.381
PINP, ng/ml	61.271 ± 25.127	65.175 ± 27.018	< **0.001**
Serum creatinine	72.758 ± 23.360	77.967 ± 24.713	< **0.001**
ALP, U/L	83.607 ± 23.654	89.094 ± 27.890	< **0.001**
Serum P, mmol/L	1.307 ± 0.458	1.321 ± 0.507	0.447
Serum Mg, mmol/L	0.933 ± 0.072	0.938 ± 0.071	0.136
Serum Ca, mmol/L	2.346 ± 0.089	2.346 ± 0.103	0.999

ALP, alkaline phosphatase; β-CTX, β-C-terminal telopeptide of type I collagen, Ca, calcium, OST, osteocalcin, P, phosphorus, PINP, N-terminal propeptide of type I collagen, Mg, magnesium, OP, osteoporosis.
Mean ± SD for continuous variables: p value was calculated by the linear regression model. Number (proportion) for categorical variables: p value was calculated by the chi-square test. BMI, body mass index, LS, lumbar spine, FN, femoral neck, BMD, bone mineral density. Group A, use fume extractors, Group B, non-use fume extractors. The significance level is defined to be p < 0.05. Bold values indicate statistical difference.

Independent association of cooking frequencies with total LS BMD

In the group of using of fume extractors, it was observed that individuals cooking frequency ≥ once a day had a lower LS BMD when compared to those cooking less than once a day (model 3: β = -0.067, 95% CI: -0.082, -0.052, $p < 0.001$), adjusting for confounding variables. Similar association existed in the group of non-use of fume extractors (Table 4).

TABLE 2 Associations of the non-use of fume extractors with total LS, femoral neck, and total hip BMD.

Outcome	Model 1, β (95% CI) *P*	Model 2, β (95% CI) *P*	Model 3, β (95% CI) *P*
Total LS BMD	-0.041 (-0.054, -0.027) < **0.001**	-0.025 (-0.038, -0.013) < **0.001**	-0.024 (-0.036, -0.012) < **0.001**
Femoral neck BMD	-0.010 (-0.027, 0.007) 0.260	-0.001 (-0.016, 0.017) 0.937	0.003 (-0.014, 0.019) 0.762
Total hip BMD	-0.019 (-0.034, -0.005) < **0.001**	-0.006 (-0.019, 0.008) 0.427	-0.004 (-0.018, 0.010) 0.591

LS, lumbar spine; BMD, bone mineral density; OP, osteoporosis. Model 1: no covariates were adjusted; model 2: age, gender, and BMI were adjusted; model 3: age, gender; BMI, marital status, smoking behavior, drinking behavior, history of the parental OP, hypertension, hyperlipidemia, diabetes, knee osteoarthritis, gout, and physical activity. The significance level is defined to be p < 0.05. Bold values indicate statistical difference.

TABLE 3 Relationship of non-use of fume extractors with individual total LS BMD.

Outcome	Model 1, β (95% CI) *P*	Model 2, β (95% CI) *P*	Model 3, β (95% CI) *P*
L1 BMD	-0.024 (-0.038, -0.011) < **0.001**	-0.013 (-0.026, -0.000) 0.047	-0.012 (-0.025, 0.001) 0.067
L2 BMD	-0.040 (-0.056, -0.024) < **0.001**	-0.024 (-0.039, -0.009) **0.002**	-0.023 (-0.038, -0.008) **0.002**
L3 BMD	-0.048 (-0.063, -0.033) < **0.001**	-0.030 (-0.043, -0.017) < **0.001**	-0.028 (-0.042, -0.015) < **0.001**
L4 BMD	-0.040 (-0.058, -0.023) < **0.001**	-0.027 (-0.044, -0.011) < **0.001**	-0.026 (-0.043, -0.010) **0.002**

LS, lumbar spine, BMD, bone mineral density, OP, osteoporosis. Model 1: no covariates were adjusted; model 2: age, gender, and BMI were adjusted; model 3: age, gender; BMI, marital status, smoking behavior, drinking behavior, history of the parental OP, hypertension, hyperlipidemia, diabetes, knee osteoarthritis, gout, and physical activity. The significance level is defined to be p < 0.05. Bold values indicate statistical difference.

Stratification analysis

In the subgroup analysis stratified by age, the adverse effects of not using fume extractors were only observed in the population aged 45-60 years (β = -0.051, 95% CI: -0.075, -0.027, $p < 0.001$). In the subgroup analysis stratified by gender, smoking behavior, and drinking behavior, the detrimental impact of not using fume extractors appeared to be more significant among males (males, β = -0.028, 95%CI: -0.050, -0.006, $p = 0.014$; female, β = -0.018, 95% CI: -0.032, -0.003, $p = 0.016$), smokers (smokers, β = -0.042, 95%CI: -0.077, -0.006, p = 0.022; never smoking, β = -0.019, 95%CI: -0.032, -0.006, $p = 0.004$), and drinkers (drinker, β = -0.039, 95%CI: -0.070, -0.007, $p = 0.016$; never drinking, β = -0.020, 95%CI: -0.033, -0.006, $p = 0.004$) (Table 5).

10.3389/fendo.2023.1280429

TABLE 4 Association of cooking frequencies with total LS BMD.

Groups	Cooking frequencies	Model 1, β (95% CI) *P*	Model 2, β (95% CI) *P*	Model 3, β (95% CI) *P*
Use fume extractors	≥once a day	Reference	Reference	Reference
	< once a day	0.122 (0.107, 0.137) **<0.001**	0.068 (0.053, 0.083) **<0.001**	0.067 (0.052, 0.082) **<0.001**
Non-use fume extractors	≥once a day	Reference	Reference	Reference
	< once a day	0.095 (0.070, 0.121) **<0.001**	0.043 (0.017, 0.068) **0.001**	0.049 (0.022, 0.075) **<0.001**

LS, lumbar spine, BMD, bone mineral density, OP, osteoporosis. Model 1: no covariates were adjusted; model 2: age, gender; and BMI were adjusted; model 3: age, gender, BMI, marital status, smoking behavior, drinking behavior, history of the parental OP, hypertension, hyperlipidemia, diabetes, knee osteoarthritis, gout, and physical activity. The significance level is defined to be p < 0.05. Bold values indicate statistical difference.

Association of non-use of fume extractors with bone metabolic markers level

The results of the linear regression model without using fume extractors and bone metabolic markers showed significant positive associations of non-use of fume extractors with PINP (model 3: β = 4.363, 95% CI, 2.371, 6.356, $p < 0.001$) and ALP (model 3: β = 4.555, 95% CI, 2.593, 6.517, $p < 0.001$) levels. There was no correlation between the non-use of fume extractors and β-CTX and other markers after adjusting the factors (Table 6).

TABLE 5 The results of stratification.

Stratified variable	Total LS BMD		
	Model 1, β (95% CI) *P*	Model 2, β (95% CI) *P*	Model 3, β (95% CI) *P*
Age			
45-60 years	-0.031 (-0.056, -0.006) **0.016**	-0.051 (-0.075, -0.027) < **0.001**	-0.051 (-0.075, -0.027) < **0.001**
60-75 years	-0.008 (-0.026, 0.009) 0.350	-0.013 (-0.028, 0.002) 0.095	-0.009 (-0.024, 0.006) 0.245
≥75 years	-0.022 (-0.059, 0.015) 0.241	-0.006 (-0.038, 0.026) 0.706	0.005 (-0.027, 0.036) 0.772
Gender			
male	-0.047 (-0.070, -0.024) < **0.001**	-0.034 (-0.056, -0.012) **0.002**	-0.028 (-0.050, -0.006) **0.014**
female	-0.053 (-0.069, -0.036) < **0.001**	-0.018 (-0.032, -0.003) **0.017**	-0.018 (-0.032, -0.003) **0.016**
Smoking behavior			
Never	-0.040 (-0.055, -0.026) < **0.001**	-0.020 (-0.033, -0.007) **0.003**	-0.019 (-0.032, -0.006) **0.004**
Current or past	-0.062 (-0.099, -0.025) **0.011**	-0.049(-0.085, -0.014) 0.007	-0.042 (-0.077, -0.006) **0.022**
Drinking behavior			
Never	-0.040 (-0.055, -0.025) < **0.001**	-0.021 (-0.035, -0.008) **0.002**	-0.020 (-0.033, -0.006) **0.004**
Current or past	-0.046 (-0.079, -0.013) **0.007**	-0.042 (-0.073, -0.010) **0.009**	-0.039 (-0.070, -0.007) **0.016**

LS, lumbar spine, BMD, bone mineral density, OP, osteoporosis. Model 1: no covariates were adjusted; model 2: age, gender, and BMI were adjusted; model 3: age, gender; BMI, marital status, smoking behavior, drinking behavior, history of the parental OP, hypertension, hyperlipidemia, diabetes, knee osteoarthritis, gout, and physical activity. The significance level is defined to be p < 0.05.
*In the subgroup analysis stratified, the model is not adjusted for the stratification variable itself. Bold values indicate statistical difference.

Association of cooking fuel type and food frying with total LS BMD

Among the people who use oil fume extractors, 2294 people have recorded cooking fuel types, including 2088 participants who use clean fuel (natural gas, liquefied gas, or electricity), 206 participants who use solid fuel (coal). Compared with clean fuel, the results of model indicated that there was a negative correlation between solid fuel use and total LS BMD (model 3: β = -0.049, 95% CI: - 0.074, -0.024, $p < 0.001$).

There were 2,692 participants using fume extractors who had records of frying food, including 2,160 who often liked fried food

TABLE 6 Associations of the non-use of fume extractors with bone metabolic markers level.

Bone metabolic markers	Model 1, β (95% CI) *P*	Model 2, β (95% CI) *P*	Model 3, β (95% CI) *P*
β-CTX	-0.013 (-0.026, -0.001) **0.037**	-0.002 (-0.015, 0.011) 0.735	-0.003 (-0.016, 0.009) 0.615
OST	0.256 (-0.316, 0.829) 0.381	0.430 (-0.140, 0.999) 0.139	0.366 (-0.195, 0.928) 0.201
PINP	3.904 (1.901, 5.907) < **0.001**	4.595 (2.588, 6.602) < **0.001**	4.363 (2.371, 6.356) < **0.001**
Serum creatinine	5.210 (3.356, 7.064) < **0.001**	0.971 (-0.683, 2.624) 0.250	1.007 (-0.640, 2.655) 0.231
ALP	5.488 (3.552, 7.424) < **0.001**	4.584 (2.624, 6.544) < **0.001**	4.555 (2.593, 6.517) < **0.001**
Serum P	0.014 (-0.023, 0.051) 0.447	0.014 (-0.023, 0.051) 0.459	0.014 (-0.023, 0.052) 0.451
Serum Mg	0.004 (-0.001, 0.010) 0.136	-0.001 (-0.007, 0.004) 0.673	-0.001 (-0.007, 0.004) 0.689
Serum Ca	-0.000 (-0.007, 0.007) 0.999	0.003 (-0.004, 0.010) 0.403	0.004 (-0.003, 0.011) 0.273

ALP, alkaline phosphatase; β-CTX, β-C-terminal telopeptide of type I collagen, Ca, calcium; OST, osteocalcin, P, phosphorus; PINP, N-terminal propeptide of type I collagen, Mg, magnesium, OP, osteoporosis.
Model 1: no covariates were adjusted; model 2: age, gender, and BMI were adjusted; model 3: age, gender; BMI, marital status, smoking behavior, drinking behavior, history of the parental OP, hypertension, hyperlipidemia, diabetes, knee osteoarthritis, gout, and physical activity. The significance level is defined to be p < 0.05. Bold values indicate statistical difference.

and 532 who never fried food. The results of model indicated that there was no significant correlation between frying food and total LS BMD (model 3: β = -0.004, 95%CI: -0.019, 0.011, p = 0.607) (Table 7).

Discussion

In this prospective cross-sectional study of China, we systematically assessed the relationship between COFs extractors use and total LS, FN, and total hip BMD in adults ≥ 45 age. The results confirmed that long-term use of COFs extractors is an effective measure to prevent bone loss, particularly among groups of 45-60 years old, males, smokers (current or past smokers) and drinkers (current or past smokers). The higher the cooking frequency, the greater the decrease in LS BMD. Additionally, we found that solid fuel use was associated with lower total LS BMD among COFs extractor users.

Long-term exposure to air pollution was a significant independent risk factor for bone mass decline (27). A study from rural areas of Henan Province in China demonstrated that PM content in the air was positively correlated with OP (19). A study based on the UK Biobank manifested that people exposed to $PM_{2.5}$, NO_2, and NO_X increased the incidence of OP (28). A large national cohort study in South Korea proved that long-term exposure to SO_2 was associated with an increased risk of osteoporotic fractures (29). Aldehydes were one of the environmental pollutants. Gu et al. deemed that mixed aldehydes can significantly reduce BMD in males (30). Duan et al. considered that 2-hydroxy fluorene was associated with increased odds of OP (31). The above evidence indicates that air pollution was related to lower BMD. COFs were the main culprit of indoor air pollution. Most harmful substances in COFs are similar to outdoor air pollution, such as PM (31).

Biologically, exposure to high concentrations of PM may stimulate inflammatory responses in alveolar macrophages and airway epithelial cells, which significantly increase the levels of serum monocytes, NK cells, and helper T cells and induce the expression of proinflammatory cytokines including tumor necrosis factor α, monocyte chemoattractant protein-1, interleukin-8, macrophage inflammatory protein-1 α, IL-6, IL-1 β and granulocyte-macrophage colony-stimulating factor (32–34). Subsequently, some inflammatory factors may increase receptor activators of nuclear factor κ B expression in osteoclast precursors and macrophage colony-stimulating factor expression in stromal cells. Eventually, an imbalance of osteoblasts and osteoclasts leads to bone loss (18, 35) (Figure 2).

The fume extractors can effectively discharge the lampblack produced during cooking. Notwithstanding, in many rural areas of China, the use of fume extractors is not all widespread. Currently, few researchers have investigated the relationship between the use of fume extractors and human BMD. Thereby, we conducted a cross-sectional study of southern China. Our study verified that using fume extractors in family cooking can effectively prevent the loss of total LS BMD aged 45-60 in southern China, which might provide evidence for the local government to formulate valuable policies. We recommend that the kitchen be equipped with a fume extractor and use this device when cooking to reduce the unfavorable impact of COFs on public bones. Incidentally, we found no evidence of an association between the use of a fume extractor and hip or femoral neck BMD. Although there is no direct experimental evidence for the susceptibility of different bones to air pollution, Ranzani et al. believed that trabecular bone was more affected than cortical bone (36). Further study on the effect of different parts of BMD is necessary.

As for the relationship between the use of COFs extractors and single LS BMD, the results of L2, L3, and L4 were consistent with the overall lumbar BMD except for L1. This may involve the biomechanical effects of the LS. The L1 segment has a large range of motion, and it is the transition point from thoracic kyphosis to lumbar kyphosis. The L1 trabecular bone tissue possesses distinctive characteristics, serving as a pivotal site in vertebral fractures. Among the fragility fractures of the lumbar vertebrae, L1 has the highest incidence (37). For this reason, the effect COFs on L1 was different from other LS.

What is worth mentioning was the result of the hierarchical analysis. After the adjustment of the model, the total LS BMD of people aged 45-60 without using fume extractors were significantly lower than that of using fume extractor, and that phenomenon disappeared over 60. One possible explanation was that the activity of osteoclasts and osteoblasts of the elderly decreases with age (38, 39). The adverse effect of COFs was less prominent in the competition between osteoclasts and osteoblasts with reduced activity (40). In the stratification analysis of gender, although the negative correlation between the non-use of fume extractor and total LS BMD was present in both males and females, bone loss was more severe in males. This result was different from previous studies in Taiwan (41). It was speculated that the women in this study are all 45 years old and older, most of whom were postmenopausal. Postmenopausal women lack the combination of hormone factors and particulate matter. Moreover, total LS BMD declines in smokers were more severe than in non-smokers, which was

TABLE 7 Association of fuel type and food frying with LS BMD in the population using fume extractors.

	Model 1 (β, 95% CI, P)	Model 2 (β, 95% CI, P)	Model 3 (β, 95% CI, P)
Fuel type			
Clean fuel (n=2088)	Reference	Reference	Reference
Solid fuel (n=206)	-0.068 (-0.094, -0.043) < **0.001**	-0.039 (-0.061, -0.016) < **0.001**	-0.045 (-0.067, -0.022) < **0.001**
Food frying			
No (n=2160)	Reference	Reference	Reference
Yes (n=532)	-0.019 (-0.036, -0.002) **0.032**	-0.001 (-0.016, 0.014) 0.918	-0.004 (-0.019, 0.011) 0.607

LS, lumbar spine, BMD, bone mineral density, OP, osteoporosis. Model 1: no covariates were adjusted; model 2: age, gender, and BMI were adjusted; model 3: age, gender; BMI, marital status, smoking behavior, drinking behavior, history of parental OP, hypertension, hyperlipidemia, diabetes, knee osteoarthritis, gout and physical activity. Bold values indicate statistical difference.

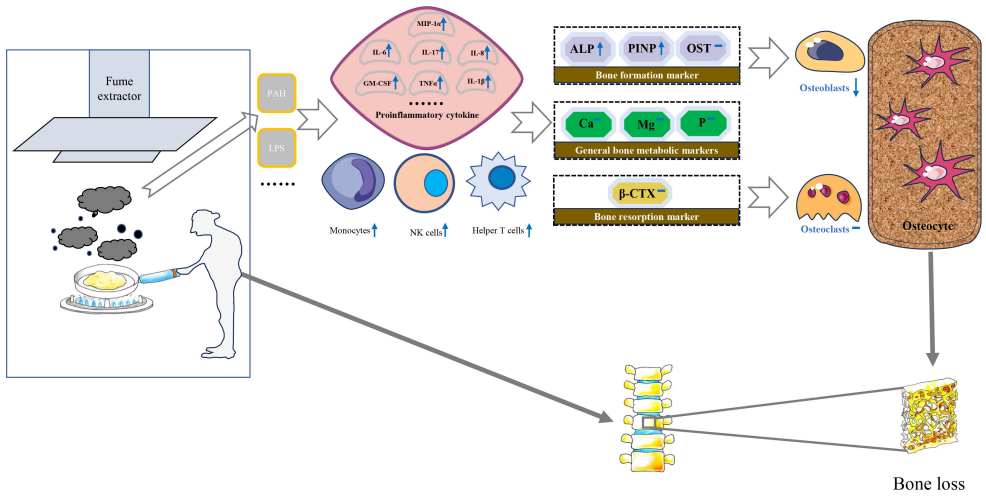

FIGURE 2
Possible molecular and cellular mechanisms for the impact of cooking oil fume on bone mineral density. IL, Interleukin; MCSF, Macrophage colony-stimulating factor; TNF-α, Tumor necrosis factor-alpha; PAH, polycyclic aromatic hydrocarbons; LPS, lipopolysaccharide; MIP-1α, Macrophage inflammatory protein 1α; ALP, alkaline phosphatase; β-CTX, β-C-terminal telopeptide of type I collagen; Ca, calcium; OST, osteocalcin; P, phosphorus; PINP, N-terminal propeptide of type I collagen; Mg, magnesium.

consistent with previous studies (42, 43). Several toxic components in tobacco smoke were the same as those in particulates. Nicotine and other toxic components in tobacco smoke can promote osteoclast differentiation, which was the superimposed harmful factor of COFs (44). Similarly, total LS BMD declines in drinkers were more severe than in non-drinkers. The effect of alcohol intake on BMD has always been controversial, and studies had shown that the effect of alcohol on BMD depends on the amount consumed (45). As a consequence, this study strongly recommends that certain groups of people aged 45-60 years, males, smokers, or drinkers focus on using fume extractors to prevent loss of LS BMD while cooking.

The user of solid fuel had lower total LS BMD compared to the clean fuel in the population of using fume extractors. A cohort study covering 28 villages in southern India reported that black carbon was associated with lower levels of BMD in the hips and LS, although not statistically significant (36). On the one hand, the primary mechanism by which the toxic components produced by black charcoal burning affect bone loss may stimulate pro-inflammatory cytokines to induce RANKL secretion (46). On the other hand, black carbon exposure is negatively correlated with parathyroid hormone levels (47). Our study revealed that the behavior of food frying had no significant effect on total LS BMD while using fume extractors.

The detection of serum biochemical markers can indirectly reflect the status of bone metabolism in the whole body to some extent (48). Bone turnover markers are divided into bone formation markers and bone resorption markers. PINP, ALP and OST belong to bone formation markers. ALP was an extracellular enzyme secreted by osteoblasts. Its physiological function was to hydrolyze phosphate and pyrophosphate during osteogenesis (49). When bone mineralization was blocked, osteoblasts would synthesize a large amount of ALP. In addition, type I collagen was the only type of collagen in mineralized bone in the human body. The amino terminal additional peptide removed from procollagen was called PINP. PINP is recognized as the best marker for evaluating bone formation (50). The increased expression of PINP indicates that the synthesis rate of type I collagen was fast and bone turnover is active (51). β-CTX primarily serves as an indicator of osteoclast activity and bone resorption levels, thereby indirectly gauging the extent of osteoporosis (52). Liu et al. observed a significant positive correlation between exposure to air pollutants and bone calcium and β-CTX levels of children (53). Conversely, the investigation led by Feizabad et al. yielded no noteworthy differentiation in β-CTX levels between adolescents inhabiting polluted and unpolluted locales (54). A basic study found that rats exposed to air pollutants had significantly higher ALP levels than the control group (55). There was limited research on the correlation between air pollution and PINP, which made it challenging to compare our current findings with previous research. In our study, serum levels of PINP and ALP were significantly lower in individuals with using fume extractors compared to without using fume extractors. This condition is not reflected in β-CTX and other bone metabolic markers. Therefore, we speculate that the biological mechanism of BMD loss caused by COFs exposure may destroy the balance of bone remodeling mainly by affecting the process of bone formation (Figure 2).

To the best of our knowledge, this study is the first to investigate the association between household fume extractors use and BMD based on cross-sectional population. Admittedly, there are certain limitations in this study. Firstly, the exposure variables in this study were based on self-reported results, which memory errors of a small number of participants may have been biased. Secondly, the exposure factors in this study were qualitative, while the content of COFs was not quantified. We will further refine the COFs

content in the ongoing cohort study. Last but not least, there was the bias caused by certain unavoidable potential confounding factors, such as the type of COFs.

Conclusion

In a nutshell, this study verified that the use of fume extractors was an efficacious measure to prevent bone loss. The use of fume extractors may keep serum PINP and ALP at a low level. For the sake of public bone health, we recommended that people should install a fume extractor in the kitchen and use it routinely when cooking. Particularly, the specific population aged 45-60, males, smokers, or drinkers are required to follow this recommendation. In addition, clean fuel should be used as much as possible when cooking to reduce the adverse impact on LS BMD.

Data availability statement

The original contributions presented in the study are included in the article/supplementary material. Further inquiries can be directed to the corresponding author.

Ethics statement

The cross-sectional study has been approved by the Institutional Review Committee of Longhua Hospital, Shanghai University of Traditional Chinese Medicine (No. 2016LCSY065). This study was conducted in strict accordance with the Declaration of Helsinki, and all participants signed informed consent.

Author contributions

HZ: Data curation, Formal analysis, Investigation, Methodology, Software, Visualization, Writing – original draft. BShi: Data curation, Investigation, Methodology, Software, Writing – original draft. CY: Data curation, Formal analysis, Investigation, Methodology, Software, Supervision, Writing – original draft. CH: Data curation, Investigation, Methodology, Writing – original draft. TH: Data curation, Investigation, Writing – original draft. ZL: Data curation, Investigation, Writing – review & editing. WZhu: Data curation, Formal analysis, Investigation, Methodology, Software, Validation, Visualization, Writing – original draft. WZho: Data curation, Investigation, Writing – review & editing. HX: Data curation, Investigation, Software, Validation, Writing – original draft. JJ: Data curation, Investigation, Software, Writing – original draft. FC: Data curation, Investigation, Writing – original draft. YC: Data curation, Investigation, Writing – original draft. PS: Data curation, Investigation, Writing – original draft. XZ: Data curation, Investigation, Writing – review & editing. ZY: Data curation, Investigation, Writing – review & editing. JW: Data curation, Methodology, Formal analysis, Supervision, Writing – review & editing. BShu: Writing – review & editing, Project administration, Supervision. QL: Supervision, Writing – review & editing, Validation. QS: Supervision, Writing – review & editing, Conceptualization. CX: Conceptualization, Supervision, Writing – review & editing, Funding acquisition. DT: Conceptualization, Supervision, Writing – review & editing, Project administration, Resources, Funding acquisition. YW: Conceptualization, Project administration, Resources, Supervision, Writing – review & editing, Funding acquisition.

Funding

The author(s) declare financial support was received for the research, authorship, and/or publication of this article. This work was partially supported by the Inheritance and Innovation Team Project of National Traditional Chinese Medicine (ZYYCXTD-C-202202), the National Key R&D Program of China (2018YFC1704300), the National Natural Science Foundation of China (81730107, 81973883), the Program for Innovative Research Team of Ministry of Education of China (IRT1270), the Program for Innovative Research Team of Ministry of Science and Technology of China (2015RA4002), the Ningxia Hui Autonomous Region science and technology benefit people project (2022CMG03030).

Conflict of interest

The authors declare that the research was conducted in the absence of any commercial or financial relationships that could be construed as a potential conflict of interest.

Publisher's note

References

1. Johnston CB, Dagar M. Osteoporosis in older adults. *Med Clinics North America* (2020) 104(5):873–84. doi: 10.1016/j.mcna.2020.06.004

2. Consensus development conference: diagnosis, prophylaxis, and treatment of osteoporosis. *Am J Med* (1993) 94(6):646–50. doi: 10.1016/0002-9343(93)90218-e

3. Looker AC, Sarafrazi Isfahani N, Fan B, Shepherd JA. Trends in osteoporosis and low bone mass in older US adults, 2005-2006 through 2013-2014. *Osteoporosis Int J established as result cooperation between Eur Foundation Osteoporosis Natl Osteoporosis Foundation USA* (2017) 28(6):1979–88. doi: 10.1007/s00198-017-3996-1

4. Dempster DW. Osteoporosis and the burden of osteoporosis-related fractures. *Am J managed Care* (2011) 17 Suppl 6:S164–9.

5. Yu F, Xia W. The epidemiology of osteoporosis, associated fragility fractures, and management gap in China. *Arch osteoporosis* (2019) 14(1):32. doi: 10.1007/s11657-018-0549-y

6. Straif K, Baan R, Grosse Y, Secretan B, El Ghissassi F, Cogliano V. Carcinogenicity of household solid fuel combustion and of high-temperature frying. *Lancet Oncol* (2006) 7(12):977–8. doi: 10.1016/S1470-2045(06)70969-X

7. Wei F, Nie G, Zhou B, Wang L, Ma Y, Peng S, et al. Association between Chinese cooking oil fumes and sleep quality among a middle-aged Chinese population. *Environ pollut (Barking Essex 1987)* (2017) 227:543–51. doi: 10.1016/j.envpol.2017.05.018

8. Hou X, Mao Z, Song X, Kang N, Zhang C, Li R, et al. Kitchen ventilation alleviated adverse associations of domestic fuel use and long-duration cooking with platelet indices as biomarkers of cardiovascular diseases. *Sci Total Environ* (2022) 834:155341. doi: 10.1016/j.scitotenv.2022.155341

9. Hou J, Sun H, Zhou Y, Zhang Y, Yin W, Xu T, et al. Environmental exposure to polycyclic aromatic hydrocarbons, kitchen ventilation, fractional exhaled nitric oxide, and risk of diabetes among Chinese females. *Indoor air* (2018) 28(3):383–93. doi: 10.1111/ina.12453

10. Jia PL, Zhang C, Yu JJ, Xu C, Tang L, Sun X. The risk of lung cancer among cooking adults: a meta-analysis of 23 observational studies. *J Cancer Res Clin Oncol* (2018) 144(2):229–40. doi: 10.1007/s00432-017-2547-7

11. Singh A, Chandrasekharan Nair K, Kamal R, Bihari V, Gupta MK, Mudiam MK, et al. Assessing hazardous risks of indoor airborne polycyclic aromatic hydrocarbons in the kitchen and its association with lung functions and urinary PAH metabolites in kitchen workers. *Clinica chimica acta; Int J Clin Chem* (2016) 452:204–13. doi: 10.1016/j.cca.2015.11.020

12. Sjaastad AK, Jørgensen RB, Svendsen K. Exposure to polycyclic aromatic hydrocarbons (PAHs), mutagenic aldehydes and particulate matter during pan frying of beefsteak. *Occup Environ Med* (2010) 67(4):228–32. doi: 10.1136/oem.2009.046144

13. Yao Z, Li J, Wu B, Hao X, Yin Y, Jiang X. Characteristics of PAHs from deep-frying and frying cooking fumes. *Environ Sci pollut Res Int* (2015) 22(20):16110–20. doi: 10.1007/s11356-015-4837-4

14. Ding L, Sui X, Yang M, Zhang Q, Sun S, Zhu F, et al. Toxicity of cooking oil fume derived particulate matter: Vitamin D(3) protects tubule formation activation in human umbilical vein endothelial cells. *Ecotoxicol Environ Saf* (2020) 188:109905. doi: 10.1016/j.ecoenv.2019.109905

15. Ke Y, Huang L, Xia J, Xu X, Liu H, Li YR. Comparative study of oxidative stress biomarkers in urine of cooks exposed to three types of cooking-related particles. *Toxicol Lett* (2016) 255:36–42. doi: 10.1016/j.toxlet.2016.05.017

16. Li YC, Qiu JQ, Shu M, Ho SSH, Cao JJ, Wang GH, et al. Characteristics of polycyclic aromatic hydrocarbons in PM(2.5) emitted from different cooking activities in China. *Environ Sci pollut Res Int* (2018) 25(5):4750–60. doi: 10.1007/s11356-017-0603-0

17. Guo J, Huang Y, Bian S, Zhao C, Jin Y, Yu D, et al. Associations of urinary polycyclic aromatic hydrocarbons with bone mass density and osteoporosis in U.S. adults, NHANES 2005-2010. *Environ pollut (Barking Essex 1987)* (2018) 240:209–18. doi: 10.1016/j.envpol.2018.04.108

18. Prada D, López G, Solleiro-Villavicencio H, Garcia-Cuellar C, Baccarelli AA. Molecular and cellular mechanisms linking air pollution and bone damage. *Environ Res* (2020) 185:109465. doi: 10.1016/j.envres.2020.109465

19. Qiao D, Pan J, Chen G, Xiang H, Tu R, Zhang X, et al. Long-term exposure to air pollution might increase prevalence of osteoporosis in Chinese rural population. *Environ Res* (2020) 183:109264. doi: 10.1016/j.envres.2020.109264

20. Yang Y, Li R, Cai M, Wang X, Li H, Wu Y, et al. Ambient air pollution, bone mineral density and osteoporosis: Results from a national population-based cohort study. *Chemosphere* (2023) 310:136871. doi: 10.1016/j.chemosphere.2022.136871

21. Feng S, Shen X, Hao X, Cao X, Li X, Yao X, et al. Polycyclic and nitro-polycyclic aromatic hydrocarbon pollution characteristics and carcinogenic risk assessment of indoor kitchen air during cooking periods in rural households in North China. *Environ Sci pollut Res Int* (2021) 28(9):11498–508. doi: 10.1007/s11356-020-11316-8

22. Chen TY, Fang YH, Chen HL, Chang CH, Huang H, Chen YS, et al. Impact of cooking oil fume exposure and fume extractor use on lung cancer risk in non-smoking Han Chinese women. *Sci Rep* (2020) 10(1):6774. doi: 10.1038/s41598-020-63656-7

23. Wang J, Chen L, Zhang Y, Li CG, Zhang H, Wang Q, et al. Association between serum vitamin B(6) concentration and risk of osteoporosis in the middle-aged and older people in China: a cross-sectional study. *BMJ Open* (2019) 9(7):e028129. doi: 10.1136/bmjopen-2018-028129

24. Wang J, Shu B, Tang DZ, Li CG, Xie XW, Jiang LJ, et al. The prevalence of osteoporosis in China, a community based cohort study of osteoporosis. *Front Public Health* (2023) 11:1084005. doi: 10.3389/fpubh.2023.1084005

25. Kanis JA, Delmas P, Burckhardt P, Cooper C, Torgerson D. Guidelines for diagnosis and management of osteoporosis. *Eur Foundation Osteoporosis Bone Disease. Osteoporosis Int J established as result cooperation between Eur Foundation Osteoporosis Natl Osteoporosis Foundation USA* (1997) 7(4):390–406. doi: 10.1007/BF01623782

26. von Elm E, Altman DG, Egger M, Pocock SJ, Gøtzsche PC, Vandenbroucke JP. The Strengthening the Reporting of Observational Studies in Epidemiology (STROBE) statement: guidelines for reporting observational studies. *Lancet* (2007) 370 (9596):1453–7. doi: 10.1016/S0140-6736(07)61602-X

27. Torkashvand J, Jonidi Jafari A, Pasalari H, Shahsavani A, Oshidari Y, Amoohadi V, et al. The potential osteoporosis due to exposure to particulate matter in ambient air: Mechanisms and preventive methods. *J Air Waste Manage Assoc (1995)* (2022) 72 (9):925–34. doi: 10.1080/10962247.2022.2085820

28. Xu C, Weng Z, Liu Q, Xu J, Liang J, Li W, et al. Association of air pollutants and osteoporosis risk: The modifying effect of genetic predisposition. *Environ Int* (2022) 170:107562. doi: 10.1016/j.envint.2022.107562

29. Heo S, Kim H, Kim S, Choe SA, Byun G, Lee JT, et al. Associations between long-term air pollution exposure and risk of osteoporosis-related fracture in a nationwide cohort study in South Korea. *Int J Environ Res Public Health* (2022) 19(4):2404. doi: 10.3390/ijerph19042404

30. Gu L, Wang Z, Liu L, Luo J, Pan Y, Sun L, et al. Association between mixed aldehydes and bone mineral density based on four statistical models. *Environ Sci Pollut Res Int* (2023) 30(11):31631–46. doi: 10.1007/s11356-022-24373-y

31. Duan W, Meng X, Sun Y, Jia C. Association between polycyclic aromatic hydrocarbons and osteoporosis: data from NHANES, 2005-2014. *Arch osteoporosis* (2018) 13(1):112. doi: 10.1007/s11657-018-0527-4

32. Pope CA 3rd, Bhatnagar A, McCracken JP, Abplanalp W, Conklin DJ, O'Toole T. Exposure to fine particulate air pollution is associated with endothelial injury and systemic inflammation. *Circ Res* (2016) 119(11):1204–14. doi: 10.1161/CIRCRESAHA.116.309279

33. Alfaro-Moreno E, Torres V, Miranda J, Martínez L, García-Cuellar C, Nawrot TS, et al. Induction of IL-6 and inhibition of IL-8 secretion in the human airway cell line Calu-3 by urban particulate matter collected with a modified method of PM sampling. *Environ Res* (2009) 109(5):528–35. doi: 10.1016/j.envres.2009.02.010

34. Becker S, Dailey L, Soukup JM, Silbajoris R, Devlin RB. TLR-2 is involved in airway epithelial cell response to air pollution particles. *Toxicol Appl Pharmacol* (2005) 203(1):45–52. doi: 10.1016/j.taap.2004.07.007

35. Kitaura H, Kimura K, Ishida M, Kohara H, Yoshimatsu M, Takano-Yamamoto T. Immunological reaction in TNF-α-mediated osteoclast formation and bone resorption *in vitro* and *in vivo*. *Clin Dev Immunol* (2013) 2013:181849. doi: 10.1155/2013/181849

36. Ranzani OT, Milà C, Kulkarni B, Kinra S, Tonne C. Association of ambient and household air pollution with bone mineral content among adults in peri-urban south India. *JAMA Network Open* (2020) 3(1):e1918504. doi: 10.1001/jamanetworkopen.2019.18504

37. Yeni YN, Kim DG, Divine GW, Johnson EM, Cody DD. Human cancellous bone from T12-L1 vertebrae has unique microstructural and trabecular shear stress properties. *Bone* (2009) 44(1):130–6. doi: 10.1016/j.bone.2008.09.002

38. Cauley JA, Chalhoub D, Kassem AM, Fuleihan Gel H. Geographic and ethnic disparities in osteoporotic fractures. *Nat Rev Endocrinol* (2014) 10(6):338–51. doi: 10.1038/nrendo.2014.51

39. Zeng Q, Li N, Wang Q, Feng J, Sun D, Zhang Q, et al. The prevalence of osteoporosis in China, a nationwide, multicenter DXA survey. *J Bone mineral Res Off J Am Soc Bone Mineral Res* (2019) 34(10):1789–97. doi: 10.1002/jbmr.3757

40. Shen L, Zhou S, Glowacki J. Effects of age and gender on WNT gene expression in human bone marrow stromal cells. *J Cell Biochem* (2009) 106(2):337–43. doi: 10.1002/jcb.22010

41. Lin YH, Wang CF, Chiu H, Lai BC, Tu HP, Wu PY, et al. Air pollutants interaction and gender difference on bone mineral density T-score in Taiwanese adults. *Int J Environ Res Public Health* (2020) 17(24):9165. doi: 10.3390/ijerph17249165

42. Thompson AR, Joyce M, Stratton K, Orwoll ES, Carlson HL, Carlson NL, et al. Lifetime smoking history and prevalence of osteoporosis and low bone density in U.S. Adults, national health and nutrition examination survey 2005-2010. *J women's Health* (2023) 32(3):323–31. doi: 10.1089/jwh.2022.0153

43. Alvaer K, Meyer HE, Falch JA, Nafstad P, Søgaard AJ. Outdoor air pollution and bone mineral density in elderly men - the Oslo Health Study. *Osteoporosis Int J established as result cooperation between Eur Foundation Osteoporosis Natl Osteoporosis Foundation USA* (2007) 18(12):1669–74. doi: 10.1007/s00198-007-0424-y

44. Weng W, Bovard D, Zanetti F, Ehnert S, Braun B, Uynuk-Ool T, et al. Tobacco heating system has less impact on bone metabolism than cigarette smoke. *Food Chem Toxicol an Int J published Br Ind Biol Res Assoc* (2023) 173:113637. doi: 10.1016/j.fct.2023.113637

45. Gaddini GW, Turner RT, Grant KA, Iwaniec UT. Alcohol: A simple nutrient with complex actions on bone in the adult skeleton. *Alcoholism Clin Exp Res* (2016) 40 (4):657–71. doi: 10.1111/acer.13000

46. Saha H, Mukherjee B, Bindhani B, Ray MR. Changes in RANKL and osteoprotegerin expression after chronic exposure to indoor air pollution as a result of cooking with biomass fuel. *J Appl Toxicol JAT* (2016) 36(7):969–76. doi: 10.1002/jat.3275

47. Prada D, Zhong J, Colicino E, Zanobetti A, Schwartz J, Dagincourt N, et al. Association of air particulate pollution with bone loss over time and bone fracture risk: analysis of data from two independent studies. *Lancet Planetary Health* (2017) 1(8): e337–e47. doi: 10.1016/S2542-5196(17)30136-5

48. Wu CH, Chang YF, Chen CH, Lewiecki EM, Wüster C, Reid I, et al. Consensus statement on the use of bone turnover markers for short-term monitoring of osteoporosis treatment in the asia-pacific region. *J Clin densitometry Off J Int Soc Clin Densitometry* (2021) 24(1):3–13. doi: 10.1016/j.jocd.2019.03.004

49. Brown JP, Don-Wauchope A, Douville P, Albert C, Vasikaran SD. Current use of bone turnover markers in the management of osteoporosis. *Clin Biochem* (2022) 109-110:1–10. doi: 10.1016/j.clinbiochem.2022.09.002

50. Watts NB, Camacho PM, Lewiecki EM, Petak SM. American association of clinical endocrinologists/american college of endocrinology clinical practice guidelines for the diagnosis and treatment of postmenopausal osteoporosis-2020 update. *Endocrine Pract Off J Am Coll Endocrinol Am Assoc Clin Endocrinologists* (2021) 27 (4):379–80. doi: 10.1016/j.eprac.2021.02.001

51. Choi R, Lee SG, Lee EH. Intra-individual changes in total procollagen-type 1 N-terminal propeptide in a korean adult population. *Diagnostics (Basel Switzerland)* (2022) 12(10):2399. doi: 10.3390/diagnostics12102399

52. Eastell R, Pigott T, Gossiel F, Naylor KE, Walsh JS, Peel NFA. DIAGNOSIS OF ENDOCRINE DISEASE: Bone turnover markers: are they clinically useful? *Eur J Endocrinol* (2018) 178(1):R19–r31. doi: 10.1530/EJE-17-0585

53. Liu C, Fuertes E, Flexeder C, Hofbauer LC, Berdel D, Hoffmann B, et al. Associations between ambient air pollution and bone turnover markers in 10-year old children: results from the GINIplus and LISAplus studies. *Int J hygiene Environ Health* (2015) 218(1):58–65. doi: 10.1016/j.ijheh.2014.07.006

54. Feizabad E, Hossein-Nezhad A, Maghbooli Z, Ramezani M, Hashemian R, Moattari S. Impact of air pollution on vitamin D deficiency and bone health in adolescents. *Arch Osteoporosis* (2017) 12(1):34. doi: 10.1007/s11657-017-0323-6

55. Kheirouri S, Alizadeh M, Abad RMS, Barkabi-Zanjani S, Mesgari-Abbasi M. Effects of sulfur dioxide, ozone, and ambient air pollution on bone metabolism related biochemical parameters in a rat model. *Environ Analysis Health Toxicol* (2020) 35(4): e2020023–0. doi: 10.5620/eaht.2020023

Frontiers in Endocrinology

Explores the endocrine system to find new therapies for key health issues

The second most-cited endocrinology and metabolism journal, which advances our understanding of the endocrine system. It uncovers new therapies for prevalent health issues such as obesity, diabetes, reproduction, and aging.

Discover the latest Research Topics

See more →

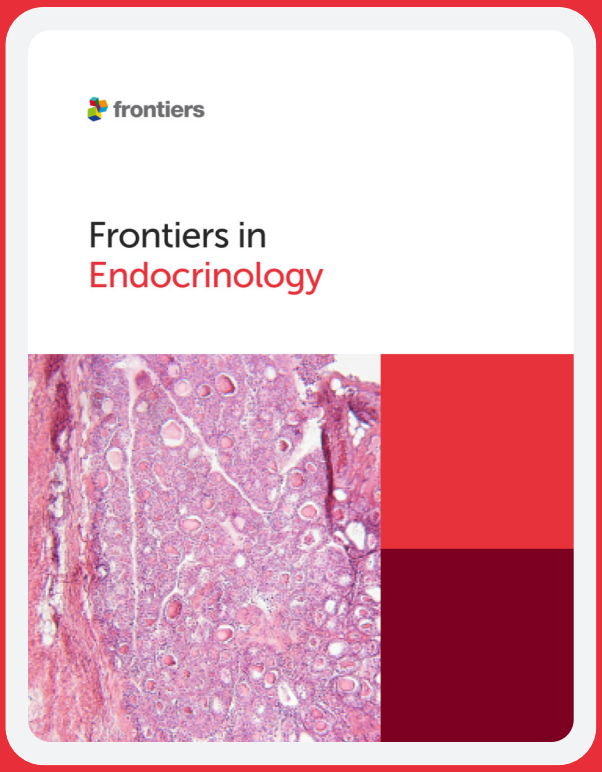

Frontiers

Avenue du Tribunal-Fédéral 34
1005 Lausanne, Switzerland
frontiersin.org

Contact us

+41 (0)21 510 17 00
frontiersin.org/about/contact